U.PORTO

FACULDADE DE FARMÁCIA
UNIVERSIDADE DO PORTO

NEW PERSPECTIVES ON MELANOMA THERAPY: INSIGHTS ON THE ROLE OF ADENOSINE AND ADENOSINE RECEPTORS

ANA SOFIA FALCATO SOARES

TESE DO 3º CICLO DE ESTUDOS CONDUCENTE AO GRAU DE DOUTORAMENTO EM CIÊNCIAS FARMACÊUTICAS
ESPECIALIDADE DE FARMACOLOGIA E FARMACOTERAPIA

Trabalho realizado sob a orientação da Professora Doutora Paula Maria Façanha da Cruz Fresco, Professora Associada da Faculdade de Farmácia da Universidade do Porto, e da Professora Doutora Carmen Diniz Pereira, Professora Auxiliar da Faculdade de Farmácia da Universidade do Porto.

MARÇO, 2014

DECLARAÇÃO

Ao abrigo do nº2 do artigo 8º do Decreto-Lei nº388/70, declara-se que fazem parte integrante desta tese os seguintes trabalhos publicados ou submetidos. Para esses trabalhos, o autor da tese contribuiu maioritariamente na execução das experiências laboratoriais, interpretação de resultados e preparação dos manuscritos.

PUBLICAÇÕES

I. **Falcato-Soares A**, Diniz C, Fresco P. Characterization of adenosine receptors in human and mouse melanoma cells. Medimond International Proceedings: 6th European Congress of Pharmacology, Granada (Spain) 2013:29-34.

II. **Soares AF**, Diniz C, Fresco P. A_3 adenosine receptor effects on malignant melanoma cells. FEBS J 2012;279(Suppl. 1):547.

III. **Soares AS**, Costa VM, Diniz C, P F. Inosine strongly enhances human C32 melanoma cells proliferation through PLC-PKC-MEK1/2-ERK1/2 and PI3K pathways (Submitted).

IV. **Soares AS**, Costa VM, Diniz C, Fresco P. Potentiation of cytotoxicity of paclitaxel in combination with Cl-IB-MECA in human C32 metastatic melanoma cells: A new possible therapeutic strategy for melanoma. Biomedicine & pharmacotherapy 2013;67:777-789.

V. **Soares AS**, Costa VM, Diniz C, Fresco P. Combination of Cl-IB-MECA with paclitaxel is a highly effective cytotoxic therapy causing mTOR-dependent autophagy and mitotic catastrophe on human melanoma cells. Journal of cancer research and clinical oncology DOI: 10.1007/s00432-014-1645-z.

VI. **Soares AS**, Costa VM, Diniz C, Fresco P. The combination of Cl-IB-MECA with paclitaxel: A new anti-metastatic therapeutic strategy for melanoma (Submitted).

AGRADECIMENTOS

"Ninguém escapa ao sonho de voar, de ultrapassar os limites do espaço onde nasceu, de ver novos lugares e novas gentes. Mas saber ver em cada coisa, em cada pessoa, aquele algo que a define como especial, um objecto singular, um amigo – é fundamental. Navegar é preciso, reconhecer o valor das coisas e das pessoas é mais preciso ainda!"

Antoine de Saint-Exupéry

Deixo apenas algumas palavras, poucas, mas um sentido e profundo agradecimento a todas as pessoas que directa ou indirectamente contribuiram para a elaboração deste trabalho.

À Professora Doutora Paula Fresco, um agradecimento muito especial pela oportunidade que me deu, pela orientação deste trabalho e por ter partilhado comigo a sua experiência e conhecimentos científicos. Agradeço ainda por me ter permitido seguir o meu próprio trajeto. Obrigada por todo o carinho, disponibilidade e amizade em todos os momentos, principalmente nas alturas de desânimo!

À Professora Doutora Carmen Diniz, pelo apoio e orientação deste trabalho, pelos conselhos, sugestões e sentido crítico, além da sua simpatia e palavras de ânimo. Obrigada pela sua amizade.

À Vera, com quem tive o privilégio de colaborar, agradeço todos os estímulos e desafios que muito contribuiram para este trabalho. Um agradecimento especial, pela disponibilidade e pela ajuda, apoio e preocupação nos momentos de aflição e, acima de tudo, pelo seu rigor científico. Foste incansável! Obrigada pela amizade e pelos bons momentos de discussão de Ciência.

Ao grupo da Farmacologia pela amizade, pela ajuda em todas as ocasiões, compreensão, companheirismo e boa disposição em todos os momentos, pessoas com as quais criei um laço verdadeiro, e que certamente se identificarão nestas minhas palavras, sem ter que dizer muito mais. Obrigada Amigas!

Aos colegas e amigos da Faculdade de Farmácia pelo apoio, ajuda e boa disposição.

Aos familiares e amigos pelo apoio, compreensão, amizade e momentos fantásticos de descontração.

Ao João, pelo companheirismo com que sempre me apoiou e acompanhou ao longo deste trabalho. Sempre que necessário soube aconselhar e soube criticar... Pelas alegrias, momentos felizes, desânimos, angústias mas, principamente, pela compreensão e por estares sempre ao meu lado, muito obrigada!

Ao meu irmão Luís e à Susana pela amizade e carinho, pelo apoio prestado, pela compreensão e incentivo, pela partilha dos bons (e menos bons) momentos e, claro, por estarem sempre a torcer por mim. Muito obrigada!

Aos meus pais, Maria e José, pela forma como me incutiram a alegria de viver, pelo incentivo para fazer tudo o melhor possível e por me apoiarem incondicionalmente em todas as decisões. Um agradecimento muito especial pelo amor e carinho diários, e pela transmissão de confiança e de força, em todos os momentos. Obrigada por escutarem os intermináveis desabafos ao telemóvel! Obrigada por acreditarem sempre em mim! Obrigada, simplesmente, por tudo!

Deixo aqui, também, os agradecimentos às seguintes instituições pelo seu apoio a esta tese:

À Fundação para a Ciência e Tecnologia (FCT) pela bolsa de Doutoramento SFRH/BD/64911/2009 e aos fundos do Programa Operacional Factores de Competitividade (COMPETE) sem os quais a realização desta tese não teria sido possível.

Ao Laboratório de Farmacologia do Departamento de Ciências do Medicamento da Faculdade de farmácia da Universidade do Porto e REQUIMTE por providenciarem as instalações e apoio logístico necessário ao trabalho aqui incluído.

ABSTRACT

Melanoma is one of the most aggressive malignant tumours, due to its high metastatic potential and resistance to current treatment modalities. Patients with metastatic melanoma present poor prognosis, with an overall survival of 8 to 18 months and limited meaningful therapeutic strategies. Systemic treatment options for advanced melanoma include single-agent or combination chemotherapies. Paclitaxel is recommended as a first or second-line strategy for systemic therapy of metastatic melanoma, both in monotherapy and in combination with platinum compounds. However, paclitaxel as all other currently available treatment options are associated with limited efficacy and combinations increased toxicities without significantly improve survival rates. Therefore, alternative therapeutic strategies for metastatic melanoma are urgently needed.

Several lines of evidence have hypothesized a role of adenosine in tumour development and growth. Studies suggest a contradictory role of adenosine in the viability of normal and cancer cells, ascribed to the stimulation of the four adenosine receptor subtypes, named A_1, A_{2A}, A_{2B}, and A_3, which couple to different signal transduction pathways and can be co-expressed in the same cell.

The overall aim of this thesis was to study the role of adenosine/adenosine receptors in the complex interplay of proliferation, cell death mechanisms and metastatic progression of melanoma, and to provide clues for the development of new therapeutic strategies for metastatic melanoma.

The expression of A_1, A_{2A}, A_{2B} and A_3 adenosine receptors, on human C32 and A375 and mouse K1735-M2 melanoma cells, was shown. Activation of adenosine receptor subtypes A_1, A_{2A}, and A_3 did not affect cell proliferation of A375 and K1735-M2 cells. However, proliferation of C32 cells was increased, after activation of A_3 adenosine receptor, by micromolar concentrations of adenosine or nanomolar concentrations of the selective A_3 agonist, Cl-IB-MECA. However, Cl-IB-MECA, at micromolar concentrations, caused marked cytotoxicity, through A_3-independent mechanisms.

Results indicate a major role for A_3 adenosine receptors in C32 cell proliferation induced by inosine, through PLC-PKC-MEK1/2-ERK1/2 pathway activation. However, activation of the PI3K pathway, mediated by $P2Y_1$ receptors, was also found to be involved. Inosine also enhanced proliferation of the A375 cell line and stimulated the metastatic processes evaluated in both cell lines (migration, adhesion, invasion and colony-formation), through A_3 adenosine receptor activation. These results suggest inosine as an aggressiveness agent for these human melanoma cell models. Furthermore, the observed inosine pro-angiogenic effect (microvessel sprouting) is A_3-independent.

The combination of Cl-IB-MECA and paclitaxel was studied, emerging as a promising cytotoxic combination for metastatic melanoma, acting through the induction of multiple mechanisms of cell death (apoptosis with the involvement of mitotic catastrophe, and mTOR-dependent autophagy) and inhibition of the aforementioned metastatic processes, involved in melanoma progression. This new therapeutic strategy seems to be able to overcome melanoma chemotherapy multiresistance, through activation of alternative cell death mechanisms, and to stop, or delay, melanoma progression, potentially improving treatment and prognosis of patients with metastatic melanoma.

Keywords

Melanoma, adenosine receptors, Cl-IB-MECA, paclitaxel, cell death mechanisms

RESUMO

O melanoma é um dos tumores malignos mais agressivos, devido ao seu elevado potencial metastático e resistência às modalidades de tratamento disponíveis. Doentes com melanoma metastático têm mau prognóstico, com uma sobrevida global de 8 a 18 meses, e estratégias terapêuticas limitadas. Opções de tratamento sistémico para o melanoma avançado incluem monoterapias e combinações de agentes quimoterápicos. O paclitaxel é recomendado como agente de primeira ou segunda linha para a terapêutica sistémica do melanoma metastático, em monoterapia ou em combinação com compostos de platina. No entanto, o paclitaxel tal como todas as opções terapêuticas actualmente disponíveis estão associadas a baixa eficácia terapêutica e as combinações apresentam aumento de toxicidade sem melhorar significativamente as taxas de sobrevida. Por estas razões, são necessárias, urgentemente, estratégias terapêuticas alternativas para o melanoma metastático.

Vários trabalhos sugerem que a adenosina desempenha um papel importante no desenvolvimento e crescimento tumorais. Este nucleósido foi descrito como afectando, de modo diferencial, a viabilidade das células normais e cancerosas, através da ativação dos quatro subtipos de recetores de adenosina, denominados A_1, A_{2A} , A_{2B} e A_3, que podem acoplar a vias de transdução de sinal diferentes e ser co-expressos numa mesma célula.

O objetivo geral desta tese foi estudar o papel da adenosina e dos seus recetores na complexidade das interações entre a proliferação, os mecanismos de morte celular e a progressão metastática do melanoma, e encontrar indicações para o desenvolvimento de novas estratégias terapêuticas para o melanoma metastático.

Foi mostrada a expressão dos recetores da adenosina A_1, A_{2A}, A_{2B} e A_3, em células C32 e A375 de melanoma humano e células K1735-M2 de melanoma de ratinho. A ativação dos subtipos dos receptores da adenosina A_1, A_{2A} e A_3 não afetou a proliferação celular das células A375 e K1735-M2. No entanto, a proliferação das células C32 foi aumentada, após a activação do receptor A_3 da adenosina, por concentrações micromolares de adenosina ou nanomolares do agonista selectivo A_3, Cl-IB-MECA. No entanto, Cl-IB-MECA, em concentrações micromolares, causou citotoxicidade, através de mecanismos independentes da activação dos recetores A_3.

Os resultados indicam um papel importante para os recetores A_3 da adenosina na proliferação das células C32, induzida pela inosina, através da ativação da via da PLC-PKC-MEK1/2-ERK1/2. No entanto, a ativação da via da PI3K, mediada por recetores $P2Y_1$, também está envolvida. A inosina promoveu ainda a proliferação das células A375 e estimulou os processos metastáticos avaliados em ambas as linhas celulares (migração, adesão, invasão e formação de colónias), através da ativação do recetor A_3 da adenosina.

Estes resultados sugerem a inosina como um agente de agressividade nestes modelos celulares de melanoma humano. Além disso, o efeito pró-angiogénico estimulado pela inosina (formação de microvasos a partir de anéis de aorta de ratinho) é independente da activação dos receptores A_3.

Estudou-se a combinação terapêutica Cl-IB-MECA e paclitaxel, que se revelou uma combinação promissora para o tratamento do melanoma metastático, através da indução de múltiplos mecanismos de morte celular (apoptose com o envolvimento de catástrofe mitótica e autofagia dependente do mTOR) e inibição dos processos metastáticos acima mencionados e que estão envolvidos na progressão do melanoma. Esta nova estratégia terapêutica parece ser capaz de superar a resistência do melanoma à quimioterapia, através da ativação de mecanismos alternativos de morte celular, e de parar, ou atrasar, a progressão do melanoma, melhorando, potencialmente, o tratamento e prognóstico dos doentes com melanoma metastático.

Palavras-chave

Melanoma, recetores da adenosina; Cl-IB-MECA; paclitaxel; mecanismos de morte celular

TABLE OF CONTENTS

LIST OF FIGURES

ABBREVIATIONS AND SYMBOLS

AC	adenylyl cyclase
Ac-DEVD-CHO	*N*-acetyl-asp-glu-val-asp-al
ADA	adenosine deaminase
ADO	adenosine
ADP	adenosine diphosphate
AIF	apoptosis inducing factor
AK	adenosine kinase
AMP	adenosine monophosphate
AR	adenosine receptors
ATP	adenosine triphosphate
cAMP	cyclic adenosine monophosphate
CGS 15943	9-chloro-2-(2-furanyl)-[1,2,4]triazolo[1,5-*c*]quinazolin-5-amine
CGS 21680	4-[2-[[6-amino-9-(*N*-ethyl-β-D-ribofuranuronamidosyl)-9*H*-purin-2-yl]amino]ethyl]benzenepropanoic acid hydrochloride
Cl-IB-MECA	1-[2-chloro-6-[[(3-iodophenyl)methyl]amino]-9*H*-purin-9-yl]-1-deoxy-*N*-methyl-β-D-ribofuranuronamide
CPA	*N*-cyclopentyladenosine
DNA	deoxyribonucleic acid
ECM	extracellular matrix
ERK	extracellular signal-regulated kinase
IAP	inhibitors of apoptosis
IL-2	interleukin-2
IMP	inosine monophosphate
INO	inosine
MAPK	mitogen-activated protein kinase
MEK	mitogen-activated protein kinase kinase
MRE 3008F20	*N*-[2-(2-furanyl)-8-propyl-8*H*-pyrazolo[4,3-*e*][1,2,4]triazolo[1,5-*c*]pyrimidin-5-yl]-*N*'-(4-methoxyphenyl)urea
mTOR	mammalian target of rapamycin
NBTI	*S*-(4-nitrobenzyl)-6-thioinosine
NECA	5'-*N*-ethylcarboxamidoadenosine
NT	nucleoside transporters
NTase	nucleotidase

PI3K	phosphoinositide 3-kinase
PKA	protein kinase A
PKC	protein kinase C
PLC	phospholipase C
PXT	paclitaxel
ROS	reactive oxygen species
SAH	*S*-adenosylhomocysteine
UV	ultraviolet
VEGF	vascular endothelial growth factor

CHAPTER I

General Introduction

A. LITERATURE REVIEW

1. MELANOMA

Metastatic melanoma is considered one of the most aggressive malignant tumours, representing the deadliest form of skin cancer [1]. This serious disease, whose cells are derived from transformed epidermal melanocytes, has, currently, an alarming increase in incidence rates [2]. Although melanoma is less common than other types of skin cancer, the incidence of cutaneous melanoma is rising faster than any other solid tumour [3], accounting for a global incidence of about 160 thousands new cases each year [4]. This increased incidence may be a consequence of more people chronically exposed to natural/artificial UV radiation and/or higher detection rates associated with enhanced public awareness [5]. In Portugal, melanoma incidence is estimated to be 8/100,000 persons *per* year, with an overall increasing incidence of 6-7% *per* year [6].

1.1 Melanocytes and skin

Melanocytes are pigment-producing cells of the skin in humans and other vertebrates [7]. They are originated from embryonic neural crest cells (melanoblasts) that gradually become more differentiated during development [8]. The life cycle of melanocytes consists in i) migration and proliferation of melanoblasts, ii) differentiation into melanocytes, iii) maturation of melanocytes (melanin production in melanosomes, dendritic morphology), iv) transport of melanosomes to keratinocytes and v) eventual cell death [9]. Although pigment cells are found throughout the skin, they are also present in the hair, eye, inner ear, central nervous system, mucosal membranes, heart, and muscle [10]. It is well accepted that melanocytes establish dynamic interactions with the skin microenvironment, in particular with keratinocytes (Figure 1) [9].

Melanocytes are found in the basal layer of epidermis where they form the epidermal melanin units. These are defined as functional units composed of one melanocyte and approximately 36 associated keratinocytes [11]. It is accepted that each melanocyte, through its multiple dendrites, transports melanin-containing melanosomes to keratinocytes, although the precise transfer process is not completely understood [12]. Melanin, produced in melanocytes through the involvement of tyrosinase activity, absorbs

and scatters ultraviolet (UV) radiation, preventing DNA damage of keratinocytes and melanocytes [13].

Complex signalling networks between keratinocytes, melanocytes, fibroblasts, and extracellular matrix (ECM) include not only the transfer of melanin to keratinocytes, but extensive cytokine, hormonal, and growth factor signalling, which maintains skin homeostasis [10,14].

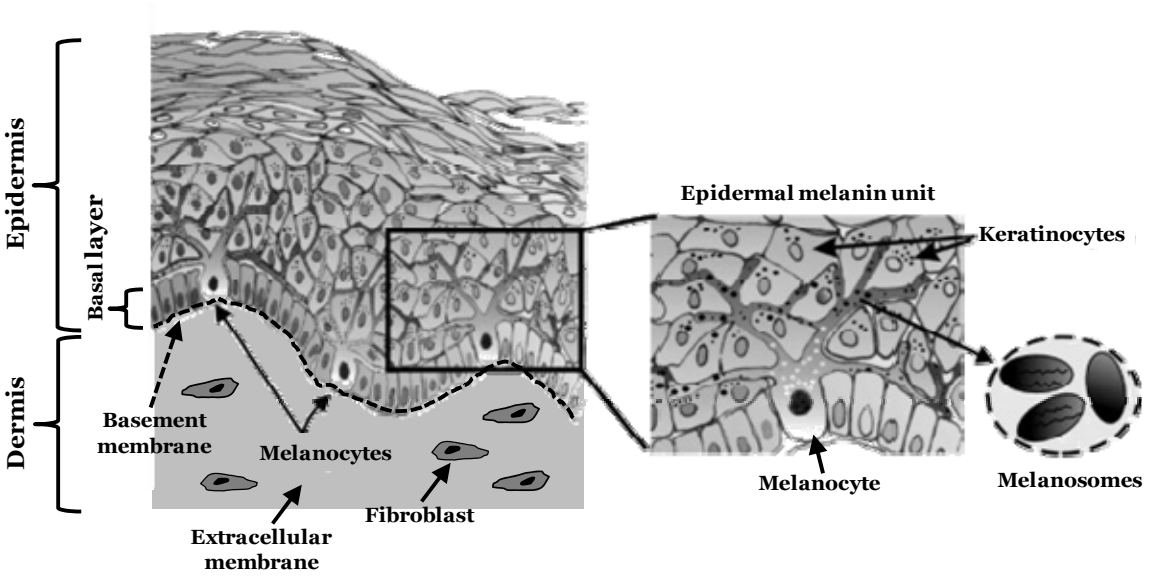

Figure 1. The human skin is constituted of two distinct layers, the epidermis and the dermis, which are separated by the basement membrane. Melanocytes, found in the epidermal basal layer, synthesize melanin in melanosomes, which are then transported into keratinocytes, through dendritic processes. Modified from [9].

1.2 Melanoma development

Currently, divergent hypothesis are proposed to explain melanoma development. In individuals with a tendency to develop large numbers of nevi, melanomas are initiated after modest solar radiation exposure, after which host factors drive further progression; on the contrary, in individuals with little or no tendency to develop nevi, chronic exposure to the sun seems crucial for melanoma development [10]. This could justify the different mutation patterns found in skin areas, chronically or non-chronically, exposed to solar radiation [15]. Nevertheless, approximately 75% of melanomas arise from normal skin in the absence of pre-existing nevi [16].

Endogenous risk factors like previous family history of melanoma, and multiple dysplastic or benign nevi, blond or red hair, and pale skin have revealed a strong association with melanoma development [1]. However, exogenous risk factors including long term sun exposure, photochemotherapy, and photographic chemicals exposure are also reported to favour the development of melanoma [17].

Solar UV radiation has been linked to skin cancer, both in non-melanoma (transformed keratinocytes) and melanoma (transformed melanocytes) cancers [18]. Skin malignant changes promoted by UV solar radiation (i) cause DNA mutagenic effects; (ii) increase the production of growth factors by skin cellular constituents; (iii) reduce the cutaneous immune defences; and (iv) promote reactive oxygen species (ROS) formation [19].

Although epidemiological studies have linked solar UV radiation to melanoma [20], the specific contribution of UVB and UVA radiation exposure in the risk of developing melanoma is controversial. UVB, the minor but the most damaging solar light component, causes direct DNA damage on cells of skin epidermal basal layer, since UVB wavelengths are within the DNA absorption spectrum [21]. UVA wavelengths (more abundant) penetrate into the epidermis and dermis of the skin, generating ROS that can damage cellular components, including DNA [22]. Nevertheless, evidence suggests that both UVA and UVB radiation act together to promote the development and progression of melanoma [23,24].

Skin has endogenous defence systems that limit the potential damage caused by UV radiation, such as melanin, antioxidant enzymes, and DNA repair enzymes [21]. However, these endogenous photoprotective mechanisms are not always sufficient to neutralize the adverse effects caused by UV radiation. Thus, melanocytes that have accumulated abnormalities in their DNA may develop melanoma. The abnormalities can promote a malignant phenotype, which include cell proliferation and impaired apoptosis, stimulation of angiogenesis, escape from the immune system, tumour invasion, and finally metastasis [19].

1.3 Melanoma progression

Despite the origins for melanoma remain controversial, with melanoma development starting either from a nevus or directly from cutaneous melanocyte, melanomas generally undergo several stages of growth (Figure 2).

Initially, cells proliferate in a radial-like fashion within the epidermis (radial growth phase). These lesions can then progress with cells breaking through the basement membrane and invading the dermis (vertical growth phase) [25]. At this stage, cells become autonomous, producing their own growth factors independently from keratinocytes, being able to invade blood and lympha [26,27]. These events first lead to local metastasis and eventually to distant metastasis [26]. However not all melanomas have these individual stages [28]. Both radial and vertical growth phases can develop directly from either single melanocytes or nevi, and both can progress directly to metastatic melanoma [29].

Some melanomas retain physical characteristics of melanocytes, namely pigmentation, giving melanomas a highly pigmented phenotype, whereas others lose this ability and are amelanotic. Overall, melanomas present heterogeneity concerning cell morphology and pigmentation level [30].

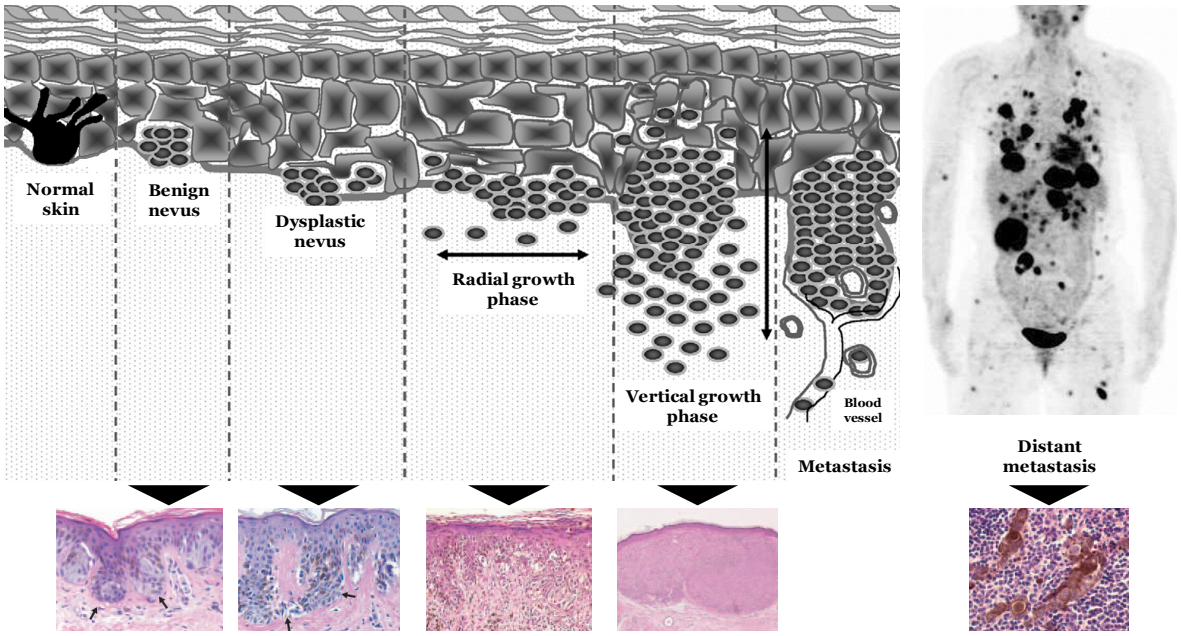

Figure 2. Different stages of human melanoma. Aberrant proliferation of normal melanocytes results in the formation of benign or dysplastic nevus. In the radial growth phase, melanoma exhibits the ability to grow intra-epidermally, followed by invasion of the dermis in the vertical growth phase, and culminating with metastasis. Note that not all melanomas arise from nevi, and progression can occur without going through all the stages depicted. Modified from [25,29,31].

Malignancy hallmarks of cancers, including rapid and uncontrolled proliferation, invasion, and distant organs colonization, can be attributed, in part, to deregulation of

interactions between neoplastic cells and cellular microenvironment [32]. Following malignant transformation, melanoma cells become autonomous and no longer respond to keratinocytes trophic stimulation signals [27]. Development of melanoma metastasis starts with cell migration from the primary tumour, followed by re-adhesion and tissue invasion [33]. Proteolytic degradation of basement membrane and ECM represents a critical step for melanoma invasion and metastasis, since it displaces the surrounding matrix, which is required for cells to move into surrounding tissues [28]. In addition, anchorage-independent growth (colony formation) is also important for malignant cell transformation as this ability identifies tumours with metastatic potential [34]. As such, new colonies of melanoma cells dramatically increase the consumption of oxygen and nutrients, eventually leading to cell starvation and hypoxia on the tumour site [35]. These increasing demands induce the development of additional vasculature in order to increase blood supply, triggering angiogenesis [25].

1.3.1 Signalling pathways involved in melanoma progression

Disruption in crucial signalling pathways that regulate normal melanocyte function is strongly linked to melanoma development and progression [36,37]. Several signalling pathways were found to be constitutively activated in melanoma. Among them, the mitogen-activated protein kinase (MAPK) and phosphoinositide 3-kinase (PI3K)-AKT signalling pathways are activated in melanoma and appear to play major roles in cell proliferation, melanoma development and its progression [38]. Both were found to be constitutively activated in most melanomas [4,39]. Moreover, intrinsic resistance to apoptosis is also involved in the regulation of melanoma progression [40].

1.3.1.1 Mitogen-activated protein kinase pathway

Aberrant MAPK pathway [Ras–Raf–mitogen-activated protein kinase kinase (MEK)–extracellular signal-regulated kinase (ERK)] activation is being implicated in the regulation of cancer, namely cellular proliferation, differentiation, and survival [41]. Briefly, stimulation of Ras causes activation of Raf, which then phosphorilates MEK, leading to activation of ERK (Figure 3).

Activation of the MAPK pathway is a frequent and early event in melanoma development [42]. During the process of malignant transformation, melanocytes acquire the ability to secrete autocrine and paracrine growth factors [43]. Many of these factors

contribute to the increased ERK activity in melanoma through direct activation of the Ras-Raf pathway [39]. Moreover, this activation may also occur *via* phospholipase C (PLC)-protein kinase C (PKC) (Figure 3), since PKC can induce direct activation of Raf, triggering MEK1/2 cascade activation (reviewed in [44]). In addition, the ERK1/2 activation involved in cellular proliferation was also reported to be dependent of G protein-PKC-MEK1/2 signalling [45].

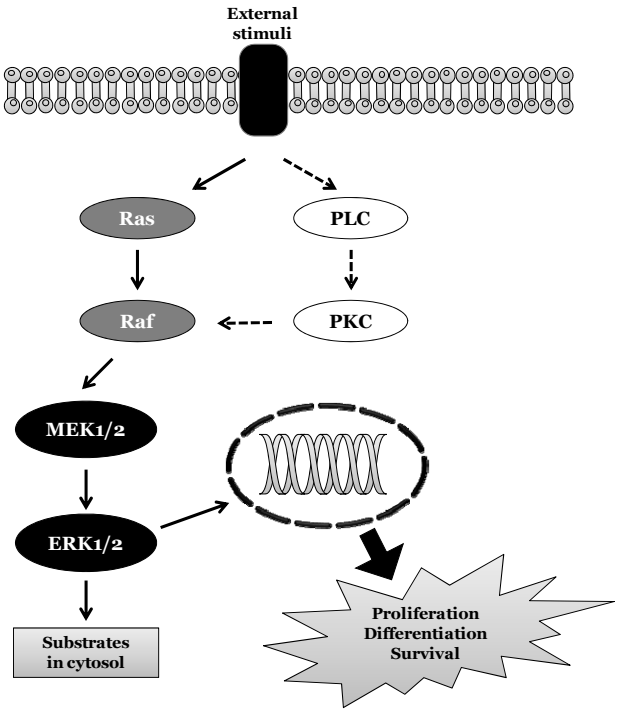

Figure 3. Schematic representation of the MAPK (Ras-Raf-MEK1/2-ERK1/2) signalling pathway in melanoma cells. An extracellular factor interacts with its receptor and induces activation of Ras which in turns phosphorilates Raf. Activated Raf then phosphorylates and activates MEK1/2 which phosphorylates and activates ERK1/2. Nevertheless, extracellular factors may also activate PLC-PKC (through a G protein-mediated effect) which can also activate MEK1/2. Activated ERK1/2 has substrates in the cytosol but can also enter the nucleus and regulate gene expression.

Mutations of N-Ras or B-Raf, autocrine and paracrine growth factors, and adhesion receptor activation represent some of the multiple mechanisms through which Ras-Raf-MEK-ERK signalling pathway is activated in melanoma [39]. Extracellular signals generated through the interaction of ligand-receptor are transmitted to the interior of melanoma cells, activating downstream signalling cascades (Figure 3). Finally, ERK1/2 either phosphorylates cytoplasmic targets or migrates to the nucleus, where it phosphorylates and activates several transcription factors, such as c-Fos or Elk-1 [46].

Evidence indicates that MEK1/2 inhibitors can block ERK activity of human melanoma cell lines, leading to melanoma cell cycle arrest [47]. Therefore, the MAPK pathway seems essential for cellular proliferation.

1.3.1.2 Phosphatidylinositol-3-kinase pathway

Constitutive activation of the PI3K-AKT pathway can trigger a cascade of responses, going from cell growth and proliferation to survival and motility [48]. Briefly, PI3K is activated by receptor protein tyrosine kinases or receptors coupled with G proteins. The substrate for class I PI3K is phosphatidylinositol-4,5-biphosphate, leading to the production of phosphatidylinositol-3,4,5-triphosphate (PIP3). Then, PIP3 recruits signalling proteins, namely AKT (also named protein kinase B) inducing conformational changes. Active AKT translocates to the nucleus, mediates the activation and inhibition of several targets, leading to cellular survival and proliferation [39] (Figure 4).

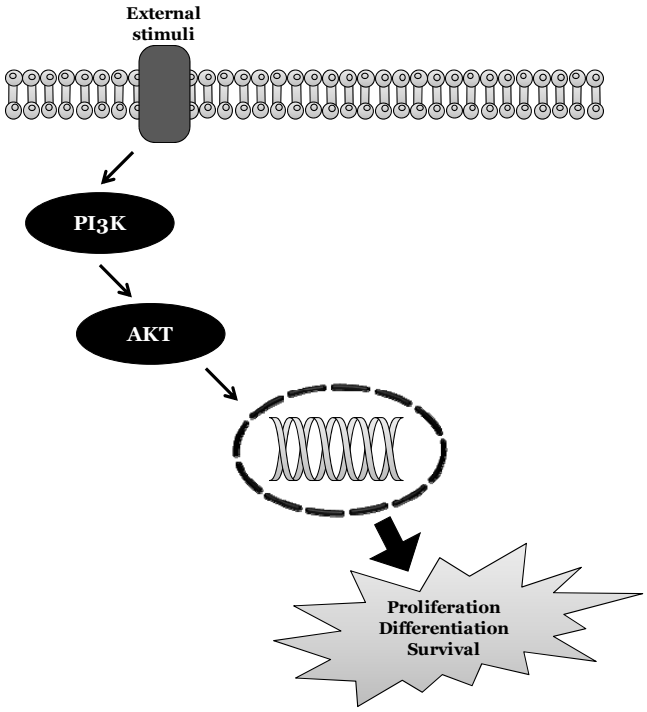

Figure 4. Schematic representation of the PI3K-AKT signalling pathway in melanoma cells. Extracellular signals after interaction of ligand-receptor are transmitted to the interior of the melanoma cells, that activate PI3K, leading to phosphorylation of AKT. Finally, AKT migrates to the nucleus where it mediates the activation and/or inhibition of several targets. This results in cellular survival, proliferation, and differentiation, promoting melanoma progression.

Although in melanoma PI3K itself is rarely mutated [49] or overexpressed [50], activation of downstream signalling components, namely AKT, have been implicated in melanoma progression [51]. As such, interaction of extracellular signals with the respective receptor is transmitted to the interior of melanoma cells, activating downstream cascades [39]. This will lead to the activation of AKT which is crucial for melanoma progression, through regulation of adhesion molecules [39] (Figure 4). Constitutive activation of AKT was observed in melanoma cell lines and melanoma samples in different progression stages [52]. Moreover, increased phospho-AKT expression is also associated with melanoma progression and worst patient prognosis [53].

1.3.1.3 Apoptosis dysregulation

Several studies reported that melanoma cells have low levels of spontaneous apoptosis comparatively to other tumour cells (reviewed in [40]). Apoptotic cell death is the major underlying mechanism of therapies targeting cancer cells [54]. The two major apoptotic pathways, the intrinsic (or mitochondrial) and extrinsic (or death receptor) pathways [55] are targets to aberrant pro-survival signalling, which are implicated in melanoma resistance to anticancer therapies [56].

Briefly, the intrinsic pathway of apoptosis involves the permeabilization of the outer mitochondrial membrane through cooperation of proapoptotic proteins (such as Bax, Bak) [57], leading to the release of apoptogenic proteins into the cytosol, namely cytochrome c [58]. Once cytochrome c is released it binds to Apaf-1, inducing the formation of the apoptosome complex that recruits the initiator caspase 9. This caspase is then activated, leading to the activation of executioner caspases, such as caspase 3, causing DNA fragmentation [59] (Figure 5). On the other hand, the extrinsic pathway involves the activation of membrane death receptors [60]. Upon activation of these receptors, caspase 8 is recruited and activated, leading to direct cleavage of downstream executioner caspases, including caspase 3 [61] (Figure 5).

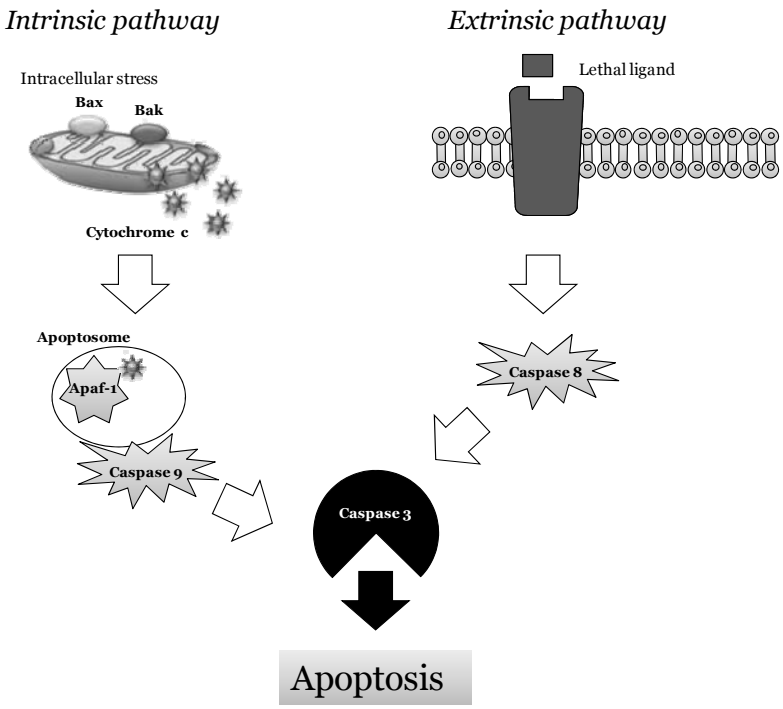

Figure 5. Schematic representation of the two main molecular pathways leading to apoptosis. In the intrinsic pathway, the release of cytochrome c from the mitochondria results in the formation of the apoptosome and activation of caspase 9. In the extrinsic pathway upon ligand binding to specific receptors, caspase 8 is activated. Caspase 8 and 9 (initiator caspases) then activate downstream caspases such as caspase 3, resulting in cell death.

Apoptosis can also be caspase-independent, mostly involving the translocation to the nucleus of the mitochondrial protein, apoptosis inducing factor (AIF) [55]. Caspase-dependent and/or independent processes result in apoptosis and occurrence of morphological features, which include cell shrinkage, nuclear fragmentation, and membrane blebbing phenotype [62].

In melanoma, apoptotic events are blocked by the overexpression or over-activation of pro-survival proteins, such as Bcl-2, Mcl-1, Bcl-XL, and inhibitors of apoptosis (IAP), namely XIAP and cIAP1 [63]. In fact, the inability of induce apoptosis following genetic errors is one of the main features for cancer progression. Moreover, failure to activate apoptotic pathways, in response to drug treatment, may explain the observed resistance of melanoma to anticancer therapies [64]. Alternative strategies to overcome resistance in melanoma cells and, therefore, improve melanoma therapy can be the targeting of those overexpressed/over-activated pro-survival proteins or the exploring of non-apoptotic cell death mechanisms.

1.4 Therapies for metastatic melanoma

Metastatic melanoma is highly resistant to chemotherapy, radiotherapy, hormonal therapy and immunotherapeutic approaches (reviewed in [65]). In the last few decades, overall survival has improved slightly, mainly due to earlier diagnosis. Nevertheless, no significant impact on remission of patients with metastatic melanoma has been made despite improvements in response rates achieved with new drugs or new combinations of drugs [66].

Dacarbazine is one of the most effective chemotherapeutic agents for metastatic melanoma and remains the classical mono-chemotherapeutic regimen used for the deadliest form of skin cancer [66]. This alkylating DNA agent is used as a single agent and showed an approximately 20% response rate [67]. Although it has low activity in monotherapy, intravenous dacarbazine has remained the basis for many chemotherapeutic combinations [68], including with cisplatin and tubular toxins. However, these combinations had limited impact on overall survival with increased toxicity [69].

Anti-microtubular agents, such as paclitaxel (PXT; natural product-based taxane) that act through stabilisation of polymerised microtubules, have been reported to have modest activity in patients with metastatic melanoma (16.4% response rate) but comparable with that of dacarbazine, cisplatin, or interleukin-2 (IL-2) [70]. However, a combination of PXT and tamoxifen demonstrated an overall response rate of 24% in phase II trial [71]. Interestingly, a phase I/II trial of sorafenib (non-selective B-Raf inhibitor) administered in combination with carboplatin and PXT demonstrated preliminary antitumor activity in metastatic melanoma with a favorable safety profile [72]. Moreover, PXT is currently used on a phase II trial in combination with carboplatin and axitinib, a selective second-generation inhibitor of vascular endothelial growth factor (VEGF) receptors, on metastatic melanoma patients. However, final data is not yet published (Clinicaltrials.gov identifier: NCT01174238).

High dose IL-2, an immunodulatory agent, seems to benefit some patients with metastatic melanoma, presenting an overall response of 16%, with complete and partial responses rates of 6% and 10%, respectively [73]. IL-2 mediates its effects by binding to IL-2 receptors, which are expressed by lymphocytes, the cells that are responsible for immunity. Unfortunately, these more effective rates were found to be also associated with greater toxicities [74].

Ipilimumab, a monoclonal antibody that blocks cytotoxic T lymphocyte-associated antigen-4, being a negative regulator of T-cells [75], has recently been approved as a single agent therapy for the treatment of late stage melanoma. With the approval of ipilimumab,

the role of high dose IL-2 remains in question. While the clinical benefit of high dose IL-2 is roughly similar to ipilimumab, the toxicity is worse and tolerability is less [76]. Nevertheless, ipilimumab has relatively modest overall survival improvement, and toxicities associated to this therapy can be severe, long-lasting, or both, although most are reversible with appropriate treatment [75].

Considering the overall low efficacy of the drugs presented, novel therapies that target specific alterations associated with melanoma are being tested for the treatment of metastatic melanoma patients [77]. As described previously, one altered pathway in melanoma is the MAPK signalling pathway, with mutations in N-Ras and B-Raf being essential for tumour growth and maintenance [39]. In fact, tipifarnib (R115777), a Ras inhibitor, has shown to have anti-tumour effects in both human cell cultures and *in vivo* model of melanoma [78]. However, tipifarnib never reached clinical trials as a single-agent and when in combination with the sorafenib (non-selective B-Raf inhibitor), this combination did not significant improve sorafenib efficacy [79].

The selective B-Raf inhibitors, vemurafenib and dabrafenib, demonstrated an impressive single agent activities against melanoma, in clinical trials [80,81]. However, both also showed development of squamous cell carcinomas as side effects [80,81]. Patients become resistant to the B-Raf inhibitor treatment, which was attributed to reactivation of the MAPK pathway and enhanced tumour growth through c-Raf [82]. Therefore, combination therapy with MEK inhibitors may be most adequate, as all isoforms of both Ras and Raf signal through MEK, leading to complete inhibition of the MAPK pathway. Phase I and II trials of a combined treatment with dabrafenib and trametinib (a selective MEK inhibitor) have shown increased progression free survival but without significant reduction in the appearance of squamous cell carcinoma [83].

Other molecular targets, which are being investigated as possible therapeutic strategies for melanoma, include inhibitors of the PI3K pathway. However, the dual PI3K/mammalian target of rapamycin (mTOR) inhibitor, PI-103, promoted immunosuppression, *in vivo* tumour growth and increases in survival of sorafenib-treated melanoma cells [84], while sorafenib in combination with temsirolimus (mTOR inhibitor), tested in a phase II trial, demonstrated that this combination did not show sufficient activity to justify its further use [79].

Limited efficacy of the presented therapies and their increased toxicities emphasize, therefore, the importance of developing novel treatment strategies and redirect investigations towards new targets. Understanding and overcoming resistance pathways, combining current and future agents, identifying biomarkers to improve patient selection, and discovering future therapeutic targets will hopefully lead to further advances in treatment.

2. ADENOSINE

The purine nucleoside adenosine (ADO) is a structural element of nucleic acids and has a central role in the energy metabolism of all living organisms. This nucleoside is considered a major local regulator of tissue function through the activation of adenosine receptors (AR), especially when energy supply cannot fulfil cellular energy demand [85]. Moreover, several studies highlight a crucial role for ADO signalling in regulating several processes of cancer development [86].

Intracellular ADO is produced either by breakdown of adenosine monophosphate (AMP) promoted by the enzyme 5' nucleotidase (5'NTase), or by the hydrolysis of S-adenosylhomocysteine (SAH) [87] (Figure 6). Extracellular ADO is formed by AMP hydrolysis catalysed by ecto-5' nucleotidase (ecto-5'NTase) [88]. Nevertheless, levels of this nucleoside may also be regulated by nucleoside transporters (NT) [89], which rapidly transport ADO into/out of the cell [89] (Figure 6). Metabolism of ADO by phosphorylation (forming AMP) or degradation into inosine (INO) is catalysed by adenosine kinase (AK) and adenosine deaminase (ADA), respectively [90] (Figure 6).

Physiological concentrations of ADO in body fluids are minimal, ranging from 20-200 nM [91], and are dependent of body energy consumption. Therefore, is not surprising that under metabolic stress conditions, such as hypoxia and ischemia, where breakdown of adenosine triphosphate (ATP) is enhanced, ADO extracellular levels can reach concentrations as high as 30 μM [91]. The concentration of the ADO metabolite, INO, follows the fluctuations of ADO levels, resulting in similar levels of ADO and INO [92]. Nevertheless, INO can also be independently formed by direct hydrolysis of inosine monophosphate (IMP) (Figure 5), being able to bind to AR and initiate intracellular signalling events or affect cell function via receptor-independent pathways [93].

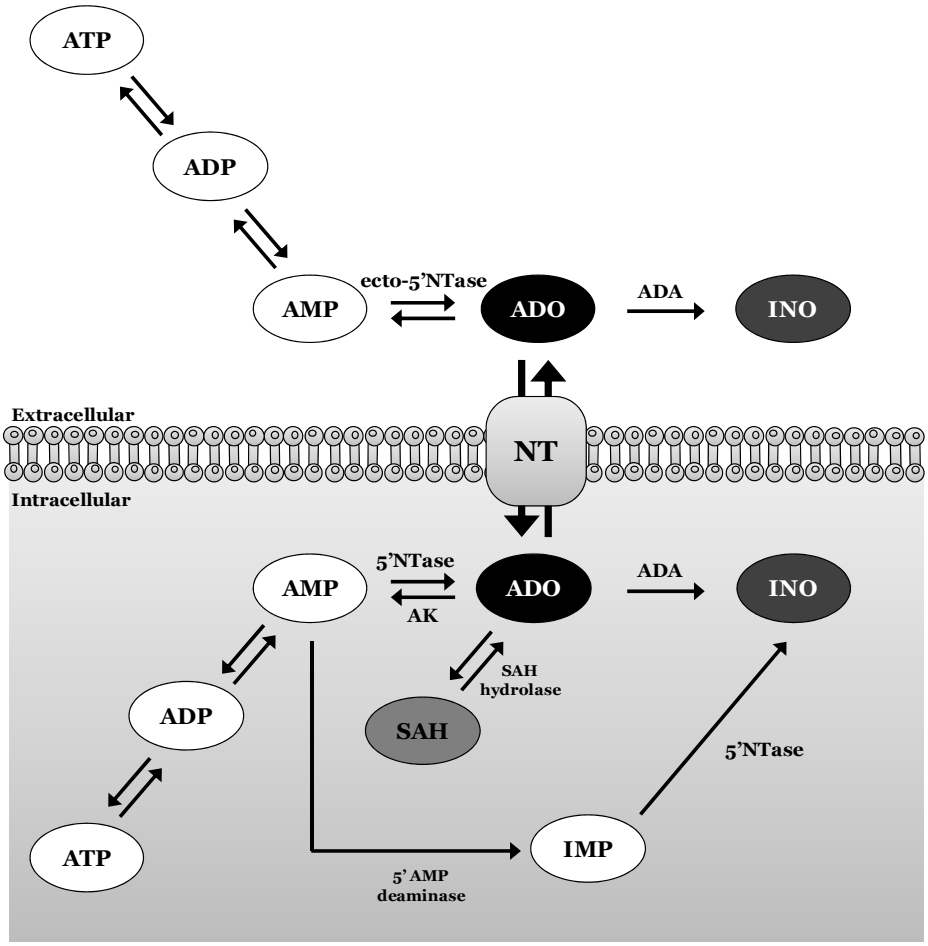

Figure 6. Schematic summary of the regulation of intra- and extracellular levels of adenosine (ADO) and inosine (INO). Within the cell, ADO is continually recycled depending on energy requirements through dephosphorylation and phosphorylation steps mediated by 5′-nucleotidase (5′NTase) and adenosine kinase (AK), respectively. ADO can also be generated after the hydrolysis of S-adenosylhomocysteine (SAH). Levels of this nucleoside may also be regulated by nucleoside transporters (NT), which rapidly transport ADO *via* facilitated diffusion into/out of the cell. Excess ADO may also be irreversibly deamidated to INO by the enzyme adenosine deaminase (ADA). Hydrolysis of inosine monophosphate (IMP) is another source of INO.

2.1 Adenosine receptors

The cellular effects of ADO are mediated through activation of a family of four G-protein-coupled AR, named A_1, A_{2A}, A_{2B}, and A_3 [94]. These receptors, also termed P1 receptors, are seven transmembrane glycoproteins that differ in their affinity for ADO, in the G proteins recruited, and finally in the activation of downstream signalling pathways of target cells (Figure 7). The A_1 and A_{2A} display high affinity for ADO while the A_{2B} and A_3 show low affinity for this nucleoside [95]. The A_1AR and A_3AR, coupled to G_i proteins, inhibit the enzyme adenylyl cyclase (AC), thereby decreasing the levels of intracellular

cyclic AMP (cAMP) [94]. However, they also activate other intracellular signal transducers, such as PKC, PI3K, and ERK1/2 [96]. Additionally, A_3AR is also able to signal through the PLC pathway *via* G_q proteins [97]. The A_{2A}AR and A_{2B}AR, coupled to G_s proteins, activate AC, leading to the increase of cAMP levels. This increase results in the activation of protein kinase A (PKA) pathway [94]. Moreover, A_{2A}AR has been described to activate G protein-independent pathways [98] and A_{2B}AR is also able to couple G_q, as well as to activate other pathways, such as MAPK and PI3K [96] (Figure 7). Accordingly, MAPK and PI3K signalling and hence cell proliferation might be amenable to manipulation through specific AR in tumour cells. For a review see [99].

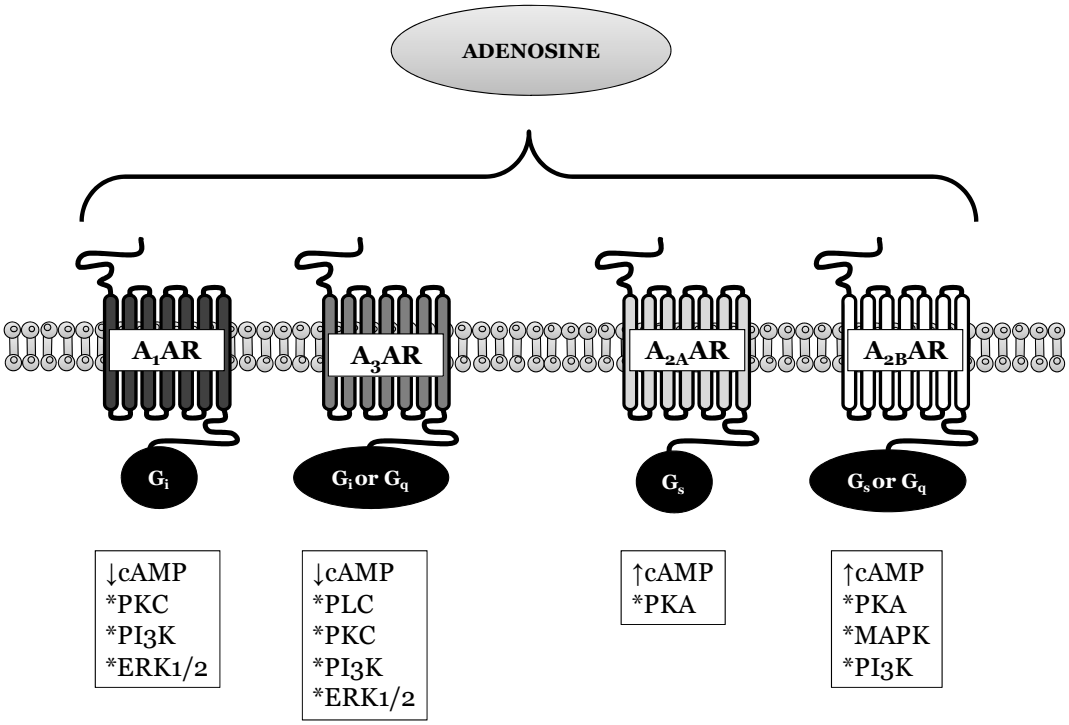

Figure 7. Schematic representation of the four AR subtypes (A_1, A_{2A}, A_{2B}, and A_3), coupling to G proteins, and respective downstream signalling pathways (*:activation; ↑:increase; and ↓:decrease).

2.2 Adenosine receptors and cancer

The effects of extracellular ADO are pleiotropic, being the cellular response to this nucleoside dependent on the expression of the different AR subtypes on each tissue. They can be co-expressed in the same cell, activating different signal transduction pathways. AR have been actively studied as potential therapeutic targets in several disorders, including cancer (reviewed in [86]).

Increasing evidence indicates that ADO, the end product of ATP hydrolysis, is an autocrine and paracrine regulatory factor that can rapidly increase its concentration in response to pathophysiological conditions, and therefore may accumulate in the tumour microenvironment [100,101]. Indeed, alterations in purine metabolism that facilitate ADO production, contribute to tumour development and progression [102]. Moreover, increased levels of ADO also contribute to angiogenesis that is essential for tumour growth [103]. ADO may regulate tumour growth through both receptor-mediated and receptor-independent pathways [104]. Extracellular ADO acts mainly through the activation of AR, and it is considered a full agonist for all AR [101]. Moreover, reduction of extracellular levels of ADO, by an increase in ADA activity, has been also suggested to reduce tumour promotion or progression [105]. On the contrary, studies reported that levels of ADA are increased in serum of patients with cancer [106]. Nevertheless, ADO also showed growth-inhibitory effects, and anti-apoptotic or even pro-apoptotic effects, depending on the tumour type (reviewed in [101]), suggesting that the activation of AR subtypes involved in tumour progression remains largely unknown. Although both *in vitro* studies and animal models have confirmed that targeting AR has tremendous potential for treating cancers [100], the translation into clinical practice will require a more thorough understanding of how ADO and AR regulate cancer.

2.2.1 A_3AR and melanoma

The research results to date indicate that in melanoma, activation of A_3AR showed to have an important role in controlling melanoma growth, showing also that only two studies report the involvement A_{2A}AR in murine melanoma cells, through the use of antagonists (reviewed in [100]).

Targeting A_3AR, by ADO or synthetic agonists, has been described to cause differential effects on tumour or on normal cells, inhibiting cell growth of various tumour types such as melanoma while favours normal cells development [107]. Primary and metastatic tumour tissues were found to express high A_3AR levels [108]. Interestingly, expression of A_3AR was found to be low in most body tissues, while it is highly expressed in tumour cell lines [109-111], thus suggesting A_3AR as a potential target for tumour growth inhibition.

Expression and pharmacological characterization of A_1, A_{2A}, A_{2B} and A_3 receptor subtypes were described on human melanoma cells, for the first time, in A375 cells, showing that A_1 and A_3 messenger RNAs (mRNAs) were less expressed than A_{2A} and A_{2B} mRNAs [109]. The ability of IB-MECA, a selective A_3AR agonist, to decrease levels of PKA,

a downstream effector of cAMP, and AKT, leading to cell growth suppression, was described in mouse B16-F10 melanoma cells [112]. Moreover, activation of A_3AR by IB-MECA in mice melanoma tumours inhibited PKA and AKT signalling proteins, which resulted in tumour growth suppression [113]. The ADO analogue, cordycepin (3'-deoxyadenosine) was also able to inhibit the growth of another mouse melanoma cell line (B16-BL6), through A_3AR activation [114].

Oral administration of Cl-IB-MECA, also considered a selective A_3AR agonist, to melanoma-bearing mice, suppressed the development of melanoma lung metastases, causing synergistic anti-tumour effect when in combination with cyclophosphamide [115].

The activation of A_3AR with Cl-IB-MECA, on human A375 melanoma cells, results in PI3K-dependent phosphorylation of AKT, leading to the reduction of basal levels of ERK1/2 phosphorylation, which in turn inhibits cell proliferation [116]. However, ADO, the natural ligand, displays contradictory effects on A375 cells: it improves cell proliferation through A_3AR activation, while it may also induce apoptosis and impair cell survival *via* A_{2A}AR signalling pathway, which involves PKC and MAPK [117]. The blocking of A_3AR, using the selective A_3AR antagonist MRE3008F20, decreases VEGF secretion in melanoma cells treated with etoposide and doxorubicin, thus improving the ability of the chemotherapeutic regimen to block angiogenesis [118].

Although previous studies demonstrated that A_3AR agonists, such as IB-MECA or Cl-IB-MECA, at micromolar concentrations, induced apoptosis in different tumour cells, this was not true for all cells tested. As such, Cl-IB-MECA led to apoptosis in leukemic (30 μM) and thyroid carcinoma (≥10 μM) cells through A_3AR-independent mechanisms [119-121], suggesting the possibility that these effects are most likely dependent on the intracellular level of Cl-IB-MECA. Nevertheless, Cl-IB-MECA is currently being evaluated in clinical trials (phase I and phase II) on patients with hepatocellular carcinoma, showing good oral bioavailability with no serious drug-related adverse events nor dose-limiting toxicities [122].

B. OBJECTIVES

While primary melanoma is highly curable with surgery, patients with metastatic disease carry the worst prognosis [5]. One of the major problems of metastatic melanoma has been the lack of efficient treatments [66], which could be related to an incomplete understanding of mechanisms that regulate tumour initiation and metastatic progression. Indeed, melanoma is the most treatment-resistant human cancer [123], remaining one of the greatest challenges in oncotherapy.

It is well accepted that the limited success of most current therapeutic strategies used in metastatic melanoma is due, at least in part, to cancer cells ability in escaping apoptosis, thus leading to drug resistance [40]. Drugs that activate pathways overcoming melanoma's apoptosis resistance and inducing cell death have, therefore, great potential for melanoma therapeutic interventions. ADO is being associated to cancer development, progression and metastasis [100]. However, mechanisms involved in these processes are still poorly understood. Therefore, identifying key regulator agents involved in melanoma progression will provide a tool for development of more effective therapies to impair metastatic spread.

The overall aims of this thesis were to study the role of ADO-AR system in the complex interplay of proliferation, cell death and metastatic progression of melanoma cells, and to provide clues for the development of new therapeutic approaches, that will improve metastatic melanoma treatment.

In order to achieve these goals, the following specific objectives were pursued:

- Characterization of the AR in human and mouse melanoma cells and establishment of each receptor subtype contribution in proliferation and/or cytotoxicity in these models.
- Investigation of the effects of ADO and its metabolic degradation on melanoma cells and the mechanisms involved in these effects.
- Characterization of the metastatic potential of melanoma cells.
- Evaluation of the cytotoxic and anti-metastatic effects of the combination of Cl-IB-MECA with the chemotherapeutic agent, PXT, on melanoma cells, and clarification of the underlying mechanisms.

CHAPTER II

Experimental section

1. MANUSCRIPT I

Characterization of adenosine receptor expression in melanoma cell lines

Published in *Medimond International Proceedings*

Characterization of Adenosine Receptors in Human and Mouse Melanoma Cells

A. Falcato-Soares, C. Diniz and P.Fresco

REQUIMTE/FARMA, University of Porto – Faculty of Pharmacy, Department of Drug Sciences, Laboratory of Pharmacology (Portugal)
anafalcatosoares@gmail.com, cdiniz@ff.up.pt, pfresco@ff.up.pt

Abstract
Melanoma is one of the most aggressive malignant tumours due to its high metastasis incidence and resistance to multiple forms of treatment. It has been reported that adenosine (ADO) has tumour promoting activities mediated by adenosine receptors (ARs) activation. However, activation of A_3 adenosine receptor (A_3AR) by synthetic agonists induces inhibitory effects on melanoma cell growth.
The present work aimed at evaluating the expression of ARs in human and mouse melanoma cells and the proliferative and/or cytotoxic effects induced by ARs activation.
The presence of ARs in human A375 and C32 and mouse K1735-M2 melanoma cells was determined by immunocytochemistry. The proliferative/cytotoxic effects of ADO and selective ARs agonists were assessed using the MTT assay (A_{570}). Results showed the presence of the four ARs on melanoma cells. However, A_3AR evidenced the lowest staining pattern. CPA, CGS 21680 and Cl-IB-MECA (0.1–100 nM; 24h) did not affect cell viability of A375 and K1735-M2 cells. For C32 cells, ADO concentrations (0.1–100 μM; 24 h) promoted cell proliferation up to 117.90±2.52 (n=15; p<0.001, from control). This effect was abolished by the selective A_3AR antagonist MRS 1220 (100 nM): 96.07±2.40 (n=3). Cl-IB-MECA (0.1–100 nM) showed a proliferative effect at lower concentrations: 100 nM (1h): 14.31%±2.04 (n=18; p<0.05); 0.1 nM (24h): 29.92%±4.80 (n=22; p<0.001). The proliferative effect was abolished by MRS 1220 (100 nM). Higher concentrations of Cl-IB-MECA (30-100 μM) caused cytotoxicity in C32 cells (EC_{50}(1h)=36 μM and EC_{50}(24h)=70 μM). Cytotoxicity effects were not abolished by MRS 1220. Moreover, these effects were not time dependent (1-72h). In the presence of NBTI (10 μM), the cytotoxic effect mediated by 50 μM of Cl-IB-MECA (-38.22±2.48 n=4; p<0.001) was increased (-55.35±2.13; n=4; p<0.001). Our findings show for the first time the presence of ARs on human C32 and mouse K1735-M2 melanoma cells. A_3AR showed the lowest staining pattern. In C32 cells, cell proliferation elicited by exogenous ADO seems to be mediated by A_3AR. Nanomolar Cl-IB-MECA concentrations increases C32 cell proliferation and micromolar concentrations causes a non time-dependent cytotoxicity, not mediated by A_3AR activation. Moreover, we have gathered evidence that endogenous ADO may protect human C32 melanoma cells from the cytotoxicity induced by high concentrations of Cl-IB-MECA.

Keywords: Adenosine receptors, melanoma cells, Cl-IB-MECA, NBTI.

1. INTRODUCTION

Melanoma has been, in recent decades, one of the cancers with greatest incidence increase in the white human population worldwide [1] being the most serious skin cancer due to its high mortality rates [2]. Success of systemic therapy of melanoma has been minimal and associated with limiting toxicity, which often results in discontinuation of treatment [3]. The development of new and more effective strategies for this type of cancer is, therefore, crucial. Studies have shown that adenosine (ADO) levels are high in the tumour microenvironment. The physiological concentrations of ADO produced under such conditions are sufficient to activate ARs present in tumour cells [4]. A_3 adenosine receptor (A_3AR) has been known to be involved in several pathological processes including ischemia, inflammation, and tumorigenesis [1]. Therefore, agonists or antagonists to A_3AR have been considered as drug candidates for the treatment of various human diseases. Especially, A_3AR agonists IB-MECA and Cl-IB-MECA exhibited potent anti-tumour activity in various in vitro and in vivo models [5]. Activation of A_3 adenosine receptor (A_3AR) by synthetic agonists induces inhibitory effects on melanoma cell growth [6]. Here, we aimed at evaluating the expression of ARs in human and mouse melanoma cells and the proliferative and/or cytotoxic effects induced by ARs activation.

2. METHODOLOGY

Materials
Hoechst 33258, 3-(4,5-dimethylthiazol-2-yl)-2,5-diphenyl tetrazolium bromide (MTT), Adenosine, CGS21680, CPA and NBTI and all other chemicals employed in this study were of analytical grade and purchased from Sigma-Aldrich. Cl-IB-MECA was purchased from Tocris Bioscience. Anti-A_1, anti-A_{2A}, anti-A_{2B} and anti-A_3 were purchased from Santa Cruz Biotechnology Inc. and Alexa Fluor 488 from Invitrogen Laboratories Inc.

Cell lines and culture conditions
Human A375 melanoma cells and mouse K1735-M2 melanoma cells were gently provided by Prof. Maria Paula Marques (Unidade de Química-Física Molecular, University of Coimbra, Portugal) and Dr. Paulo Jorge Oliveira (Centro de Neurociências e Biologia Celular – CNC, University of Coimbra, Portugal), respectively. Human C32 melanoma cells were purchased from ECACC (Sigma-Aldrich). Cells were cultured in DMEM-HG medium with 10% FBS, penicillin (10000 U/mL) and streptomycin (10 mg/mL), pH 7.4. Cells were incubated at 37 ºC in a humidified atmosphere of 95% air and 5% CO_2. All experiments were performed with cells from batches at passage <50.

Adenosine Receptor Subtypes expression determined by immunocytochemistry
Cells from exponentially growing cultures were seeded in chamber slide systems (3.0×10^4 cells/cm^2), fixed in 4% paraformaldehyde for 10 min at RT and then, incubated with blocking solution of BSA (2% in PBS) for 30 min at RT. Then, cells were incubated with anti-ARs (1:300 in PBS) overnight at 4 ºC. After cell washing with PBS, incubation with Hoechst 33258 for 15 min (RT) followed by Alexa Fluor 488 (1:1000 in PBS) for 1 h (RT) was performed in the absence of light. Parallel negatives controls were also performed. Subsequently, cells were analyzed using the fluorescence microscope coupled to a digital camera.

Proliferation/Cytotoxicity assay
Cells were prepared using an initial cell density of 3.0×10^4 cells/cm^2. Twenty-four hours after cell seeding, ADO or Agonists solutions were added. Control and blank wells were incubated only with DMEM-HG. Cell viability was assessed by MTT assay (A_{570}), 24, 48 and 72 h after addition of compounds solutions. EC_{50} values were determined using the program GraphPad PRISM Software Inc (version 4.0). Results are expressed as percentage of the respective control (mean±SEM) and *n* denotes the number of experiments performed in triplicate, initiated and processed in parallel; $p<0,05$ was taken to reflect statistically significant differences (Student's *t* test).

3. RESULTS AND DISCUSSION

In the present study we have investigated, for the first time, the expression of purinergic P1 receptors in human C32 and in mouse K1735-M2 melanoma cells by immunocytochemistry (Fig. 1). Morphological results showed that all subtypes of adenosine receptors (A_1, A_{2A}, A_{2B} and A_3) are present in human C32 and A375 and in mouse K1735-M2 melanoma cells. However, we could not establish a profile for all AR subtypes in melanoma cells since the distribution of ARs was not similar in the three types of melanoma cells. Nevertheless, images showed that the A_3AR has the lowest staining pattern of all melanoma cells used in this study. This fact is in agreement with the results obtained by RT-PCR, showing that A_1 and A_3 mRNAs were less expressed then A_{2A} and A_{2B} mRNAs in human A375 melanoma cells [7]. However, A_3AR has been reported to be highly expressed in primary tumours, such as colon carcinoma, breast carcinoma, small cell lung carcinoma, pancreatic carcinoma, and melanoma [6]. This is not true for all types of cancer cells: human MCF-7 breast cancer cells appeared to be devoid of any detectable amount of ARs, whereas human MDA-MB-231 breast cancer cells only express high levels of A_{2B} receptor subtype [8].
ADO is a cell signalling molecule which binds to specific cell surface receptors and modulate intracellular signalling, resulting in the regulation of physiological processes. ADO binds and activates four AR subtypes, A_1, A_{2A}, A_{2B} and the A_3. Since most cells express different ARs and their activation may lead to opposite effects, selective synthetic agonists are used to induce specific effects on particular cell types.

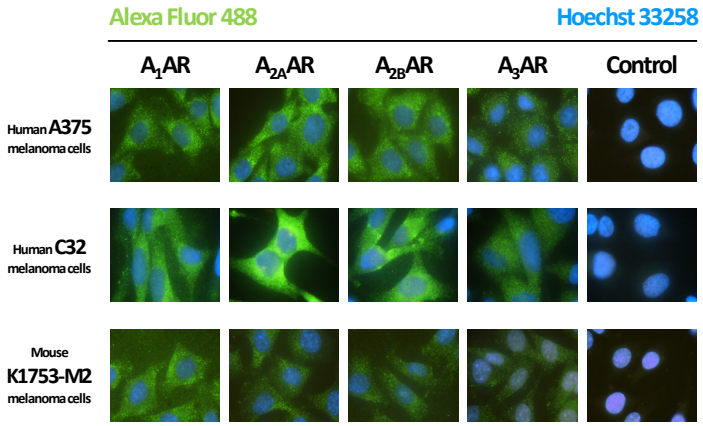

Fig. 1. Adenosine receptor subtypes (A_1AR, A_{2A}AR, A_{2B}AR and A_3AR) in human A-375 and C32 and mouse K1735-M2 melanoma cells (magnification of 1000 times - 10x from ocular lens and 100x from objective lens).

To investigate the effects caused by the activation of AR subtypes by the natural ligand (ADO) or selective agonists, cytotoxic studies were carried out on human (A375 and C32) and mouse (K1735-M2) melanoma cells and the percentage of viable cells (from control) was determined by the MTT assay.

First, we tested the effect of ADO (0.1–100 μM) on human A375 and mouse K1735-M2 melanoma cells (data not showed), after 24 h of incubation. Results showed that the natural ligand did not significantly affect cell viability, in these conditions. However, exogenous ADO promoted human C32 cell proliferation up to 117.90±2.52 (n=15; p<0.001, from control) and this effect was abolished by the selective A_3AR antagonist MRS 1220 (100 nM): 96.07±2.40 (n=3) (Fig.2). This fact suggests that activation of A_3AR by the natural ligand is responsible for human C32 melanoma cell proliferation. The same effect was reported for colon carcinoma cells [9]. Nevertheless, our results showed that this stimulatory proliferation effect is concentration-independent. Extracellular ADO could increase up to micromolar range concentrations as the result of the transport and/or diffusion of intracellular adenosine, formed from the large pools of intracellular ATP in tumour microenvironment [10]. The physiological concentrations of adenosine produced under such conditions are sufficient enough to activate ARs present on tumour cells [11]. ADO has been previously reported to induce cell proliferation, through AR activation, in human breast cancer [12] and melanoma cells [13].

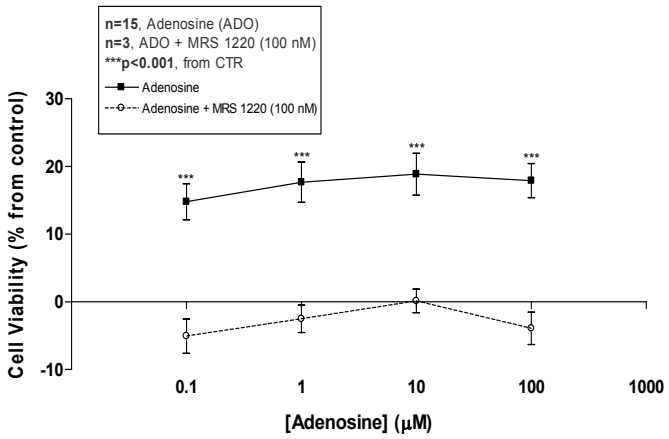

Fig. 2. Effect of increasing concentrations of ADO (0.1–100 μM) on human C32 melanoma cells, after 24h of incubation; and in the presence of a selective A_3AR antagonist, MRS 1220 (100 nM).

Thereafter, to better evaluate if ARs activation could interfere with cell proliferation and/or cell death, cells were treated with selective agonists. Increasing concentrations of CPA, CGS21680 and Cl-IB-MECA (selective A_1, A_{2A} and agonist A_3 agonists, respectively) did not cause significant effects in human A375 and mouse K1735-M2 melanoma cell viability, after 24 h of incubation (Fig. 3). The lack of a selective A_{2B} agonist did not allow us to evaluate the role of this adenosine

receptor subtype on these cell lines. For human C32 melanoma cells, CPA and CGS21680 also did not cause any effect on cell viability (data not showed).

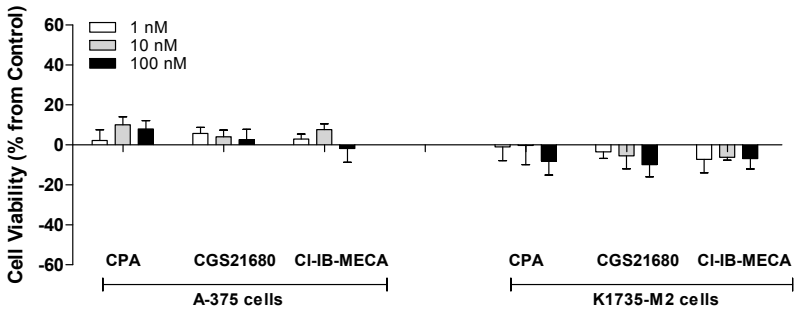

Fig. 3. Effect of increasing concentrations (1-100 nM) of CPA, CGS21680 and Cl-IB-MECA (selective A_1AR, A_{2A}AR and A_3AR agonists, respectively) on cell viability of human A-375 and mouse K1735-M2 melanoma cells, after 24 hours of incubation (n=3).

Based on the fact that ADO induced C32 cell proliferation mediated by A_3AR activation, we examined the effect of increasing concentrations of Cl-IB-MECA in these cells (Fig.4a). Concentrations of this selective A_3AR agonist in the nanomolar range (0.1-100 nM) promote cell proliferation after 24 h of incubation (0.1 nM: 29.92%±4.80 (*n*=22; *p*<0.001)). This result was also observed immediately after 1 h of incubation with the A_3AR agonist (100 nM: 14.31%±2.04 (*n*=18; *p*<0.05), data not showed). In view of the fact that Cl-IB-MECA is a synthetic nucleoside with anti-tumour activity [14] we also tested higher concentrations of Cl-IB-MECA (micromolar range) to evaluate if it causes a cytotoxic effect on C32 melanoma cells. Micromolar concentrations of Cl-IB-MECA (30-100 μM) exhibit a cytotoxic effect on human C32 melanoma cells with an EC_{50} of 36 μM (1 h of incubation, data not showed) and an EC_{50} of 70 μM after 24 h of incubation (Fig.4a). The selective A_3AR agonist, Cl-IB-MECA, showed a biphasic effect for different concentrations (proliferation/cytotoxicity) on human C32 melanoma cells (Fig.4a). The proliferative effect caused by Cl-IB-MECA was abolished by a selective A_3AR antagonist, MRS 1220 (100 nM, Fig.4b). On the contrary, cytotoxicity effects produced by Cl-IB-MECA in human C32 melanoma cells were not prevented by MRS 1220 (Fig. 4b). A similar biphasic effect of Cl-IB-MECA was also reported in human Caco2 and DLD1 colon cancer cells, after 24 h of incubation with the agonist [9]. Moreover, in astrocytoma cells, Cl-IB-MECA promotes protection against apoptosis through A_3AR activation and promotes cell death of micromolar concentrations, which is not mediated by A_3AR [15].

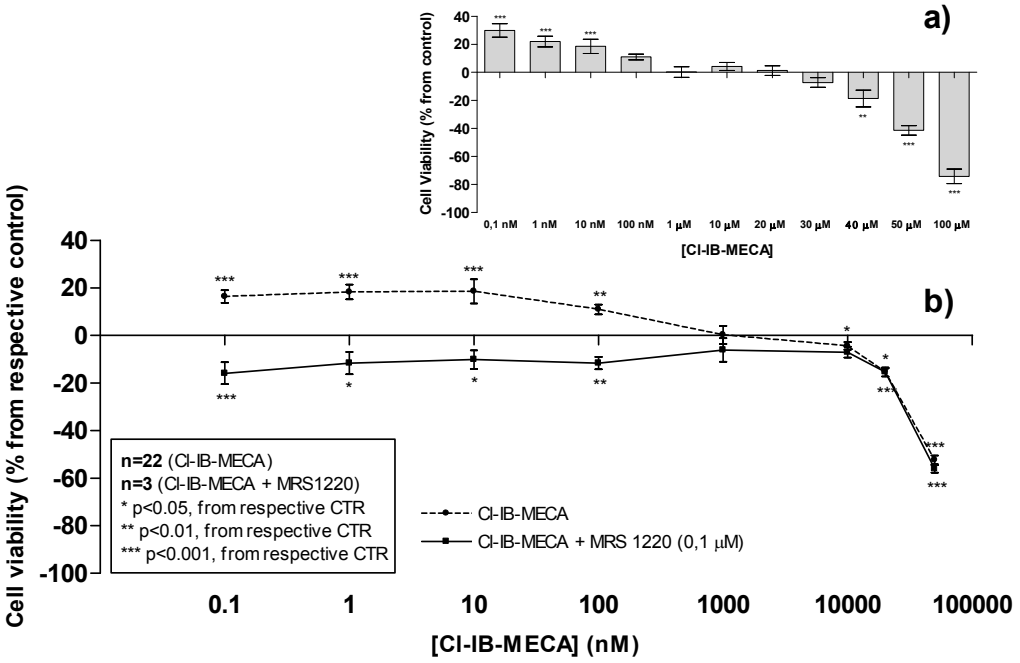

Fig. 4. Effect of increasing concentrations of Cl-IB-MECA (0,1 nM – 100 μM) in C32 cells after 24h of incubation (a) and in the presence of a selective A_3AR antagonist, MRS 1220 (100 nM (b)).

In addition, increasing concentrations of Cl-IB-MECA (5–80 μM, 24 h) in NPA cells (human papillary thyroid carcinoma) also inhibited cell proliferation, by a mechanism independent of classical adenosine receptors [16]. The different effects exhibited by nanomolar and micromolar concentrations of Cl-IB-MECA could be explained by loss of A_3AR selectivity (possible activation of other adenosine subtypes receptor) and/or A_3AR desensibilization [17].
After evaluation of the effect caused by increasing concentrations of Cl-IB-MECA on human C32 melanoma cells, we tested the dependence of a lower and intermediate EC_{50} concentrations (10 and 50 μM) over time (1h-72h, Fig.5). After each incubation time, we found that Cl-IB-MECA did not induce a time-dependent cytotoxicity. The same was true for recent selective A_3AR agonist, Thio-Cl-IB-MECA (0-100 μM), in human lung cancer cells [18].

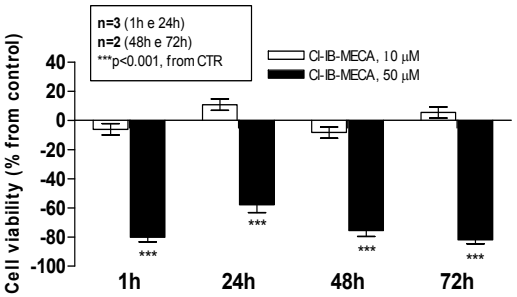

Fig. 5. Effect of Cl-IB-MECA (10 and 50 μM) on C32 cells after 1, 24, 48 and 72 h of incubation.

We also verified the possibility of Cl-IB-MECA can act intracellulary, as a second messenger, after being transported into the cells. NBTI, a nucleoside transporter inhibitor, used at a final concentration of 10 μM, which is an excess of IC_{50} values for inhibition of nucleoside transporters [19] failed to inhibit or reduce the effects of 50 μM Cl-IB-MECA (-38.22±2.48 n=4; p<0.001) (Fig. 6). This result is consistent with what was described for human NPA thyroid cancer cells: 40 μM of Cl-IB-MECA inhibited cell proliferation by neither A3AR activation nor through a nucleoside transporter-dependent mechanism [16]. On the contrary, our results reveal an increase in the cytotoxic effect caused by the addition of 10 μM of NBTI to 50 μM of Cl-IB-MECA (-55.35±2.13; n=4; p<0.001), which suggest that endogenous ADO can protect human C32 melanoma cells against cell death. Perhaps, in the presence of NBTI, endogenous ADO was unable to access the extracellular space, activate the A_3AR and promote cell proliferation.

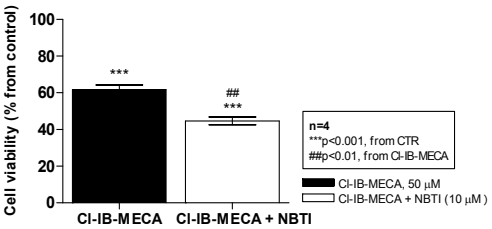

Fig. 6. Effect of Cl-IB-MECA (50 μM) on C32 cells in the presence and absence of NBTI (10 μM), after 24 h of incubation.

4. CONCLUSIONS

To our knowledge, our findings show for the first time, the presence of all four AR subtypes (A_1AR, A_{2A}AR, A_{2B}AR and A_3AR) on human C32 and mouse K1735-M2 melanoma cells. Moreover, a sparser presence of A_3R was observed in the three studied melanoma cells lines (human A375 and C32 and mouse K1735-M2 cells), when compared to the other AR subtypes. The selective AR agonists CPA (A_1AR), CGS 21680 (A_{2A}AR) and Cl-IB-MECA (A_3AR) did not affect cell viability in human A-375 and mouse K1735-M2 melanoma cells.
Human C32 melanoma cell proliferation elicited by exogenous ADO seems to be mediated by A_3AR. Nanomolar Cl-IB-MECA concentrations increased C32 cell proliferation; micromolar Cl-IB-MECA concentrations caused cytotoxicity which was neither time-dependent, nor mediated by A_3AR. Endogenous ADO may protect cells from the cytotoxicity induced by high concentrations of Cl-IB-MECA. These results further highlight the therapeutic potential of Cl-IB-MECA in melanoma.

Acknowledgements: FCT(SFRH/BD/64911/2009); This work is financed by FEDER founds through Operacional Program Competitivity– COMPETE and national funding from FCT – Fundação para a Ciência e a Tecnologia.

REFERENCES

[1] Greinert, R. (2009) Skin cancer: new markers for better prevention. Pathobiology 76, pp 64–81.

[2] Keilholz, U. (2003) Biochemotherapy of melanoma. Forum (Genova) 13, pp 158–169.

[3] Soengas, M.S. & Lowe S.W. (2003) Apoptosis and melanoma chemoresistance. Oncogene. 22, pp 3138–3151.

[4] Ohta, A. et al. (2006) A2A adenosine receptor protects tumors from antitumor T cells. PNAS. 35, pp 13132–13137.

[5] Fishman, P. et al. (2009) Adenosine Receptors and Cancer. Handbook of Experimental Pharmacology 193, pp 399–441.

[6] Madi, L. (2004) The A3 Adenosine Receptor Is Highly Expressed in Tumor versus Normal Cells: Potential Target for Tumor Growth Inhibition. Clin Cancer Res 10, pp 4472–4479.

[7] Merighi, S. et al. (2001) Pharmacological and biochemical characterization of adenosine receptors in the human malignant melanoma A375 cell line. British Journal of Pharmacology 134, pp 1215–1226.

[8] Panjehpour, M. et al. (2005) Human breast cancer cell line MDA-MB-231 expresses endogenous A2B adenosine receptors mediating a Ca2þ signal. British Journal of Pharmacology 145, pp 211–218.

[9] Gessi, S. et al. (2007) Adenosine Receptors in Colon Carcinoma Tissues and Colon Tumoral Cell Lines: Focus on the A3 Adenosine Subtype. J. Cell. Physiol. 211, pp 826–836.

[10] Sitkovsky, M.V., Ohta, A. (2005) The 'danger' sensors that STOP the immune response: the A2 adenosine receptors? Trends Immunol 26, pp 299–304.

[11] Ohta, A. et al. (2006) A2A adenosine receptor protects tumors from antitumor T cells. PNAS 103, pp 13132–13137.

[12] Panjehpour, M., Karami-Tehrani, F. (2007) Adenosine modulates cell growth in the human breast cancer cells via adenosine receptors. Oncol Res 16, pp 575–585.

[13] Merighi, S. et al. (2002) Adenosine Receptors as Mediators of Both Cell Proliferation and Cell Death of Cultured Human Melanoma Cells. J Invest Dermatol 119, pp 923–933.

[14] Fishman, P. et al. (2001) The A3 Adenosine Receptor as a New Target for Cancer Therapy and Chemoprotection. Experimental Cell Research 269, pp 230–236.

[15] Trincavelli, M.L. et al. (2002) A3 Adenosine Receptors in Human Astrocytoma Cells: Agonist-Mediated Desensitization, Internalization, and Down-Regulation. Mol Pharmacol 62, pp 1373–1384.

[16] Morello, S. et al. (2008) Cl-IB-MECA inhibits human thyroid cancer cell proliferation independently of A3 adenosine receptor activation. Cancer Biology & Therapy 7(2), pp 278-284.

[17] Klaasse, E. et al. (2008) Internalization and desensitization of adenosine receptors. Purinergic Signalling 4, pp 21–37.

[18] Kim, S.J. et al. (2008) Inhibition of cell proliferation through cell cycle arrest and apoptosis by thio-Cl-IB-MECA, a novel A3 adenosine receptor agonist, in human lung cancer cells. Cancer Letters 264, pp 309–315.

[19] Griffith, D.A., Jarvis, S.M. (1996) Nucleoside and nucleobase transport systems of mammalian cells. Biochim Biophys Acta 1286, pp 153-181.

2. MANUSCRIPT II

Inosine strongly enhances human C32 melanoma cells proliferation through PLC-PKC-MEK1/2-ERK1/2 and PI3K pathways

Manuscript submitted for publication

Title page

Inosine strongly enhances human C32 melanoma cells proliferation through PLC-PKC-MEK1/2-ERK1/2 and PI3K pathways

Ana Sofia Soares[1], Vera Marisa Costa[2], Carmen Diniz[1] and Paula Fresco[1].

Affiliations

[1]REQUI*M*TE/Laboratório de Farmacologia, Departamento de Ciências do Medicamento, Faculdade de Farmácia, Universidade do Porto, Porto, Portugal

[2]REQUI*M*TE/Laboratório de Toxicologia, Departamento de Ciências Biológicas, Faculdade de Farmácia, Universidade do Porto, Porto, Portugal

Running title: Inosine enhances C32 melanoma cells proliferation

Corresponding author:

Paula Fresco (pfresco@ff.up.pt)

Departamento de Farmacologia
Faculdade de Farmácia, Universidade do Porto, Rua de Jorge Viterbo Ferreira, 228,
4050-313 Porto, Portugal
Telephone 00351-220428609

Abstract

Malignant melanoma is the most deadly type of skin cancer. The lack of effective pharmacological approaches could be related to the incomplete understanding of the pathophysiological mechanisms involved in cell melanoma proliferation. Adenosine has growth-promoting and growth-inhibitory effects on tumour cells. We aimed to investigate effects of adenosine and its metabolic product, inosine, on human C32 melanoma cells and the signalling pathways involved.

The 3-(4,5-dimethylthiazol-2-yl)-2,5-diphenyl tetrazolium bromide (MTT) reduction and bromodeoxyuridine (BrdU) proliferation assays were used to evaluate adenosine, adenosine deaminase and inosine effects, in the absence or presence of AR, A_3AR and $P2Y_1$R antagonists; and PLC, PKC, MEK1/2, and PI3K inhibitors. ERK1/2 levels were determined using an ELISA kit. Adenosine and inosine levels were quantified using an enzyme-coupled assay.

Adenosine caused cell proliferation through AR activation. Adenosine deaminase increased inosine levels (nanomolar concentrations) on the extracellular space, in a time-dependent manner, inducing proliferation through A_3AR activation. Micromolar concentrations of inosine enhanced proliferation through A_3AR activation, causing an increase in ERK1/2 levels, and $P2Y_1$R activation via ENT-dependent mechanisms.

We propose the simultaneous activation of PLC-PKC-MEK1/2-ERK1/2 and PI3K pathways as the main mechanism responsible for the proliferative effect elicited by inosine and its significant role in melanoma cancer progression.

Keywords: Inosine, proliferation, melanoma, A_3AR, ERK1/2, PI3K.

Abbreviations

AC: adenyl cyclase

ADA: adenosine deaminase

ADO: adenosine

AK: adenosine kinase

AMP: adenosine monophosphate

AOPCP: adenosine 5′-(α,β-methylene)diphosphate

AR: adenosine receptor

ATP: adenosine triphosphate

BrdU: bromodeoxyuridine

cAMP: cyclic AMP

CD73: ecto-5'-nucleotidase

CGS 19543: 5-amino-9-chloro-2-(2-furyl)1,2,4-triazolo[1,5-*c*]quinazoline

CNTs: Na^+-dependent concentrative nucleoside transporters

CTR: control

DMSO: dimethyl sulfoxide

DMEM-HG: dulbecco's modified eagle's medium – high glucose

ENTs: Na^+-independent equilibrative nucleoside transporters

ERK: extracellular signal-regulated kinase

FBS: foetal bovine serum

H89: *N*-[2-[[3-(4-bromophenyl)-2-propenyl]amino]ethyl]-5-isoquinolinesulfonamide dihydrochloride

HRP: horseradish peroxidase

INO: inosine

ITU: 5-iodotubericidin

LY294002: 2-(4-morpholinyl)-8-phenyl-4*H*-1-benzopyran-4-one hydrochloride

MAPK: mitogen-activated protein kinase

MEK: mitogen-activated protein kinase kinase

MRE 3008F20: *N*-[2-(2-furanyl)-8-propyl-8*H*-pyrazolo[4,3-*e*][1,2,4]triazolo[1,5-*c*]pyrimidin-5-yl]-*N*'-(4-methoxyphenyl)urea

MRS 2500: N^6-methyl-(*N*)-methanocarba-2′-deoxyadenosine-3′,5-bisphosphate

MTT: 3-(4,5-dimethylthiazol-2-yl)-2,5-diphenyl tetrazolium bromide

NBTI: 6-*S*-[(4-nitrophenyl)methyl]-6-thioinosine

NT: nucleoside transporters

$P2Y_1R$: $P2Y_1$ receptor

PI3K: phosphoinositide 3-kinase

PKA: protein kinase A

PKC: protein kinase C

PLC: phospholipase C

PNP: purine nucleoside phosphorylase

RO 32-0432: 3-[(8*S*)-8-[(dimethylamino)methyl]-6,7,8,9-tetrahydropyrido[1,2-*a*]indol-10-yl]-4-(1-methyl-1*H*-indol-3-yl)-1*H*-pyrrole-2,5-dione hydrochloride

U0126: 1,4-diamino-2,3-dicyano-1,4-*bis*[2-aminophenylthio]butadiene

U73122: 1-[6-[[(17β)-3-methoxyestra-1,3,5(10)-trien-17-yl]amino]hexyl]-1*H*-pyrrole-2,5-dione

U73343: 1-[6-[[(17*β*)-3-methoxyestra-1,3,5(10)-trien-17-yl]amino]hexyl]-2,5-pyrrolidinedione

XO: xanthine oxidase

Introduction

Malignant melanoma is the most deadly type of skin cancer. Although melanoma is less common than other types of skin cancers, the incidence of cutaneous melanoma is rising faster than any other solid tumour [1], accounting for a global incidence of about 160 thousands new cases each year [2]. This increased incidence may be a consequence of more people chronically exposed to natural/artificial UV radiation and/or as a result of higher detection rates associated with enhanced public awareness [3]. While primary melanoma is highly curable with surgery, patients with metastatic disease carry the worst prognosis, with a median survival time of less than 1 year [3]. One of the major problems of metastatic melanoma has been the lack of efficient treatments [4]. The absence of an effective pharmacological approach could be, at least in part, due to an incomplete understanding of the pathophysiological mechanisms involved in melanoma cells proliferation and, ultimately, tumour initiation and progression.

Melanoma progression is associated to abnormal activation of pathways that regulate the proliferation of melanocytes [5]. Mitogen-activated protein kinase (MAPK) and phosphoinositide 3-kinase (PI3K) pathways are constitutively activated in most melanomas [2, 6].

Increasing evidence indicates that complex interactions of tumour cells with the tumour microenvironment may be related with secretory products released by these cells, which appear to be fundamental for tumourigenesis [7]. Adenosine (ADO), the end product of adenosine triphosphate (ATP) hydrolysis, is one of those trophic products, being increased in the tumour microenvironment [reviewed in [8]]. High levels of extracellular ADO are caused, at least in part, by the ecto-5'-nucleotidase (CD73), overexpressed in various types of cancer, which catalyses the hydrolysis of extracellular adenosine monophosphate (AMP) into ADO [9]. This nucleoside may then regulate the growth and development of

tumour cells through adenosine receptor (AR)-dependent and/or independent pathways [10].

Extracellular ADO acts mainly through the activation of four subtypes of AR (A_1, A_{2A}, A_{2B}, and A_3), members of the G protein-coupled receptor superfamily, and it is considered a full agonist for all AR [8]. Stimulation of A_3AR, which is upregulated in different tumours, by ADO is reported to have distinct and tumour specific actions, since ADO can have growth-promoting as well as growth-inhibitory effects, anti-apoptotic or even pro-apoptotic effects, depending on the tumour type [reviewed in [8]].

Alternatively to AR-mediated actions, ADO may be rapidly transported into the cell by nucleoside transporters (NT). Two major types of NT have been distinguished based on their mechanism of action: Na^+-dependent concentrative nucleoside transporters (CNTs), active transport; and bidirectional Na^+-independent equilibrative nucleoside transporters (ENTs), passive transport [11, 12]. Additionally, the expression of these transporters is found to be changed in certain tumours. Once inside the cell, ADO can be converted to AMP via adenosine kinase (AK) or to inosine (INO) via adenosine deaminase (ADA) [13]. Nevertheless, INO can be formed both intracellular and extracellularly, and it can also bind to AR and initiate intracellular signalling events or affect cell function via receptor-independent pathways [14].

Evidence suggests that an increase in ADA activity can cause a reduction in the concentration of ADO in the extracellular medium, thus reducing tumour promoting functions [15]. However, serum ADA has been shown to be increased in patients with bladder [16], breast [17], and lung cancer [18]. ADA serum levels in patients with melanoma were never evaluated and a full study of the effects of its metabolic product (INO) in human melanoma cells is still lacking.

The purpose of the present work was to investigate the effects of ADO and particularly of its metabolic product INO, on human C32 melanoma cells and to gather further insights into the signal transduction pathways involved. We report that INO caused cell growth mainly through the direct activation of A_3AR. Surprisingly, indirect P2Y1R activation also contributes to the INO-induced proliferative effect. Intracellularly, INO-induced proliferation is due to the simultaneous activation of PLC-PKC-MEK1/2-ERK1/2 and PI3K pathways as the molecular mechanisms able to explain the proliferative activity of INO on human C32 melanoma cells.

Materials and Methods

Chemicals

MRE 3008F20, CGS 15943, MRS 2500, and pentostatin were obtained from Tocris Bioscience (Bristol, United Kingdom). Bromodeoxyuridine (BrdU) cell proliferation assay kit and STAR ERK1/2 ELISA kit were purchased from Merck-Millipore (Interface, Amadora, Portugal). Bio-Rad RC DC protein assay kit was purchased to Biorad (Amadora, Portugal). Foetal bovine serum (FBS), Glutamax, and Trypsin/EDTA were obtained from Gibco – Invitrogen, Alfagene (Carcavelos, Portugal). Dulbecco's Modified Eagle's Medium – High Glucose (DMEM-HG), penicillin/streptomycin (10 000 U/mL; 10 mg/mL), 3-(4,5-dimethylthiazol-2-yl)-2,5-diphenyl tetrazolium bromide (MTT), dimethyl sulfoxide (DMSO), 5-iodotubericidin (ITU), adenosine 5′-(α,β-methylene)diphosphate (AOPCP), 6-*S*-[(4-Nitrophenyl)methyl]-6-thioinosine (NBTI), dipyridamole, RO 32-0432, U73343, U73122, H89, U0126, LY294002, ADA type X (EC 3.5.4.4), purine nucleoside phosphorylase (PNP; EC 2.4.2.1), xanthine oxidase (XO; EC 1.17.3.2), horseradish peroxidase (HRP; EC 1.11.1.7), Amplex Red reagent, ADO, INO, hypoxanthine, uridine, and all other chemicals were purchased from Sigma-Aldrich (Sigma-Aldrich-Química SA, Sintra, Portugal) of the highest purity available.

Melanoma cell culture

Human C32 melanoma cells obtained from ECACC - SIGMA (Sigma-Aldrich-Química SA, Sintra, Portugal) were used in this study. Cells were seeded in DMEM-HG medium with 10% of FBS, 1% of a mixture of penicillin/ streptomycin (10 000 U/mL; 10 mg/mL) and 1% of Glutamax, pH 7.4. Cells were incubated at 37 ºC in a humidified atmosphere (95% air; 5% CO_2). For cell culture maintenance, cells were grown in monolayer and sub-cultivated twice a week. Cell passaging was done by trypsinization. All experiments were

carried out with cells at 70−80% confluence and from batches with passage number lower than 50.

Cell treatment

Human C32 melanoma cells were prepared using an initial cell density of 5.0×10^4 cells/cm^2. Cells were allowed to attach for 24h and then were treated with ADA [0.3 U/mL [19]] or increasing concentrations of nucleosides (ADO or INO) for different time-points (1 – 48h), depending on the experiment performed. When antagonists [MRE 3008F20 (selective A_3AR, 10 nM [20]); CGS 15943 (non-selective AR, 100 nM [20]); MRS 2500 (selective $P2Y_1R$, 1 μM [21]] were used, these compounds were added 30 min prior to the addition of other compounds.

Experiments with ENTs inhibitors [dipyridamole and NBTI, 10 μM [22]] were performed incubating cells with these inhibitors for 1h, before the addition of other compounds (for dipyridamole), or 15 min after addition of pentostatin plus ITU (for NBTI), since NBTI also prevents pentostatin [23] and ITU [22] uptake. Simultaneous addition of uridine [300 μM [24]] with INO was performed when this substrate for ENTs and CNTs was used.

Pentostatin [ADA inhibitor, 10 nM [25]], ITU [adenosine kinase (AK) inhibitor, 100 nM [22]], AOPCP [CD73 inhibitor, 100 μM [26]], U-73122 [selective phospholipase C (PLC) inhibitor, 1 μM [27, 28]], U-73343 [selective PLC inhibitor analogue, 1 μM [27]], RO 32-0432 [selective PKC inhibitor, 1 μM [27]], H-89 [selective PKA inhibitor, 1 μM [27]], U0126 [selective MEK1/2 inhibitor, 10 μM [29, 30]] and LY294002 [potent PI3K inhibitor, 1 μM [31, 32]] were added 1h prior to the addition of other compounds.

All conditions, including vehicle (cells exposed to DMSO at maximum final concentration of 0.1% v/v) and blank (without cells) wells were initiated and processed in parallel.

MTT reduction assay

C32 cells were seeded in 96-well plates. After cell treatment, mitochondrial function was evaluated as an index of cell proliferation or cytotoxicity, since mitochondrial dehydrogenases of living cells can reduce the MTT (yellow) to formazans [33]. At the end of the incubation (48h), cells were processed as already described by us [20].

Determination of ERK1/2 levels

C32 cells were seeded in 6-well plates. After cell treatment, quantitative evaluation of ERK1/2 levels was done with the STAR ERK1/2 ELISA kit, according to the manufacturer's instructions, after 24h incubation.

Protein content determination

Protein content of cellular fractions in total cell lysates for ERK1/2 assays was determined using the Bio-Rad RC DC protein assay kit, in accordance to the manufacturer instructions. Stock solutions of bovine serum albumin were used as standards.

BrdU proliferation assay

C32 cells were seeded in 96-well plates. After cell treatment, BrdU was added to the cells 5h prior to the end of the incubation period (48h). Quantitative detection of newly synthesized DNA of actively proliferating cells was determined with the BrdU kit, according to the manufacturer's instructions.

Metabolism of ADO and INO

Cells were incubated at 37 ºC in 24-well plates in the absence and presence of ADA (0.3 U/mL). After 1h, 6h and 48h incubation, cell medium was collected, immediately heat-

inactivated (5 min at 60 ºC) and assayed for ADO and INO levels, as specified in the enzyme-coupled assay (fluorometric detection) developed by Helenius *et al.* [19]. Stock solutions of ADO, INO, and hypoxanthine were used as standards. Calibrations curves were generated for each experiment using identical coupled reactions.

Statistical analysis

Results are presented as mean ± SEM for *n* experiments. Statistical comparisons between groups were performed with One-Way ANOVA, after Shapiro-Wilk test normality evaluation. Significance was accepted at p values <0.05. The Student–Newman–Keuls *post hoc* test was used once a significant p was achieved.

Results

Micromolar concentrations of exogenous ADO causes proliferation of human C32 metastatic melanoma cells through AR activation

Cells were exposed to increasing concentrations of ADO (0.1–1000 μM) and mitochondrial functionality of these cells was evaluated at 48h (Figure 1A). A significant increase in cell proliferation, indicated by the MTT reduction assay, was already observed for the lowest ADO concentration tested (0.1 μM, $p<0.001$), when compared to vehicle. Furthermore, concentrations of ADO up to 100 μM caused a significant increase in cell proliferation ($p<0.001$), when compared to vehicle. However, this effect was not concentration-dependent. For the highest ADO concentration used (1000 μM), MTT reduction assay showed mitochondrial dysfunction ($p<0.01$, comparatively to vehicle), indicating that this concentration is cytotoxic.

To investigate whether exogenous ADO elicited proliferative/cytotoxic effects on human C32 melanoma cells through AR activation, cells were incubated with the same concentrations of ADO (0.1–1000 μM), in the presence of CGS 15943, a potent and non-selective AR antagonist, for 48h (Figure 1A). CGS 15943 completely blocked the proliferative effect caused by concentrations of ADO up to 100 μM. These results suggest that, C32 cells proliferation caused by exogenous ADO (0.1–100 μM) is mediated by AR activation. However, CGS 15943 was not able to prevent the cytotoxicity elicited by the highest ADO concentration tested (1000 μM), suggesting that the cytotoxic effects caused by millimolar concentrations of ADO, on human C32 melanoma cells, are not AR-mediated.

Increased endogenous ADO has AR-dependent proliferative effects on human C32 melanoma cells

Cells were incubated with the ADA inhibitor, pentostatin (10 nM), alone or in combination with the AK inhibitor, ITU (100 nM), in order to evaluate whether similar effects could be triggered by endogenous ADO. The proliferative ability of C32 cells was evaluated at 48h (Figure 1B). Significant increase in cell proliferation was observed for C32 cells treated with pentostatin ($p<0.001$) or ITU ($p<0.01$), when compared to vehicle. This effect was even more pronounced when cells were treated simultaneously with pentostatin and ITU ($p<0.01$, comparatively to pentostatin alone). These results confirm that when enzymes involved in ADO catabolism are inhibited, endogenous ADO levels are involved in the enhancement of cell proliferation.

In order to examine whether increased levels of endogenous ADO induces proliferation of human C32 melanoma cells by intracellular or extracellular mechanisms, cells were pre-treated with pentostatin (10 nM) and ITU (100 nM), and then incubated with the bidirectional ENT inhibitor (10 μM of NBTI), for 48h (Figure 1B). NBTI completely blocked the proliferative effect caused by the combination of pentostatin and ITU ($p<0.001$), indicating that proliferation of C32 cells is caused by extracellular ADO.

To assess whether AR activation has any relevant role in the observed cell proliferation caused by the increased levels of endogenous ADO in the extracellular space, MTT test was performed in cells pre-treated with 100 nM of CGS 15943 and incubated with pentostatin in combination with ITU. CGS 15943 completely blocked the proliferative effect caused by the extracellular accumulation of endogenous ADO ($p<0.001$, Figure 1B). Overall, results suggest that C32 cells proliferation caused by endogenous ADO is mediated by AR activation. These data are in agreement with the results obtained with exogenously added ADO.

Additionally, in order to prevent ADO production, an inhibitor of CD73 (AOPCP, 100 μM) was added, (Figure 1B). AOPCP induced cytotoxic effects on C32 cells ($p<0.001$, comparatively to vehicle), after 48h incubation, demonstrating the importance of endogenous ADO on the proliferation and survival of these cells.

Metabolic product of exogenous ADA causes human C32 melanoma cells proliferation through A_3AR activation

Effects of ADO catabolism (through the addition of ADA) and consequent increased levels of its metabolic product (INO) were studied on C32 cells. Cells were treated with pentostatin (10 nM) plus ITU (100 nM) and with ADA (0.3 U/mL) for 48h. Surprisingly, results obtained by the MTT reduction assay indicated that addition of ADA did not reduce the proliferative effect caused by increased levels of endogenous ADO, after co-incubation of pentostatin and ITU (Figure 2). The effect of ADA alone showed that degradation of endogenous ADO leads to a significant increase on C32 proliferation ($p<0.001$, comparatively to vehicle), suggesting that not only ADO but also its ADA metabolic product, INO, are able to induce proliferation of these cells.

In order to evaluate whether endogenous INO induces proliferation of human C32 melanoma cells through intracellular or extracellular mechanisms, cells were treated with ADA, in the presence of the ENT inhibitor, dipyridamole, which prevents the uptake of nucleosides. Cells were pre-treated with dipyridamole (10 μM), and then incubated with ADA for 48h. This ENT inhibitor could not prevent the cell proliferation caused by the addition of ADA (Figure 2). This result indicates that the proliferative effect induced by INO is mainly due to the extracellular accumulation of INO rather than an intracellular mechanism.

To assess whether AR activation has any relevant role in the proliferation observed by increased extracellular levels of INO, cells were pre-treated with the non-selective AR antagonist, CGS 15943 (100 nM) or the selective A_3AR antagonist, MRE 3008F20 (10 nM) after which cells were incubated with ADA for 48h. CGS 15943 completely blocked the proliferation caused by endogenous INO ($p<0.001$, Figure 2). Similar results were obtained for the selective A_3AR antagonist, MRE 3008F20 ($p<0.001$, Figure 2). Taken together, these results demonstrate that endogenously produced INO also promotes C32 cell proliferation through A_3AR activation.

Exogenous INO enhances proliferation of human C32 melanoma cells by direct A_3AR activation and indirect $P2Y_1$R activation through ENT-dependent mechanisms

To evaluate the effect of exogenous INO on C32 cells and compare with the observed effects of exogenous ADO, cells were incubated with two concentrations of INO (50 and 100 μM) for 48h (Figure 3). Results of MTT test on C32 cells treated with INO demonstrated significant cell proliferation, when compared to vehicle ($p<0.001$; Figure 3). However, this proliferative effect was not concentration-dependent. This observation is similar to the effect elicited by exogenous ADO, although exogenous INO caused a higher increment on the C32 cells proliferation percentage (in similar concentrations) than exogenous ADO on the same model and incubation period.

Since endogenously formed INO induces C32 cell proliferation by activation of A_3AR, experiments were carried out in order to determine whether exogenous INO could also mediate cell proliferation via AR-mediated mechanisms. To address this goal, cells were pre-treating with MRE 3008F20 (10 nM) or CGS 15943 (100 nM) and then incubated with INO (50 μM) for 48h. Both selective A_3AR and non-selective AR antagonists, were only able to partially and to the same extent block proliferation caused by 50 μM of INO

($p<0.001$; Figure 3). This fact suggests that, although most of the proliferation caused by exogenous INO is mediated by A_3AR activation, other mechanisms may also be involved in the INO-induced proliferative effect (at this INO concentration). As such, cells were treated with INO (50 μM) in the presence of uridine (300 μM), a substrate for ENTs and CNTs. Simultaneous addition of uridine and INO, for 48h, caused approximately 21% inhibition of proliferation of C32 cells ($p<0.05$; Figure 3), suggesting that the proliferative effect caused by INO is also nucleoside transporters (NT)-dependent. To assess whether this effect was mediated by ENTs or CNTs, cells were pre-treated with the ENTs inhibitor, dipyridamole (10 μM), and then incubated with INO (50 μM) for 48h. Dipyridamole blocked approximately 24% of C32 cells proliferation caused by the addition of INO ($p<0.05$; Figure 3), similar to the inhibition percentage elicited by uridine. These results confirmed the role of INO uptake mediated by ENTs on proliferation of C32 cells. In an attempt to clarify which possible intracellular mechanisms could be involved in the proliferative effect caused by exogenous INO, cells were also pre-treated with the selective $P2Y_1R$ antagonist (MRS 2500, 1 μM) in the presence of 50 μM of INO (Figure 3): results showed that MRS 2500 was not able to completely block the INO-induced proliferative effect ($p<0.05$), with an inhibition percentage similar to those caused by the ENT inhibitor; when cells were co-incubated with the selective A_3AR and $P2Y_1R$ antagonists, the proliferative effect elicited by INO was completely blocked. In addition, the combination of these two antagonists, in the absence of added INO, caused a significant C32 cells cytotoxicity ($p<0.05$), indicating that A_3AR and $P2Y_1R$ are constitutively activated in these melanoma cells.

Simultaneous activation of PLC-PKC-MEK-ERK and PI3K pathways are the main mechanisms responsible for the proliferative effect of exogenous INO

To get further insights on the intracellular mechanisms that cause proliferation of human C32 melanoma cells elicited by exogenous INO (50 μM), cells were pre-treated with the PKA inhibitor, H-89 (1 μM) for 48h. The proliferative effect of added INO was not blocked nor attenuated by H-89, indicating that PKA signalling pathway does not contribute to the observed proliferative effect (data not shown).

C32 cells were then incubated with 50 μM of INO in the absence or in the presence of inhibitors of PLC (U-73122), PKC (RO 32-0432), MEK1/2 (U0126) and PI3K (LY294002) to evaluate proliferation after 48h. Figure 4A showed that the proliferative effect caused by INO was significantly decreased by 1 μM of PLC inhibitor (approximately 67%), but not by its inactive analogue U-73343 (1 μM). The PKC inhibitor (1 μM) and the MEK1/2 inhibitor (10 μM) also counteracted the INO-induced proliferating effect (approximately 65% and 68%, respectively). These data suggest that PLC-PKC-MEK1/2 pathway has a significant role on INO-mediated proliferation of C32 cells. However, it was not the only pathway involved since total ablation of the effects was not achieved. Therefore, human C32 melanoma cells were incubated with INO after a pre-treatment with 1 μM of LY294002 (PI3K inhibitor). This pre-treatment attenuated (~32%) the proliferative effect (Figure 4A). When INO was tested in the presence of combinations of PLC and PI3K inhibitors (U-73122 plus LY294002) or MEK1/2 and PI3K inhibitors (U0126 plus LY294002), the proliferative effect was completely blocked, suggesting that micromolar concentration of exogenous INO caused proliferation of human C32 melanoma cells through simultaneous activation of PLC-MEK1/2 and PI3K pathways. Moreover, the inhibitors combinations tested, in the absence of added INO, caused significant C32

cellular cytotoxicity ($p<0.05$), indicating that PLC- MAPK and PI3K pathways are constitutively activated in these human melanoma cells.

To evaluate the role of ERK1/2 expression, final molecule of MEK pathway, on C32 cell proliferation induced by exogenous and endogenous INO, cells were treated with INO (50 μM) or ADA (0.3 U/mL) in the absence or in the presence of the selective A_3AR antagonist (MRE 3008F20, 10 nM), the MEK1/2 inhibitor (U0126, 10 μM) or the PI3K inhibitor (LY294002, 1 μM) for 24h. Increased levels of ERK1/2, obtained with the ELISA kit, are dependent on A_3AR and MEK1/2 activation, since only MRE 3008F20 and U0126 were able to completely block the increased levels of ERK1/2 induced by endogenous and exogenous INO (Figure 4B). Involvement of PI3K pathway on rising ERK1/2 levels was excluded because LY294002 was not able to block the increase in ERK1/2 levels (Figure 4B), thus demonstrating that PI3K activation occurs independently.

BrdU cell proliferation assay confirms the INO-induced proliferative effects on human C32 melanoma cells

The golden standard assay for cell proliferation, BrdU assay, was performed to confirm whether the results obtained by the MTT reduction assay were, in fact, representative of cell proliferation. For this purpose only conditions considered crucial were tested. Human C32 melanoma cells were pre-treated with selective A_3AR and/or $P2Y_1$R antagonists (10 nM of MRE 3008F20 and 1 μM of MRS 2500, respectively) and then incubated with INO (50 μM) for 48h. As shown in Figure 5, exogenous INO significantly enhanced C32 cells proliferation ($p<0.001$), when compared to vehicle, confirming those proliferative effects obtained using the MTT reduction assay (Figure 3). MRE 3008F20 was not able to completely block the proliferative effect caused by 50 μM of INO (approximately 77 %; Figure 5). Total prevention of this effect was only achieved when cells were pre-treated

with the combination of the A_3AR and $P2Y_1R$ antagonists, thus corroborating the results already obtained with the MTT test.

Activation of MEK1/2 in proliferation of cells induced by exogenous INO was also confirmed with the BrdU test. Cells were pre-treated with the MEK1/2 inhibitor, U0126 (10 μM) and then incubated with INO (50 μM) for 48h. Results confirm the involvement of MAPK pathway in the proliferation of C32 cells, already suggested by the MTT test (approximately 68%; Figure 4A), since MEK1/2 inhibitor was only able to partially block the INO-induced proliferative effect (approximately 72%; Figure 5).

Crucial conditions for endogenous INO (addition of ADA) already tested with the MTT test were also confirmed with the BrdU test: ADO deamination catalysed by ADA significantly enhanced C32 cells proliferation ($p<0.001$), when compared to vehicle (Figure 5). In cells pre-treated with the selective A_3AR antagonist (MRE 3008F20, 10 nM) or the MEK1/2 inhibitor (U0126, 10 μM), and then incubated with ADA (0.3 U/mL) for 48h, cell proliferation was also completely blocked ($p<0.001$; Figure 5), as in MTT test.

Exogenous ADA increases INO levels on the extracellular space in a time-dependent manner

Quantification of extracellular ADO and INO levels was performed using an enzyme-coupled assay, in order to determine the concentrations of endogenous ADO and INO present in the cellular medium with or without addition of ADA (Figure 6). Results showed that extracellular concentrations of ADO (Figure 6A) and INO (Figure 6B) were in the nanomolar range. For both vehicle and ADA conditions, ADO concentrations decreased with time (Figure 6A). For the vehicle condition, a starting concentration of 386 nM (1h) suffered an approximately 1.5-fold decrease at 6h ($p<0.001$) and an approximately 2.5-fold decrease at 48h incubation ($p<0.001$), comparatively to 1h. In cells treated with

ADA (0.3 U/mL), concentration of ADO was 308 nM (1h), followed by an approximately 4-fold decrease at 6h ($p<0.001$) and by an approximately 10-fold decrease at 48h incubation ($p<0.001$), when compared to 1h incubation. That ADO decrease was accompanied by an increase in INO levels in the extracellular space. Vehicle and ADA conditions presented significant increases in INO concentration, in a time-dependent manner (Figure 6B). An INO concentration of 91 nM was quantified on vehicle-treated cells, at 1h incubation, followed by significant increases of an approximately 1.1-fold at 6h ($p<0.01$) and by an approximately 3.5-fold at 48h ($p<0.001$). Results obtained with the medium collected from cells treated with ADA, showed significantly higher INO concentrations at all time points: after 1h incubation INO reached 142 nM, accompanied by an approximately 1.6-fold increase at 6h ($p<0.001$) and by an approximately 3-fold increase at 48h incubation ($p<0.001$).

Discussion

ADO is a ubiquitous molecule formed in almost all cells and present at increased levels in the tumour microenvironment [8]. In fact, cancer cell growth may be affected by extracellular levels of ADO, the expression of different AR subtypes, and related signalling pathways activated [34, 35]. In the present work, we demonstrated that exogenous ADO concentrations of 0.1-100 μM caused increased proliferation on human C32 melanoma cells through AR activation (Figure 1A). These ADO concentrations, that mimic concentrations found within the tumour microenvironment, were already described to induce AR-dependent proliferation on colorectal carcinoma [29, 36] and glioma [37] cells. However, ADO at millimolar concentration caused C32 cell cytotoxicity through AR-independent mechanisms (Figure 1A). Similar cytotoxic AR-independent effects were found in mouse N1E-115 neuroblastoma cells for millimolar concentrations of ADO [38]. This biphasic effect of exogenous ADO (proliferation *vs.* cytotoxicity) was also described in human colon [29] and epithelial [39] cancer cells.

Moreover, we found that addition of pentostatin and ITU (ADA and AK inhibitors, respectively) enhanced proliferation of C32 cells, probably due to an increase in endogenous ADO levels (Figure 1B). This fact is in agreement with a previous report that described an increase in ADO levels in extracellular fluids of solid carcinomas after the addition of ADA and AK inhibitors, thus preventing the degradation of ADO into INO and the formation of AMP from ADO, respectively [40]. Currently, it is known that following ADO cellular release, or after its extracellular formation, ADO diffuses to the extracellular space where it binds and activates AR [41]. Consistent with this finding, we showed that it is fundamental for the proliferative effect observed that increased levels of endogenous ADO access the extracellular space in order to activate AR-dependent cell proliferation (Figure 1B). This fact was confirmed by i) addition of NBTI (ENTs inhibitor) prevented the increase of cellular proliferation by blocking increased levels of endogenous ADO

from being released into the extracellular space through NT and ii) pre-incubation of cells with CGS 15943 (non-selective AR antagonist) blocked ADO interactions with membrane AR (Figure 1B).

Assuming that ADO promotes proliferation of cancer cells, and that AR signalling is controlled, at least in part, by extracellular levels of ADO, which are regulated by CD73 and ADA [enzymes that produce and degrade ADO, respectively [35]], we have speculated that inhibiting production of ADO (using AOPCP, a CD73 inhibitor) or promoting its degradation (adding ADA) would block the proliferative effect of C32 cells. The relative importance of these two enzymes varies from cell to cell [42]. We found that addition of AOPCP significantly reduces cell proliferation (Figure 1B), suggesting that increased levels of AMP, in contrast to ADO, have an inhibitory effect on C32 cell proliferation. Similar results obtained with AOPCP were reported in glioma [43] and breast [44] cancer cells. We also found, after adding ADA, that the metabolic product of ecto-ADA, endogenous INO, was also able to significantly induce proliferation of C32 cells (Figure 2). Although mainly cytosolic, ecto-ADA associated with CD26 (multifunctional cell membrane glycoprotein) also exists in cancer cells [45], but we added this enzyme since it has been reported that melanoma cells do not express extracellular CD26 [46], thus suggesting the lack of ecto-ADA activity in these cells. Previously, ADO (100 μM) and INO (300 μM) were reported to increase proliferation of rat kidney cells [47]. Thus, our subsequent studies were re-focused to characterize the proliferative effect of INO on C32 melanoma cells.

Approximately 430 nM (48h, Figure 6B) of endogenous INO (produced by the addition of ADA) induced significant C32 cell proliferation (Figure 2). Dipyridamole in a concentration reported to block all ENTs, thus preventing nucleoside uptake [38] did not alter cellular proliferation. Therefore, proliferation is induced by endogenous INO via

extracellular mechanisms. Moreover, pre-treated cells with CGS 15943 (non-selective AR antagonist) completely blocked the proliferative effect induced by the addition of ADA (Figure 2). The same effect was achieved when the selective A_3AR antagonist (MRE 3008F20) was used. Based on these facts, we suggest that the proliferation of C32 cells caused by increased levels of endogenous INO (ADA addition) is A_3AR-mediated. Formerly, other studies reported that when metabolism of ADO is high, INO production is increased [48, 49]. Accordingly, we found nanomolar concentrations of ADO and INO (Figure 6) and while ADO levels decreased with time, INO levels increased in a time-dependent manner. High basal levels of ADO could be justified by the presence of foetal bovine serum (FBS) in all conditions, including the vehicle, since a full composition of FBS is unknown and varies between batches [50]. In fact, FBS contains nucleotidase activity, even after serum inactivation [51], explaining the high levels of ADO found at 1h incubation in vehicle conditions.

Results involving increased levels of ADA found in some cancer patients and malignancy could be linked to our results since we found proliferative effects caused by endogenous INO (Figure 2) and by addition of ADO (Figure 1A), suggesting a relevant role of the metabolic product of ADO in cancer.

Micromolar concentrations of INO were previously described as being able to activate the A_3AR [49]. Our findings are in agreement with this possibility as we found that stimulation of the A_3AR, and not other AR subtypes, with 50 μM of INO can exert proliferative effects in our model system (Figure 3 and 5). Moreover, A_3AR-responses induced by exogenous INO were higher than AR-responses induced by exogenous ADO (Figure 1A), in similar conditions. This fact could be justified, at least in part, by the removal of a possible inhibitory effect of ADO mediated by other AR subtypes that are insensitive to INO [48]

or by the fact that some modulatory actions of extracellular ADO are mediated by INO, after ADO uptake and conversion to INO [14], thus representing a delay on the final effect. Our results indicated a major role for cell-surface A_3AR in the proliferative effects of exogenous INO, but the potential involvement of AR-independent (intracellular pathways) effects cannot be ruled out (Figure 3). We showed that CNTs could not mediate INO uptake since uridine (competing substrate for CNTs and ENTs) had an identical effect to that elicited by dipyridamole (ENTs inhibitor), both capable of nucleoside uptake inhibition [38], indicating that the proliferative effect is ENT-dependent (Figure 3). This fact was not observed for endogenous INO (Figure 2) perhaps because nanomolar concentrations of endogenous INO could only activate A_3AR, contrary to micromolar concentrations that enter the cell besides the activation of A_3AR. Although INO binds mainly to A_3AR to promote its effects, there are studies reporting that INO uptake-dependent mechanisms can also be involved [47, 52].

The selective $P2Y_1$R antagonist (MRS 2500) was able to block the INO-induced proliferative effect, with an inhibition percentage similar to that caused by the ENT inhibitor (Figure 3). The most likely interpretation of this finding, proposed in Figure 7, is that after INO uptake, INO serves as an alternative source to produce ATP [53]. Then, cells release ATP [54] which activates plasma-membrane $P2Y_1$ receptors and thereby modulates cellular function through specific signalling pathways [54, 55]. Expression of $P2Y_1$R was reported in human melanomas [56] and activation of this P2Y subtype receptor by ATP was found to induce proliferation of retinal cells [57].

Here in, we demonstrated that co-incubation of C32 cells with the selective A_3AR and P2Y1R antagonists completely prevented the proliferative effect elicited by INO (Figure 3 and 5). Moreover, the combination of these two antagonists, in the absence of added INO,

induced already a significant cytotoxicity in C32 cells, confirming the relevance of these two receptors in C32 cell survival (Figure 3 and 5).

Efforts were also made in order to disclose the intracellular pathways sustained by exogenous INO on proliferation of C32 cells. To the best of our knowledge, we showed, for the first time, that INO affected cell proliferation through PLC-PKC-MEK1/2-ERK1/2 and PI3K signalling pathways, the first being more relevant for C32 cell proliferation (Figure 4 and 7). A_3AR are known to couple to G proteins, thereby inhibiting AC and activating PLC [34]. We propose that activation of A_3AR by INO, in this melanoma cell line, is couple to activation of PLC-PKC-MEK1/2-ERK1/2 to enhance cell proliferation (Figure 7) since U73122, RO 32-0432, and U0126 (inhibitors of PLC, PKC, and MEK1/2, respectively) were able to similarly attenuate the proliferative effect induced by INO (Figure 4A) and the increasing ERK1/2 levels observed are completely dependent on MEK1/2 and A_3AR activation (both completely block the effect), excluding the involvement of other pathways, namely PI3K, on rising ERK1/2 levels (Figure 4B). Suppression of PKC-MEK-ERK pathway was already described as a possible target to metastatic melanoma treatment, in mouse melanoma cells [58] and activation of A_3AR is related to colon cancer cell proliferation through MEK-ERK [29].

We also found that PI3K activation was responsible for the remaining of C32 cell proliferation caused by INO (approximately 30%; Figure 4A) without ERK1/2 involvement. We suggest that PI3K activation is mediated by indirect activation of $P2Y_1R$ (Figure 7). As such, the decrease on the INO-induced proliferation of both LY294002 and MRS 2500 are similar (Figure 3 and Figure 4A). Previously, stimulation of P2 receptors by ATP on human U138-MG glioma [59] and breast MCF-7 [60] cells were reported to cause cell proliferation mediated by PI3K. Activation of this pathway mediated by $P2Y_1R$ was also described in retinal cells proliferation [57].

Accordingly, it seems that PLC-PKC-MEK-ERK and PI3K pathways are independent but both responsible for the final proliferative effect caused by exogenously added INO (Figure 7) since the combinations of U73122 (PLC inhibitor) with LY294002 (PI3K inhibitor) and U0126 (MEK1/2 inhibitor) with LY294002 (PI3K inhibitor) completely prevented C32 cell proliferation (Figure 4A). In fact, there was no cross-talk between ERK and PI3K pathways in proliferation of C6 glioma cells [61] and combined targeting of MEK and PI3K effector pathways was necessary to effectively inhibit NRAS mutant melanoma *in vitro* and *in vivo* [62]. Moreover, we observed that PLC-MAPK and PI3K pathways are important for C32 cell survival since the combinations tested, without INO, induced cell cytotoxicity (Figure 4A), corroborating the findings that MAPK and PI3K pathways are constitutively activated in most melanomas and these pathways are known to play critical roles on cell proliferation [2, 63].

In conclusion, we have demonstrated that INO causes proliferation of human C32 melanoma cells through A_3AR activation and an ENT-dependent mechanism, which seems to be related to indirect $P2Y_1R$ activation. PLC-PKC-MEK-ERK and PI3K activation are the signalling pathways responsible by INO-induced human C32 melanoma cell proliferation (Figure 7). According to our results, it would be reasonable to conclude that INO might have a significant role in melanoma cancer progression. Nevertheless, future studies using clinically relevant animal models are needed for a better understanding of these pathways in melanoma and what impact our discover can have on the cancer therapeutics.

Acknowledgments

Work was funded by FEDER through the Program Operational Competitiveness Factors – COMPETE and National Funds through FCT – Foundation for Science and Technology. ASS and VMC thank FCT for their PhD grant (SFRH/BD/64911/2009) and Post-doc grant (SFRH/BPD/63746/2009), respectively.

Statement of conflicts of interest

None.

References

1. MacKie RM, Hauschild A, Eggermont AM. Epidemiology of invasive cutaneous melanoma. Annals of oncology. 2009;20 Suppl 6:vi1-7.

2. Eggermont AM, Spatz A, Robert C. Cutaneous melanoma. Lancet. 2013.

3. Erdei E, Torres SM. A new understanding in the epidemiology of melanoma. Expert review of anticancer therapy. 2010;10:1811-23.

4. Bhatia S, Tykodi SS, Thompson JA. Treatment of metastatic melanoma: an overview. Oncology. 2009;23:488-96.

5. Jones V, Katiyar SK. Emerging phytochemicals for prevention of melanoma invasion. Cancer letters. 2013;335:251-8.

6. Meier F, Schittek B, Busch S, Garbe C, Smalley K, Satyamoorthy K, et al. The Ras/Raf/MEK/ERK and PI3K/AKT signaling pathways present molecular targets for the effective treatment of advanced melanoma. Front Biosci. 2005;10:2986-3001.

7. Bergamin LS, Braganhol E, Zanin RF, Edelweiss MI, Battastini AM. Ectonucleotidases in tumor cells and tumor-associated immune cells: an overview. Journal of biomedicine & biotechnology. 2012;2012:959848.

8. Burnstock G, Di Virgilio F. Purinergic signalling and cancer. Purinergic signalling. 2013.

9. Allard B, Turcotte M, Stagg J. CD73-generated adenosine: orchestrating the tumor-stroma interplay to promote cancer growth. Journal of biomedicine & biotechnology. 2012;2012:485156.

10. Ceruti S, Abbracchio MP. Adenosine signaling in glioma cells. Advances in experimental medicine and biology. 2013;986:13-30.

11. Zhang J, Visser F, King KM, Baldwin SA, Young JD, Cass CE. The role of nucleoside transporters in cancer chemotherapy with nucleoside drugs. Cancer metastasis reviews. 2007;26:85-110.

12. Leitão-Rocha A, Sousa J, Diniz C. Adenosinergic System in the Mesenteric Vessels. In: Gaze DC, editor. The Cardiovascular System - Physiology, Diagnostics and Clinical Implications: InTech; 2012.

13. Hasko G, Cronstein BN. Adenosine: an endogenous regulator of innate immunity. Trends in immunology. 2004;25:33-9.

14. Hasko G, Sitkovsky MV, Szabo C. Immunomodulatory and neuroprotective effects of inosine. Trends in pharmacological sciences. 2004;25:152-7.

15. Stagg J, Smyth MJ. Extracellular adenosine triphosphate and adenosine in cancer. Oncogene. 2010;29:5346-58.

16. Pirincci N, Gecit I, Gunes M, Yuksel MB, Kaba M, Tanik S, et al. Serum adenosine deaminase, catalase and carbonic anhydrase activities in patients with bladder cancer. Clinics. 2012;67:1443-6.

17. Aghaei M, Karami-Tehrani F, Salami S, Atri M. Adenosine deaminase activity in the serum and malignant tumors of breast cancer: the assessment of isoenzyme ADA1 and ADA2 activities. Clinical biochemistry. 2005;38:887-91.

18. Zanini D, Schmatz R, Pelinson LP, Pimentel VC, da Costa P, Cardoso AM, et al. Ectoenzymes and cholinesterase activity and biomarkers of oxidative stress in patients with lung cancer. Molecular and cellular biochemistry. 2013;374:137-48.

19. Helenius M, Jalkanen S, Yegutkin G. Enzyme-coupled assays for simultaneous detection of nanomolar ATP, ADP, AMP, adenosine, inosine and pyrophosphate concentrations in extracellular fluids. Biochimica et biophysica acta. 2012;1823:1967-75.

20. Soares AS, Costa VM, Diniz C, Fresco P. Potentiation of cytotoxicity of paclitaxel in combination with Cl-IB-MECA in human C32 metastatic melanoma cells: A new possible therapeutic strategy for melanoma. Biomedicine & pharmacotherapy. 2013;67:777-89.

21. Pinho D, Quintas C, Sardo F, Cardoso TM, Queiroz G. Purinergic modulation of norepinephrine release and uptake in rat brain cortex: contribution of glial cells. Journal of neurophysiology. 2013;110:2580-91.

22. Sinclair CJ, Powell AE, Xiong W, LaRiviere CG, Baldwin SA, Cass CE, et al. Nucleoside transporter subtype expression: effects on potency of adenosine kinase inhibitors. British journal of pharmacology. 2001;134:1037-44.

23. Fernandez-Calotti PX, Colomer D, Pastor-Anglada M. Translocation of nucleoside analogs across the plasma membrane in hematologic malignancies. Nucleosides, nucleotides & nucleic acids. 2011;30:1324-40.

24. Molina-Arcas M, Casado FJ, Pastor-Anglada M. Nucleoside transporter proteins. Current vascular pharmacology. 2009;7:426-34.

25. Niitsu N, Yamamoto-Yamaguchi Y, Kasukabe T, Okabe-Kado J, Umeda M, Honma Y. Antileukemic efficacy of 2-deoxycoformycin in monocytic leukemia cells. Blood. 2000;96:1512-6.

26. Mandapathil M, Szczepanski MJ, Szajnik M, Ren J, Lenzner DE, Jackson EK, et al. Increased ectonucleotidase expression and activity in regulatory T cells of patients with head and neck cancer. Clinical cancer research : an official journal of the American Association for Cancer Research. 2009;15:6348-57.

27. Quintas C, Fraga S, Goncalves J, Queiroz G. Opposite modulation of astroglial proliferation by adenosine 5'-O-(2-thio)-diphosphate and 2-methylthioadenosine-5'-diphosphate: mechanisms involved. Neuroscience. 2011;182:32-42.

28. Lawal AO, Ellis EM. Phospholipase C mediates cadmium-dependent apoptosis in HEK 293 cells. Basic & clinical pharmacology & toxicology. 2012;110:510-7.

29. Gessi S, Merighi S, Varani K, Cattabriga E, Benini A, Mirandola P, et al. Adenosine receptors in colon carcinoma tissues and colon tumoral cell lines: focus on the A(3) adenosine subtype. Journal of cellular physiology. 2007;211:826-36.

30. Weng SH, Tsai MS, Chiu YF, Kuo YH, Chen HJ, Lin YW. Enhancement of mitomycin C-induced cytotoxicity by curcumin results from down-regulation of MKK1/2-ERK1/2-mediated thymidine phosphorylase expression. Basic & clinical pharmacology & toxicology. 2012;110:298-306.

31. Greco S, Storelli C, Marsigliante S. Protein kinase C (PKC)-delta/-epsilon mediate the PKC/Akt-dependent phosphorylation of extracellular signal-regulated kinases 1 and 2 in MCF-7 cells stimulated by bradykinin. The Journal of endocrinology. 2006;188:79-89.

32. Li GW, Xing WJ, Bai SZ, Hao JH, Guo J, Li HZ, et al. The calcium-sensing receptor mediates hypoxia-induced proliferation of rat pulmonary artery smooth muscle cells through MEK1/ERK1,2 and PI3K pathways. Basic & clinical pharmacology & toxicology. 2011;108:185-93.

33. Mosmann T. Rapid colorimetric assay for cellular growth and survival: application to proliferation and cytotoxicity assays. Journal of immunological methods. 1983;65:55-63.

34. Fredholm BB, AP IJ, Jacobson KA, Linden J, Muller CE. International Union of Basic and Clinical Pharmacology. LXXXI. Nomenclature and classification of adenosine receptors-an update. Pharmacological reviews. 2011;63:1-34.

35. Ghiringhelli F, Bruchard M, Chalmin F, Rebe C. Production of adenosine by ectonucleotidases: a key factor in tumor immunoescape. Journal of biomedicine & biotechnology. 2012;2012:473712.

36. Mujoomdar M, Hoskin D, Blay J. Adenosine stimulation of the proliferation of colorectal carcinoma cell lines. Roles of cell density and adenosine metabolism. Biochemical pharmacology. 2003;66:1737-47.

37. Morrone FB, Jacques-Silva MC, Horn AP, Bernardi A, Schwartsmann G, Rodnight R, et al. Extracellular nucleotides and nucleosides induce proliferation and increase nucleoside transport in human glioma cell lines. Journal of neuro-oncology. 2003;64:211-8.

38. Schrier SM, van Tilburg EW, van der Meulen H, Ijzerman AP, Mulder GJ, Nagelkerke JF. Extracellular adenosine-induced apoptosis in mouse neuroblastoma cells: studies on involvement of adenosine receptors and adenosine uptake. Biochemical pharmacology. 2001;61:417-25.

39. Barry CP, Lind SE. Adenosine-mediated killing of cultured epithelial cancer cells. Cancer research. 2000;60:1887-94.

40. Blay J, White TD, Hoskin DW. The extracellular fluid of solid carcinomas contains immunosuppressive concentrations of adenosine. Cancer research. 1997;57:2602-5.

41. Fredholm BB. Adenosine receptors as drug targets. Experimental cell research. 2010;316:1284-8.

42. Hashikawa T, Hooker SW, Maj JG, Knott-Craig CJ, Takedachi M, Murakami S, et al. Regulation of adenosine receptor engagement by ecto-adenosine deaminase. FASEB journal : official publication of the Federation of American Societies for Experimental Biology. 2004;18:131-3.

43. Bavaresco L, Bernardi A, Braganhol E, Cappellari AR, Rockenbach L, Farias PF, et al. The role of ecto-5'-nucleotidase/CD73 in glioma cell line proliferation. Molecular and cellular biochemistry. 2008;319:61-8.

44. Mazurek S, Michel A, Eigenbrodt E. Effect of extracellular AMP on cell proliferation and metabolism of breast cancer cell lines with high and low glycolytic rates. Journal of Biological Chemistry. 1997;272:4941-52.

45. Gonzalez-Gronow M, Hershfield MS, Arredondo-Vega FX, Pizzo SV. Cell surface adenosine deaminase binds and stimulates plasminogen activation on 1-LN human prostate cancer cells. The Journal of biological chemistry. 2004;279:20993-8.

46. Houghton AN, Albino AP, Cordon-Cardo C, Davis LJ, Eisinger M. Cell surface antigens of human melanocytes and melanoma. Expression of adenosine deaminase binding protein is extinguished with melanocyte transformation. The Journal of experimental medicine. 1988;167:197-212.

47. Modis K, Gero D, Nagy N, Szoleczky P, Toth ZD, Szabo C. Cytoprotective effects of adenosine and inosine in an in vitro model of acute tubular necrosis. British journal of pharmacology. 2009;158:1565-78.

48. Jin X, Shepherd RK, Duling BR, Linden J. Inosine binds to A3 adenosine receptors and stimulates mast cell degranulation. The Journal of clinical investigation. 1997;100:2849-57.

49. Jacobson KA. Introduction to adenosine receptors as therapeutic targets. Handbook of experimental pharmacology. 2009:1-24.

50. Jochems CE, van der Valk JB, Stafleu FR, Baumans V. The use of fetal bovine serum: ethical or scientific problem? Alternatives to laboratory animals : ATLA. 2002;30:219-27.

51. Gendaszewska-Darmach E, Maszewska M, Zaklos M, Koziolkiewicz M. Degradation of extracellular nucleotides and their analogs in HeLa and HUVEC cell cultures. Acta biochimica Polonica. 2003;50:973-84.

52. Idzko M, Panther E, Bremer HC, Windisch W, Sorichter S, Herouy Y, et al. Inosine stimulates chemotaxis, Ca2+-transients and actin polymerization in immature human dendritic cells via a pertussis toxin-sensitive mechanism independent of adenosine receptors. Journal of cellular physiology. 2004;199:149-56.

53. Modis K, Gero D, Stangl R, Rosero O, Szijarto A, Lotz G, et al. Adenosine and inosine exert cytoprotective effects in an in vitro model of liver ischemia-reperfusion injury. International journal of molecular medicine. 2013;31:437-46.

54. Fitz JG. Regulation of cellular ATP release. Transactions of the American Clinical and Climatological Association. 2007;118:199-208.

55. Corriden R, Insel PA. Basal release of ATP: an autocrine-paracrine mechanism for cell regulation. Science signaling. 2010;3:re1.

56. White N, Ryten M, Clayton E, Butler P, Burnstock G. P2Y purinergic receptors regulate the growth of human melanomas. Cancer letters. 2005;224:81-91.

57. Ornelas IM, Ventura AL. Involvement of the PI3K/AKT pathway in ATP-induced proliferation of developing retinal cells in culture. International journal of developmental neuroscience : the official journal of the International Society for Developmental Neuroscience. 2010;28:503-11.

58. Tsubaki M, Matsuoka H, Yamamoto C, Kato C, Ogaki M, Satou T, et al. The protein kinase C inhibitor, H7, inhibits tumor cell invasion and metastasis in mouse melanoma via suppression of ERK1/2. Clinical & experimental metastasis. 2007;24:431-8.

59. Jacques-Silva MC, Bernardi A, Rodnight R, Lenz G. ERK, PKC and PI3K/Akt pathways mediate extracellular ATP and adenosine-induced proliferation of U138-MG human glioma cell line. Oncology. 2004;67:450-9.

60. Bilbao PS, Santillan G, Boland R. ATP stimulates the proliferation of MCF-7 cells through the PI3K/Akt signaling pathway. Archives of biochemistry and biophysics. 2010;499:40-8.

61. Van Kolen K, Slegers H. Integration of P2Y receptor-activated signal transduction pathways in G protein-dependent signalling networks. Purinergic signalling. 2006;2:451-69.

62. Posch C, Moslehi H, Feeney L, Green GA, Ebaee A, Feichtenschlager V, et al. Combined targeting of MEK and PI3K/mTOR effector pathways is necessary to effectively inhibit NRAS mutant melanoma in vitro and in vivo. Proceedings of the National Academy of Sciences of the United States of America. 2013;110:4015-20.

63. Meier F, Busch S, Lasithiotakis K, Kulms D, Garbe C, Maczey E, et al. Combined targeting of MAPK and AKT signalling pathways is a promising strategy for melanoma treatment. Brit J Dermatol. 2007;156:1204-13.

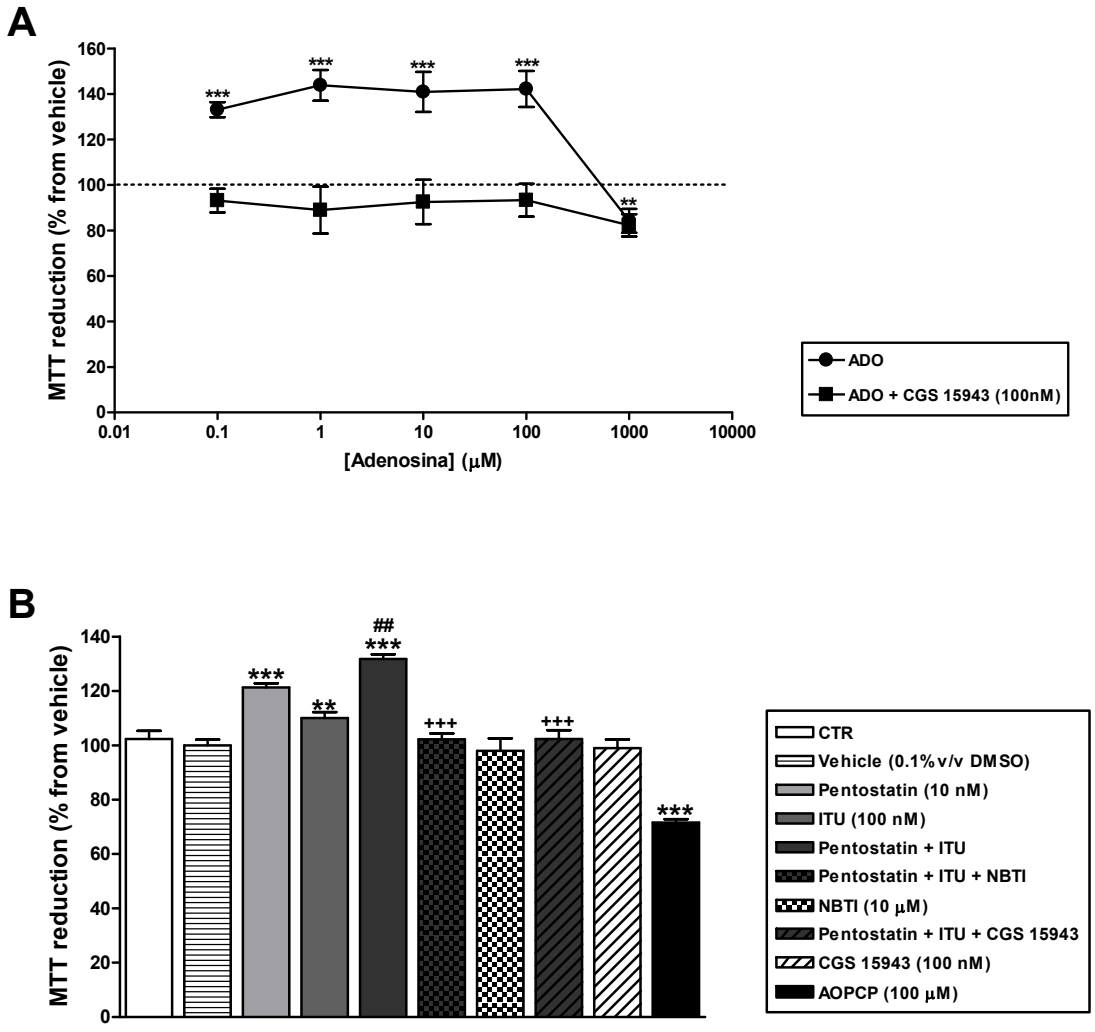

Figure 1. Effects of ADO on human C32 melanoma cells. (A) Increasing concentrations of exogenous ADO (0.1–1000 μM), in the absence (•) or presence (■) of the AR antagonist, CGS 15943 (100 nM). DMSO (final concentration of 0.1% v/v) in DMEM-HG was used as vehicle. Results presented are means ± SEM, n=12 of 4 independent experiments. MTT reduction (% from vehicle) was evaluated at 48h incubation. Significant differences (One-Way ANOVA test, followed by the Student-Newman-Keuls post-hoc test): **p<0.01 vs. vehicle; ***p<0.001 vs. vehicle. (B) Cells treated with vehicle (DMSO in DMEM-HG, final concentration of 0.1% v/v), ADA inhibitor (pentostatin, 10 nM) and AK inhibitor (ITU, 100 nM), in the absence or presence of the bidirectional ENT inhibitor (NBTI, 10 μM) or the AR antagonist (CGS 15943, 100 nM). Cells were also treated with

the CD73 inhibitor (AOPCP, 100 μM). Results presented are means ± SEM, n=12 of 4 independent experiments. MTT reduction (% from vehicle) was evaluated after 48h incubation. Significant differences (One-Way ANOVA test, followed by the Student-Newman-Keuls post-hoc test): **p<0.01 vs. vehicle; ***p<0.001 vs. vehicle; $^{\#\#}$p<0.01 vs. pentostatin; $^{+++}$p<0.001 vs. (pentostatin + ITU).

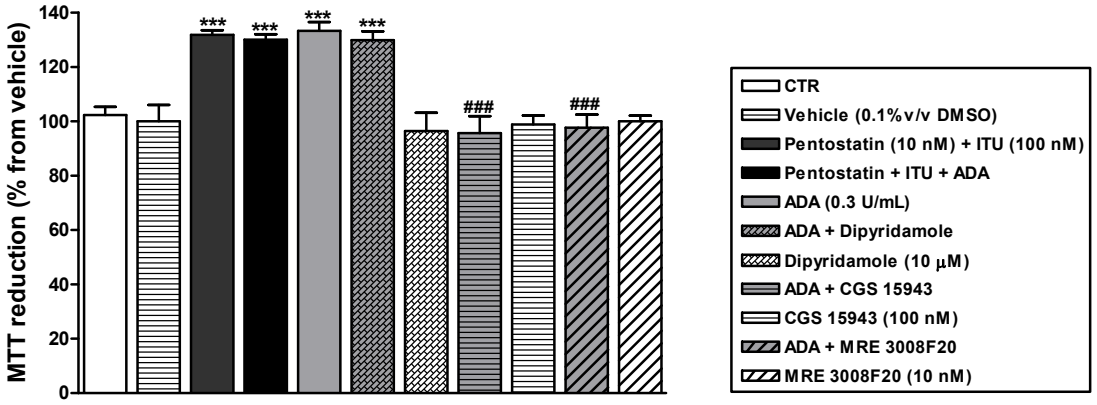

Figure 2. Addition of exogenous ADA increased INO levels which caused human C32 melanoma cells proliferation through A_3AR activation. Cells were treated with ADA (0.3 U/mL) in the absence or presence of ENT inhibitor (dipyridamole, 10 μM), non-selective AR antagonist (CGS 15943, 100 nM), and selective A_3AR antagonist (MRE 3008F20, 10 nM). DMSO (final concentration of 0.1% v/v) in DMEM-HG was used as vehicle. Results presented are means ± SEM, n=12 of 4 independent experiments. MTT reduction (% from vehicle) was evaluated at 48h incubation. Significant differences (One-Way ANOVA test, followed by the Student-Newman-Keuls post-hoc test): ***$p<0.001$ vs. vehicle; $^{###}p<0.001$ vs. ADA.

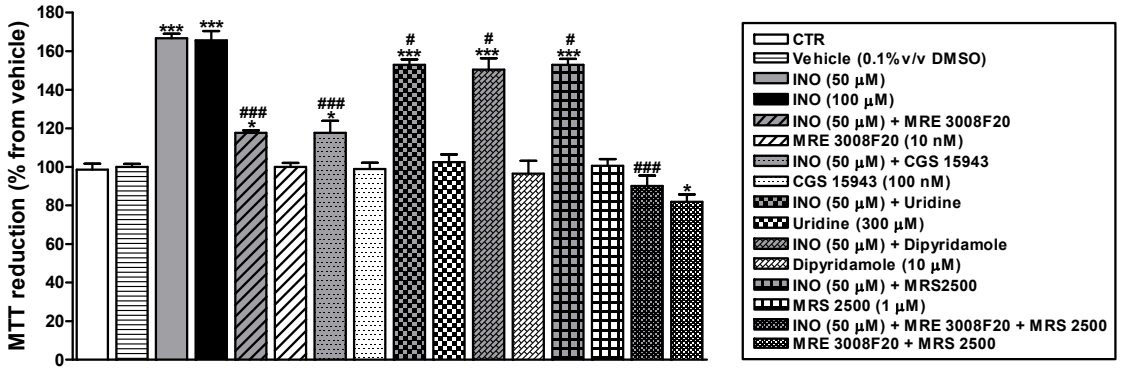

Figure 3. Exogenous INO (50 and 100 μM) enhanced human C32 melanoma cells proliferation through A_3AR direct activation and indirect $P2Y_1$R activation triggered by an intracellular mechanism. For the lowest INO concentration (50 μM), cells were incubated in the absence or presence of selective A_3AR antagonist (MRE 3008F20, 10 nM), non-selective AR antagonist (CGS 15943, 100 nM), substrate for ENTs and CNTs (uridine, 300 μM), ENT inhibitor (dipyridamole, 10 μM), and selective $P2Y_1$R antagonist (MRS 2500, 1 μM). DMSO (final concentration of 0.1% v/v) in DMEM-HG was used as vehicle. Results presented are means ± SEM, n=12 of 4 independent experiments. MTT reduction (% from vehicle) was evaluated at 48h incubation. Significant differences (One-Way ANOVA test, followed by the Student-Newman-Keuls post-hoc test): *$p<0.05$ vs. vehicle; ***$p<0.001$ vs. vehicle; $^{\#}p<0.05$ vs. INO (50 μM); $^{\#\#\#}p<0.001$ vs. INO (50 μM).

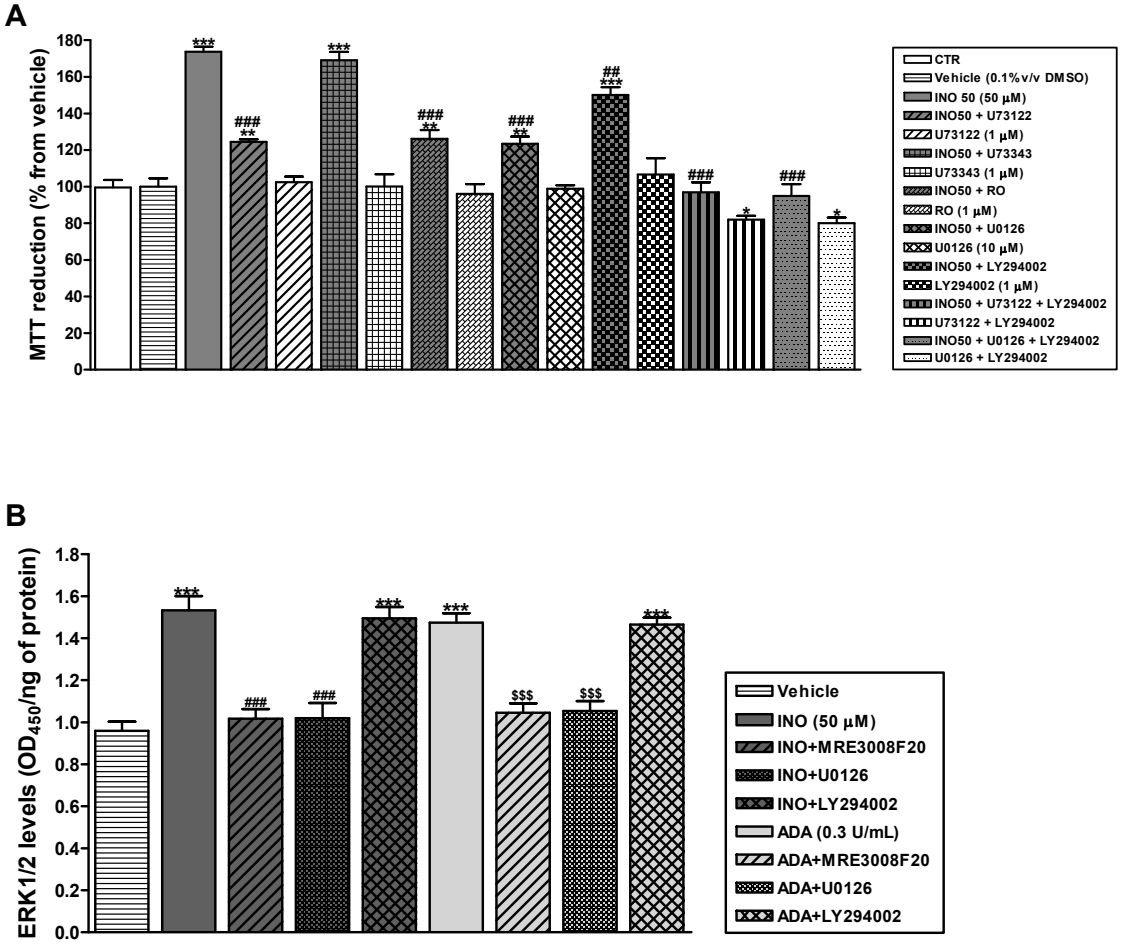

Figure 4. Simultaneous activation of PLC-PKC-MEK1/2-ERK1/2 and PI3K pathways induced by exogenous INO caused proliferation of human C32 melanoma cells. (A) Cells were treated with INO (50 μM), in the absence or presence of U-73122 (selective PLC inhibitor, 1 μM), U-73343 (PLC inactive analogue inhibitor, 1 μM), RO 32-0432 (selective PKC inhibitor, 1 μM), U0126 (selective MEK1/2 inhibitor, 10 μM) and/or LY294002 (potent PI3K inhibitor, 1 μM). DMSO (final concentration of 0.1% v/v) in DMEM-HG was used as vehicle. Results presented are means ± SEM, n=12 of 4 independent experiments. MTT reduction (% from vehicle) was evaluated at 48h incubation. Significant differences (One-Way ANOVA test, followed by the Student-Newman-Keuls post-hoc test): *$p<0.05$ vs. vehicle; **$p<0.01$ vs. vehicle; ***$p<0.001$ vs. vehicle; $^{\#\#}p<0.01$ vs. INO (50 μM); $^{\#\#\#}p<0.001$ vs. INO (50 μM). (B) Increase of ERK1/2 levels (OD_{450}/ng of protein) on human C32 melanoma cells induced by INO, through

A_3AR-MEK1/2 activation. Cells were treated with INO (50 μM) or ADA (0.3 U/mL), in the absence or presence of MRE 3008F20 (A_3AR antagonist, 10 nM), U0126 (selective MEK1/2 inhibitor, 10 μM) or LY294002 (potent PI3K inhibitor, 1 μM) at 24h incubation. DMSO (final concentration of 0.1% v/v) in DMEM-HG was used as vehicle. Results presented are means ± SEM of 3-4 independent experiments. Significant differences (One-Way ANOVA test, followed by the Student-Newman-Keuls post-hoc test): ***$p<0.001$ vs. vehicle; $^{###}p<0.001$ vs. INO; $^{\$\$\$}p<0.001$ vs. ADA.

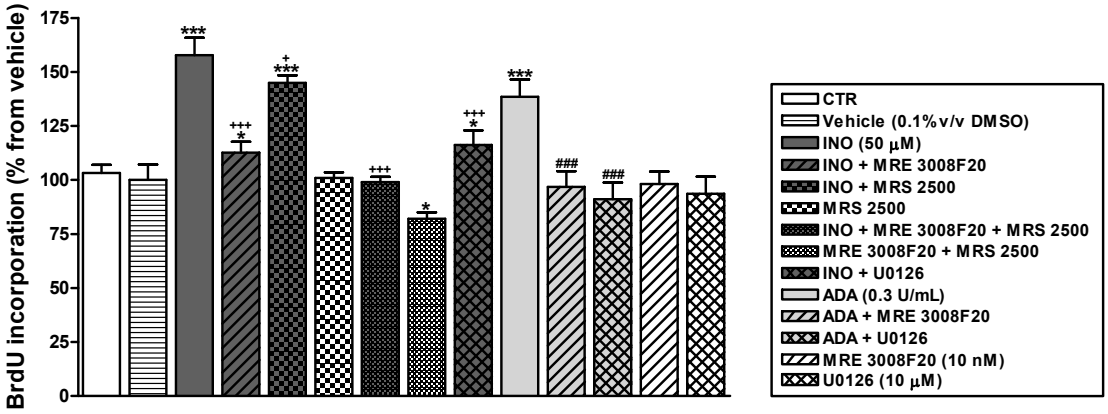

Figure 5. BrdU incorporation (% from vehicle) evaluated at 48h incubation. Human C32 melanoma cells were treated with INO (50 μM) or ADA (0.3 U/mL), in the absence or presence of selective A_3AR antagonist (MRE 3008F20, 10 nM), selective $P2Y_1R$ antagonist (MRS 2500, 1 μM) or selective MEK1/2 inhibitor (U0126, 10 μM). Results presented are means ± SEM, n=9–12 of 3–4 independent experiments. Significant differences (One-Way ANOVA test, followed by the Student-Newman-Keuls post-hoc test): *$p<0.05$ vs. vehicle; ***$p<0.001$ vs. vehicle; $^{+}p<0.05$ vs. INO (50 μM); $^{+++}p<0.001$ vs. INO (50 μM); $^{\#\#\#}p<0.001$ vs. ADA.

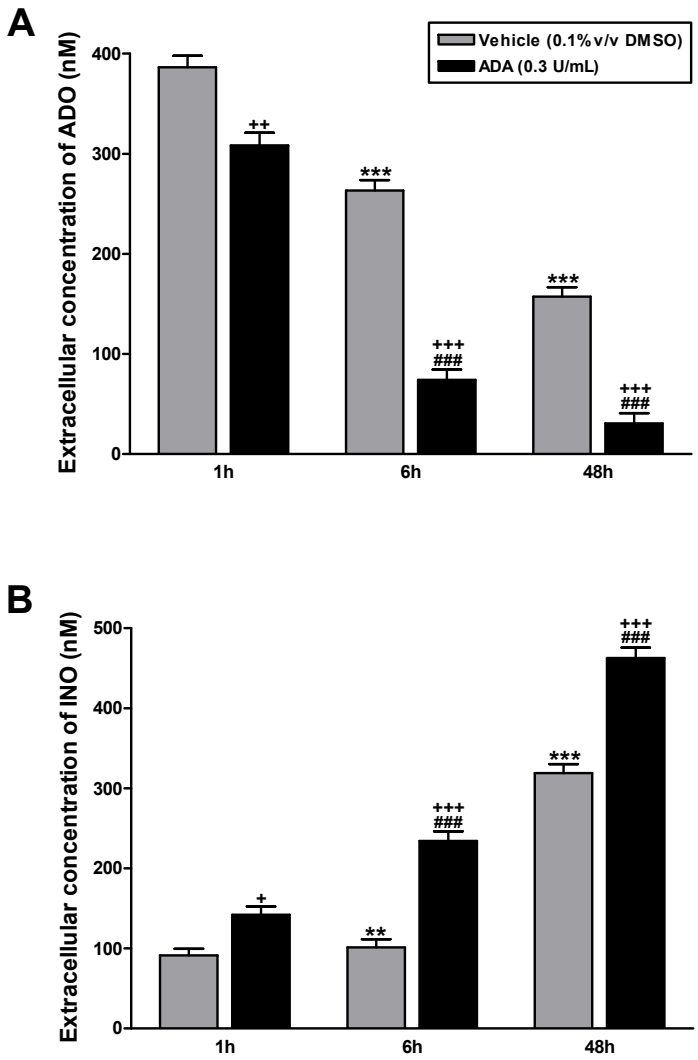

Figure 6. Extracellular concentrations of endogenous ADO and INO in human C32 melanoma cells. Medium was collected from cells treated with vehicle (0.1% v/v of DMSO; black bars) or ADA (0.3 U/mL; grey bars), after 1, 6, and 48h incubation. Results presented are means ± SEM, n=12 of 4 independent experiments. (A) Extracellular concentration of ADO (nM) at 1, 6 and 48h incubation. Significant differences (One-Way ANOVA test, followed by the Student-Newman-Keuls post-hoc test): ***$p<0.001$ vs. vehicle (1h); $^{###}p<0.001$ vs. ADA (1h); $^{++}p<0.01$ vs. vehicle at same time point; $^{+++}p<0.001$ vs. vehicle at same time point. (B) Extracellular concentration of INO (nM) at 1h, 6h and 48h incubation. Significant differences (One-Way ANOVA test, followed by the Student-Newman-Keuls post-hoc test): **$p<0.01$ vs. vehicle (1h); ***$p<0.001$ vs. vehicle (1h);

$^{###}p<0.001$ vs. ADA (1h); $^{+}p<0.05$ vs. vehicle at same time point; $^{+++}p<0.001$ vs. vehicle at same time point.

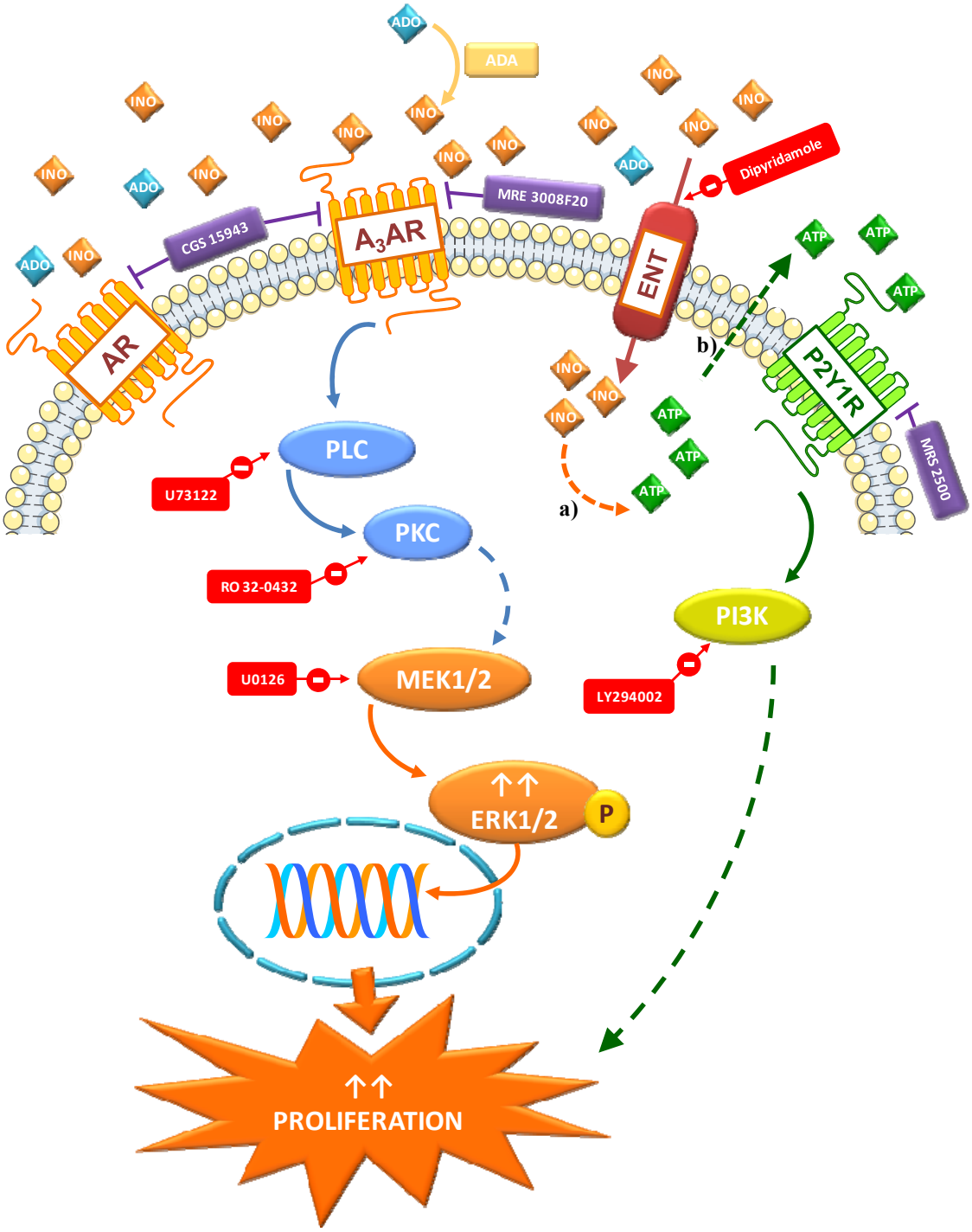

Figure 7. Proposed signalling pathways involved in proliferation of human C32 melanoma cells caused by INO through direct A_3AR activation and indirect $P2Y_1$R activation. INO activates, primarily, PLC-PKC-MEK1/2-ERK1/2 pathway after binding to A_3AR, causing cell proliferation. Simultaneously, INO can also enter into the cell through the ENT, being converted into ATP [(a) [50]] and release to the extracellular space [(b)

[51]]. Then, ATP activates PI3K, through the interaction with $P2Y_1R$, contributing to cell proliferation. Red and purple boxes represent selective inhibitors and antagonists, respectively. Dashed arrows represent indirect pathways.

3. MANUSCRIPT III

Potentiation of cytotoxicity of paclitaxel in combination with Cl-IB-MECA in human C32 metastatic melanoma cells: a new possible therapeutic strategy for melanoma

Published in the *Biomedicine & Pharmacotherapy* journal.

Biomedicine & Pharmacotherapy 67 (2013) 777–789

Available online at SciVerse ScienceDirect www.sciencedirect.com

Elsevier Masson France EM|consulte www.em-consulte.com/en

Original article

Potentiation of cytotoxicity of paclitaxel in combination with Cl-IB-MECA in human C32 metastatic melanoma cells: A new possible therapeutic strategy for melanoma

Ana S. Soares [a], Vera M. Costa [b], Carmen Diniz [a], Paula Fresco [a,*]

[a] REQUIMTE/Laboratório de Farmacologia, Departamento de Ciências do Medicamento, Faculdade de Farmácia, Universidade do Porto, Porto, Portugal
[b] REQUIMTE/Laboratório de Toxicologia, Departamento de Ciências Biológicas, Faculdade de Farmácia, Universidade do Porto, Porto, Portugal

ARTICLE INFO

Article history:
Received 3 July 2013
Accepted 10 August 2013

Keywords:
Paclitaxel
Cl-IB-MECA
Melanoma

Abbreviations:
Ac-DEVD-CHO, N-Ac-Asp-Glu-Val-Asp-CHO
AR, Adenosine receptor
Cl-IB-MECA, 2-chloro-*N*(6)-(3-iodobenzyl)-adenosine-5′-*N*-methyl-uronamide
DMSO, Dimethyl sulfoxide
DMEM-HG, Dulbecco's Modified Eagle's Medium–High Glucose
FBS, Fetal bovine serum
IAP, Inhibitors of apoptosis
LDH, Lactate dehydrogenase
MTT, 3-(4,5-dimethylthiazol-2-yl)-2,5-diphenyl tetrazolium bromide
NR, Neutral red
NAC, *N*-acetyl-cysteine
PXT, Paclitaxel
ROS, Reactive oxygen species
TNF, Tumour necrosis factor

ABSTRACT

Metastatic melanoma monotherapies with drugs such as dacarbazine, cisplatin or paclitaxel (PXT) are associated with significant toxicity and low efficacy rates. These facts reinforce the need for development of novel agents or combinatory strategies. Cl-IB-MECA is a small molecule, orally bioavailable, well tolerated and currently under clinical trials as an anticancer agent. Our aim was to investigate a possible combinatory therapeutic strategy using PXT and Cl-IB-MECA on human C32 melanoma cells and its underlying mechanisms. Cytotoxicity was evaluated using MTT reduction, lactate dehydrogenase leakage and neutral red uptake assays, for different concentrations and combinations of both agents, at 24 and 48 h. Apoptosis was also assessed using fluorescence microscopy and through the evaluation of caspases 8, 9, and 3 activities. We demonstrated, for the first time, that combination of PXT and Cl-IB-MECA significantly increases cytotoxicity for clinically relevant concentrations. This combination seems to act synergistically in disrupting membrane integrity, but also causing lysosomal and mitochondrial dysfunction. When using the lowest PTX concentration (10 ng/mL), co-incubation with Cl-IB-MECA (micromolar concentrations) potentiated overall cytotoxic effects and morphological signs of apoptosis. All combinations studied enhanced caspase 8, 9, and 3 activities, suggesting the involvement of both intrinsic and extrinsic apoptotic pathways. The possibility that cytotoxicity elicited by Cl-IB-MECA, alone or in combination with PXT, involves adenosine receptor activation was discarded and results confirmed that oxidative stress is only involved in cytotoxicity after treatment with PXT, alone. Being melanoma a very apoptosis-resistance cancer, this combination seems to hold promise as a new therapeutic strategy for melanoma.

1. Introduction

Malignant melanoma incidence is rising worldwide [1]. This deadliest form of skin cancer is highly aggressive and has a metastatic potential that is considerably greater than that of any other solid tumours [2]. Moreover, malignant melanoma presents high resistance to conventional chemotherapy and radiotherapy, especially once the metastatic process has begun [3]. Therefore, patients with metastatic melanoma have a poor prognosis, with an overall survival of 8 to 18 months [1]. Resistance to conventional chemotherapy is often related to overexpression of multidrug resistance proteins [3], efficient DNA repair mechanisms [4], overall resistance to endoplasmic reticulum stress [5] and pro-survival machinery that maintains melanoma cells alive by counteracting therapy- and microenvironment-induced apoptotic stimuli during tumour development and metastasis [6]. This last possibility is reinforced by studies, which reported melanoma cells to have low levels of spontaneous apoptosis, *in vivo*, comparatively to other tumour cells [6].

Apoptotic cell death is the major underlying mechanism of therapies targeting cancer cells [7]. The two major apoptotic

* Corresponding author. Tel.: +351 22 20428609.
E-mail address: pfresco@ff.up.pt (P. Fresco).

0753-3322/$ – see front matter © 2013 Elsevier Masson SAS. All rights reserved.
http://dx.doi.org/10.1016/j.biopha.2013.08.003

pathways, the intrinsic or mitochondrial pathway, and the extrinsic or death receptor pathway [8], are subject to aberrant pro-survival signaling in cancer cells, being this mechanism implicated in the resistance of melanoma to standard anticancer therapies [9]. The intrinsic pathway involves outer mitochondrial membrane permeabilization through cooperation of proapoptotic Bcl genes family, including *BAD*, *BAX*, *BAK*, and *BNIP3L* [10]. Once mitochondrial membrane is disrupted, apoptogenic proteins are released into the cytosol, including cytochrome c, AIF, HtrA2/Omi, and Smac/DIABLO [11]. These proteins trigger caspases (cysteine aspartate proteases) cascade activation, beginning with initiator caspases like caspase 9. Upon activation of the executioner caspases, they cleave different cytoplasmic and nuclear substrates, resulting into DNA fragmentation [12]. On the other hand, extrinsic pathway involves cell membrane–bound death receptors activation, which belong to TNF receptor gene family, including CD95 and TRAIL-R1 [13]. Activation of CD95 or TRAIL-R1 by Fas or TRAIL, respectively, results in aggregation of these receptors and recruitment of FADD and caspase 8. Activation of caspase 8 can then initiate apoptosis by direct cleavage of downstream executioner caspases, including caspase 3 [14]. Moreover, TRAIL is able to induce both extrinsic and intrinsic apoptosis pathways in melanoma [15]. However, pre-existing TRAIL resistance, related with down regulation of caspase 8, was also seen in melanoma cells [16]. Thus, initiator caspases, like caspase 8, may control melanoma cell sensitivity to TRAIL, and strategies that result in their up regulation, may be useful for enhancement of TRAIL sensitivity in melanoma.

Caspase-dependent and/or independent processes result in lethal apoptosis, including features of cell shrinkage, nuclear fragmentation, and membrane blebbing [17]. Nevertheless, apoptotic events can be antagonized by pro-survival Bcl-2 proteins and inhibitors of apoptosis (IAP) [18]. Members of both families are widely overexpressed or over activated in melanoma [19]. Overexpression of Bcl-2, Mcl-1, Bcl-XL, NF-κB, TRAF-2, surviving, living, and chromosome x-linked IAP (XIAP) were found to occur in melanoma models [19,20]. This overexpression results in the blockage or hampering of apoptosis. Failure to activate apoptotic pathways, in response to drug treatment, may explain the observed resistance of melanoma to anticancer therapies [20]. Therefore, drugs that induce caspase activation, overcoming melanoma's apoptosis impairment and promoting cell death, have great potential for melanoma therapeutic intervention.

Drugs that target the mitotic spindle are among the most effective anticancer therapeutics currently in use. Taxanes, like paclitaxel (PXT), induce microtubules stabilization, leading to the arrest of cell proliferation and apoptosis [21]. PXT is widely used in many types of cancers, including melanoma [22]. Previous studies showed that PXT is an effective anti-melanoma agent in preclinical models [23,24] and it has been used in clinical trials since 1990 [25]. It is presently used in patients with metastatic melanoma, including patients whose disease has progressed after previous chemotherapy sessions [26]. PXT, as a single agent, showed comparable anticancer activity to common melanoma monotherapy [27]. Unfortunately, PXT is associated with high multidrug resistance [28] that limits the efficacy of this agent, especially when used alone [29]. Therefore, PXT is often given as part of a combination chemotherapy regimen [30]. PXT is used in combination with carboplatin in the treatment of patients with metastatic melanoma. However, this combination added significantly haematological toxicity without improving response or survival rates [31].

Targeting A_3 adenosine receptor (AR) by adenosine or synthetic agonists has been described to cause a differential effect on tumour or on normal cells, inhibiting cell growth of various tumour types such as melanoma [32]. Previously, our group demonstrated that micromolar concentrations of 2-chloro-*N*(6)-(3-iodobenzyl)-adenosine-5′-*N*-methyl-uronamide (Cl-IB-MECA), a synthetic and selective A_3AR agonist, promotes cytotoxic effects on malignant melanoma cells [33]. Moreover, oral administration of Cl-IB-MECA to melanoma-bearing mice suppressed the development of melanoma lung metastases [34]. Additionally, Cl-IB-MECA is currently being evaluated in clinical trials (Phase1 and Phase 2) on patients with hepatocellular carcinoma, showing no serious drug-related adverse events or dose-limiting toxicities and good oral bioavailability [35]. Overall, Cl-IB-MECA is considered safe for non-cancer cells, therefore representing a promising therapeutic strategy for cancer treatment. In fact, the use of Cl-IB-MECA, alone or in combination, can improve the therapeutic index of a chemotherapeutic therapy, reducing the clinical dose while preserving efficacy against the cancer.

The aim of the present study was to investigate the potential synergistic cytotoxic effects of the combination of PXT with Cl-IB-MECA, on human C32 melanoma cells, using the lowest concentrations possible of both agents. Human C32 melanoma cells are a well-accepted model to evaluate cytotoxic compounds that can be of interest against melanoma [36]. In fact, PXT is a commonly used cytotoxic agent used on melanoma and Cl-IB-MECA is an oral drug with good potential anticancer properties. In this paper we provide evidence of a potentiation of C32 cells cytotoxicity by simultaneous treatment with PXT and Cl-IB-MECA, leading to apoptosis and necrosis. Based on the results we suggest a possible mechanism for this combination with the special focus on apoptotic pathways. The combination can, in fact, reveal a good potential on melanoma treatment by allowing to decrease PTX dosage and consequently decreasing its adverse effects and its multiresistance recurrence in melanoma.

2. Materials and methods

2.1. Chemicals

All reagents used were of analytical grade. Cl-IB-MECA, MRS 1220, MRE 3008F20, and CGS 15943 were obtained from Tocris Bioscience (Bristol, United Kingdom). Lactate dehydrogenase (LDH) assay kit was purchased from Promega Bioscience (VWR, Porto, Portugal). Caspase 3 and caspase 8 substrates and caspase inhibitor (*N*-Ac-Asp-Glu-Val-Asp-CHO, Ac-DEVD-CHO) were purchased from Calbiochem (Merck-Millipore, Interface, Amadora, Portugal). Bio-Rad RC DC protein assay kit was purchased to Bio-Rad (Amadora, Portugal). Fetal bovine serum (FBS), Glutamax, and Trypsin/EDTA were obtained from Gibco–Invitrogen, Alfagene (Carcavelos, Portugal). Dulbecco's Modified Eagle's Medium–High Glucose (DMEM-HG), penicillin/streptomycin (10,000 U/mL); PXT, 3-(4,5-dimethylthiazol-2-yl)-2,5-diphenyl tetrazolium bromide (MTT), neutral red (NR), Hoechst 33258, caspase 9 substrate, *N*-acetyl-cysteine (NAC), dimethyl sulfoxide (DMSO) and all other chemicals were purchased from Sigma-Aldrich (Sigma-Aldrich-Química SA, Sintra, Portugal) of the highest purity available.

2.2. Melanoma cell culture

Human C32 melanoma cells obtained from ECACC – SIGMA (Sigma-Aldrich-Química SA, Sintra, Portugal) were used in this study. Cells were seeded in DMEM-HG medium with 10% of FBS, 1% of a mixture of penicillin/streptomycin (10,000 U/mL; 10 mg/mL) and 1% of Glutamax, pH 7.4. Cells were incubated at 37 °C in a humidified atmosphere (95% air; 5% CO_2). For cell culture maintenance, cells were grown in monolayer and sub-cultivated twice a week. Cell passaging was done by trypsinization. All experiments were carried out with cells at 70%–80% confluence and from batches with passage number lower than 50.

2.3. Cytotoxicity and apoptosis assays

Human C32 melanoma cells were prepared using an initial cell density of 5.0×10^4 cells/cm^2. Cells were allowed to attach for 24 h and then were treated with PXT and/or Cl-IB-MECA solutions for different time-points (24 h or 48 h). During all the experimental period, cells were maintained at 37 °C with 5% CO_2. Vehicle (cells exposed to DMSO at maximum final concentration of 0.1% v/v) and blank (without cells) wells were also incubated at 37 °C, for the corresponding time-point. All conditions were initiated and processed in parallel.

2.3.1. LDH leakage assay

C32 cells were seeded in 96-well plates. After cell treatment, cell death (measurement of membrane integrity evaluated by the percentage of LDH release over the total LDH) was assessed using a LDH assay kit according to the manufacturer instructions. A_3AR selective antagonists MRS 1220 (10 nM), MRE 3008F20 (10 nM) [37] or the non-selective AR antagonist CGS 15943 (100 nM) [38] were added 30 min prior to the addition of PXT and/or Cl-IB-MECA solutions. For experiments with caspase 3 inhibitor Ac-DEVD-CHO (50 μM) [39] or with the antioxidant NAC (1 mM) [40], addition of these compounds was done 1 h prior to the addition of PXT and/or Cl-IB-MECA solutions. All conditions were performed in triplicate.

Measurements of absorbance were performed in an automated microplate reader (PowerWaveXS, Bio-Tek Instruments Inc, Vermont, USA).

2.3.2. MTT reduction assay

C32 cells were seeded in 96-well plates. After cell treatment, mitochondrial function was evaluated since mitochondrial dehydrogenases of living cells can reduce the MTT (yellow) to formazans, which are purple compounds [41]. At the end of incubations, cell medium was removed and 100 μL/well of MTT solution (0.5 mg/mL in PBS) were added. Then, plates were incubated for 3 h (at 37 °C, protected from light). After this period, MTT solution was removed and DMSO (100 μL/well) was added to solubilize the formazan crystals. Absorbance was measured at 570 nm in an automated microplate reader (PowerWaveXS, Bio-Tek Instruments Inc, Vermont, USA). Results were compared with vehicle wells whose media of values was set to 100%. A_3AR antagonists MRS 1220 (10 nM), MRE 3008F20 (10 nM) or the non-selective AR antagonist CGS 15943 (100 nM) were added 30 min prior to the addition of PXT and/or Cl-IB-MECA solutions. All conditions were performed in triplicate.

2.3.3. NR uptake assay

C32 cells were seeded in 96-well plates. After cell treatment, lysosomal functionality was spectrophotometrically evaluated and represented as percentage of NR dye incorporated in the cells. This dye easily penetrates viable cell membranes and accumulates intracellularly in lysosomes [42]. At the end of incubations, cell medium was removed and 250 μL/well of NR solution (33 μg/mL of NR in DMEM-HG) were added. Then, plates were incubated for 3 h (at 37 °C, protected from light). After this time, NR solution was removed and 100 μL/well of the solvent (50% ethanol/1% acetic acid) were added to extract the NR dye from viable cells. The plates were then placed in a microplate shaker for 30 min, at room temperature. Absorbance was measured at 540 nm, in an automated microplate reader (PowerWaveXS, Bio-Tek Instruments Inc, Vermont, USA), and results were compared with vehicle wells whose media of values was set to 100%. All conditions were performed in triplicate.

2.3.4. Apoptotic nuclei fluorescent staining

C32 cells were seeded in chamber slide systems. After cell treatment, cells were washed with PBS and fixed in 4% paraformaldehyde (10 min, room temperature). Cells were then stained with the nuclear dye Hoechst 33258 (5 μg/mL in PBS) for 15 min, at room temperature (protected from light), and then examined in a Nikon Eclipse E400 fluorescence microscope coupled to a digital camera (Nikon Digital Sight DS-5Mc, New Jersey, USA). Images from ten random fields were captured per well (magnification of 200 times – 10× from ocular lens and 20× from objective lens). Apoptotic cells were identified as blue-coloured nuclei with typical morphologic apoptotic features including chromatin condensation and nuclear fragmentation, and increased staining intensity [43].

2.4. Caspase 8, 9, and 3 activity assays

The activities of caspase 8, 9 and 3 were determined using colorimetric assays, as previously described [39]. Briefly, hydrolysis of the peptide substrates Ac-Ile-Glu-Thr-Asp-*p*-nitroanilide, Ac-Leu-Glu-His-Asp-*p*-nitroanilide and Ac-Asp-Glu-Val-Asp-*p*-nitroanilide by caspase 8, 9 and 3, respectively, causes the release of the *p*-nitroaniline (*p*NA) moiety, which presents a high absorbance at 405 nm. Cells were seeded in six well plates using an initial cell density of 5.0×10^4 cells/cm^2 and allowed to attach for 24 h. After 16 h (caspase 8 and 9) or 24 h (caspase 3) of Cl-IB-MECA (10, 20 and 50 μM) incubation in the absence or in the presence of PXT (10 ng/mL), cells were collected with a cell scraper and lysed in lysis buffer [50 mM HEPES, 1 mM DTT, 0.1 mM EDTA, 0.1% CHAPS (pH 7.4)] for 5 min on ice (without protease inhibitors). Cell lysate was added to the assay buffer [100 mM NaCl, 50 mM HEPES, 10 mM DTT, 1 mM EDTA, 10% Glycerol, 0.1% CHAPS (pH 7.4)] containing final concentrations of 80 μM, 200 μM and 200 μM of the colorimetric substrates for caspase 3, 9 and 8, respectively. After incubation at 37 °C for 24 h, absorbance was measured in an automated microplate reader (PowerWaveXS, Bio-Tek Instruments Inc, Vermont, USA) at 405 nm. Results were expressed as optic density (OD) and normalised to protein content of cell lysate. Protein concentration of each condition was determined using the protocol referred in the following section.

2.4.1. Protein content determination

Protein content of cellular fractions in total cell lysates for caspase activity assays was determined using the Bio-Rad RC DC protein assay kit, in accordance to the manufacturer instructions. Stock solutions of bovine serum albumin were used as standards.

2.5. Statistical analysis

Results are presented as mean ± SEM for n experiments performed. Statistical comparisons between groups were performed with One-Way ANOVA (when a normal distribution was found) or Kruskal–Wallis test (one-way ANOVA on ranks when distribution was not normal), after Shapiro–Wilk test normality evaluation. Significance was accepted at P values < 0.05. The Student-Newman–Keuls post-hoc test was used once a significant P was achieved. Details of statistical analysis are found in the legend of the figures.

3. Results

3.1. Cytotoxicity induced by increasing concentrations of PXT is potentiated by Cl-IB-MECA (50 μM) in human C32 metastatic melanoma cells

Human C32 metastatic melanoma cells were exposed to increasing concentrations of PXT (10, 25 and 50 ng/mL) in the absence or in the presence of 50 μM of Cl-IB-MECA, for 24 h or 48 h incubation (Fig. 1). Cell death (LDH leakage assay) caused by increasing concentrations of PXT was only significant after 48 h

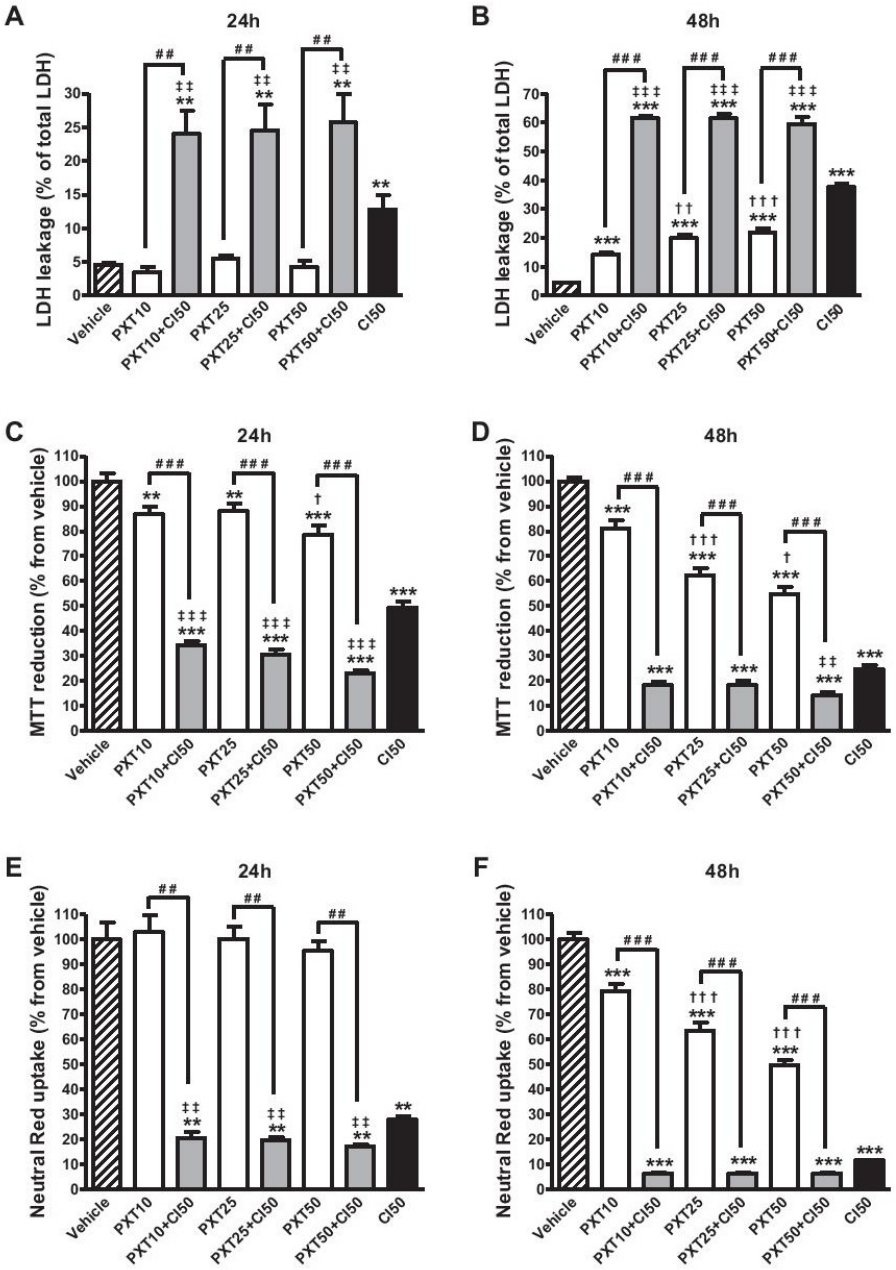

Fig. 1. Human C32 melanoma cells cytotoxicity elicited by increasing concentrations of PXT (10, 25 and 50 ng/mL; PXT10, PXT25 and PXT50) in the absence (open bars) or in the presence (grey bars) of Cl-IB-MECA (50 μM; CI50; black bars), after 24 (A, C and E) or 48 h (B, D and F) incubation. DMSO (final concentration of 0.1% v/v) in DMEM-HG was used as vehicle (hatched bars). Results presented are means ± SEM, $n = 12$ of four independent experiments. A. LDH leakage (% of total LDH) at 24 h incubation. Significant differences (Kruskal–Wallis test, followed by the Student-Newman–Keuls post-hoc test): $^{**}P < 0.01$ vs. vehicle; $^{‡‡}P < 0.01$ vs. CI50; $^{\#\#}P < 0.01$ vs. PXT + CI50. B. LDH leakage (% of total LDH) at 48 h incubation. Significant differences (One-Way ANOVA test, followed by the Student-Newman–Keuls post-hoc test): $^{***}P < 0.001$ vs. vehicle; $^{‡‡‡}P < 0.001$ vs. CI50; $^{††}P < 0.01$ vs. PXT10; $^{†††}P < 0.001$ vs. PXT10; $^{\#\#\#}P < 0.001$ vs. PXT + CI50. C. MTT reduction (% from vehicle) at 24 h incubation. Significant differences (One-Way ANOVA test, followed by the Student-Newman–Keuls post-hoc test): $^{**}P < 0.01$ vs. vehicle; $^{***}P < 0.001$ vs. vehicle; $^{‡‡‡}P < 0.001$ vs. CI50; $^{†}P < 0.05$ vs. lower PXT concentrations; $^{\#\#\#}P < 0.001$ vs. PXT + CI50. D. MTT reduction (% from vehicle) at 48 h incubation. Significant differences (One-Way ANOVA test, followed by the Student-Newman–Keuls post-hoc test): $^{***}P < 0.001$ vs. vehicle; $^{‡‡}P < 0.01$ vs. CI50; $^{†}P < 0.05$ vs. PXT concentration immediately below; $^{†††}P < 0.001$ vs. PXT concentration immediately below; $^{\#\#\#}P < 0.001$ vs. PXT + CI50. E. Neutral red uptake (% from vehicle) at 24 h incubation. Significant differences (Kruskal–Wallis test, followed by the Student-Newman–Keuls post-hoc test): $^{**}P < 0.01$ vs. vehicle; $^{‡‡}P < 0.01$ vs. CI50; $^{\#\#}P < 0.01$ vs. PXT + CI50. F. Neutral red uptake (% from vehicle) at 48 h incubation. Significant differences (One-Way ANOVA test, followed by the Student-Newman–Keuls post-hoc test): $^{***}P < 0.001$ vs. vehicle; $^{†††}P < 0.001$ vs. PXT concentration immediately below; $^{\#\#\#}P < 0.001$ vs. PXT + CI50.

incubation, in a concentration-dependent manner. Significant increase in cell death caused by 50 μM of Cl-IB-MECA was already observed at 24 h when compared to vehicle, and that cytotoxicity was time-dependent. In contrast, cell death promoted by all combinations of PXT with Cl-IB-MECA, evaluated by the LDH leakage assay, was already significant at 24 h (Fig. 1A) being more pronounced at 48 h incubation (Fig. 1B), when compared to cells treated with the corresponding PXT concentration. Importantly, the increase in cell death was significantly higher in C32 cells treated with combinations of PXT and Cl-IB-MECA, when compared to Cl-IB-MECA alone.

In contrast to the LDH leakage assay, the MTT reduction assay showed statistically significant mitochondrial dysfunction caused by increasing concentrations of PXT (10, 25 and 50 ng/mL), already at 24 h incubation (Fig. 1C). This effect was also more marked at 48 h incubation (Fig. 1D), showing that cytotoxicity is time and concentration-dependent. Additionally, Cl-IB-MECA alone promoted mitochondrial dysfunction in a time-dependent manner. Importantly, higher levels of mitochondrial dysfunction (lower levels of MTT reduction) were found for all combinations of PXT and Cl-IB-MECA at 24 h or 48 h, when compared to the effect of Cl-IB-MECA or the corresponding PXT concentration, individually.

The cytotoxic effect of increasing concentrations of PXT (10, 25 and 50 ng/mL) and 50 μM of Cl-IB-MECA was also monitored using the NR uptake assay. No significant differences on active lysosomal uptake were detected for each PXT concentrations used alone, after 24 h incubation, when compared to vehicle (Fig. 1E). Nevertheless, statistically significant decrease in lysosomal uptake was found for all PXT concentrations, at 48 h, when compared to vehicle (Fig. 1F). Cl-IB-MECA alone also promoted lysosomal uptake dysfunction, in a time-dependent manner. Cytotoxicity elicited by combinations of PXT with Cl-IB-MECA, evaluated by this assay, was already significant at 24 h, but was more pronounced after 48 h incubation, when compared to the effect of Cl-IB-MECA or the corresponding PXT concentration, individually. However, the effects elicited by combinations were already significantly different when compared to Cl-IB-MECA alone, after 24 h of exposure.

Overall, there was a marked increased cytotoxicity in human C32 metastatic melanoma cells that was potentiated by the addition of Cl-IB-MECA to the three different PXT concentrations used, including the lowest concentration of PXT used (10 ng/mL) at the first end-point time evaluated (24 h incubation).

Fluorescence microscopy with Hoechst 33258, a blue nuclei staining dye, was used to visualize morphological features of apoptosis as a result of increasing concentrations of PXT (10, 25 and 50 ng/mL) in the absence or in the presence of 50 μM of Cl-IB-MECA (Fig. 2). After cell treatment, we found morphological features of programmed cell death, namely nuclear fragmentation and chromatin condensation, for all conditions used, except for vehicle, after 24 h incubation (Fig. 2A). Apoptosis features were more frequent when combinations of PXT and Cl-IB-MECA were evaluated, and accompanied with a decrease in cell number per

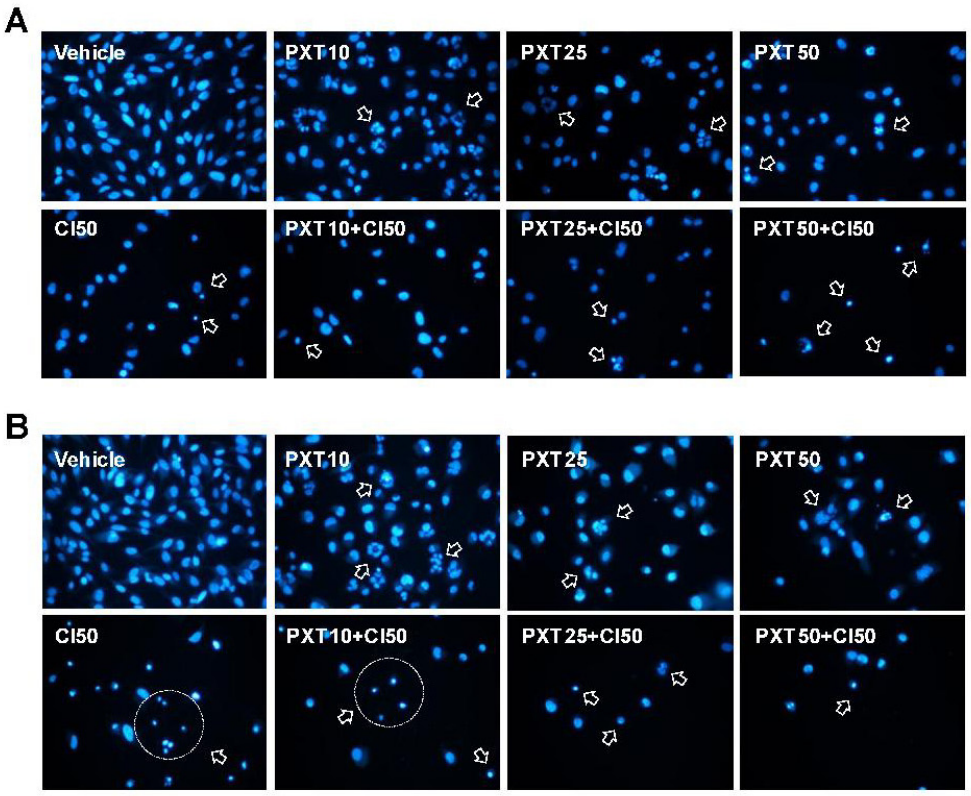

Fig. 2. Morphological changes of human C32 melanoma cells, after exposure to increasing concentrations of PXT (10, 25 and 50 ng/mL; PXT10, PXT25 and PXT50) in the absence or in the presence of Cl-IB-MECA (50 μM; CI50). Cells were treated with vehicle (DMSO in DMEM-HG, final concentration of 0.1% v/v), Cl-IB-MECA, PXT or PXT + CI50 for 24 (A) or 48 h (B). Cells were then fixed and stained with Hoechst 33258 (5 μg/mL in PBS) and observed by fluorescence microscopy. Images (magnification of 200 times: 10× from ocular lens and 20× from objective lens) are representative of three independent experiments. Arrows indicate cells apoptosis features.

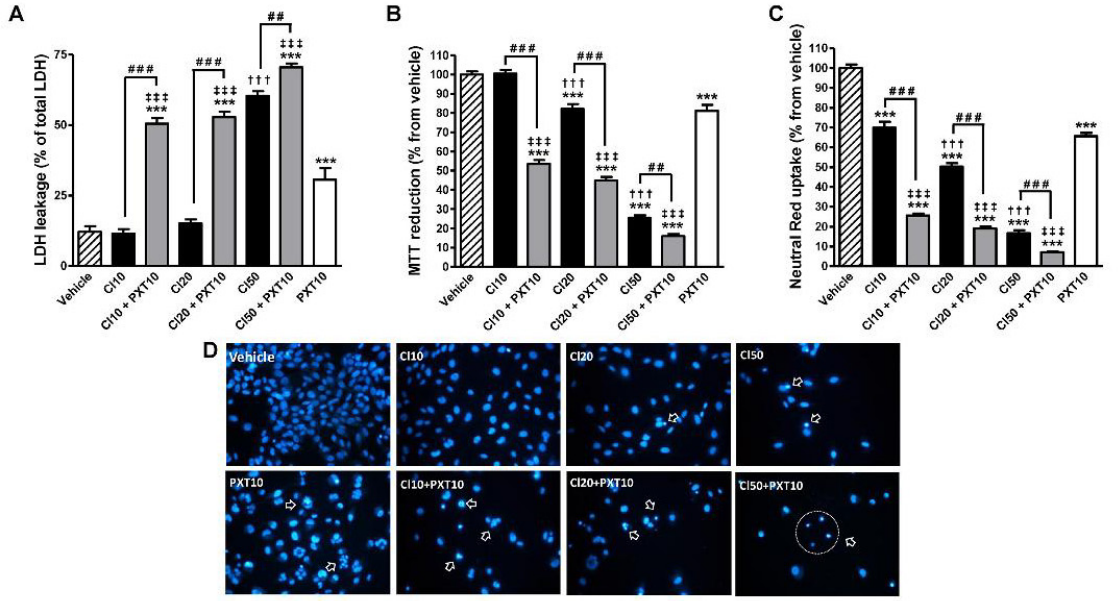

Fig. 3. Cytotoxicity and morphological changes in human C32 melanoma cells elicited by increasing concentrations of Cl-IB-MECA (10, 20 and 50 μM; Cl10, Cl20 and Cl50), in the absence (black bars) or in the presence (grey bars) of PXT (10 ng/mL; PXT10; open bars), after 48 h incubation. DMSO (final concentration of 0.1% v/v) in DMEM-HG was used as vehicle (hatched bars). A. LDH leakage (% of total LDH). Significant differences (One-Way ANOVA test, followed by the Student-Newman–Keuls post-hoc test): $^{***}P < 0.001$ vs. vehicle; $^{‡‡‡}P < 0.001$ vs. PXT10; $^{†††}P < 0.001$ vs. lower Cl concentrations; $^{\#\#}P < 0.01$ vs. Cl + PXT10; $^{\#\#\#}P < 0.001$ vs. Cl + PXT10. B. MTT reduction (% vs. vehicle). Significant differences (One-Way ANOVA test, followed by the Student-Newman–Keuls post-hoc test): $^{***}P < 0.001$ vs. vehicle; $^{‡‡‡}P < 0.001$ vs. PXT10; $^{†††}P < 0.001$ vs. Cl concentration immediately below; $^{\#\#}P < 0.01$ vs. Cl + PXT10; $^{\#\#\#}P < 0.001$ vs. Cl + PXT10. C. Neutral red uptake (% vs. vehicle). Significant differences (One-Way ANOVA test, followed by the Student-Newman–Keuls post-hoc test): $^{***}P < 0.001$ vs. vehicle; $^{‡‡‡}P < 0.001$ vs. PXT10; $^{†††}P < 0.001$ vs. Cl concentration immediately below; $^{\#\#\#}P < 0.001$ vs. Cl + PXT10. Results presented are means ± SEM, $n = 12$ of four independent experiments. D. Fluorescence microscopy images of human C32 melanoma cells after Hoechst 33258 staining. Images are representative of three independent experiments (magnification of 200 times: 10× from ocular lens and 20× from objective lens). Arrows indicate cells undergoing apoptosis.

well. Similar effects were observed at 48 h incubation (Fig. 2B) for all the conditions performed (except for vehicle), being the apoptotic signs more notorious.

3.2. Increasing concentrations of Cl-IB-MECA, in combination with PXT (10 ng/mL), caused concentration-dependent cytotoxicity in human C32 metastatic melanoma cells

Since we found significant cytotoxic effects in human C32 melanoma cells treated with the lowest PXT concentration, in combination with 50 μM of Cl-IB-MECA, the next step was to evaluate whether these effects could be also observed for this lower concentration of PXT (10 ng/mL) in combination with lower concentrations of Cl-IB-MECA.

Human C32 metastatic melanoma cells were treated with increasing concentrations of Cl-IB-MECA (10, 20 and 50 μM), alone or in combination with 10 ng/mL of PXT10, for 48 h (Fig. 3).

Human C32 metastatic melanoma cell death (LDH leakage assay) was assessed at 48 h (Fig. 3A), as described in the Methods section (Section 2). Although 10 and 20 μM of Cl-IB-MECA did not lead to cell death, this effect was statistically significant when these Cl-IB-MECA concentrations were tested in combination with PXT (10 ng/mL). For the highest concentration of Cl-IB-MECA used (50 μM), alone or in combination with PXT, and for PXT alone, results were in agreement with those presented in Fig. 1, showing the occurrence of significant C32 cell death, when compared to vehicle.

Mitochondrial functionality of human C32 metastatic melanoma cells was also evaluated (MTT reduction assay), for the same conditions. Results showed that mitochondrial function was not affected by the lowest concentration of Cl-IB-MECA tested (10 μM, Fig. 3B). However, even the lowest Cl-IB-MECA concentration when in combination with PXT was able to statistically decrease the activity of the mitochondrial enzymatic machinery. Significant mitochondrial dysfunction was also observed for cells individually treated with 20, 50 μM of Cl-IB-MECA or 10 ng/mL of PXT. These effects were more pronounced when Cl-IB-MECA concentrations were used in combination with PXT.

Active lysosomal uptake (NR uptake assay) was also evaluated in the conditions described above (Fig. 3C). All concentrations of Cl-IB-MECA used, or PXT, alone, were able to reduce lysosomal NR uptake when compared to vehicle. Moreover, this reduction in lysosomal activity was more marked when increasing concentrations of Cl-IB-MECA were used in combination with PXT (10 ng/mL).

Overall, increasing concentrations of Cl-IB-MECA in combination with 10 ng/mL of PXT caused a concentration-dependent cytotoxicity in human C32 metastatic melanoma cells. In addition, these cytotoxic effects were corroborated by morphologic cellular evaluation. C32 cells exposed to increasing concentrations of Cl-IB-MECA (10, 20 and 50 μM), in the absence or in the presence of 10 ng/mL of PXT, were also analysed for morphologic signs of apoptosis at 48 h (Fig. 3D). Images revealed apoptosis morphological features (nuclear fragmentation and chromatin condensation) for all conditions used, except for vehicle and the lowest Cl-IB-MECA concentration (10 μM). Programmed cell death features were, once again, more marked when combinations of Cl-IB-MECA and PXT were used, comparatively to individual treatments. Those

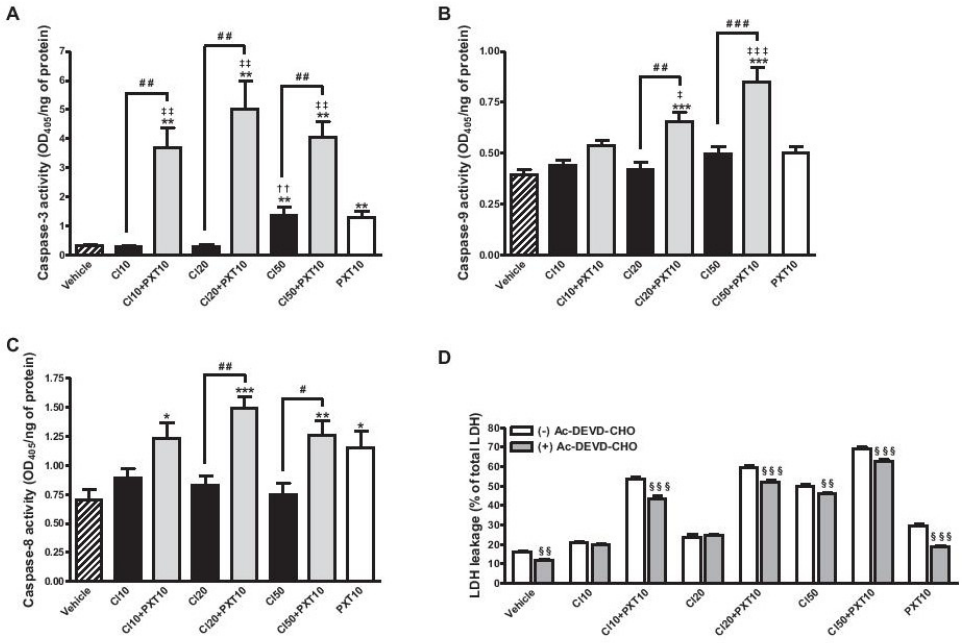

Fig. 4. Enhancement of caspase 3, 9, and 8 enzyme activities in human C32 melanoma cells by increasing concentrations of Cl-IB-MECA (10, 20 and 50 μM; Cl10, Cl20 and Cl50) in the absence (black bars) or in the presence (grey bars) of PXT (10 ng/mL; PXT10; open bars). DMSO (final concentration of 0.1% v/v) in DMEM-HG was used as vehicle (hatched bars) (A–C). A. Caspase 3 activity [optic density (OD) 405/ng of protein] at 24 h incubation. Results presented are means ± SEM, $n = 7$ independent experiments. Significant differences (Kruskal–Wallis test, followed by the Student-Newman–Keuls post-hoc test): $^{**}P < 0.01$ vs. vehicle; $^{\ddagger\ddagger}P < 0.01$ vs. PXT10; $^{\dagger\dagger}P < 0.01$ vs. lower Cl concentrations; $^{\#\#}P < 0.01$ vs. Cl + PXT10. B. Caspase 9 activity (OD405/ng of protein) at 16 h incubation. Results presented are means ± SEM, $n = 8$ independent experiments. Significant differences (One-Way ANOVA test, followed by the Student-Newman–Keuls post-hoc test): $^{***}P < 0.001$ vs. vehicle; $^{\ddagger}P < 0.05$ vs. PXT10; $^{\ddagger\ddagger\ddagger}P < 0.001$ vs. PXT10; $^{\#\#}P < 0.01$ vs. Cl + PXT10; $^{\#\#\#}P < 0.001$ vs. Cl + PXT10. C. Caspase 8 activity (OD405/ng of protein) at 16 h incubation. Results presented are means ± SEM, $n = 6$ independent experiments. Significant differences (One-Way ANOVA test, followed by the Student-Newman–Keuls post-hoc test): $^{*}P < 0.05$ vs. vehicle; $^{**}P < 0.01$ vs. vehicle; $^{***}P < 0.001$ vs. vehicle; $^{\#}P < 0.05$ vs. Cl + PXT10; $^{\#\#}P < 0.01$ vs. Cl + PXT10. D. Human C32 melanoma cells death (LDH leakage assay) elicited by increasing concentrations of Cl-IB-MECA (10, 20, and 50 μM; Cl10, Cl20, and Cl50), paclitaxel (10 ng/mL; PXT10) and all Cl + PXT10 combinations, after 48 h incubation in the absence (open bars) or in the presence of the caspase inhibitor, Ac-DEVD-CHO (50 μM; grey bars). DMSO (final concentration of 0.1% v/v) in DMEM-HG was used as vehicle. Results presented are means ± SEM, $n = 12$ of four independent experiments. Significant differences (One-Way ANOVA test, followed by the Student-Newman–Keuls post-hoc test): $^{\S}P < 0.05$ vs. corresponding condition in the absence of Ac-DEVD-CHO; $^{\S\S}P < 0.01$ vs. corresponding condition in the absence of Ac-DEVD-CHO. Other significant differences were similar to Fig. 3A.

were also accompanied by a decrease in the cell number per well, probably resulting from necrosis and/or cell detachment.

Cytotoxicity was not statistically significant when these Cl-IB-MECA concentrations were tested alone or in combination with PXT (10 ng/mL), at 24 h incubation (data not shown).

3.3. Cytotoxicity promoted by Cl-IB-MECA in combination with PXT (10 ng/mL) is accompanied by caspases (8, 9 and 3) activation

In order to examine the role of apoptotic pathways involving activation of caspases, in the cytotoxicity elicited by increasing Cl-IB-MECA concentrations (10, 20 and 50 μM), in the absence or in the presence of 10 ng/mL of PXT, we measured the proteolytic activity of the initiators caspase 9 and 8 and the executioner caspase 3, as described in Methods section (Section 2). C32 cell lysates were collected at 16 h for caspase 9 and 8 or 24 h for caspase 3, after cell treatment (Fig. 4). As shown in Fig. 4A, all combinations of different Cl-IB-MECA concentrations with PXT caused significant increase of caspase 3 proteolytic activity. The highest concentration of Cl-IB-MECA used (50 μM) and PXT (10 ng/mL), alone, also had a significant increase in caspase 3 activity, although lower than that observed for all tested combinations of Cl-IB-MECA with PXT. Significant increase in caspase 9 activity was observed only for 20 and 50 μM Cl-IB-MECA in combination with PXT (Fig. 4B), indicating that caspase 9 is only activated for higher Cl-IB-MECA concentrations, in the presence of PXT. Results showed that all combinations of Cl-IB-MECA with PXT10 caused a significant increase in caspase 8 activity (Fig. 4C). PXT alone significantly increased the caspase 8 activity, when compared to vehicle. Taken together, these results indicate that activation of caspase 8, 9 and 3 is involved in apoptosis induced by combinations of Cl-IB-MECA and PXT.

To assess whether caspase activation had any relevant role in the cytotoxicity observed by increasing concentrations of Cl-IB-MECA, PXT (10 ng/mL) or all combinations of Cl-IB-MECA with PXT, we measured LDH leakage at 48 h incubation with or without Ac-DEVD-CHO, a caspase 3 inhibitor (Fig. 4D), in the absence/presence of the caspase inhibitor. Pre-incubation with 50 μM of Ac-DEVD-CHO, followed by cell treatment at the conditions described above, significantly reduced C32 cell death for 50 μM of Cl-IB-MECA, for 10 ng/mL of PXT and for all combinations of Cl-IB-MECA with PXT, after 48 h incubation (Fig. 4D). Furthermore, AC-DEVD-CHO did not lead to any protection against the mitochondrial dysfunction elicited by Cl-IB-MECA with or without PXT (data not shown).

3.4. Possible involvement of endogenous adenosine protection against Cl-IB-MECA and PXT cytotoxicity

To investigate whether Cl-IB-MECA or combinations of Cl-IB-MECA and PXT elicited the cytotoxic effects observed A_3AR

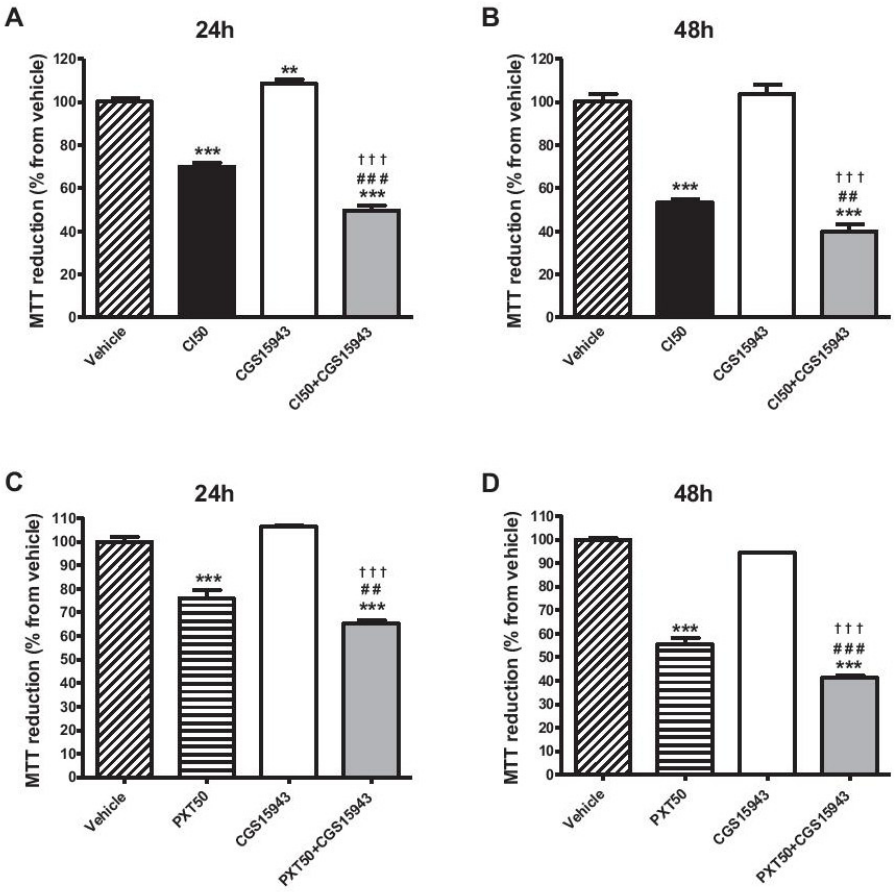

Fig. 5. Human C32 melanoma cells cytotoxic effects of Cl-IB-MECA (50 μM; Cl50, black bars) (A and B) or PXT [50 ng/mL; PXT50, horizontally hatched bars (C and D)] in the presence of the AR antagonist, CGS 15943 (100 nM, grey bars), at 24 or 48 h incubation. DMSO (final concentration of 0.1% v/v) in DMEM-HG was used as vehicle (diagonally hatched bars). Results presented are means ± SEM, $n = 12$ of four independent experiments. A. MTT reduction (% from vehicle) at 24 h incubation. Significant differences (One-Way ANOVA test, followed by the Student-Newman–Keuls post-hoc test): $^{**}P < 0.01$ vs. vehicle; $^{***}P < 0.001$ vs. vehicle; $^{\#\#\#}P < 0.001$ vs. Cl50; $^{\dagger\dagger\dagger}P < 0.001$ vs. CGS 15943. B. MTT reduction (% from vehicle) at 48 h incubation. Significant differences (One-Way ANOVA test, followed by the Student-Newman–Keuls post-hoc test): $^{***}P < 0.001$ vs. vehicle; $^{\#\#}P < 0.01$ vs. Cl50; $^{\dagger\dagger\dagger}P < 0.001$ vs. CGS 15943. C. MTT reduction (% from vehicle) at 24 h incubation. Significant differences (One-Way ANOVA test, followed by the Student-Newman–Keuls post-hoc test): $^{***}P < 0.001$ vs. vehicle; $^{\#\#}P < 0.01$ vs. PXT50; $^{\dagger\dagger\dagger}P < 0.001$ vs. CGS 15943. D. MTT reduction (% from vehicle) at 48 h incubation. Significant differences (One-Way ANOVA test, followed by the Student-Newman–Keuls post-hoc test): $^{***}P < 0.001$ vs. vehicle; $^{\#\#\#}P < 0.001$ vs. PXT50; $^{\dagger\dagger\dagger}P < 0.001$ vs. CGS 15943.

activation, human C32 metastatic melanoma cells were treated with increasing concentrations of Cl-IB-MECA (10, 20 and 50 μM), PXT (10 ng/mL) or combinations of Cl-IB-MECA with PXT, in the absence or presence of MRE 3008F20 (10 nM) or MRS 1220 (10 nM), selective A_3AR antagonists, as described in the Methods section (Section 2). Cell death (LDH leakage assay) and mitochondrial impairment (MTT reduction assay) induced by 50 μM of Cl-IB-MECA and all combinations of Cl-IB-MECA with PXT were not statistically different from the respective condition in the presence of each of A_3AR antagonists used, at 48 h incubation (data not shown). These results suggest that, at these experimental conditions, cytotoxicity is not mediated by A_3AR activation.

We also used a potent and non-selective AR antagonist, CGS 15943. Human C32 metastatic melanoma cells were pre-treated with 100 nM of CGS 15943 for 30 min, and then incubated with Cl-IB-MECA (50 μM) or PXT (50 ng/mL) for a 24 h or a 48 h (Fig. 5). Results obtained for mitochondrial dysfunction showed that CGS 15943 was not able to prevent the cytotoxicity induced by Cl-IB-MECA or PXT. On the contrary, these cytotoxic effects were even more pronounced when compared with single incubations with Cl-IB-MECA or PXT, suggesting the involvement of endogenous adenosine on the protection of melanoma cells.

3.5. NAC partially reverts PXT-induced cell death

To determine whether cell death (LDH leakage assay) promoted by Cl-IB-MECA (10, 20 and 50 μM), PXT (10 ng/mL) or combinations of Cl-IB-MECA with PXT was affected by reactive oxygen species (ROS), cells were pre-incubated with 1 mM of NAC [(ROS) scavenger] for 1 h, followed by 48 h incubation with the compounds (Table 1). Pre-incubation with NAC did not prevent C32 cell death for any cell treatment tested, with the exception of 10 ng/mL of PXT. In 10 ng/mL PXT treated cells, NAC was able to partially counteract the cytotoxicity observed by PTX. Moreover, no cytotoxicity protection was observed, in the presence of NAC, against mitochondrial dysfunction elicited by Cl-IB-MECA either in

Table 1
Effect of NAC (1 mM) on the cytotoxicity elicited by increasing concentrations of Cl-IB-MECA (10, 20 and 50 μM; Cl10, Cl20 and Cl50), in the absence or in the presence of PXT (10 ng/mL; PXT10), on human C32 melanoma cells. DMSO (final concentration of 0.1% v/v) in DMEM-HG was used as vehicle. LDH leakage (% of total LDH) at 48 h incubation.

48 h	LDH leakage (% from total LDH)	
	(−) NAC (mean ± SEM)	(+) NAC (mean ± SEM)
Vehicle	4.07 ± 0.11	3.05 ± 0.20
Cl10	4.84 ± 0.11	4.60 ± 0.14
Cl10 + PXT10	35.13 ± 0.87	32.88 ± 0.93
Cl20	6.08 ± 0.16	5.76 ± 0.15
Cl20 + PXT10	39.67 ± 1.16	40.25 ± 1.53
Cl50	40.06 ± 3.25	40.35 ± 3.88
Cl50 + PXT10	62.05 ± 1.35	63.60 ± 1.30
PXT10	14.05 ± 0.20	10.37 ± 0.18[§]

Significant differences (One-Way ANOVA test, followed by the Student-Newman–Keuls post-hoc test): [§]$P < 0.05$ vs. corresponding condition in the absence of NAC. Results presented are means ± SEM, $n = 9$ of three independent experiments. Other significant differences were similar to Fig. 3A.

the absence or in the presence of 10 ng/mL of PXT (data not shown).

4. Discussion

Metastatic melanoma remains a challenging disease to treat, since metastatic melanoma cells are usually resistant to chemo- and radiotherapy [3]. Despite the new promising drugs emerging, the need for alternative treatment options is crucial. In fact, the 10-year survival rate for patients with metastatic melanoma is still less than 10% [44]. Cytotoxic chemotherapeutic drugs including alkylating agents (dacarbazine), platinum analogues (cisplatin, carboplatin) and anti-microtubular agents (PXT) have been used, alone or in combination, in metastatic melanoma treatment for more than three decades [26]. Combinations of cytotoxic agents may yield a slightly higher survival rate than monotherapy. However, these combinations are associated with higher toxicity [45]. Furthermore, melanoma usually relapses because most patients eventually develop resistance to the chemotherapeutic agents used, e.g. PXT [46]. Therefore, it is of the utmost importance to find new strategies that are safe, cost-effective, available, and able to sensitize melanoma cells or decrease the multiresistance to drugs without life-threatening toxic effects [47]. In this study, we aimed to determine whether Cl-IB-MECA is an agent able to potentiate the PXT cytotoxicity in human C32 melanoma cells, and if so, how this combination exerts its effects.

We demonstrated, for the first time, that cytotoxicity elicited by PXT is significantly increased by combining Cl-IB-MECA, at clinically relevant concentrations. This combination seems to act synergistically in disrupting membrane integrity, but also lysosomal and mitochondrial functionality. The proposed therapeutic combination showed morphological apoptotic signs and enhanced caspase 9, 8 and 3 activities, which seems also to be synergistically increased. It is unlikely that enhanced cytotoxicity and apoptosis observed is due to an additive effect, since potentiation of effects also occurs in cases where one of the combination constituents does not elicit an effect. Although Cl-IB-MECA is a very potent and selective A_3AR agonist, cytotoxicity promoted by this compound alone or in combination with PXT, in our melanoma model, does not involve AR activation (Fig. 6).

We found that incubating human C32 metastatic melanoma cells with increasing PXT concentrations (10, 25 and 50 ng/mL) or with 50 μM Cl-IB-MECA resulted in time-dependent cytotoxicity (Fig. 1). Similar PXT concentrations have been reported to cause tumour cell death [48]. Moreover, similar cytotoxic effects were also observed in A375 and NCTC 2544 melanoma cells [49]. PXT concentrations used in our study do not represent collateral toxicity as fortyfold higher concentrations were already tested without affecting human bone marrow cells viability [50]. Moreover, concentrations up to 80 ng/mL PXT were found in plasma ultra filtrate of cancer patients [51].

The initial Cl-IB-MECA concentration tested in the present study was previously reported, by our group, to promote marked cytotoxicity on human C32 metastatic melanoma cells [33]. Previous studies have also shown that micromolar concentrations of this synthetic and selective A_3AR agonist is able to cause tumour cell death [52,53]. Interestingly, A_3AR agonists do not inhibit normal cell growth, revealing differential effects on normal and malignant cells [32]. Indeed, these ligands can potentially act as cytoprotective agents, preventing, for example, myelotoxic effects of chemotherapy [34], caused by treatments with PXT [54].

We measured cytotoxic effects using three different cytotoxicity assays: LDH leakage, MTT reduction, and NR uptake assays. Results showed significant differences when PXT and Cl-IB-MECA were used alone. This observation can be explained by the fundamentals of each assay [55]. Different concentrations and time-points were performed in order to avoid over or under-estimation of cytotoxicity and to allow to distinguish between effects on specific organelles or general cytotoxicity. Based on the end-points and assays performed, we can summarize that PXT-induced mitochondria dysfunction occurs earlier than lysosomal injury and loss of membrane integrity. These results are in agreement with the reported PXT-induced mitochondrial stress on melanoma cells [56]. Furthermore, necrosis, as observed in our study, which involves disruption of cell membrane integrity, usually a late event, was already described to occur for high PXT concentrations in tumour cells [57]. On the other hand, it seems that, in human C32 metastatic melanoma cells, Cl-IB-MECA has a profound effect on lysosomes, accounting for the high cytotoxicity observed in the NR uptake assay. This fact seems to reveal that Cl-IB-MECA causes a severe lysosomal damage in C32 cells. This effect, to the best of our knowledge, has not been previously described. Results obtained with the combinations of PXT and Cl-IB-MECA show that these joined effects in human C32 metastatic melanoma cells leads to increased general cytotoxicity observed as severe rupture of cell membrane, mitochondrial dysfunction, and lysosomal damage.

PXT treated cells showed nuclear morphological changes (chromatin condensation and nuclear fragmentation) characteristic of apoptosis. Although increasing PXT concentrations did not lead to necrosis (evaluated by cytoplasmatic membrane rupture) at 24 h incubation, apoptosis features at this time-point were already observed, even for the lowest PXT concentration (10 ng/mL). Accordingly, it has been reported that PXT induces apoptosis in breast cancer cell lines at low concentrations, causing necrosis only for prolonged time exposures or higher concentrations [57]. In other models, namely A375 and BLM melanoma cells, PXT was also reported to induce apoptosis [56]. Concerning treatments with Cl-IB-MECA, it causes apoptosis in human C32 metastatic melanoma cells, in a time-dependent manner, as revealed by morphological studies (Fig. 2). This apoptotic effect has been previously described to occur in human renal, bladder, and lung cancer cells [58–60]. However it has never been reported to occur in melanoma cells. Studies with Cl-IB-MECA in melanoma cells described only the inhibition of melanoma cell proliferation induced by this A_3AR agonist [34,61]. For all combinations of PXT with Cl-IB-MECA, we found marked apoptosis features and a decrease in cell number per well, indicative of necrosis, these facts being in agreement with the overall cytotoxic effects observed with the combination of both agents (Fig. 2).

In view of the pronounced cytotoxic effects described above, we selected the lowest PXT concentration for further experiments

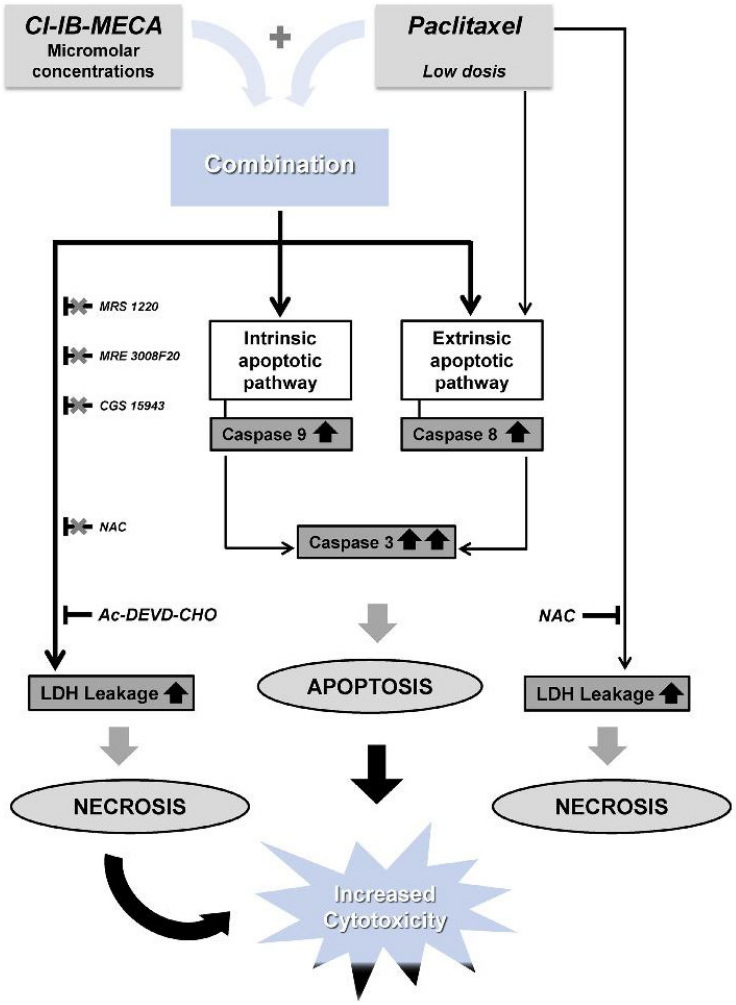

Fig. 6. Proposed mechanism for the interaction of Cl-IB-MECA (micromolar concentrations) with PXT (10 ng/mL) on human C32 melanoma cells. Combination of these two drugs enhances activity of intrinsic (caspase 9) and extrinsic (caspase 8) initiator caspase activities, and effector caspase 3 activity, triggering cell apoptosis. The prosecution of cellular injury leads to cellular disintegration. Selective (A3 adenosine receptor antagonists: MRS 1220 and MRS 3008F20) and nonselective adenosine receptor antagonists (CGS 15943) failed to prevent cell death caused by this pharmacological combination, showing that cytotoxicity does not involve adenosine receptors activation. Ac-DEVD-CHO, a caspase 3 inhibitor, only partially prevents this effect, indicating that caspase-dependent and/or -independent mechanisms can also be involved. The antioxidant *N*-acetyl-cysteine (NAC) partially blocks cell death only when cells are treated with PXT alone, showing that ROS are involved in the cytotoxicity induced by PXT but not in those induced by Cl-IB-MECA or the combinations.

(10 ng/mL) in combination with lower concentrations of Cl-IB-MECA (10 and 20 μM). These lower concentrations were not able to cause significant necrosis in C32 melanoma cells but a severe lysosomal damage was observed, suggesting that Cl-IB-MECA causes cytotoxic effects in lysosomes, prior to mitochondria dysfunction or necrosis (Fig. 3). In addition, we demonstrated that 20 μM (but not 10 μM) of Cl-IB-MECA led to apoptosis features. All combinations of Cl-IB-MECA with the lowest PXT concentration were still able to cause cytotoxicity (Fig. 3) and induce marked apoptosis in human C32 metastatic melanoma cells. This represents an important finding since decreasing PXT clinical doses could diminish/avoid possible collateral toxicity on healthy tissues.

Apoptosis in melanoma cells involves both extrinsic and intrinsic pathways that require mainly the activation of caspases [9]. Caspase 8 is related to the extrinsic pathway while caspase 9 mediates the intrinsic pathway. Once activated, caspase 8 and caspase 9 activate downstream caspase 3 that trigger cell apoptosis [8,12]. As such, we measured the activities of caspase 3, caspase 8 and caspase 9 and found that the lower concentrations of Cl-IB-MECA (10 and 20 μM) did not increase caspase activation in C32 cells. Similar results were described in thyroid carcinoma cells where 20 μM of this A_3AR agonist were not able to promote apoptosis, at 24 h [53]. For the highest Cl-IB-MECA concentration (50 μM) used alone, we only found activation of caspase 3 (Fig. 4), suggesting a possible involvement of other initiators caspases. Effector caspase 3 activation by this A_3AR agonist has been previously described in human glioma, lung, and thyroid cancer cells [40,53,62]. We also demonstrated that PXT, used alone, causes C32 apoptosis mainly through the extrinsic pathway, since treated

cells only revealed significant increases in caspase 8 and caspase 3 activities (Fig. 6). PXT has been reported to cause apoptosis in A375 and BLM melanoma cells through caspase 9 and 3 activation [56], in opposition to our results. However, during PXT-induced apoptosis in leukaemia CCRF-HSB-2 cells, caspase 3 is activated, independently of caspase 9 [63]. These differences can be ascribed to the reported cell type-specificity and concentration dependence [63,64]. We found, for all combination conditions, that the activity of the three proteases (caspase 9, 8 and 3) were increased, suggesting the involvement of both, intrinsic and extrinsic, apoptotic pathways in the apoptosis caused by combinations of Cl-IB-MECA with PXT (Fig. 6). Interestingly, activation of caspase 8 comparatively to caspase 9, seems to be more marked, in response to combinations of Cl-IB-MECA with PXT, suggesting that the apoptosis proceeds, mainly, via a caspase extrinsic mitochondrial pathway. Although combinations of Cl-IB-MECA with PXT have never been tested, activation of caspase 9, caspase 8, and caspase 3, caused by a combination of PXT with manumycin A (a farnesyltransferase inhibitor), has been previously described in thyroid cancer cells [65].

Several studies showed that TRAIL is able to promote both extrinsic and intrinsic apoptosis pathways in melanoma [15,66], suggesting that enhancement of melanoma cell sensitivity for death ligands, overcoming its natural resistance to TRAIL agonists [15], can represent a promising approach for melanoma treatment. Moreover, it has been demonstrated that Cl-IB-MECA enhanced TRAIL-mediated apoptosis in thyroid cancer cells [53] and addition of TRAIL agonists to PXT can cause apoptosis in 86M1 lung cancer cells [67]. Nevertheless, the importance of activating other pathways by Cl-IB-MECA (50 μM), PXT (10 ng/mL) and all combinations of Cl-IB-MECA with PXT was demonstrated by pre-treating cells with Ac-DEVD-CHO, a caspase 3 inhibitor. This inhibitor only partially prevented human C32 melanoma cell death, suggesting that other caspase-dependent and/or -independent cytotoxicity also occurs (Fig. 4D). Caspase-independent apoptosis mechanisms have also been described to occur after treatment with PXT, in several models of cancer cells [68,69].

We tried, therefore, to evaluate other mechanisms involved in the cytotoxicity of the potentially therapeutic relevant combination herein studied. To address this question, we tested all the conditions in the presence of two selective A_3AR antagonists (MRS 1220 and MRE 3008F20) since other groups showed that adenosine induced apoptosis in human colonic cancer cells, through activation of caspase 3, 8 and 9, occurs via ARs activation [70,71]. In our experimental conditions the cytotoxic effects elicited by Cl-IB-MECA and by all combinations of this selective A_3AR agonist with PXT were independent of A_3AR activation, as selective A_3AR antagonists failed to block the cytotoxic effects observed. It is well established that A_3AR agonists lose their selectivity at high concentrations [72] and Cl-IB-MECA could be activating other ARs. Experiments in the presence of the non-selective AR antagonist (CGS 15943) at a concentration able to block all AR subtypes [38]. We confirmed that cytotoxicity promoted by Cl-IB-MECA or PXT was not AR-mediated (Fig. 5). Although we have previously demonstrated that all AR subtypes (A_1, A_{2A}, A_{2B} and A_3) are present in human C32 metastatic melanoma cells [73], these results support the idea that the cytotoxic effect of Cl-IB-MECA and combinations of this selective A_3AR agonist with PXT most likely depend on the intracellular level of Cl-IB-MECA rather than on its interaction with ARs, as suggested by other authors [61]. In addition, Cl-IB-MECA led to apoptosis in leukemic (30 μM) and thyroid carcinoma ($\geq$ 10 μM) cells through an A_3AR-independent mechanism [52,74]. Moreover, for combinations of the AR antagonist and Cl-IB-MECA or PXT, cytotoxicity was even more pronounced (Fig. 5), suggesting that blocking of AR receptors prevents the binding of the natural ligand (probably endogenous adenosine) which could be, somehow, involved in the protection of human C32 melanoma cells. This putative protective role of endogenous adenosine observed in our study is in line with several works that ascribe tumour-promoting activity to endogenous adenosine [75,76].

PXT has also been described to increase the generation of ROS known to be involved in both apoptotic and necrotic cancer cell death [56]. NAC only alters the PXT-induced cytotoxicity in C32 cells (Table 1). NAC's protection in PXT-induced C32 cell death is in agreement with a recent work reporting that NAC modulates the cytotoxic effects of 1 μM of PXT on human A549 adenocarcinoma cells [77] and that PTX cytotoxic properties are oxidative stress related [56]. ROS generation does not seem to be involved in the cytotoxicity of any combination of Cl-IB-MECA with PXT nor with Cl-IB-MECA used alone, in opposition to what has been described in human glioma cells, where NAC (1 mM) blocked cell death promoted by 20 μM of Cl-IB-MECA [40]. The absence of this effect in C32 melanoma cells could be, at least in part, justified by the different model used in the two studies.

In conclusion, the present study provides evidence that cytotoxicity elicited by the combination between PXT and Cl-IB-MECA is significantly increased, comparatively to PXT alone, in clinically relevant concentrations, with the involvement of several mechanisms, including increased apoptosis, in melanoma human cells (Fig. 6). These findings may be the beginning for the future use of PXT in combination with Cl-IB-MECA as an anticancer strategy, to overcome the natural antiapoptotic characteristics of melanoma cells. Both compounds are clinically evaluated drugs with good potential. Nevertheless, future studies using clinically relevant animal models are needed to understand the potential of this combination in anticancer therapy towards melanoma.

Disclosure of interest

The authors declare that they have no conflicts of interest concerning this article.

Acknowledgments

Work was funded by FEDER through the Program Operational Competitiveness Factors – COMPETE and National Funds through FCT – Foundation for Science and Technology. ASS and VMC thank FCT for their PhD grant (SFRH/BD/64911/2009) and Post-doc grant (SFRH/BPD/63746/2009), respectively.

References

[1] Jemal A, Siegel R, Xu J, Ward E. Cancer statistics, 2010. CA Cancer J Clin 2010;60:277–300.
[2] Bandarchi B, Ma L, Navab R, Seth A, Rasty G. From melanocyte to metastatic malignant melanoma. Dermatol Res Pract 2010;2010:1–8.
[3] Chen KG, Valencia JC, Gillet JP, Hearing VJ, Gottesman MM. Involvement of ABC transporters in melanogenesis and the development of multidrug resistance of melanoma. Pigment Cell Melanoma Res 2009;22:740–9.
[4] Bradbury PA, Middleton MR. DNA repair pathways in drug resistance in melanoma. Anticancer Drugs 2004;15:421–6.
[5] Jiang CC, Lucas K, Avery-Kiejda KA, Wade M, deBock CE, Thorne RF, et al. Upregulation of Mcl-1 is critical for survival of human melanoma cells upon endoplasmic reticulum stress. Cancer Res 2008;68:6708–17.
[6] Soengas MS, Lowe SW. Apoptosis and melanoma chemoresistance. Oncogene 2003;22:3138–51.
[7] Fulda S, Debatin KM. Extrinsic versus intrinsic apoptosis pathways in anticancer chemotherapy. Oncogene 2006;25:4798–811.
[8] Elmore S. Apoptosis: a review of programmed cell death. Toxicol Pathol 2007;35:495–516.
[9] Sekulic A, Haluska Jr P, Miller AJ, Genebriera De Lamo J, Ejadi S, Pulido JS, et al. Malignant melanoma in the 21st century: the emerging molecular landscape. Mayo Clin Proc 2008;83:825–46.
[10] Green DR, Kroemer G. The pathophysiology of mitochondrial cell death. Science 2004;305:626–9.

[11] Saelens X, Festjens N, Vande Walle L, van Gurp M, van Loo G, Vandenabeele P. Toxic proteins released from mitochondria in cell death. Oncogene 2004;23:2861–74.
[12] Nagata S. Apoptotic DNA fragmentation. Exp Cell Res 2000;256:12–8.
[13] Walczak H, Krammer PH. The CD95 (APO-1/Fas) and the TRAIL (APO-2L) apoptosis systems. Exp Cell Res 2000;256:58–66.
[14] Chen G, Goeddel DV. TNF-R1 signaling: a beautiful pathway. Science 2002;296:1634–5.
[15] Berger A, Quast SA, Plotz M, Hein M, Kunz M, Langer P, et al. Sensitization of melanoma cells for death ligand-induced apoptosis by an indirubin derivative-Enhancement of both extrinsic and intrinsic apoptosis pathways. Biochem Pharmacol 2011;81:71–81.
[16] Kurbanov BM, Fecker LF, Geilen CC, Sterry W, Eberle J. Resistance of melanoma cells to TRAIL does not result from upregulation of antiapoptotic proteins by NF-kappaB but is related to downregulation of initiator caspases and DR4. Oncogene 2007;26:3364–77.
[17] Hengartner MO. The biochemistry of apoptosis. Nature 2000;407:770–6.
[18] Garcia-Saez AJ. The secrets of the Bcl-2 family. Cell Death Differ 2012; 19:1733–40.
[19] Hartman ML, Czyz M. Antiapoptotic proteins on guard of melanoma cell survival. Cancer Lett 2013;331:24–34.
[20] Hussein MR, Haemel AK, Wood GS. Apoptosis and melanoma: molecular mechanisms. J Pathol 2003;199:275–88.
[21] Jordan MA, Wilson L. Microtubules as a target for anticancer drugs. Nat Rev Cancer 2004;4:253–65.
[22] Steed H, Sawyer MB. Pharmacology, pharmacokinetics and pharmacogenomics of paclitaxel. Pharmacogenomics 2007;8:803–15.
[23] Wang F, Cao Y, Zhao W, Liu H, Fu Z, Han R. Taxol inhibits melanoma metastases through apoptosis induction, angiogenesis inhibition, and restoration of E-cadherin and nm23 expression. J Pharmacol Sci 2003;93:197–203.
[24] Sevko A, Michels T, Vrohlings M, Umansky L, Beckhove P, Kato M, et al. Antitumor effect of Paclitaxel is mediated by inhibition of myeloid-derived suppressor cells and chronic inflammation in the spontaneous melanoma model. J Immunol 2013;190:2464–71.
[25] Legha SS, Ring S, Papadopoulos N, Raber M, Benjamin RS. A phase II trial of taxol in metastatic melanoma. Cancer 1990;65:2478–81.
[26] Bhatia S, Tykodi SS, Thompson JA. Treatment of metastatic melanoma: an overview. Oncology 2009;23:488–96.
[27] Wiernik PH, Einzig AI. Taxol in malignant melanoma. J Natl Cancer Inst Monogr 1993;15:185–7.
[28] Kavallaris M, Annereau JP, Barret JM. Potential mechanisms of resistance to microtubule inhibitors. Semin Oncol 2008;35:S22–7.
[29] Cree IA, Neale MH, Myatt NE, de Takats PG, Hall P, Grant J, et al. Heterogeneity of chemosensitivity of metastatic cutaneous melanoma. Anticancer Drugs 1999;10:437–44.
[30] Kretzer IF, Maria DA, Maranhao RC. Drug-targeting in combined cancer chemotherapy: tumor growth inhibition in mice by association of paclitaxel and etoposide with a cholesterol-rich nanoemulsion. Cell Oncol 2012;35: 451–60.
[31] Zimpfer-Rechner C, Hofmann U, Figl R, Becker JC, Trefzer U, Keller I, et al. Randomized phase II study of weekly paclitaxel versus paclitaxel and carboplatin as second-line therapy in disseminated melanoma: a multicentre trial of the Dermatologic Co-operative Oncology Group (DeCOG). Melanoma Res 2003;13:531–6.
[32] Fishman P, Bar-Yehuda S, Madi L, Cohn I. A3 adenosine receptor as a target for cancer therapy. Anticancer Drugs 2002;13:437–43.
[33] Soares AF, Diniz C, Fresco P. A_3 adenosine receptor effects on malignant melanoma cells. FEBS J 2012;279(Suppl. 1):52–576.
[34] Fishman P, Bar-Yehuda S, Barer F, Madi L, Multani AS, Pathak S. The A3 adenosine receptor as a new target for cancer therapy and chemoprotection. Exp Cell Res 2001;269:230–6.
[35] Stemmer SM, Benjaminov O, Medalia G, Ciuraru NB, Silverman MH, Bar-Yehuda S, et al. CF102 for the treatment of hepatocellular carcinoma: a phase I/II, open-label, dose-escalation study. Oncologist 2013;18:25–6.
[36] Chodurek E, Orchel A, Gruchlik A, Aleksander E, Golabek K, Dzierzewicz Z. Valproic acid enhances cisplatin cytotoxicity in melanoma cells. Acta Pol Pharm 2012;69:1298–302.
[37] Gessi S, Merighi S, Varani K, Cattabriga E, Benini A, Mirandola P, et al. Adenosine receptors in colon carcinoma tissues and colon tumoral cell lines: focus on the A(3) adenosine subtype. J Cell Physiol 2007;211:826–36.
[38] Lakshmi S, Joshi PG. Activation of Src/kinase/phospholipase C/mitogen-activated protein kinase and induction of neurite expression by ATP, independent of nerve growth factor. Neuroscience 2006;141:179–89.
[39] Capela JP, da Costa Araujo S, Costa VM, Ruscher K, Fernandes E, Bastos Mde L, et al. The neurotoxicity of hallucinogenic amphetamines in primary cultures of hippocampal neurons. Neurotoxicology 2013;34:254–63.
[40] Kim TH, Kim YK, Woo JS. The adenosine A3 receptor agonist Cl-IB-MECA induces cell death through Ca(2)(+)/ROS-dependent down regulation of ERK and Akt in A172 human glioma cells. Neurochem Res 2012;37: 2667–77.
[41] Costa VM, Silva R, Ferreira R, Amado F, Carvalho F, de Lourdes Bastos M, et al. Adrenaline in pro-oxidant conditions elicits intracellular survival pathways in isolated rat cardiomyocytes. Toxicology 2009;257:70–9.
[42] Repetto G, del Peso A, Zurita JL. Neutral red uptake assay for the estimation of cell viability/cytotoxicity. Nat Protoc 2008;3:1125–31.
[43] Chae HJ, Park KM, Lee GY, Jeong GS, Park HR, Kim HM, et al. Je-chun-jun induced apoptosis of human cervical carcinoma HeLa cells. Acta Pharmacol Sin 2004;25:1372–9.
[44] Balch CM, Buzaid AC, Soong SJ, Atkins MB, Cascinelli N, Coit DG, et al. Final version of the American Joint Committee on Cancer staging system for cutaneous melanoma. J Clin Oncol 2001;19:3635–48.
[45] Mouawad R, Sebert M, Michels J, Bloch J, Spano JP, Khayat D. Treatment for metastatic malignant melanoma: old drugs and new strategies. Crit Rev Oncol Hematol 2010;74:27–39.
[46] van Herpen CM, Eskens FA, de Jonge M, Desar I, Hooftman L, Bone EA, et al. A phase Ib dose-escalation study to evaluate safety and tolerability of the addition of the aminopeptidase inhibitor tosedostat (CHR-2797) to paclitaxel in patients with advanced solid tumours. Br J Cancer 2010;103:1362–8.
[47] Rao RD, Holtan SG, Ingle JN, Croghan GA, Kottschade LA, Creagan ET, et al. Combination of paclitaxel and carboplatin as second-line therapy for patients with metastatic melanoma. Cancer 2006;106:375–82.
[48] Li W, Wang X, Lei P, Ye Q, Zhu H, Zhang Y, et al. Antisense RNA of survivin gene inhibits the proliferation of leukemia cells and sensitizes leukemia cell line to taxol-induced apoptosis. J Huazhong Univ Sci Technolog Med Sci 2008;28:1–5.
[49] Merighi S, Mirandola P, Varani K, Gessi S, Capitani S, Leung E, et al. Pyrazolo-triazolopyrimidine derivatives sensitize melanoma cells to the chemotherapic drugs: taxol and vindesine. Biochem Pharmacol 2003;66:739–48.
[50] Pessina A, Bonomi A, Cocce V, Invernici G, Navone S, Cavicchini L, et al. Mesenchymal stromal cells primed with paclitaxel provide a new approach for cancer therapy. PloS One 2011;6:e28321.
[51] Bulitta JB, Duffull SB, Landersdorfer CB, Kinzig M, Holzgrabe U, Stephan U, et al. Comparison of the pharmacokinetics and pharmacodynamic profile of carumonam in cystic fibrosis patients and healthy volunteers. Diagn Microbiol Infect Dis 2009;65:130–41.
[52] Morello S, Petrella A, Festa M, Popolo A, Monaco M, Vuttariello E, et al. Cl-IB-MECA inhibits human thyroid cancer cell proliferation independently of A3 adenosine receptor activation. Cancer Biol Ther 2008;7:278–84.
[53] Morello S, Sorrentino R, Porta A, Forte G, Popolo A, Petrella A, et al. Cl-IB-MECA enhances TRAIL-induced apoptosis via the modulation of NF-kappaB signalling pathway in thyroid cancer cells. J Cell Physiol 2009;221:378–86.
[54] Shin BS, Hong SH, Bulitta JB, Lee JB, Hwang SW, Kim HJ, et al. Physiologically based pharmacokinetics of zearalenone. J Toxicol Environ Health A 2009;72: 1395–405.
[55] Weyermann J, Lochmann D, Zimmer A. A practical note on the use of cytotoxicity assays. Int J Pharm 2005;288:369–76.
[56] Selimovic D, Hassan M, Haikel Y, Hengge UR. Taxol-induced mitochondrial stress in melanoma cells is mediated by activation of c-Jun N-terminal kinase (JNK) and p38 pathways via uncoupling protein 2. Cell Signal 2008;20: 311–22.
[57] Yeung TK, Germond C, Chen X, Wang Z. The mode of action of taxol: apoptosis at low concentration and necrosis at high concentration. Biochem Biophys Res Commun 1999;263:398–404.
[58] Nagaya H, Gotoh A, Kanno T, Nishizaki T. A3 adenosine receptor mediates apoptosis in in vitro RCC4-VHL human renal cancer cells by up-regulating AMID expression. J Urol 2013;189:321–8.
[59] Kanno T, Gotoh A, Fujita Y, Nakano T, Nishizaki T. A(3) adenosine receptor mediates apoptosis in 5637 human bladder cancer cells by G(q) protein/PKC-dependent AIF upregulation. Cell Physiol Biochem 2012;30:1159–68.
[60] Kanno T, Nakano T, Fujita Y, Gotoh A, Nishizaki T. Adenosine induces apoptosis in SBC-3 human lung cancer cells through A(3) adenosine receptor-dependent AMID upregulation. Cell Physiol Biochem 2012;30:666–77.
[61] Merighi S, Benini A, Mirandola P, Gessi S, Varani K, Leung E, et al. A3 adenosine receptor activation inhibits cell proliferation via phosphatidylinositol 3-kinase/Akt-dependent inhibition of the extracellular signal-regulated kinase 1/2 phosphorylation in A375 human melanoma cells. J Biol Chem 2005; 280:19516–2.
[62] Kamiya H, Kanno T, Fujita Y, Gotoh A, Nakano T, Nishizaki T. Apoptosis-related gene transcription in human A549 lung cancer cells via A(3) adenosine receptor. Cell Physiol Biochem 2012;29:687–96.
[63] Park SJ, Wu CH, Gordon JD, Zhong X, Emami A, Safa AR. Taxol induces caspase-10-dependent apoptosis. J Biol Chem 2004;279:51057–6.
[64] Le XF, Mao W, He G, Claret FX, Xia W, Ahmed AA, et al. The role of p27(Kip1) in dasatinib-enhanced paclitaxel cytotoxicity in human ovarian cancer cells. J Natl Cancer Inst 2011;103:1403–22.
[65] Pan J, Xu G, Yeung SC. Cytochrome c release is upstream to activation of caspase 9, caspase 8, and caspase 3 in the enhanced apoptosis of anaplastic thyroid cancer cells induced by manumycin and paclitaxel. J Clin Endocrinol Metab 2001;86:4731–40.
[66] Zhang XD, Franco A, Myers K, Gray C, Nguyen T, Hersey P. Relation of TNF-related apoptosis-inducing ligand (TRAIL) receptor and FLICE-inhibitory protein expression to TRAIL-induced apoptosis of melanoma. Cancer Res 1999;59:2747–53.
[67] Hunter TB, Manimala NJ, Luddy KA, Catlin T, Antonia SJ, Paclitaxel. TRAIL synergize to kill paclitaxel-resistant small cell lung cancer cells through a caspase-independent mechanism mediated through AIF. Anticancer Res 2011;31:3193–204.
[68] Huisman C, Ferreira CG, Broker LE, Rodriguez JA, Smit EF, Postmus PE, et al. Paclitaxel triggers cell death primarily via caspase-independent routes in the non-small cell lung cancer cell line NCI-H460. Clin Cancer Res 2002;8: 596–606.

[69] Ofir R, Seidman R, Rabinski T, Krup M, Yavelsky V, Weinstein Y, et al. Taxol-induced apoptosis in human SKOV3 ovarian and MCF7 breast carcinoma cells is caspase 3 and caspase 9 independent. Cell Death Differ 2002;9:636–42.
[70] Saito M, Yaguchi T, Yasuda Y, Nakano T, Nishizaki T. Adenosine suppresses CW2 human colonic cancer growth by inducing apoptosis via A(1) adenosine receptors. Cancer Lett 2010;290:211–5.
[71] Yasuda Y, Saito M, Yamamura T, Yaguchi T, Nishizaki T. Extracellular adenosine induces apoptosis in Caco-2 human colonic cancer cells by activating caspase 9/-3 via A(2a) adenosine receptors. J Gastroenterol 2009;44:56–65.
[72] Mlejnek P, Dolezel P, Frydrych I. Effects of synthetic A3 adenosine receptor agonists on cell proliferation and viability are receptor independent at micromolar concentrations. J Physiol Biochem 2013;69:405–17.
[73] Soares AF, Diniz C, Fresco P. Characterization of Adenosine Receptors in Human and Mouse Melanoma Cells<. In: 6th European Congress of Pharmacology; 2012.p. 276.
[74] Kim SG, Ravi G, Hoffmann C, Jung YJ, Kim M, Chen A, et al. p53-Independent induction of Fas and apoptosis in leukemic cells by an adenosine derivative, Cl-IB-MECA. Biochem Pharmacol 2002;63:871–80.
[75] Spychala J. Tumor-promoting functions of adenosine. Pharmacol Ther 2000;87:161–73.
[76] Stagg J, Smyth MJ. Extracellular adenosine triphosphate and adenosine in cancer. Oncogene 2010;29:5346–58.
[77] Lyle PA, Mitsopoulos P, Suntres ZE. N-acetylcysteine modulates the cytotoxic effects of Paclitaxel. Chemotherapy 2011;57:298–304.

4. MANUSCRIPT IV

Combination of Cl-IB-MECA with paclitaxel is a highly effective cytotoxic therapy causing mTOR-dependent autophagy and mitotic catastrophe on human melanoma cells

Accepted for publication in the *Journal of Cancer Research and Clinical Oncology*.
DOI: 10.1007/s00432-014-1645-z.

J Cancer Res Clin Oncol
DOI 10.1007/s00432-014-1645-z

ORIGINAL ARTICLE – CANCER RESEARCH

Combination of Cl-IB-MECA with paclitaxel is a highly effective cytotoxic therapy causing mTOR-dependent autophagy and mitotic catastrophe on human melanoma cells

Ana S. Soares · Vera M. Costa · Carmen Diniz · Paula Fresco

Received: 26 February 2014 / Accepted: 7 March 2014

Abstract
Purpose Metastatic melanoma is the deadliest form of skin cancer. It is highly resistant to conventional therapies, particularly to drugs that cause apoptosis as the main anticancer mechanism. Recently, induction of autophagic cell death is emerging as a novel therapeutic target for apoptotic-resistant cancers. We aimed to investigate the underlying mechanisms elicited by the cytotoxic combination of 2-chloro-*N*(6)-(3-iodobenzyl)-adenosine-5′-*N*-methyl-uronamide (Cl-IB-MECA, a selective A_3 adenosine receptor agonist; 10 μM) and paclitaxel (10 ng/mL) on human C32 and A375 melanoma cell lines.
Methods Cytotoxicity was evaluated using 3-(4,5-dimethylthiazol-2-yl)-2,5-diphenyl tetrazolium bromide reduction, neutral red uptake, and lactate dehydrogenase leakage assays, after 48-h incubation. Autophagosome and autolysosome formation was detected by fluorescence through monodansylcadaverine-staining and CellLight® Lysosomes-RFP-labelling, respectively. Cell nuclei were visualized by Hoechst staining, while levels of p62 were determined by an ELISA kit. Levels of mammalian target of rapamycin (mTOR) and the alterations of microtubule networks were evaluated by immunofluorescence.
Results We demonstrated, for the first time, that the combination of Cl-IB-MECA with paclitaxel significantly increases cytotoxicity, with apoptosis and autophagy the major mechanisms involved in cell death. Induction of autophagy, using clinically relevant doses, was confirmed by visualization of autophagosome and autolysosome formation, and downregulation of mTOR and p62 levels. Caspase-dependent and caspase-independent mitotic catastrophe evidencing micro- and multinucleation was also observed in cells exposed to our combination.
Conclusions The combination of Cl-IB-MECA and paclitaxel causes significant cytotoxicity on two melanoma cell lines through multiple mechanisms of cell death. This multifactorial hit makes this therapy very promising as it will help to avoid melanoma multiresistance to chemotherapy and therefore potentially improve its treatment.

Keywords Melanoma · Autophagy · mTOR · Apoptosis · Mitotic catastrophe

Abbreviations

Ac-DEVD-CHO	*N*-Ac-Asp-Glu-Val-Asp-CHO
Cl-IB-MECA	2-Chloro-*N*(6)-(3-iodobenzyl)-adenosine-5′-*N*-methyl-uronamide
CTR	Control
DMSO	Dimethyl sulfoxide
DMEM-HG	Dulbecco's modified Eagle's medium—high glucose
FBS	Foetal bovine serum
LAMP1	Lysosomal-associated membrane protein 1
LDH	Lactate dehydrogenase

A. S. Soares · C. Diniz · P. Fresco
REQUIMTE/Laboratório de Farmacologia, Departamento de Ciências do Medicamento, Faculdade de Farmácia, Universidade do Porto, Porto, Portugal

V. M. Costa
REQUIMTE/Laboratório de Toxicologia, Departamento de Ciências Biológicas, Faculdade de Farmácia, Universidade do Porto, Porto, Portugal

P. Fresco (✉)
Departamento de Farmacologia, Faculdade de Farmácia, Universidade do Porto, Rua de Jorge Viterbo Ferreira, 228, 4050-313 Porto, Portugal
e-mail: pfresco@ff.up.pt

Published online: 25 March 2014

LY294002	2-(4-Morpholinyl)-8-phenyl-4*H*-1-benzopyran-4-one hydrochloride
3-MA	3-Methyladenine
MC	Mitotic catastrophe
MDC	Monodansylcadaverine
mTOR	Mammalian target of rapamycin
MTT	3-(4,5-Dimethylthiazol-2-yl)-2,5-diphenyl tetrazolium bromide
NAC	*N*-acetylcysteine
NR	Neutral red
PI3K	Phosphoinositide 3-kinase
PXT	Paclitaxel
RFP	Red fluorescent protein
ROS	Reactive oxygen species
SQSTM1	Sequestosome 1

Introduction

Metastatic melanoma is the deadliest form of skin cancer, and its incidence is globally rising (Jemal et al. 2010). This aggressive disease has an extremely poor prognosis because it is highly resistant to conventional therapies (Tawbi and Kirkwood 2007). The overall survival of patients with metastatic melanoma is lower than 2 years (Jemal et al. 2010). Indeed, it is the most treatment-resistant human cancer (de Souza et al. 2012), remaining one of the greatest challenges in oncotherapy.

Most chemotherapeutic drugs are described to cause cell death through apoptosis (Fulda and Debatin 2006). Apoptosis is a highly structured and orchestrated cell suicide mechanism induced by physiological or pathological stimuli and controlled by specific genes and multiple signalling pathways (Elmore 2007). Activation of caspase-dependent and/or caspase-independent processes results in apoptosis that include features of cell shrinkage, nuclear fragmentation, chromatin condensation, and membrane blebbing (Hengartner 2000).

Recently, increasing evidence revealed that some chemotherapeutic drugs can also act by inducing mitotic catastrophe (MC), which is characterized by micro- and multinucleated cells, resulting in cell death (Hanahan and Weinberg 2011; Vakifahmetoglu et al. 2008). It is being reported that MC shares several biochemical hallmarks with apoptosis, in particular caspase activation, being proposed as a special case of apoptosis (Castedo et al. 2004b). However, it is not yet well established whether MC results in death that requires caspase activation or not (Mansilla et al. 2006), and the clear definition of the concepts of MC is still missing (Vakifahmetoglu et al. 2008). Nevertheless, induction of MC is an attractive strategy for developing new anticancer therapies (Hung et al. 2013).

It is well accepted that the limited success of most current therapeutic strategies used in metastatic melanoma is due, at least in part, to cancer cells ability in escaping apoptosis, thus leading to drug resistance (Soengas and Lowe 2003). Drugs that activate pathways overcoming melanoma's apoptosis resistance and inducing cell death have, therefore, great potential for melanoma therapeutic interventions. Recently, another type of cell death, autophagy, has become an alternative approach to anticancer therapy (Hanahan and Weinberg 2011), as pro-autophagic drugs seem to represent a novel therapeutic weapon for apoptosis-resistant cancers (Tsujimoto and Shimizu 2005).

Autophagy is mainly a self-destructive process that degrades intracellular structures in response to stress, contributing for both cell survival, in adverse conditions (nutrient starvation or metabolic stress), and conversely cell death (White and DiPaola 2009). This process begins with the sequestration of cytoplasmic material (cargo) in double-membrane vacuoles called autophagosomes or autophagic vacuoles, which undergo maturation, including fusion with lysosomes to form autolysosomes, where the cargo is degraded (Kung et al. 2011).

The AKT/mammalian target of rapamycin (mTOR) signalling pathway promotes tumour cell proliferation and resistance to drug-induced apoptosis (LoPiccolo et al. 2008), being highly active in several cancers including melanoma (Dai et al. 2005). This pathway is also a key negative regulator of autophagy (Jung et al. 2010). In fact, several studies have reported the importance of phosphoinositide 3-kinase (PI3K)/AKT/mTOR pathway in regulating autophagy (Jung et al. 2010; Saiki et al. 2011), although, at this point, little is known in cancer regulation. Class I and class III PI3K regulate autophagy differently: class I PI3K/AKT/mTOR pathway inhibits autophagy and class III PI3K, by contrast, promotes the sequestration of cytoplasmic material that occurs during autophagy, at the trans-Golgi network (Liu et al. 2013; Kihara et al. 2001). Currently, it has been proposed that the use of PI3K/AKT/mTOR pathway inhibitors may be a successful strategy to treat melanoma (Gao et al. 2013).

Evidence suggests that tumour cells can undergo both apoptosis and autophagic cell death in response to therapy because these pathways might be triggered by the same signal (Maiuri et al. 2007). However, the precise crosstalk regarding the relation between these two cell death mechanisms is complex and sometimes contradictory (Shen et al. 2011). Therefore, understanding the mechanisms underlying apoptosis–autophagy interaction is crucial for the development of therapeutic strategies to improve the efficacy of anticancer agents.

Recently, we provided evidence that simultaneous treatment with Cl-IB-MECA (2-chloro-*N*(6)-(3-iodobenzyl)-adenosine-5′-*N*-methyl-uronamide, a selective A_3 adenosine receptor agonist) and paclitaxel (PXT) potentiates human C32 melanoma cells cytotoxicity, mainly through

apoptotic pathways (Soares et al. 2013), however, through A_3 adenosine receptor-independent mechanisms. The combination revealed a good potential on melanoma treatment since it allows PTX doses reduction and consequently the decrease in adverse effects and multiresistance recurrence in melanoma. However, in this previous work, not all cytotoxicity induced by Cl-IB-MECA and PXT combinations could be explained just by apoptosis-mediated cell death. In the present work, efforts were made in order to elucidate the possible involvement of other cell death pathways, namely autophagy. To address this question, we investigated the cytotoxic effects induced by Cl-IB-MECA (10 μM) and PXT (10 ng/mL), alone or in combination, on two human melanoma cell lines (C32 and A375 cells) as to increase knowledge on this potentially useful anticancer therapeutic strategy.

Materials and methods

Chemicals

All reagents used were of analytical grade. Cl-IB-MECA and 3-methyladenine (3-MA) were obtained from Tocris Bioscience (Bristol, UK). Lactate dehydrogenase (LDH) assay kit was purchased from Promega Bioscience (VWR, Porto, Portugal). Caspase inhibitor (*N*-Ac-Asp-Glu-Val-Asp-CHO, Ac-DEVD-CHO) was purchased from Calbiochem (Millipore, Interface, Amadora, Portugal). Sequestosome 1(SQSTM1)/p62 ELISA kit was purchased to Cell Signaling Technology (Izasa, Lisboa, Portugal). Bio-Rad RC DC protein assay kit was purchased to Biorad (Amadora, Portugal). Foetal bovine serum (FBS), Glutamax, trypsin/EDTA, Alexa Fluor® 594 (anti-mouse), Alexa Fluor® 568 (anti-goat) and CellLight® Lysosomes-RFP-BacMam 2.0 were obtained from Invitrogen (Alfagene, Carcavelos, Portugal). Goat anti-mTOR antibody was purchased to Santa Cruz Biotechnology (Reagente 5, Porto, Portugal). Dulbecco's modified Eagle's medium-high glucose (DMEM-HG), penicillin/streptomycin (10 000 U/mL), PXT, LY294002, 3-(4,5-dimethylthiazol-2-yl)-2,5-diphenyl tetrazolium bromide (MTT), neutral red (NR), monodansylcadaverine (MDC), Hoechst 33258, mouse anti-α-tubulin antibody, dimethyl sulfoxide (DMSO), *N*-acetylcysteine (NAC), and all other chemicals were purchased from Sigma-Aldrich (Sigma-Aldrich-Química SA, Sintra, Portugal) of the highest purity available.

Cell culture

Human C32 and A375 metastatic melanoma cells obtained from ECACC to SIGMA (Sigma-Aldrich-Química SA, Sintra, Portugal) were used in this study. Cells were seeded in DMEM-HG medium with 10 % of FBS, 1 % of a mixture of penicillin/streptomycin and 1 % of Glutamax, pH 7.4. Cells were incubated at 37 °C in a humidified atmosphere (95 % air; 5 % CO_2). For cell culture maintenance, cells were grown in monolayer and sub-cultivated twice a week. Cell passaging was done by trypsinization. All experiments were carried out with cells at 70–80 % confluence and from batches with passage numbers lower than 50.

Cell treatment

Cells were prepared using an initial cell density of 3.0×10^4 cells/cm^2 (A375 cells) and 5.0×10^4 cells/cm^2 (C32 cells), and allowed to attach for 24 h. Cells were then treated with Cl-IB-MECA [10 μM (Soares et al. 2013)] and/or PXT [10 ng/mL (Soares et al. 2013)] for 24 or 48 h. When the class III PI3K inhibitor, 3-MA [2.5 mM (Santoni et al. 2013)], and/or the caspase inhibitor, Ac-DEVD-CHO [50 μM (Soares et al. 2013)], were used to prevent autophagy and/or apoptosis, respectively, they were added 1 h prior to the addition of other compounds. The antioxidant NAC [1 mM (Martins et al. 2013)], when used, was also added 1 h prior to the addition of Cl-IB-MECA and/or PXT. During all the experimental period, cells were maintained at 37 °C with 5 % CO_2.

Cytotoxicity assays

Cells were seeded in 96-well plates and treated as in section *Cell treatment*. Vehicle (cells exposed to DMSO at maximum final concentration of 0.1 % v/v) and blank (without cells) wells were also incubated at 37 °C, for 48 h. Treatments, vehicle, and blank conditions were performed in triplicate, initiated, and processed in parallel.

MTT reduction assay

Mitochondrial function was evaluated as an index of cell cytotoxicity, since mitochondrial dehydrogenases of living cells can reduce the MTT (yellow) to formazans (Mosmann 1983). At the end of the treatment incubation period (48 h), cells were processed as previously described by our group (Soares et al. 2013).

NR uptake assay

Lysosomal functionality was spectrophotometrically evaluated and represented as the percentage of NR dye incorporated in the cells. This dye easily penetrates viable cells and accumulates intracellularly in lysosomes (Repetto et al. 2008). At the end of treatment incubation period (48 h), cells were processed as already described by us (Soares et al. 2013). Cells labelled with NR were also analysed by an AE2000 Motic® inverted microscope coupled to a

Moticam 5 digital camera (Spectra Services, VWR International, Carnaxide, Portugal). Images from six random fields/well were captured (magnification of 400×).

LDH leakage

Cell death (measurement of membrane integrity evaluated by the percentage of LDH released over total LDH) was assessed using a LDH assay kit according to the manufacturer's instructions. At the end of the treatment incubation period (48 h), cells were processed as previously described (Soares et al. 2013).

Autophagosome and lysosome staining

Cells were seeded in chamber slide systems and treated according to section *Cell treatment*. The PI3K (class I) inhibitor, LY294002 [50 μM (Xing et al. 2008)], was used as a positive control for autophagy. Lysosomal morphology was evaluated after the addition of a lysosomal associated membrane protein 1-red fluorescent protein (LAMP1-RFP) fusion construct (CellLight® Lysosomes-RFP; 20 particles/cell), according to the manufacturer's instructions. After 48-h incubation with the compounds, media was removed and cells were incubated with 0.05 mM MDC (autofluorescent dye) in PBS at 37 °C for 10 min (protected from light) (Biederbick et al. 1995). Cells were then washed with PBS and analysed by a Nikon Eclipse E400 fluorescence microscope coupled to a digital camera (Nikon Digital Sight DS-5Mc, New Jersey, USA). Images from ten random fields *per* condition were captured (magnification of 1,000×). Merged images were obtained using Adobe Photoshop CS5 software. MDC-stained autophagosomes are displayed in green and LAMP1-stained lysosomes in red.

Determination of p62 levels

Cells were seeded in 6-well plates. Twenty-four hours after cell treatment (section *Cell treatment*), p62 levels were evaluated using the p62 ELISA kit, according to the manufacturer's instructions. The p62 levels were only assessed in the conditions where the MDC-stained autophagosomes were observed. LY294002 [50 μM (Xing et al. 2008)] was used as a positive control for autophagy. The levels of p62 were expressed as optic density (OD) *per* amount of protein.

Protein content determination

Protein content of cellular fractions, in total cell lysates, for p62 assays was determined using the Bio-Rad RC DC protein assay kit, in accordance with the manufacturer's instructions. Stock solutions of bovine serum albumin were used as standards.

Immunofluorescence assay

Cells were seeded in chamber slide systems and treated as in section *Cell treatment*. LY294002 [50 μM (Xing et al. 2008)] was used as a positive control for autophagy. After cell treatment, cells were washed with PBS and fixed in 4 % paraformaldehyde (10 min, room temperature). Cells were blocked and permeabilized with 1 % (v/v) FBS containing 0.25 % (v/v) Tween 20, for 30 min, at 4 °C. Next, cells were incubated with the primary antibodies, goat anti-mTOR (1:200), or mouse anti-α tubulin (1:500), depending on the experiment goal, overnight at 4 °C. After washing with PBS, cells were incubated with Hoechst 33258 (5 μg/mL) for 15 min and then incubated with the respective secondary antibodies, Alexa Fluor® 568 (1:1,500) or Alexa Fluor® 594 (1:1,000) for 1 h (room temperature, protected from light). Finally, slides were washed with PBS and mounted with PBS/glycerol solution (3:1). Cells were examined in a Nikon Eclipse E400 fluorescence microscope coupled to a digital camera (Nikon Digital Sight DS-5Mc, New Jersey, USA). Images from ten random fields *per* condition were captured (magnification of 1,000×). Merged images were obtained using Adobe Photoshop CS5 software. Depending on the experiment performed, Alexa Fluor® 568-stained mTOR and Alexa Fluor® 594-stained α-tubulin (microtubules) are displayed in red. Hoechst 33258-labelled nuclei are displayed in blue. Image processing for quantification of cell nuclei with typical morphologic mitotic catastrophe (MC) features (micro- and multinucleated cells) (Vakifahmetoglu et al. 2008) was done using ImageJ software. Ratios of MC and normal nuclei were obtained using images from ten random fields *per* condition (magnification of 400×).

Statistical analysis

Results are presented as mean ± SEM for n experiments. Statistical comparisons between groups were performed with one-way ANOVA, after Shapiro–Wilk test normality evaluation. Statistical significance was accepted at p values <0.05. The Student–Newman–Keuls post hoc test was used once a significant p was achieved.

Results

Cl-IB-MECA in combination with PXT causes cytotoxicity in human metastatic melanoma cells

Human C32 and A375 melanoma cells were treated with 10 μM of Cl-IB-MECA (Cl10), 10 ng/mL of PXT (PXT10), and the combination of the two (Cl10 + PXT10), for 48 h (Fig. 1).

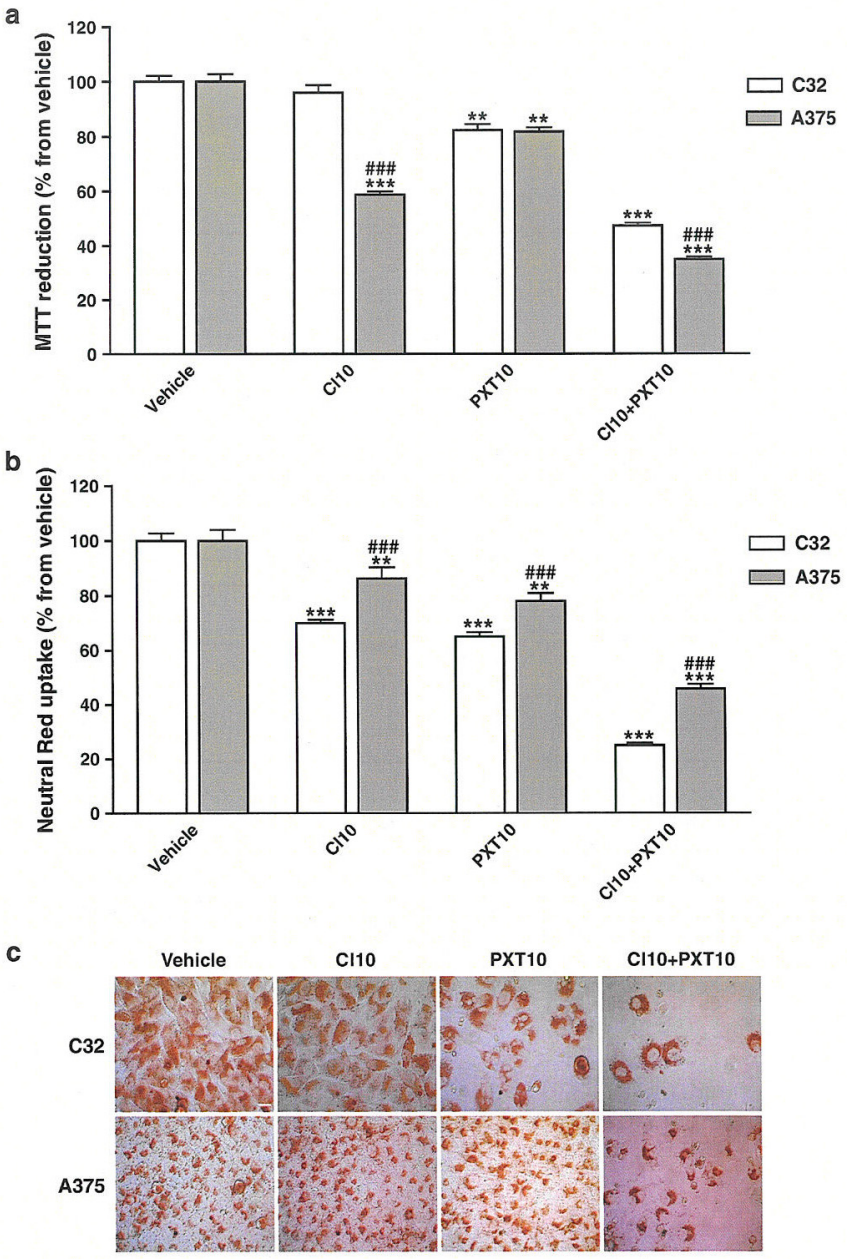

Fig. 1 Cytotoxic effects elicited by Cl-IB-MECA (10 μM; Cl10) and/or PXT (10 ng/mL; PXT10) on human C32 (*white bars*) and A375 (*grey bars*) melanoma cells, after 48-h incubation. DMSO (final concentration of 0.1 % v/v) in DMEM-HG was used as vehicle. **a** Results of MTT reduction (% from vehicle) are presented as mean ± SEM, $n = 12$ of 4 independent experiments. Significant differences (one-way ANOVA test, followed by the Student–Newman–Keuls post hoc test): $^{**}p < 0.01$ versus vehicle; $^{***}p < 0.001$ versus vehicle; $^{\#\#\#}p < 0.001$ versus C32 cells for the same condition. **b** Results of NR uptake (% from vehicle) are presented as mean ± SEM, $n = 12$ of 4 independent experiments. Significant differences (one-way ANOVA test, followed by the Student–Newman–Keuls post hoc test): $^{**}p < 0.01$ versus vehicle; $^{***}p < 0.001$ versus vehicle; $^{\#\#\#}p < 0.001$ versus C32 cells for the same condition. **c** Representative photographs of C32 and A375 cells after NR staining. Scale bar, 10 μm

Results from the MTT reduction assay showed that mitochondrial function of cells incubated with CI10 had different outcomes in C32 and A375 cells (Fig. 1a): No cytotoxicity was observed in C32 cells, whereas significant mitochondrial dysfunction occurred on A375 cells. However, both cell lines treated with PXT10 demonstrated a significant and similar decrease in mitochondrial activity (Fig. 1a). When combined, Cl10 and PXT10 (Cl10 + PXT10) caused a higher cytotoxicity in both cell lines, although more pronounced on A375 cells, comparatively to the effect caused by this treatment on C32 cells (Fig. 1a).

Active lysosomal uptake (NR uptake assay) was also evaluated in the conditions described above (Fig. 1b). Cl10

and PXT10 were able to reduce lysosomal NR uptake in both cell lines, although with a higher NR uptake impairment on C32 cells. Moreover, lysosomal uptake was clearly impaired when the combination of Cl10 with PXT10 (Cl10 + PXT10) was tested in both melanoma cell lines, when compared to the effects elicited by the individual compounds.

The cytotoxic effects observed with the NR uptake were also visualized (Fig. 1c). Images of A375 and, particularly, of C32 cells revealed that NR uptake was clearly compromised in all treatment groups when compared to the vehicle. In fact, especially in C32 cells, it is observable in Cl10 that although a similar number of cells *per* field is seen, NR uptake is clearly diminished. For both cell lines, the combination of drugs caused a significant decrease in the number of cells *per* field, whereas incubation of cells with individual compounds affects NR uptake without significantly compromising cells integrity (Fig. 1c).

Cell death elicited by the combination of Cl-IB-MECA and PXT is mediated by autophagy and apoptosis with dissimilar importance on C32 and A375 cells

To explore the role of autophagy and/or apoptosis in the cytotoxicity induced by Cl-IB-MECA (10 μM), PXT (10 ng/mL), the combination of both human C32 and A375 melanoma cells were incubated with these compounds, in the absence or in the presence of an autophagy inhibitor, 3-MA (2.5 mM) and/or a caspase inhibitor, Ac-DEVD-CHO (50 μM), as described in the Methods section. Cell death (LDH leakage assay) was assessed at 48 h (Fig. 2). Although Cl10 did not lead to C32 cell death (Fig. 2a), this effect was statistically significant on A375 cells (Fig. 2b). Moreover, pre-treatment of A375 cells with the caspase inhibitor (Ac-DEVD-CHO) did not prevent cell death, while the autophagy inhibitor (3-MA) completely blocked A375 cell death induced by Cl10. These data suggest that cytotoxicity caused by Cl10 in A375 cells is mediated only by autophagy (Fig. 2b).

Incubations of C32 and A375 cells with PXT10 induced significant cell death, when compared to vehicle. Furthermore, pre-incubation of cells with the caspase inhibitor (Ac-DEVD-CH) completely prevented cell death in both cell lines (Fig. 2), whereas 3-MA (autophagy inhibitor) had no effect upon the PXT10 cytotoxic effect. This result indicates that the cytotoxic effect induced by PXT10 in melanoma cells occurs through caspase-dependent apoptotic events.

Cell death was more pronounced when melanoma cells were treated simultaneously with Cl10 and PXT10 (Cl10 + PXT10), comparatively to vehicle and individual treatments at 48 h (Fig. 2). Moreover, the combination of drugs caused a higher increment of LDH leakage on C32 (Fig. 2a) than on A375 cells (Fig. 2b). Pre-treatment of C32 cells with the caspase inhibitor (Ac-DEVD-CHO) significantly attenuated cytotoxicity (Fig. 2a) but did not totally abrogate this effect, suggesting that apoptosis is not the only event involved in cytotoxicity occurring in C32 cells. Cells were also incubated with the combination of Cl10 and PXT10, after treatment with 3-MA, an autophagy inhibitor. This compound demonstrated to be more efficient in preventing LDH leakage than the caspase inhibitor, but total ablation of the cytotoxic effect was only achieved when C32 cells were pre-treated simultaneously with both inhibitors (Fig. 2a). These results suggest that Cl10 with PXT10 caused C32 cell death through activation of both autophagic and apoptotic events, with autophagy activation having the major role in cell death.

A375 cells were treated in the previously referred conditions and for the same incubation time (Fig. 2b). The caspase inhibitor (Ac-DEVD-CHO) or the autophagy inhibitor (3-MA) were only able to partially, and to a similar extent, prevent LDH leakage caused by Cl10 in combination with PXT10. Moreover, the mixture of inhibitors did not completely block the cytotoxic effect elicited by the combination of Cl10 and PXT10 (Fig. 2a). These results suggest that although autophagic and apoptotic cell deaths seem to contribute equally for the cytotoxic effect caused by Cl10 in combination with PXT10, these are not the only pathways involved, since total prevention of A375 cell death was not achieved (Fig. 2b).

Importantly, the simultaneous treatment with the two inhibitors did not cause any cellular cytotoxicity, indicating that autophagy and apoptosis are not constitutively activated in human C32 or A375 melanoma cells (Fig. 2).

Autophagosomes fusion with lysosomes is induced by Cl-IB-MECA on A375 cells and by the combination of Cl-IB-MECA with PXT on C32 and A375 cells

Human C32 and A375 melanoma cells were incubated with Cl-IB-MECA (10 μM, Cl10), PXT (10 ng/mL, PXT10), and the combination of both (Cl10 + PXT10), in the absence or in the presence of an autophagy inhibitor, 3-MA (2.5 mM), for 48 h, as described in the Methods section. LY294002 (50 μM) was used as a positive control for autophagy. Imaging of autophagosomes was done by using the fluorescent dye MDC and showed that, in C32 cells treated with Cl10 + PXT10, in A375 cells treated with Cl10 and Cl10 + PXt10 (conditions where there was prior indication of autophagy assessed by LDH assay, Fig. 2), and in both cell lines treated with the positive control of autophagy LY294002, autophagosomes appeared as green larger condensed structures (white arrows, Fig. 3). Similarly, the spatial distribution of lysosomes (Lyso-RFP) is altered after these treatments, showing larger red structures

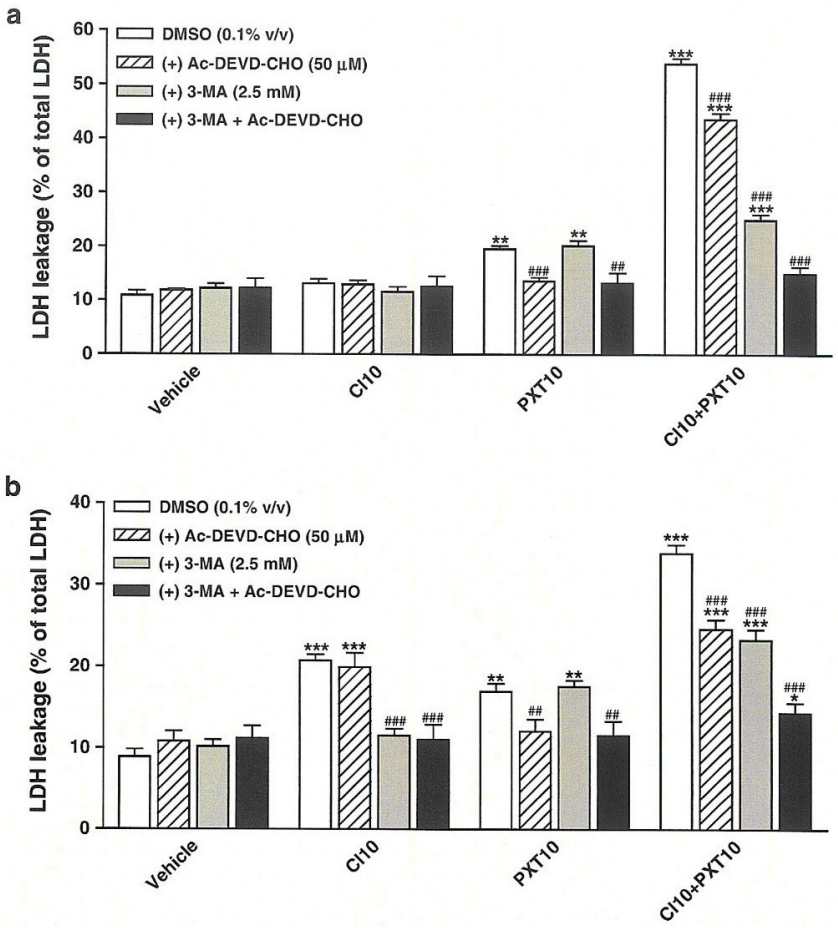

Fig. 2 Cl-IB-MECA in combination with PXT caused melanoma cell death mediated by apoptosis and autophagy. **a** C32 and **b** A375 melanoma cells treated with Cl-IB-MECA (10 μM; Cl10) and/or PXT (10 ng/mL; PXT10), after 48-h incubation, in the absence (*white bars*) or in the presence of the caspase inhibitor, Ac-DEVD-CHO (50 μM; *hatched bars*), the autophagy inhibitor, 3-MA (2.5 mM, *grey bars*), or both (*black bars*). DMSO (final concentration of 0.1 % v/v) in DMEM-HG was used as vehicle. Results of LDH leakage (% of total LDH) are presented as mean ± SEM, $n = 12$ of 4 independent experiments. Significant differences (one-way ANOVA test, followed by the Student–Newman–Keuls post hoc test): $^{*}p < 0.05$ versus vehicle; $^{**}p < 0.01$ versus vehicle; $^{***}p < 0.001$ versus vehicle; $^{\#\#}p < 0.01$ versus same condition with DMSO (0.1 % v/v); $^{\#\#\#}p < 0.001$ versus same condition with DMSO (0.1 % v/v)

(white arrows, Fig. 3). Formation of autolysosomes, as a result of the fusion between autophagosomes with lysosomes, was confirmed by observation of co-localization of the structures in the above conditions (yellow structures in merged images, white arrows, Fig. 3).

On the contrary, in conditions where there was no indication of autophagy (Fig. 2), autophagosomes were visualized as small punctate scattered structures (dots). Moreover, in those conditions (vehicle, 3-MA, Cl10 and PXT10 for C32 cells; vehicle, 3-MA, PXT10 for A375), lysosome labelling was very tenuous and yellow structures (autolysosomes) were not observed on merged images (Fig. 3). These findings indicate that, in these cell treatments, the occurrence of autophagy can be discarded.

Images from cells pre-incubated with the autophagy inhibitor 3-MA, showed decreased MDC and lysosomal staining, suggesting that A375 cells treated with Cl10 and both lines treated with the combination Cl10 + PXT10 present autophagic cell death, to some extent.

p62 levels are decreased in Cl-IB-MECA-induced A375 autophagic cell death and in Cl-IB-MECA plus PXT-induced autophagic melanoma cell death in both cell lines

Considering the fact that p62 is rapidly degraded during autophagy, analysis of its intracellular levels was performed by an ELISA kit at 24 h, as to confirm the involvement of autophagic cell death in the conditions where autophagy is suspected to occur, based on the results obtained by LDH leakage and MDC staining assays. C32 cells were incubated with the combination of Cl10 with PXT10 (Cl10 + PXT10), and A375 cells with Cl10 and Cl10 + PXT10 in the absence or in the presence of an autophagy inhibitor, 3-MA (2.5 mM), for 24 h, as described in methods section. LY294002 (50 μM) was, once more, used as a positive control for autophagy.

C32 and A375 human melanoma cell lines have similar basal levels of p62 protein and cell treatments with

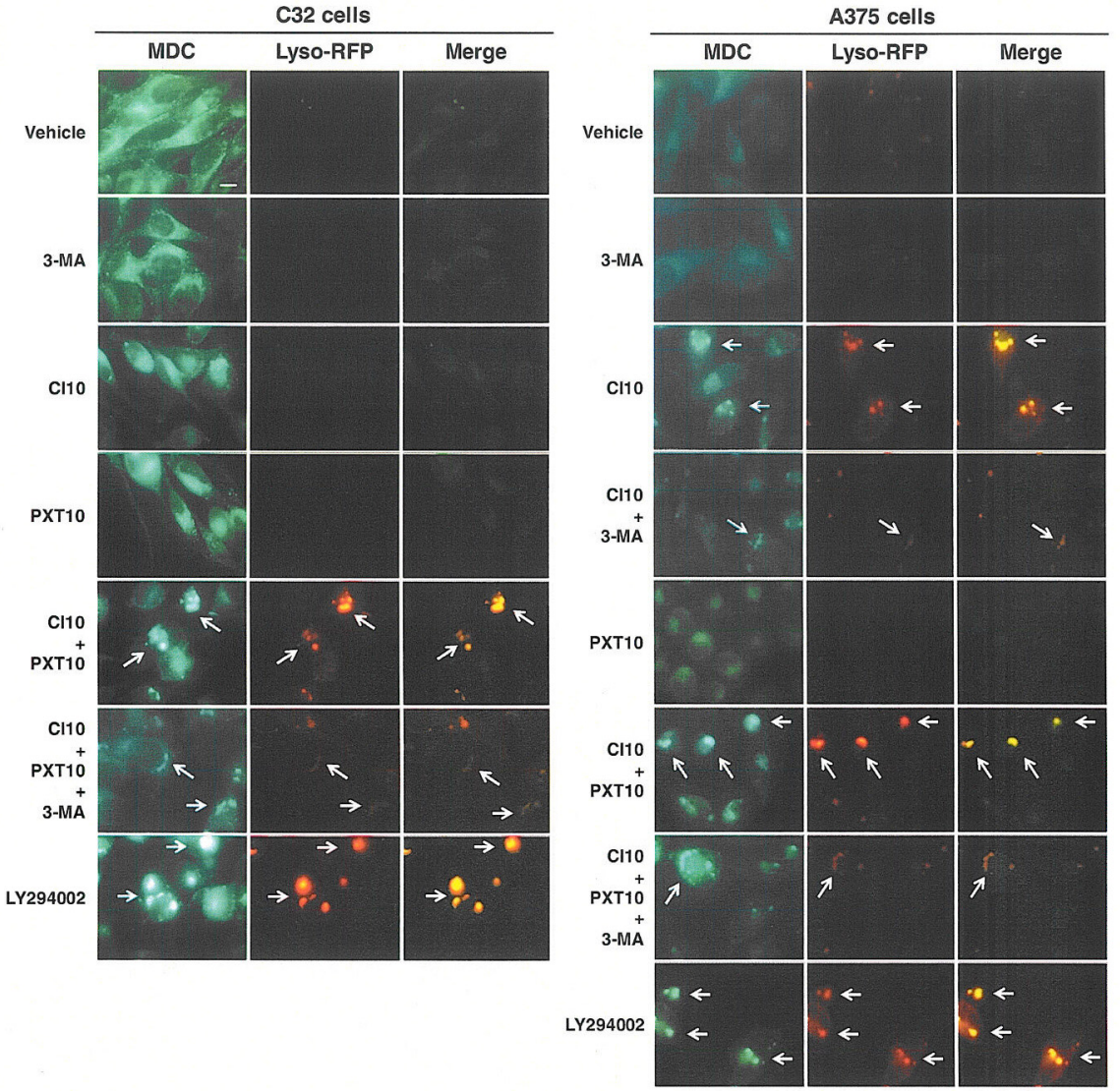

Fig. 3 Autophagosomes fusion with lysosomes induced by Cl-IB-MECA$_3$ (10 μM; Cl10) and/or PXT (10 ng/mL; PXT10) on human C32 and A375 melanoma cells, after 48-h incubation, in the absence or in the presence of the autophagy inhibitor, 3-MA (2.5 mM). DMSO (final concentration of 0.1 % v/v) in DMEM-HG was used as vehicle and LY294002 (50 μM) as a positive control for autophagy. Representative photographs of C32 and A375 cells after MDC (autophagosomes; *green*) and Lyso-RPF (lysosomes; *red*) staining ($n = 4$ independent experiments). Merged images indicate fusion of autophagosomes with lysosomes (*yellow*). Scale bar, 10 μm. *Arrows* indicate condensed autophagosomes (MDC) and lysosomes (Lyso-RPF) and intense autolysosomes formation (merge)

LY294002 resulted in significant reduction in p62 levels on both cell lines, after 24-h incubation (Fig. 4), as expected.

C32 cells present significant p62 protein levels reduction, after 24-h incubation with Cl10 + PXT10, when compared to the levels measured in cells treated with vehicle only (Fig. 4a). Moreover, the autophagy inhibitor (3-MA) was able to completely prevent this p62 degradation (Fig. 4a).

For A375 cells, treatment with Cl10 caused a significant decrease in p62 levels, being this effect more marked when cells were simultaneously treated with Cl10 and PXT10 (Fig. 4b). In this cell line, 3-MA was only able to partially prevent the degradation of p62 induced by both treatments (Cl10 and Cl10 + PXT10), although being more efficient in counteracting the degradation of p62 caused by Cl10 alone.

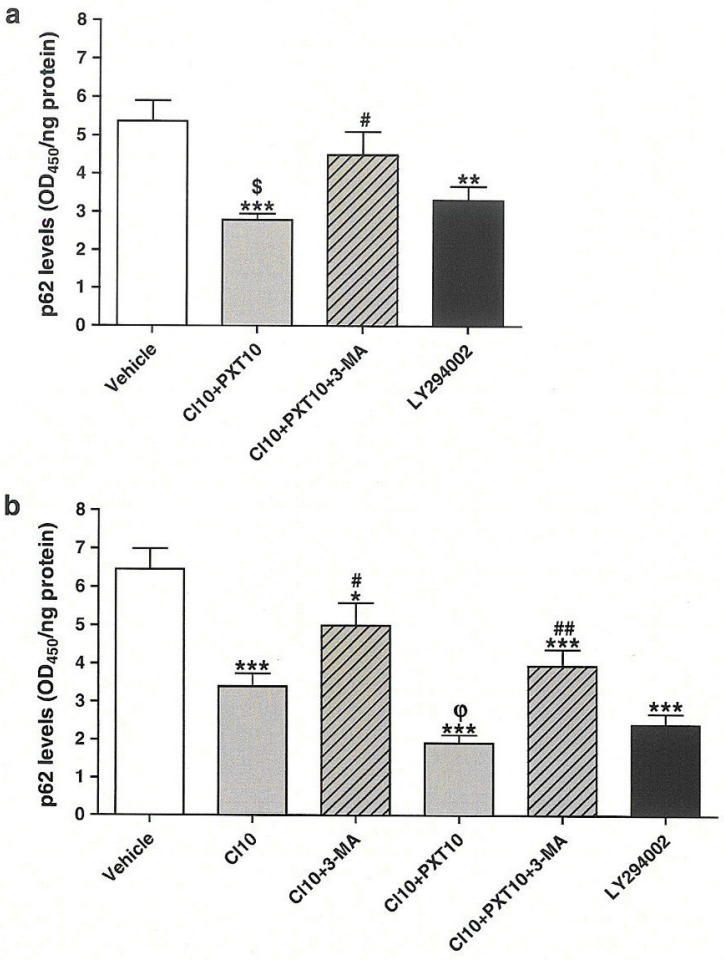

Fig. 4 Levels of p62 on human C32 (**a**) and A375 (**b**) melanoma cells treated with Cl-IB-MECA (10 μM; Cl10; *grey bars*) or in combination with PXT (10 ng/mL; Cl10 + PXT; *grey bars*), after 24-h incubation, in the absence or in the presence of the autophagy inhibitor, 3-MA (2.5 mM, *grey hatched bars*). DMSO (final concentration of 0.1 % v/v) in DMEM-HG was used as vehicle (*white bars*) and LY294002 (50 μM, *black bars*) as a positive control for autophagy. Results of levels of p62 [optic density at 450(OD_{450})/ng protein] are presented as mean ± SEM, $n = 12$ of 4 independent experiments. Significant differences (one-way ANOVA test, followed by the Student–Newman–Keuls post hoc test): $^{*}p < 0.05$ versus vehicle; $^{***}p < 0.001$ versus vehicle; $^{\#}p < 0.05$ versus same treatment without 3-MA; $^{\#\#}p < 0.01$ versus same condition in the absence of 3-MA; $^{\$}p < 0.05$ versus LY294002; $^{\varphi}p < 0.05$ versus Cl10

Reduction in mTOR levels is related to autophagic cell death activation triggered by Cl-IB-MECA in A375 cells and by Cl-IB-MECA with PXT in A375 and C32 melanoma cells

Evaluation of mTOR, a downstream effector of the PI3K/AKT signalling pathway that suppresses autophagy, was also performed by immunofluorescence, after cell treatments where autophagy occurs. As such, cells were incubated with Cl10, PXT10, and combination of Cl10 with PXT10 (Cl10 + PXT10), in the absence or in the presence of an autophagy inhibitor, 3-MA (2.5 mM), for 24 h, as described in the Methods section. LY294002 (50 μM) was used as a positive control for autophagy.

Images presented in Fig. 5 showed cells intensely stained (red) in conditions where there is no autophagy activation, as a result of high levels of mTOR protein in those conditions. C32 cells treated with Cl10 in combination with PXT10, and A375 cells treated with Cl10 and Cl10 in combination with PXT10 for 24 h, presented a decrease in mTOR expression revealed by a decrease in red fluorescence intensity. A similar low pattern of red fluorescence was also observed in cells, from both cell lines, incubated with the positive control for autophagy, after 24-h incubation (Fig. 5). These results suggest the involvement of the mTOR pathway on autophagic melanoma cell death induced by Cl10 on A375 cells and by Cl10 in combination with PXT10 on both human melanoma cell lines.

Mitotic catastrophe is induced by caspase-dependent and caspase-independent mechanisms triggered by PXT and Cl-IB-MECA in combination with PXT

Since PXT-induced cell death is solely related with apoptosis, only when combined with Cl-IB-MECA autophagy was seen, efforts were also made in order to further explore

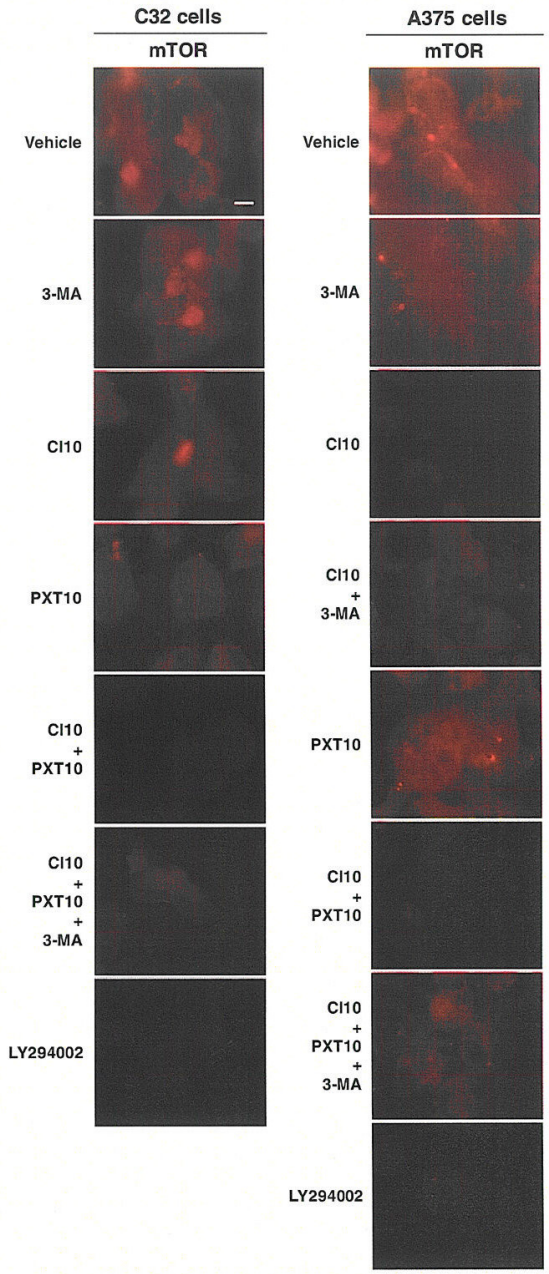

Fig. 5 Levels of mTOR on melanoma cells treated with Cl-IB-MECA (10 μM; Cl10) and/or with PXT (10 ng/mL; PXT10), after 24-h incubation, in the absence or in the presence of the autophagy inhibitor, 3-MA (2.5 mM). DMSO (final concentration of 0.1 % v/v) in DMEM-HG was used as vehicle and LY294002 (50 μM) as a positive control for autophagy. Representative photographs of C32 and A375 cells after mTOR (*red staining*) of $n = 4$ independent experiments. *Scale bar* 10 μm

the mechanisms of PTX-induced apoptosis. Images from PXT treatments labelled with Hoechst 33258 highlighted the occurrence of micro- and multinucleated cells, typical of MC (Fig. 5). To confirm the occurrence of MC, effects of PXT alone or in combination with Cl-IB-MECA on microtubule cytoskeleton (alpha-tubulin displayed in red) disruption were also examined by immunofluorescence. Human C32 and A375 melanoma cells were treated with Cl10, PXT10, and with the combination Cl10 + PXT10, in the absence or in the presence of a caspase inhibitor (Ac-DEVD-CHO, 50 μM), for 48 h (Fig. 6; Table 1). The vehicle and Cl10 alone showed typical radial and diffuse microtubule arrays (red alpha-tubulin) and normally shaped nuclei (blue) in both melanoma cell lines (Fig. 6), with similar MC/normal nuclei ratios (Table 1).

Red immunofluorescence staining showed that cell treatment with PXT (alone or in combination) disrupted microtubule networks in both melanoma cell lines (white arrows, Fig. 6). Furthermore, this effect was accompanied by the formation of micro- and multinucleated cells (blue stained nuclei, Fig. 6), morphological features associated with MC. The occurrence of such features was more significant when both cell lines were treated with Cl10 + PXT10 (Table 1). Moreover, the caspase inhibitor (Ac-DEVD-CHO) completely blocked the PXT-induced MC (Fig. 6; Table 1) but only partially prevent the effect caused by Cl10 + PXT10 (Fig. 6; Table 1). Taken together these results suggest that PXT10 causes MC by a caspase-dependent mechanism and when in combination with Cl10 causes MC by both caspase-dependent and caspase-independent mechanisms.

Enhanced cell death (LDH leakage assay) caused by PXT alone in A375 melanoma cells was completely prevented by NAC and significantly attenuated by this powerful antioxidant when cells were treated with Cl10 in combination with PXT10 (Table 2). These data suggest that PXT can induce reactive oxygen species (ROS) generation, leading to its cytotoxicity.

Discussion

The present study provides evidence that Cl-IB-MECA in combination with PXT can induce mTOR-dependent autophagic cell death, and caspase-dependent and or/independent MC-related apoptosis, on human C32 and A375 melanoma cells (Fig. 7). The activation of these mechanisms may prove to be useful towards the therapy of one of the most deadly and therapeutically challenging cancers, the melanoma.

We previously showed that Cl-IB-MECA and PXT, alone or in combination, caused caspase-dependent apoptosis on C32 cells, as a cytotoxic mechanism (Soares et al.

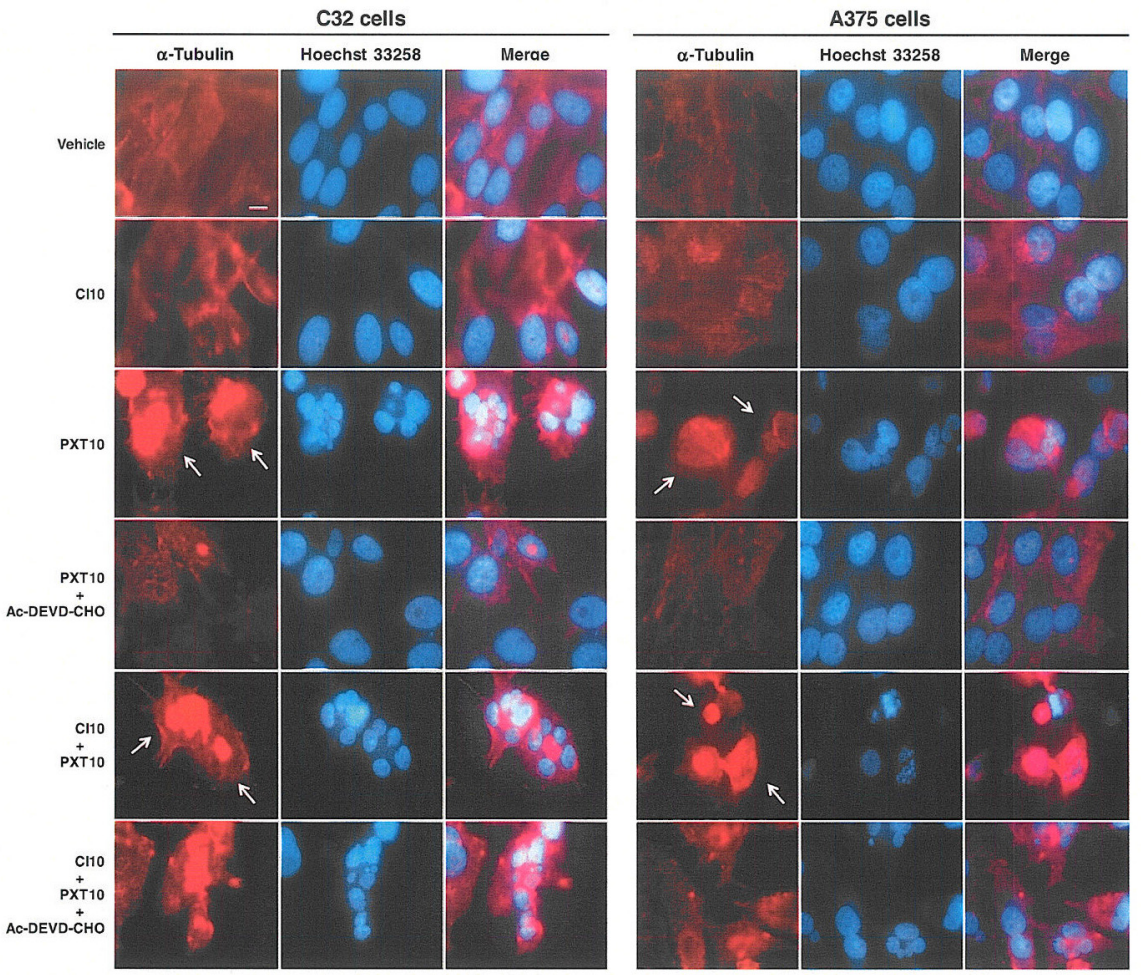

Fig. 6 Evaluation of mitotic catastrophe induced by PXT (10 ng/mL, PXT10) and/or by Cl-IB-MECA (10 μM, Cl10), after 48-h incubation, in the absence or in the presence of the caspase inhibitor, Ac-DEVD-CHO (50 μM). DMSO (final concentration of 0.1 % v/v) in DMEM-HG was used as vehicle. Representative photographs of C32 and A375 cells after alpha-tubulin (*red*) and nuclei (*blue*) staining ($n = 4$ independent experiments). *Scale bar* 10 μm. *Arrows* indicate microtubules disruption (*red*)

2013). In fact, we demonstrated that the activity of caspase 3 (and also 8 and 9) was augmented after cell treatment with this combination (Soares et al. 2013). However, it is of great interest to examine the efficacy of the proposed therapeutic strategy on other melanoma cellular models and the other possible mechanisms involved. As such, we used the lowest concentrations of Cl-IB-MECA (10 μM, Cl10) and PXT (10 ng/mL, PXT10) tested in the previous work, and the combination of both, on human C32 and A375 metastatic melanoma cells. These are clinically relevant concentrations since Cl-IB-MECA showed no serious drug-related adverse effects or dose-limiting toxicities, and good oral bioavailability in clinical trials (Stemmer et al. 2013), and PXT concentrations found in plasma cancer patients were 2.6 times higher than the one used in this study (Rodriguez et al. 2012). Cytotoxic effects were measured using several assays, MTT reduction and NR uptake assays and also the LDH leakage assay, to increase the reliability of the results obtained. Results now presented are the first demonstration that Cl-IB-MECA in combination with PXT is also an effective cytotoxicity inducer in another melanoma cellular model: A375 cells. Each cell line seems to have different sensibility towards Cl10, whereas with PXT10 or the combination of drugs, the effects seem to be similar. In fact, C32 cells when incubated with Cl10 have their NR uptake ability strongly compromised, whereas A375 cells

Table 1 Quantification of mitotic catastrophe induced by PXT (10 ng/mL, PXT10) and/or by Cl-IB-MECA (10 μM, Cl10), after 48-h incubation, in the absence or in the presence of the caspase inhibitor, Ac-DEVD-CHO (50 μM)

48 h	Nuclei ratio (mitotic catastrophe/normal) (mean ± SEM)	
	C32 cells	A375 cells
Vehicle	0.23 ± 0.02	0.19 ± 0.04
Cl10	0.22 ± 0.01	0.23 ± 0.03
PXT10	1.94 ± 0.03***	1.27 ± 0.01***
PXT10 + Ac-DEVD-CHO	0.22 ± 0.02###	0.19 ± 0.02###
Cl10 + PXT10	1.69 ± 0.01***,††	3.70 ± 0.4***,†††
Cl10 + PXT10 + Ac-DEVD-CHO	0.53 ± 0.03***,###	0.94 ± 0.04***,###

DMSO (final concentration of 0.1 % v/v) in DMEM-HG was used as vehicle. Results of nuclei ratio (mitotic catastrophe/normal) are presented as mean ± SEM, $n = 10$ random fields of 4 independent experiments

Significant differences (one-way ANOVA test, followed by the Student–Newman–Keuls post hoc test): *** $p < 0.001$ versus vehicle; ### $p < 0.001$ versus same condition in the absence of Ac-DEVD-CHO; †† $p < 0.01$ versus PXT10; ††† $p < 0.001$ versus PXT10

Table 2 Effect of NAC (1 mM) on the cytotoxicity caused by Cl-IB-MECA (10 μM; Cl10) and/or PXT (10 ng/mL; PXT10) on human A375 melanoma cells, after 48-h incubation

48 h	LDH leakage (% from total LDH)	
	(−) NAC (mean ± SEM)	(+) NAC (mean ± SEM)
Vehicle	7.07 ± 0.42	6.83 ± 0.46
Cl10	18.58 ± 0.74	17.97 ± 0.98
PXT10	14.82 ± 0.53	7.79 ± 0.95$^{\$\$\$}$
Cl10 + PXT10	35.82 ± 1.16	32.39 ± 1.17$^{\$}$

DMSO (final concentration of 0.1 % v/v) in DMEM-HG was used as vehicle. Results of LDH leakage (% of total LDH) are presented as mean ± SEM, $n = 9$ of 3 independent experiments

Significant differences (one-way ANOVA test, followed by the Student–Newman–Keuls post hoc test): $^{\$}$ $p < 0.05$ versus same condition in the absence of NAC; $^{\$\$\$}p < 0.001$ versus same condition in the absence of NAC. Other significant differences were similar to Fig. 2b

show alterations in their cellular membrane integrity (LDH assay) in the same condition. Of relevance, the combination has the same cytotoxic profile in both cell lines, showing higher clinical potential.

The combination of Cl-IB-MECA with PXT was reported to induce apoptosis in C32 melanoma cells (Soares et al. 2013). However, other mechanisms of cell death are most definitively involved since, in this study, the caspase inhibitor only prevented approximately 10 % of the cytotoxic effects described. In the present study, we tested the combination of Cl10 with PXT10 in the presence of Ac-DEVD-CHO (a caspase inhibitor) and/or 3-MA (an autophagy inhibitor) as the our used combination seems to largely impair lysosomal functions. The LDH leakage assay was chosen to assess cell death since permanent cell membrane rupture is expected to occur at a later stage (Weyermann et al. 2005), allowing us to better distinguish between overall cytotoxicity from specific organelle damage.

Results demonstrated that Cl10 did not induce any type of cell death on C32 cells, in opposition to its effect upon A375 cells where cell death occurs exclusively mediated by autophagy. To the best of our knowledge, it is the first time that Cl10 is reported to induce autophagy in melanoma cells. Autophagy induction is currently taken to represent a novel therapeutic target for apoptosis-resistant cancers (Tsujimoto and Shimizu 2005).

The discrepancy between C32 and A375 cells concerning their susceptibility to Cl10 could be, in part, related to donator's gender, since C32 and A375 cells were collected from male to female human donators, respectively. This possibility is in agreement with the different metastatic spread patterns found on gender of patients with metastatic melanoma (Mervic 2012). This difference, however, does not alter the cytotoxic response towards PXT10. The present work provides evidence that PXT10 alone elicits exclusively caspase-dependent apoptosis on both melanoma cell lines. Indeed, PXT is a well-established mitotic spindle anticancer drug reported to induce apoptosis in many types of cancer (Steed and Sawyer 2007), including melanoma (Wang et al. 2003).

Importantly, the present work demonstrates that besides apoptosis, Cl10 in combination with PXT10 also induces autophagy, causing cell death in both melanoma cell lines (Fig. 7). Indeed, when caspase-dependent apoptosis or autophagy was inhibited, cell death was not completely prevented. Activation of these two types of cell death has also been reported to occur on ME1402 and WM1158 melanoma cells after treatment with a new binuclear palladacycle complex (Aliwaini et al. 2013). Our results also indicate that for C32 cells, autophagy represents the main cell death mechanism of the drug combination, contrary to what happens in A375 cells where apoptosis and autophagy contribute at a similar extent (Fig. 7). Moreover, the simultaneous addition of a caspase and an autophagy inhibitor was not able to completely block cell death caused by Cl10 + PXT10 on A375 cells. Although Ac-DEVD-CHO is referred as a selective caspase 3/7 inhibitor, the concentration used in the present study also blocks caspase-6 (Mintzer et al. 2012), preventing all effector caspases activation. Thus, the possibility of other effector caspases being active can be discarded and necrosis (Jain et al. 2013) can be suggested as the probable mechanism through which Cl10 in combination with PXT10 induced the non-autophagic and non-apoptotic A375 cell death.

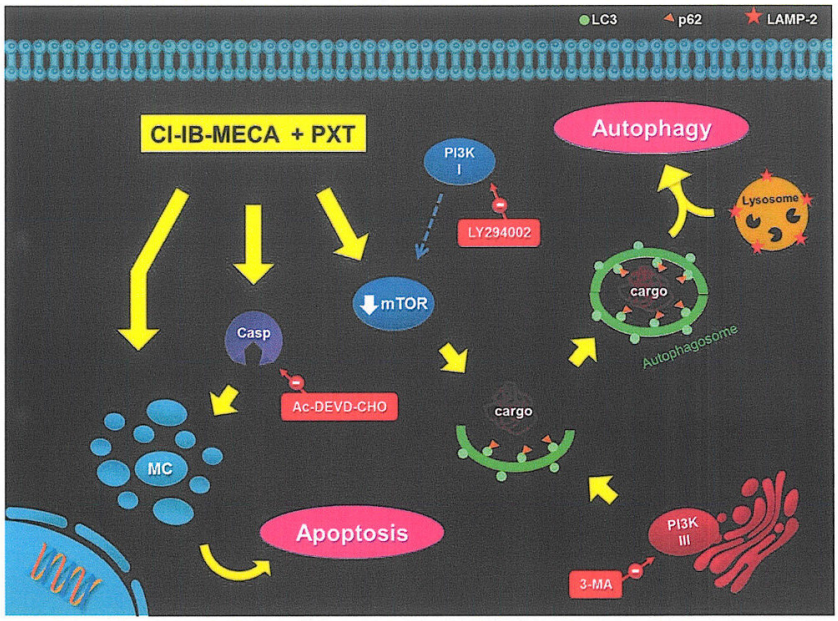

Fig. 7 Proposed signalling pathways showing the induction of autophagy through mTOR activation, with autophagosome-lysosome fusion, by the combination of Cl-IB-MECA and PXT on human C32 and A375 melanoma cell lines. This combination decreases mTOR levels, leading to the sequestration of cargo (autophagosomes) and fusion with lysosomes, leading to autophagy. Moreover, Cl-IB-MECA with PXT causes micro- and multinucleation, characteristic of mitotic catastrophe (MC), through caspase-dependent and/or independent mechanisms, followed by apoptosis. *Red boxes* represent selective inhibitors. *Dashed arrow* represents an indirect pathway

As autophagy seems to be responsible for most of the C32 and A375 cell death induced by treatment with Cl-IB-MECA and PXT, other characteristic markers of the autophagic process were also analysed to confirm this hypothesis: formation of a double-membrane vacuole (autophagosome) and subsequent fusion with lysosome (autolysosome) (Kung et al. 2011), and degradation of the intracellular levels of p62 (also called SQSTM1 in humans) (Puissant et al. 2012).

We detected a relative high accumulation of autophagosomes (through MDC staining) and their co-localization with lysosomes (through RFP fused lysosomal signal via LAMP 1 protein expression), after treatment of A375 cells with Cl10 and of both cell lines with Cl10 and PXT10. Moreover, 3-MA inhibited the formation of autophagosomes in these conditions. A class III and a class I PI3K inhibitor, 3-MA and LY294002, respectively, were used to inhibit and activate the autophagy process (Liu et al. 2013).

The understanding that p62 binds directly to LC3 (recruited to autophagosomal membranes) resulting in specific degradation of this protein by autophagy makes p62 a valuable and largely used marker for autophagy (Komatsu et al. 2012), since interaction of p62 with LC3 is required for autophagy-mediated elimination of unfolded ubiquitinated long-half-life proteins and non-ubiquitinated substrates (Puissant et al. 2012). As expected, a decrease in p62 levels from C32 cells treated with Cl10 and PXT10, and A375 cells treated with Cl10 alone or in combination with PXT10, was observed in the conditions where autophagosome formation was visualized through fluorescence microscopy. The 3-MA inhibitor was able to completely prevent the autophagic flux in C32 cells, and almost total blockade was achieved on A375 cells. Overall, these findings corroborate those obtained with the LDH leakage assay and confirm that induction of autophagy is, in fact, a cytotoxic mechanism in our conditions. Although there is a controversy whether autophagy activation promotes defensive or destructive roles in response to cancer therapy (White and DiPaola 2009), emerging evidence indicates that several cytotoxic agents are autophagic inducers of melanoma cell death (Tomic et al. 2011; Nicolau-Galmes et al. 2011).

Even though mechanisms of autophagy regulation are not completely understood, evidences have shown that mTOR, a protein kinase member of the PI3K-related family, which is involved in cell proliferation, plays a major role in controlling autophagy activation (Mizushima 2007). Moreover, targeting mTOR is considered as a promising target for cancer therapy, as dysregulation of mTOR signalling is present in a variety of human malignancies (Meric-Bernstam and Gonzalez-Angulo 2009). In agreement with these facts, we found an inverse correlation between levels of mTOR and autophagy activation. Levels of mTOR were significantly decreased in C32 cells treated with Cl10 + PXT10 and A375 cells treated with Cl10 and Cl10 + PXT10, conditions where autophagy was previously shown to occur. Autophagy was found to be regulated through the suppression of mTOR expression (Quidville et al. 2013; Wang et al. 2013). Considering current knowledge, it is conceivable that these cell treatments

inhibit class I PI3K and/or AKT, leading to downregulation of mTOR expression, since the effect was similar to that achieved with the LY294002 (Fig. 7).

Overall, it seems that Cl-IB-MECA is a more potent inducer of autophagic cell death than PXT, since the latter, when alone, did not show any signs of autophagy activation.

In fact, we found that PXT alone was fully linked to induction of apoptosis. This anticancer drug has already shown to be efficient in the treatment of different cancers, including melanoma (Wang et al. 2003). Unfortunately, the molecular mechanisms involved in PXT-induced apoptosis are poorly understood (Bhalla 2003). We characterized the microtubules network in C32 and A375 cells after treatment with PXT10 and Cl10 + PXT10 and found that PXT alone or in combination with Cl-IB-MECA strongly disrupted microtubules network and induced micro- and multinucleation, both hallmarks of MC (Fig. 7). Moreover, we demonstrated that prevention of caspase activation completely suppressed PXT10-induced MC signals in opposition to what was observed for the combination of Cl10 with PXT10, where MC was not totally prevented in either melanoma cell line. These facts indicate that PXT10 induced caspase-dependent MC in C32 and A375 cells; however, caspase-independent phenomena is also involved in the MC elicited by Cl10 + PXT10 in both cell lines. Although caspase-dependent MC is being suggested as a special case of apoptosis (Castedo et al. 2004a, b), MC cell death through caspase-dependent and caspase-independent mechanisms was also reported (Mansilla et al. 2006), corroborating our present results.

It is currently accepted that ROS generation can trigger MC (Hung et al. 2013). This possibility was checked by evaluating A375 cell death (LDH leakage assay) caused by PXT, alone or in combination with Cl-IB-MECA, in the presence of NAC. In our previous study (Soares et al. 2013), this powerful antioxidant prevented cytotoxicity on C32 cells treated with PXT10. In the present study, we found that NAC completely prevent PXT10-induced A375 cell death, suggesting that PXT induces ROS generation, which may cause MC cell death. ROS-dependent apoptosis caused by PXT has been previously described to occur in A375 cells (Selimovic et al. 2008). Interestingly, NAC was able to only slightly attenuate cytotoxicity elicited by the combination of Cl10 + PXT10, on A375 cells (Fig. 7).

In summary, the present study provides evidence that human C32 and A375 melanoma cells treated with Cl-IB-MECA and PXT undergo cell death by autophagy and MC-induced apoptosis (Fig. 7). We believe that the induction of autophagy in these cellular models, where cells are also undergoing apoptosis, provides appealing mechanisms concerning melanoma chemotherapy, since it drives more melanoma cells to die. Indeed, recently induction of autophagy was considered a very important cell death mechanism when in combination with other conventional anti-melanoma therapies (Liu et al. 2013). The combination of Cl-IB-MECA and PXT seems, therefore, to be an attractive chemotherapeutic approach to melanoma because Cl-IB-MECA seems to largely improve the effectiveness of PXT by contributing to activate other forms of cell death (Fig. 7), increasing overall melanoma cells cytotoxicity and lowering PXT chemotherapy resistance.

Acknowledgments Work was funded by FEDER through the Program of Operational Competitiveness Factors—COMPETE and National Funds through FCT—Foundation for Science and Technology. ASS and VMC thank FCT for their PhD Grant (SFRH/BD/64911/2009) and Postdoc Grant (SFRH/BPD/63746/2009), respectively.

Conflict of interest We declare that we have no conflict of interest in relation to this article.

References

Aliwaini S, Swarts AJ, Blanckenberg A, Mapolie S, Prince S (2013) A novel binuclear palladacycle complex inhibits melanoma growth in vitro and in vivo through apoptosis and autophagy. Biochem Pharmacol 86(12):1650–1663

Bhalla KN (2003) Microtubule-targeted anticancer agents and apoptosis. Oncogene 22(56):9075–9086

Biederbick A, Kern HF, Elsasser HP (1995) Monodansylcadaverine (MDC) is a specific in vivo marker for autophagic vacuoles. Eur J Cell Biol 66(1):3–14

Castedo M, Perfettini JL, Roumier T, Andreau K, Medema R, Kroemer G (2004a) Cell death by mitotic catastrophe: a molecular definition. Oncogene 23(16):2825–2837

Castedo M, Perfettini JL, Roumier T, Valent A, Raslova H, Yakushijin K, Horne D, Feunteun J, Lenoir G, Medema R, Vainchenker W, Kroemer G (2004b) Mitotic catastrophe constitutes a special case of apoptosis whose suppression entails aneuploidy. Oncogene 23(25):4362–4370

Dai DL, Martinka M, Li G (2005) Prognostic significance of activated Akt expression in melanoma: a clinicopathologic study of 292 cases. J Clin Oncol 23(7):1473–1482

de Souza CF, Morais AS, Jasiulionis MG (2012) Biomarkers as key contributors in treating malignant melanoma metastases. Dermatol Res Pract 2012:156068

Elmore S (2007) Apoptosis: a review of programmed cell death. Toxicol Pathol 35(4):495–516

Fulda S, Debatin KM (2006) Extrinsic versus intrinsic apoptosis pathways in anticancer chemotherapy. Oncogene 25(34):4798–4811

Gao S, Chen T, Choi MY, Liang Y, Xue J, Wong YS (2013) Cyanidin reverses cisplatin-induced apoptosis in HK-2 proximal tubular cells through inhibition of ROS-mediated DNA damage and modulation of the ERK and AKT pathways. Cancer Lett 333(1):36–46

Hanahan D, Weinberg RA (2011) Hallmarks of cancer: the next generation. Cell 144(5):646–674

Hengartner MO (2000) The biochemistry of apoptosis. Nature 407(6805):770–776

Hung JY, Wen CW, Hsu YL, Lin ES, Huang MS, Chen CY, Kuo PL (2013) Subamolide a induces mitotic catastrophe accompanied by apoptosis in human lung cancer cells. Evid Based Complement Altern Med 2013:828143

Jain MV, Paczulla AM, Klonisch T, Dimgba FN, Rao SB, Roberg K, Schweizer F, Lengerke C, Davoodpour P, Palicharla VR, Maddika S, Los M (2013) Interconnections between apoptotic, autophagic and necrotic pathways: implications for cancer therapy development. J Cell Mol Med 17(1):12–29

Jemal A, Siegel R, Xu J, Ward E (2010) Cancer statistics, 2010. CA Cancer J Clin 60(5):277–300

Jung CH, Ro SH, Cao J, Otto NM, Kim DH (2010) mTOR regulation of autophagy. FEBS Lett 584(7):1287–1295

Kihara A, Kabeya Y, Ohsumi Y, Yoshimori T (2001) Beclin-phosphatidylinositol 3-kinase complex functions at the trans-Golgi network. EMBO Rep 2(4):330–335

Komatsu M, Kageyama S, Ichimura Y (2012) p62/SQSTM1/A170: physiology and pathology. Pharmacol Res 66(6):457–462

Kung CP, Budina A, Balaburski G, Bergenstock MK, Murphy M (2011) Autophagy in tumor suppression and cancer therapy. Crit Rev Eukaryot Gene Expr 21(1):71–100

Liu H, He Z, Simon HU (2013) Targeting autophagy as a potential therapeutic approach for melanoma therapy. Semin Cancer Biol 23(5):352–360

LoPiccolo J, Blumenthal GM, Bernstein WB, Dennis PA (2008) Targeting the PI3K/Akt/mTOR pathway: effective combinations and clinical considerations. Drug Resist Updates 11(1–2):32–50

Maiuri MC, Zalckvar E, Kimchi A, Kroemer G (2007) Self-eating and self-killing: crosstalk between autophagy and apoptosis. Nat Rev Mol Cell Biol 8(9):741–752

Mansilla S, Priebe W, Portugal J (2006) Mitotic catastrophe results in cell death by caspase-dependent and caspase-independent mechanisms. Cell Cycle 5(1):53–60

Martins JB, Bastos Mde L, Carvalho F, Capela JP (2013) Differential effects of methyl-4-phenylpyridinium ion, rotenone, and paraquat on differentiated SH-SY5Y cells. J Toxicol 2013:347312

Meric-Bernstam F, Gonzalez-Angulo AM (2009) Targeting the mTOR signaling network for cancer therapy. J Clin Oncol 27(13):2278–2287

Mervic L (2012) Time course and pattern of metastasis of cutaneous melanoma differ between men and women. PLoS ONE 7(3):e32955

Mintzer R, Ramaswamy S, Shah K, Hannoush RN, Pozniak CD, Cohen F, Zhao X, Plise E, Lewcock JW, Heise CE (2012) A whole cell assay to measure caspase-6 activity by detecting cleavage of lamin A/C. PLoS ONE 7(1):e30376

Mizushima N (2007) Autophagy: process and function. Genes Dev 21(22):2861–2873

Mosmann T (1983) Rapid colorimetric assay for cellular growth and survival: application to proliferation and cytotoxicity assays. J Immunol Methods 65(1–2):55–63

Nicolau-Galmes F, Asumendi A, Alonso-Tejerina E, Perez-Yarza G, Jangi SM, Gardeazabal J, Arroyo-Berdugo Y, Careaga JM, Diaz-Ramon JL, Apraiz A, Boyano MD (2011) Terfenadine induces apoptosis and autophagy in melanoma cells through ROS-dependent and -independent mechanisms. Apoptosis 16(12):1253–1267

Puissant A, Fenouille N, Auberger P (2012) When autophagy meets cancer through p62/SQSTM1. Am J Cancer Res 2(4):397–413

Quidville V, Alsafadi S, Goubar A et al (2013) Targeting the deregulated spliceosome core machinery in cancer cells triggers mTOR blockade and autophagy. Cancer Res 73(7):2247–2258

Repetto G, del Peso A, Zurita JL (2008) Neutral red uptake assay for the estimation of cell viability/cytotoxicity. Nat Protoc 3(7):1125–1131

Rodriguez J, Contento AM, Castaneda G, Munoz L, Berciano MA (2012) Determination of morphine, codeine, and paclitaxel in human serum and plasma by micellar electrokinetic chromatography. J Sep Sci 35(17):2297–2306

Saiki S, Sasazawa Y, Imamichi Y, Kawajiri S, Fujimaki T, Tanida I, Kobayashi H, Sato F, Sato S, Ishikawa K, Imoto M, Hattori N (2011) Caffeine induces apoptosis by enhancement of autophagy via PI3K/Akt/mTOR/p70S6K inhibition. Autophagy 7(2):176–187

Santoni M, Amantini C, Morelli MB, Liberati S, Farfariello V, Nabissi M, Bonfili L, Eleuteri AM, Mozzicafreddo M, Burattini L, Berardi R, Cascinu S, Santoni G (2013) Pazopanib and sunitinib trigger autophagic and non-autophagic death of bladder tumour cells. Br J Cancer 109(4):1040–1050

Selimovic D, Hassan M, Haikel Y, Hengge UR (2008) Taxol-induced mitochondrial stress in melanoma cells is mediated by activation of c-Jun N-terminal kinase (JNK) and p38 pathways via uncoupling protein 2. Cell Signal 20(2):311–322

Shen S, Kepp O, Michaud M, Martins I, Minoux H, Metivier D, Maiuri MC, Kroemer RT, Kroemer G (2011) Association and dissociation of autophagy, apoptosis and necrosis by systematic chemical study. Oncogene 30(45):4544–4556

Soares AS, Costa VM, Diniz C, Fresco P (2013) Potentiation of cytotoxicity of paclitaxel in combination with Cl-IB-MECA in human C32 metastatic melanoma cells: a new possible therapeutic strategy for melanoma. Biomed Pharmacother 67(8):777–789

Soengas MS, Lowe SW (2003) Apoptosis and melanoma chemoresistance. Oncogene 22(20):3138–3151

Steed H, Sawyer MB (2007) Pharmacology, pharmacokinetics and pharmacogenomics of paclitaxel. Pharmacogenomics 8(7):803–815

Stemmer SM, Benjaminov O, Medalia G, Ciuraru NB, Silverman MH, Bar-Yehuda S, Fishman S, Harpaz Z, Farbstein M, Cohen S, Patoka R, Singer B, Kerns WD, Fishman P (2013) CF102 for the treatment of hepatocellular carcinoma: a phase I/II, open-label, dose-escalation study. Oncologist 18(1):25–26

Tawbi HA, Kirkwood JM (2007) Management of metastatic melanoma. Semin Oncol 34(6):532–545

Tomic T, Botton T, Cerezo M, Robert G, Luciano F, Puissant A, Gounon P, Allegra M, Bertolotto C, Bereder JM, Tartare-Deckert S, Bahadoran P, Auberger P, Ballotti R, Rocchi S (2011) Metformin inhibits melanoma development through autophagy and apoptosis mechanisms. Cell Death Dis 2:e199

Tsujimoto Y, Shimizu S (2005) Another way to die: autophagic programmed cell death. Cell Death Differ 12(Suppl 2):1528–1534

Vakifahmetoglu H, Olsson M, Zhivotovsky B (2008) Death through a tragedy: mitotic catastrophe. Cell Death Differ 15(7):1153–1162

Wang F, Cao Y, Zhao W, Liu H, Fu Z, Han R (2003) Taxol inhibits melanoma metastases through apoptosis induction, angiogenesis inhibition, and restoration of E-cadherin and nm23 expression. J Pharmacol Sci 93(2):197–203

Wang S, Xia P, Ye B, Huang G, Liu J, Fan Z (2013) Transient activation of autophagy via Sox2-mediated suppression of mTOR is an important early step in reprogramming to pluripotency. Cell Stem Cell 13(5):617–625

Weyermann J, Lochmann D, Zimmer A (2005) A practical note on the use of cytotoxicity assays. Int J Pharm 288(2):369–376

White E, DiPaola RS (2009) The double-edged sword of autophagy modulation in cancer. Clin Cancer Res 15(17):5308–5316

Xing C, Zhu B, Liu H, Yao H, Zhang L (2008) Class I phosphatidylinositol 3-kinase inhibitor LY294002 activates autophagy and induces apoptosis through p53 pathway in gastric cancer cell line SGC7901. Acta Biochim Biophys Sin 40(3):194–201

5. MANUSCRIPT V

The combination of Cl-IB-MECA with paclitaxel: a new anti-metastatic therapeutic strategy for melanoma

Manuscript submitted for publication

Title page

The combination of Cl-IB-MECA with paclitaxel: a new anti-metastatic therapeutic strategy for melanoma

Ana S Soares[1,2], Vera M Costa[3], Carmen Diniz[1,2], and Paula Fresco[1,2].

Affiliations

[1]REQUI*M*TE/Laboratório de Farmacologia, Departamento de Ciências do Medicamento, Faculdade de Farmácia, Universidade do Porto, Porto, Portugal

[2]MedInUP – Centro de Investigação Farmacológica e Inovação Medicamentosa, Universidade do Porto, Porto, Portugal

[3]REQUI*M*TE/Laboratório de Toxicologia, Departamento de Ciências Biológicas, Faculdade de Farmácia, Universidade do Porto, Porto, Portugal

Corresponding author

Paula Fresco (pfresco@ff.up.pt)

Departamento de Farmacologia

Faculdade de Farmácia, Universidade do Porto, Rua de Jorge Viterbo Ferreira, 228,

4050-313 Porto, Portugal

Telephone 00351-220428609

Abstract

Purpose Metastatic melanoma is considered one of the most aggressive malignant tumours, representing the deadliest form of skin cancer. Melanoma progression is associated with the abrogation of normal controls that limit cell proliferation, migration and invasion, eventually leading to metastasis. Based on the variety of cellular mechanisms involved in metastatic progression, we aimed to evaluate the effect of inosine (50 μM) and the combination of Cl-IB-MECA (10 μM) with paclitaxel (10 ng/mL) on several stages of melanoma progression.

Methods Proliferation, migration, adhesion, invasion, and colony formation were performed on human C32 and A375 metastatic melanoma cells. Levels of ERK1/2 were also determined using an ELISA kit. Moreover, mouse aortic rings were treated with vascular endothelial growth factor, as to assess the microvessel sprouting (indicator of angiogenesis) in the presence of the referred compounds.

Results We demonstrate that inosine induced, through A_3 adenosine receptors activation, proliferation, migration, adhesion, and invasion on C32 and A375 melanoma cells, although with dissimilar importance on each melanoma cell line. Inosine also increased colony formation on A375 cells. Levels of ERK1/2 were increased after inosine exposure and were also dependent on A_3 adenosine receptor activation in both cell lines. However, microvessel sprouting stimulated by inosine was not A_3 adenosine receptor-dependent but was also prevented by the combination of Cl-IB-MECA with paclitaxel.

Conclusions Cl-IB-MECA combined with paclitaxel was able to impair all the referred metastatic related mechanisms induced by inosine, making this approach a valuable tool for combination therapy against metastatic melanoma, overcoming paclitaxel common chemotherapeutic resistance.

Keywords: melanoma, Cl-IB-MECA, paclitaxel, inosine, metastatic potential

Abbreviations

AR: adenosine receptor

BME: basement membrane extract

BSA: bovine serum albumin

Cl-IB-MECA: 2-chloro-N(6)-(3-iodobenzyl)-adenosine-5'-N-methyl-uronamide

CTR: control

DMSO: dimethyl sulfoxide

DMEM-HG: dulbecco's modified eagle's medium-high glucose

ECM: extracellular matrix

ERK: extracellular signal-regulated kinase

FBS: foetal bovine serum

INO: inosine

MAPK: mitogen-activated protein kinase

MRE3008F20: *N*-[2-(2-furanyl)-8-propyl-8*H*-pyrazolo[4,3-*e*][1,2,4]triazolo[1,5-*c*]pyrimidin-5-yl]-*N*'-(4-methoxyphenyl)urea

MTT: 3-(4,5-dimethylthiazol-2-yl)-2,5-diphenyl tetrazolium bromide

Opti-MEM: opti-minimal essential medium

PBS: phosphate buffered saline

PI3K: phosphatidylinositol 3-kinase

PXT: paclitaxel

ROS: reactive oxygen species

VEGF: vascular endothelial growth factor

Introduction

Metastatic melanoma is considered one of the most aggressive malignant tumours, representing the deadliest form of skin cancer (Bandarchi et al. 2010). This serious disease, derived from transformed epidermal melanocytes, has nowadays an alarming incidence increase (Jemal et al. 2010). The propensity of melanoma to metastasize results in early and general spread and, therefore, causing very high mortality rates (Bandarchi et al. 2010). Resistance to chemotherapy and radiotherapy (Bhatia et al. 2009) is the main reason for patients with metastatic melanoma to have an overall survival of less than two years (Bandarchi et al. 2010). Chemotherapeutic drugs, including dacarbazine, cisplatin, and paclitaxel (PXT), have been used, alone or in combination, although without significant survival rate improvement (Bhatia et al. 2009). Therefore, alternative treatment options are urgently needed since mechanisms that regulate tumour initiation and metastatic progression were not yet impaired at this present and effective therapies against them are still missing. Recently, we demonstrated that Cl-IB-MECA potentiates PXT cytotoxicity in human C32 and A375 metastatic melanoma cells (Soares et al. 2013, 2014. Manuscript accepted for publication.), although the effect of this promising combination was not yet evaluated on the cellular mechanisms involved in melanoma progression.

Cellular proliferation is fundamental for tumour metastasis, being crucial, therefore, the identification of key factors involved in the induction and progression of melanoma (Madonna et al. 2012). The activation of the intracellular mitogen-activated protein kinase (MAPK) and of phosphatidylinositol 3-kinase (PI3K) is involved in melanocyte proliferation (Haass and Herlyn 2005). Abrogation of normal control of these pathways drives melanocytes to become independent, causing uncontrolled cell proliferation and, ultimately, melanoma (Haass et al. 2005). The development of metastasis starts with cell migration from the primary tumour, followed by re-adhesion and tissue invasion, with complex interactions between tumour cells and their environment (Attoub et al. 2013). An increase or decrease in tumour cells adhesion to neighbouring cells, extracellular matrix (ECM), and endothelial cells, may occur at different stages of tumour progression (Huang et al. 1997), representing the degradation of ECM and basement membrane a critical step for tumour invasion and metastasis (Yamazoe et al. 2009). In addition, anchorage-independent growth (colony formation) is also important for malignant cell transformation as this ability increases the metastatic potential (Mori et al. 2009). Another important requirement for metastatic progression is the formation of new vessels (angiogenesis), which is induced by vascular endothelial growth factors (VEGF) released by tumour cells, as to ensure tumour growth/maintenance (Abdollahi and Folkman 2010).

Based on the variety of cellular mechanisms involved in metastatic progression, attempts should be made in order to find new effective drugs that might inhibit tumour cell proliferation, cell migration and/or invasion, and also drugs with anti-angiogenic properties. Adenosine is a well-known nucleoside that plays a key role on tumour growth and angiogenesis (Spychala 2000). Results from experimental tumour models showed that reducing extracellular levels of adenosine arrests tumour progression and prevents metastasis (Stagg et al. 2011). Moreover, stimulation of A_3 adenosine receptors (A_3AR) has been reported to have growth-promoting as well as growth-inhibitory effects (Di Virgilio 2012). Previously, our group demonstrated a proliferative effect elicited by adenosine, which is even more notorious by its metabolic product, inosine (INO), on human C32 melanoma cells, through A_3AR activation (Soares et al. 2014. Manuscript submitted for publication.).

In the present study, we investigated whether INO promotes proliferation, migration, adhesion, invasion and colony formation, hallmarks of metastatic progression, on human C32 and A375 melanoma cells. The involvement of A_3AR activation and of MAPK pathway was also examined on those effects. Furthermore, in the present work, the INO role on angiogenesis was also studied. The promising anti-cancer therapeutic combination of Cl-IB-MECA with PXT was used in order to evaluate its potential against the metastatic progression.

Materials and methods

Chemicals

All reagents used were of analytical grade. Cl-IB-MECA and MRE3008F20 were obtained from Tocris Bioscience (Bristol, United Kingdom). Cultrex® human basement membrane extract (BME) was purchased from Trevigen (Reagente 5, Porto, Portugal). Collagen type I and STAR ERK1/2 ELISA kit were purchased from Merk-Millipore (Interface, Amadora, Portugal). Foetal bovine serum (FBS), Glutamax, trypsin/EDTA, and opti-minimal essential medium (Opti-MEM®) were obtained from Invitrogen (Alfagene, Carcavelos, Portugal). Dulbecco's modified eagle's medium-high glucose (DMEM-HG), penicillin/streptomycin (10 000 U/mL), INO, PXT, ECM gel, mouse VEGF, 3-(4,5-dimethylthiazol-2-yl)-2,5-diphenyl tetrazolium bromide (MTT), bovine serum albumin (BSA), crystal violet solution, sodium citrate, dimethyl sulfoxide (DMSO), and all other chemicals were purchased from Sigma-Aldrich (Sigma-Aldrich-Química SA, Sintra, Portugal) of the highest purity available.

Melanoma cell culture and treatment

Human C32 and A375 metastatic melanoma cells obtained from ECACC – SIGMA (Sigma-Aldrich-Química SA, Sintra, Portugal) were used in this study. For cell culture maintenance, cells were seeded in complete medium [DMEM-HG medium with 10% (v/v) FBS, 1% (v/v) of a mixture of penicillin/streptomycin and 1% (v/v) Glutamax, pH 7.4], incubated at 37 ºC in a humidified atmosphere (95% air; 5% CO_2) and sub-cultivated twice a week. Cell passaging was done by trypsinization. All experiments were carried out with cells from batches with passage numbers lower than 50.

Before each assay, cells were serum-starved for 4h, to allow synchronization of the cell cycle. Depending on the experiment goal, cells were treated with DMSO (maximum final concentration of 0.1% v/v; vehicle), INO (50 μM, INO50 (Soares et al. 2014), MRE3008F20 (selective A_3AR antagonist ,10 nM (Soares et al. 2013)), Cl-IB-MECA (10 μM, Cl10 (Soares et al. 2013)), PXT (10 ng/mL, PXT10 (Soares et al. 2013)), and combinations of these compounds (INO50+MRE3008F20, INO50+Cl50, INO50+PXT10, INO50+Cl10+PXT10, Cl10+PXT10), for different time-points. When MRE3008F20 was used, this compound was added 15 min prior to the addition of other compounds (Gessi et al. 2004).

MTT reduction assay

Cells were seeded in 96-well plates with 200 µL *per* well of 8.0×10^4 cells/mL and 5.0×10^4 cells/mL, for C32 and A375 cells, respectively, and allowed to attach for 4h. Thereafter, cell medium was replaced by complete medium, in the absence or in the presence of compounds referred in section *Melanoma cell culture and treatment*, and cells incubated for different time-points, depending on the experiment goal. All conditions were performed in triplicate, initiated and processed in parallel. At the end of the incubation period, mitochondrial function was evaluated as an index of cell proliferation or cytotoxicity (Soares et al. 2014), since mitochondrial dehydrogenases of living cells can reduce MTT to formazans (Mosmann 1983) being cells processed as described by our group (Soares et al. 2013).

***In vitro* scratch assay**

The *in vitro* scratch assay was performed as described previously (Liang et al. 2007), with some modifications. Cells were seeded in 12-well plates with 1 mL *per* well of 3.5×10^5 cells and 3.0×10^5 cells, for C32 and A375 cells, respectively. After 4h for cell attachment at 37 ºC, scratches were carefully made across on full confluence of cell monolayers, using a 20 µL sterile pipette tip. Cells were then washed twice with warm phosphate buffered saline with calcium chloride and magnesium chloride (PBS) and incubated with complete medium, in the absence or in the presence of the compounds referred in section *Melanoma cell culture and treatment*, for 0, 12, and 24h incubation. All conditions were performed in duplicate, initiated and processed in parallel. At the bottom of each well, two arbitrary places were marked, where the width of the scratch was photographed using an Moticam 5 digital camera coupled to a Motic® AE200 inverted microscope (100X magnification; Spectra Services, VWR International, Carnaxide, Portugal). Scratch measurements were performed using the Motic® Images Plus 2.0 software.

Cell adhesion assay

The cell adhesion assay was performed as previously described (Chaturvedi et al. 2007), with some modifications. Plates of 96 wells were coated with 50 µL of ECM (12 mg/mL) or collagen (50 µg/mL), for 5 min or 1h, respectively, at room temperature. Thereafter, coating was aspirated and plates were blocked with 0.1% of BSA (w/v), for 30 min, at room temperature. C32 and A375 cells (100 µL *per* well of the suspension of 2.5×10^5 cells/mL) were prepared in complete medium, in the absence or in the presence of compounds referred in section *Melanoma cell culture and treatment*, and incubated for 1h. All conditions were

performed in triplicate, initiated and processed in parallel. At the end of the incubation period, cell suspension was discarded and wells were gently washed with warm PBS. Cells that adhered to the wells were incubated with MTT and processed as previously described (Soares et al. 2013).

Cell invasion assay

The cell invasion assay was performed as previously described (Chaturvedi et al. 2007), with some modifications. Corning-Transwell®-96 well supports with polyethylene terephthalate membranes (8.0 μm pores) were coated with 50 μL of BME (150 μg/mL) and incubated at 37 ºC, for 2h. Coating medium was then aspirated and supports blocked with 0.1% of BSA (w/v), for 30 min, at room temperature. Complete medium (150 μL) was then added to each reservoir well, with FBS as the chemo-attractant. C32 and A375 cells were seeded in the upper chamber with 50 μL *per* well of a cell suspension prepared in serum-free medium (1.0×10^6 cells/mL), treated with the compounds referred in section *Melanoma cell culture and treatment*, and incubated for 3h. All conditions were performed in triplicate, initiated and processed in parallel. At the end of the incubation period, cell suspension and medium from the reservoir were aspirated. Each support was gently swabbed and washed with PBS. Cells that passed through and attached to the bottom of the membrane were incubated with MTT and processed as previously described (Soares et al. 2013).

Determination of ERK1/2 levels

Cells were seeded in 6-well plates with 1 mL *per* well of 1.0×10^6 cells/mL and 2 mL of serum-free medium, and allowed to attach for 4h. Thereafter, cell medium was replaced by complete medium, in the absence or in the presence of the compounds referred in section *Melanoma cell culture and treatment*, and cells were incubated for 3h. All conditions were performed in duplicate, initiated and processed in parallel. At the end of incubation period, quantitative determination of ERK1/2 levels was done using the STAR ERK1/2 ELISA kit, according to the manufacturer's instructions.

Protein content determination

Protein content of cellular fractions in total cell lysates for the ERK1/2 assay was determined using the Bio-Rad RC DC protein assay kit, in accordance to the manufacturer's instructions. Stock solutions of BSA were used as standards.

Colony formation assay

The colony formation assay was performed as described previously (Taliaferro-Smith et al. 2009), with some modifications. Cells were plated in 6-well plates with 1 mL *per* well of 1×10^3 cells/mL and 2 mL of complete medium, in the absence or in the presence of the compounds referred in section *Melanoma cell culture and treatment*. After six days, medium was removed and colonies were washed with PBS. All conditions were performed in duplicate, initiated and processed in parallel. Colonies were fixed with 4% (w/v) paraformaldehyde in PBS (5 min), stained with 0.5% (v/v) crystal violet in distilled water (5 min), and rinsed with distilled water. Wells were photographed using a Sony Cyber-shot digital camera (10.1 Mega-pixel) and a Motic® AE200 inverted microscope (40X magnification) coupled to a Moticam 5 digital camera (Spectra Services, VWR International, Carnaxide, Portugal). Colonies were manually counted. Afterward, crystal violet was eluted with sodium citrate in ethanol (0.1M) and absorbance at 540 nm was measured in an automated microplate reader (PowerWaveXS, Bio-Tek Instruments Inc, Vermont, USA).

Animals

Adult Swiss CD-1 mice (8-12 weeks old) were purchased to Charles River Laboratories (Barcelona, Spain). Throughout the experiments mice were maintained in plastic cages at 21 ± 2 ºC, on a 12h light/dark cycle with free access to food and water. Animal welfare and experimental procedures were performed in strict accordance with the care and use of laboratory animals and the related ethic regulations of our Faculty. All possible efforts were made to minimize the animals' suffering and to reduce the number of animals used.

Mouse aortic ring assay

Animals were sacrificed by cervical dislocation and aorta was removed in a laminar flow hood. The mouse aortic ring assay was performed as described previously (Baker et al. 2012), with some modifications. After dissection, thoracic aorta was cleaned, cut into rings (approximately 0.5 mm in width) and placed into 96 well-plates, containing 50 µL/well of collagen type I (1mg/mL), and then incubated at 37ºC, for 1h. The wells were then filled with150 µL of Opti-MEM® medium containing 2.5 % (v/v) FBS, 1% (v/v) of a mixture of penicillin/streptomycin, VEGF at a final concentration of 100 ng/mL (with 0.1% v/v DMSO) and the compounds referred in section *Melanoma cell culture and treatment*. At least six rings *per* condition were used in each experiment. On the ninth day, microvessel sprouting from each ring was examined using a Motic® AE200 inverted microscope (40X and 100X magnification) coupled to a Moticam 5 digital camera

(Spectra Services, VWR International, Carnaxide, Portugal). Microvessel sprouting areas were quantitative analysed with the ImageJ software.

Statistical analysis

Results are presented as mean ± SEM for *n* experiments performed. Statistical comparisons between groups, at the same time point, were performed with One-Way ANOVA, after Shapiro-Wilk test normality evaluation. Significance was accepted at p values <0.05. The Student–Newman–Keuls post hoc test was used once a significant p was achieved. Details of statistical analysis are found in the legend of each figure.

Results

Cl-IB-MECA in combination with PXT decreased cell proliferation elicited by INO on both cell lines

Human C32 and A375 melanoma cells were treated with 50 μM of INO (INO50), 10 nM of MRE3008F20, 10 μM of Cl-IB-MECA (Cl10), 10 ng/mL of PXT (PXT10), and different combinations (INO50+MRE3008F20, INO50+Cl10, INO50+PXT10, INO50+Cl10+PXT10, and Cl10+PXT10), for 1, 3 and 24h (Fig. 1). Results from the MTT reduction assay showed that none of the compounds under study caused a significant effect on cell proliferation of C32 (Fig. 1A, 1C) and A375 cells (Fig. 1B, 1D), after 1 and 3h incubation. However, after 24h, results showed that INO50 significantly increased proliferation of both cell lines, although more pronounced on C32 cells, in comparison to the effect caused by the same treatment on A375 cells (Fig. 1E, 1F). Moreover, this effect was partially prevented by MRE3008F20 (A_3AR antagonist) in both cell lines (Fig. 1E, 1F). Treatment of C32 cells with Cl10+INO50 showed that Cl10 did not interfere with INO50-induced effect. In addition, Cl10 alone did not cause any change on MTT reduction of C32 cells at 24h (Fig. 1E). On the contrary, in A375, Cl10 was able to completely block MTT metabolization elicited by INO50. In fact, significant cytotoxicity was already observed for this compound alone, at the same incubation period (Fig. 1F). Results also revealed that when PXT10 was incubated with INO50, the effect elicited by INO50 was partially blocked in C32 (Fig. 1E) and completely prevented in A375 cells (Fig. 1F). Nevertheless, PXT10 alone caused similar cytotoxicity in both cell lines (Fig. 1E, 1F). Combination of INO50+Cl10+PXT10 and Cl10+PXT10 induced cytotoxicity on both melanoma cell lines, although more pronounced on A375 cells (Fig. 1E, 1F).

MRE3008F20 and Cl-IB-MECA in combination with PXT impaired cell migration induced by INO with dissimilar importance on both melanoma cell lines

Human C32 and A375 melanoma cells were treated with 50 μM of INO (INO50), 10 nM of MRE3008F20, 10 μM of Cl-IB-MECA (Cl10), 10 ng/mL of PXT (PXT10), and different combinations (INO50+MRE3008F20, INO50+Cl10, INO50+PXT10, INO50+Cl10+PXT10, and Cl10+PXT10) at 0, 12, and 24h. Cellular migration was investigated using the classic *in vitro* scratch assay in different time points, in both cell lines (Fig. 2 and Table 1). Results showed that INO50 significantly stimulated C32 and A375 cells migration comparatively to vehicle (Fig. 2 and Table 1). Pre-treatment of cells with MRE3008F20 revealed that this A_3AR antagonist impaired the migration effects elicited by INO50, in both cell lines. However, this blocking effect was dissimilar for C32 and A375 cells, since in C32 cells migration stopped at

12h incubation, whereas in A375 cells, migration still increased, reaching values similar to vehicle cells at 24h (Fig. 2A, 2B, Table 1). Nevertheless, MRE3008F20 by itself had no effect on C32 and A375 cell migration (Fig. 1C, 1D, Table 1).

Results also indicate that Cl10 prevented the INO50-estimulated migration effect and also significantly hindered C32 cells from normal migration (Fig. 2A, Table 1). Cl10 was able to block A375 cell migration elicited by INO50, although this compound alone did not cause any effect on A375 cellular migration. PXT10 combined with INO50 or alone caused similar effects on C32 cells to those described for Cl10 (Fig. 2A, Table 1). On the contrary, PXT10 was not able to prevent A375 cell migration caused by INO50 and, when incubated alone, this compound did not show any effect on A375 cell migration (Fig. 2B, Table 1).

When C32 cells were treated with INO50+Cl10+PXT10, results indicate more pronounced effects on cells when compared to cells incubated with INO50+Cl10 or INO50+PXT10 (Fig. 2A, Table 1). However, INO50+Cl10+PXT10 only blocked A375 cell migration stimulated by INO50, whereas it did not significantly hinder cells from normal migration (Fig. 2B, Table 1).

Melanoma cell adhesion induced by INO is A_3AR and substrate dependent and the combination of Cl-IB-MECA and PXT interferes with this effect

Melanoma cells were treated with 50 μM of INO (INO50), 10 nM of MRE3008F20, 10 μM of Cl-IB-MECA (Cl10), 10 ng/mL of PXT (PXT10), and different combinations (INO50+MRE3008F20, INO50+Cl10, INO50+PXT10, INO50+Cl10+PXT10, and Cl10+PXT10), at 1h. The extracellular matrix, ECM gel (Fig. 3A and 3C), and collagen type I (not present in ECM; Fig. 3B and 3D) were used to evaluate the interference of these compounds on cellular adhesion. Results revealed that both cell lines show significant increased adhesion to both substrates, when compared to wells without any coating (Fig. 3A, 3B, 3C and 3D). C32 cells treated with INO50 in the absence or in the presence of MRE3008F20 (A_3AR antagonist), and placed in ECM gel, showed that INO50 did not statistically affect cell adhesion (Fig. 3A), although a positive tendency was observed. However, when these cells were placed in collagen type I, INO50 significantly stimulated cell adhesion and it seems that MRE3008F20 was able, at least in part, to prevent the INO50 effect (Fig. 3B). Similar effects elicited by INO50 alone, or in combination with MRE3008F20, were also found for A375 cells, after 1h incubation (Fig. 3C and 3D). Nevertheless, MRE3008F20 by itself did not interfere with C32 (Fig. 3A and 3B) and A375 (Fig. 3C and 3D) cell adhesion in both substrates, at 1h.

Cl10 significantly reduced C32 cell adhesion stimulated by INO50, in both matrices tested (Fig. 3A and 3B). Moreover, Cl10 alone impaired C32 cell adhesion when compared with vehicle with the respective substrate (Fig. 3A and 3B). Similar effects caused by Cl10 were also observed for A375 cells, at 1h (Fig. 3C and 3D). Results also showed that PXT10, in combination with INO or alone, did not cause any effect on cellular adhesion of both cell lines and in both substrates, at 1h (Fig. 3A, 3B, 3C, and 3D). However, when PXT10 is co-incubated with Cl10 in absence or in the presence of INO50, a significant reduction in cell adhesion, of both cell lines in ECM coated wells, was observed, comparatively to the respective vehicle condition (Fig. 3A and 3B). Additionally, in ECM gel coated wells, C32 cells showed the highest decrease on cellular adhesion, for cells treated with the combination of Cl10+PXT10 (Fig. 3A). The same effect was not observed for A375 cells, since INO50+Cl10+PXT10 and Cl10+PXT10 had similar percentage inhibition for cellular adhesion (Fig. 3C). Melanoma C32 and A375 cells treated with INO50+Cl10+PXT10 or with Cl10+PXT10, placed on collagen type I (Fig. 3B and 3D), showed similar results to those obtained for ECM coated wells.

Cell invasion is potentiated by INO50 through A_3AR mechanisms, while Cl-IB-MECA with PXT causes different effects on cellular invasion in both melanoma cell lines

Melanoma cells were treated with 50 μM of INO (INO50), 10 nM of MRE3008F20, 10 μM of Cl-IB-MECA (Cl10), 10 ng/mL of PXT (PXT10), and different combinations (INO50+MRE3008F20, INO50+Cl10, INO50+PXT10, INO50+Cl10+PXT10, and Cl10+PXT10), at 3h. Human BME coated inserts were used to assess whether these compounds, or their combination, affect cellular invasion, at 3h (Fig. 4). Results indicated that INO50 was able to significantly stimulate C32 cells invasion ability (Fig. 4A), being this effect even more pronounced in A375 cells incubated with INO50 (Fig. 4B). Moreover, it seems that the A_3AR antagonist (MRE3008F20) was able to completely prevent this INO50 effect on C32 (Fig. 4A) whereas on A375 cells, MRE3008F20 was only able to partially block the increase of cell invasion elicited by INO50 (Fig. 4B). Combination of INO50 with Cl10 showed that Cl10 significantly impaired INO-induced invasion in both cell lines (Fig. 4A and 4B). Furthermore, Cl10 alone already inhibited cellular invasion on both cell lines, although more significantly in A375 cells, when compared to respective vehicle cells (Fig. 4A and 4B). When PXT10 is co-incubated with INO50, no changes were observed in either cell line (Fig. 4A and 4B). Results also showed that C32 and A375 cells treated with PXT10 alone had no alteration on cell invasion, comparatively to vehicle (Fig. 4A and 4B).

C32 cells treated with INO50+Cl10+PXT10 had lower invasion levels indicating that Cl10+PXT10 caused significant reduction of cellular invasion stimulated by INO50 (Fig. 4A). Nevertheless, the use of the combination Cl10+PXT10 revealed the highest inhibitory effect on invasion on these cells (Fig. 4A). Significant reduction of cellular invasion was observed for A375 cells incubated with INO50+Cl10+PXT10 (Fig. 4B), although this effect was inferior to that caused by INO50+Cl10. Similarly, Cl10 alone elicited a higher inhibitory cell invasion effect than that caused by Cl10+PXT10 alone (Fig. 4B).

INO-dependent increase on ERK1/2 levels is A_3AR-mediated and ERK1/2 levels are reduced by the combination of Cl-IB-MECA with PXT on melanoma cell lines

Melanoma cells were treated with 50 μM of INO (INO50) in the absence or in the presence of MRE3008F20 (10 nM), Cl-IB-MECA (10 μM, Cl10), PXT (10 ng/mL, PXT10), and Cl10+PXT10, for 3h incubation (Fig. 5). Results obtained with the ERK1/2 ELISA kit revealed that INO50 significantly increased ERK1/2 levels on C32 cells (Fig. 5A) although this effect was more pronounced in A375 cells (Fig. 5B). Cells pre-incubated with MRE3008F20 showed that this A_3AR antagonist was able to completely prevent the effect elicited by INO50, on both melanoma cells (Fig. 5). Results with Cl10 and INO50 indicated that this compound set the ERK1/2 levels comparable to vehicle levels, on C32 cells (Fig. 5A). For A375 cells, Cl10 besides suppressing the INO50-induced effect also decreased ERK1/2 levels to levels below values found in the vehicle (Fig. 5B). On the contrary, PXT10 proved to be ineffective on blocking the increase of ERK1/2 levels elicited by INO 50, on both cell lines (Fig. 5). The combination of INO50+Cl10+PXT10 showed that Cl10+PXT10 significantly reduced ERK1/2 levels induced by INO50, on C32 cells (Fig. 5A). Significant decrease in ERK1/2 levels was also observed for A375 cells incubated with INO50+Cl10+PXT10, although this effect was lower than what was caused by INO50+Cl10 (Fig. 5B).

Anchorage-independent A375 cell growth was potentiated by INO50 through A_3AR activation and is reduced by Cl-IB-MECA and PXT

Melanoma cells were treated with 50 μM of INO (INO50), 10 nM of MRE3008F20, 10 μM of Cl-IB-MECA (Cl10), 10 ng/mL of PXT (PXT10), and different combinations (INO50+MRE3008F20, INO50+Cl10, INO50+PXT10, INO50+Cl10+PXT10, and Cl10+PXT10), for six days (Fig. 6). The ability of cancer cells to exhibit anchorage-independent cell growth was evaluated through the colony formation assay. Results showed that C32 melanoma cells have no colony-forming ability (data not shown). On the contrary, A375

cells not only had colony-forming ability as when treated with INO50 this ability was significantly increased (Fig. 6). Moreover, MRE3008F20 (A_3AR antagonist) was able to completely prevent the INO50-colony stimulating effect (Fig. 6). When A375 cells were co-incubated with INO50 and Cl10, colony formation is significantly reduced (Fig. 6), being the size of these colonies smaller than those observed in vehicle condition (Fig. 6A). Similar effects were achieved by Cl10 alone (Fig. 6). Results also showed that PXT10 alone or in combination with INO50 exhibited similar colony reduction ability (Fig. 6). PXT10 effects were more pronounced than those obtained with INO50+Cl10 or Cl10, although colonies size is, in average, larger than that present in all conditions with Cl10 (Fig. 6). The combination of INO50+Cl10+PXT10 showed that Cl10+PXT10 significantly reduced the increase ability of INO to increase colony formation (Fig. 6).

Increased angiogenesis elicited by INO50 is reduced by the combination of Cl-IB-MECA and PXT

Mouse aortic rings were treated with VEGF (100 ng/mL) in the absence or in the presence of 50 μM of INO (INO50), 10 nM of MRE3008F20, 10 μM of Cl-IB-MECA (Cl10), 10 ng/mL of PXT (PXT10), and different combinations (INO50+MRE3008F20, INO50+Cl10, INO50+PXT10, INO50+Cl10+PXT10, and Cl10+PXT10), for nine days, to assess angiogenesis *in vitro* (Fig. 7). Rings without VEGF were used as negative controls for microvessel sprouting. Results showed that INO50 is an important angiogenesis promotor since it significantly stimulated microvessel sprouting, when compared to VEGF alone (Fig. 7). However, this effect was not prevented by the A_3AR antagonist (MRE3008F20). Additionally, MRE3008F20 alone did not interfere with VEGF-induced sprouting (Fig. 7). Rings treated with Cl10 showed that this compound completely inhibited INO50-induced effect and microvessel sprouting was even lower than VEGF levels (Fig. 7). A similar effect was observed for Cl10 incubated alone. Results also revealed that PXT10 did not cause any effect on microvessel sprouting elicited by INO50 or VEGF (Fig. 7). Nevertheless, when PXT10 was combined with Cl10, significant reduction on microvessel sprouting induced by INO50 was observed, representing the best combination for blocking INO50 effects (Fig. 7). Additionally, the combination of Cl10 with PXT10 almost totally abrogated VEGF-induced microvessel sprouting.

Discussion

Melanoma progression is associated with the abrogation of the normal controls that limit cell migration and invasion, eventually leading to metastasis (Haass and Herlyn 2005). Patients with metastatic melanoma have low survival rates due to the high resistance to chemotherapy and radiotherapy (Bhatia et al. 2009). We previously showed that the combination of Cl-IB-MECA with PXT caused cytotoxicity, through different mechanisms, on human C32 and A375 melanoma cells, at clinically relevant concentrations (Soares et al. 2013, 2014b).

Results now presented are the first demonstration that Cl-IB-MECA (10 μM), alone or in combination with PXT (10 ng/mL), is also very efficient in preventing the metastatic process stimulated by INO (50 μM) on human melanoma cells by (i) inhibiting cell proliferation; (ii) stopping cell migration; (iii) preventing ECM and collagen cell adhesion; (iv) blocking BME cell invasion through the reduction of ERK1/2 levels; (v) diminishing colony formation ability; and (vi) reducing angiogenesis (Fig. 8). Moreover, we provided evidence that the effects enhanced by INO on cells are A_3AR-dependent, but the pro-angiogenesis effect is A_3AR-independent. Nevertheless, Cl-IB-MECA+PXT was able to abolish all of them, although with dissimilar importance on human C32 and A375 melanoma cells, and almost always more efficiently than the compounds by themselves.

Before beginning of the studies on the metastatic potential of INO and the effects of the combination Cl-IB-MECA+PXT, the MTT reduction assay was performed to evaluate cellular proliferation or cytotoxicity at the same time points of migration, adhesion, and invasion assays, in both cell lines, as to avoid confounding effects on the assessment of the metastatic potential. We observed that in the time points of adhesion and invasion (1 and 3h) no changes were seen, thus increasing the reliability to our data, instead of being attributed to the overall proliferation induced by INO. At 24h, a significant increase in INO proliferation of both cell lines was observed. The only assay performed at this time point was migration where, in fact, the proliferation ability of INO can contribute to the migration stimulating effect. The data obtained on MTT and migration is, therefore, complementary. Cellular proliferation and migration are essential to several functions, such as melanoma tumour metastasis (Haass et al. 2005). Results of the *in vitro* scratch assay demonstrate that although the proliferation elicited by INO is only partially mediated by A_3AR activation at 24h, migration caused by this nucleoside is totally A_3AR-dependent, on both melanoma cell lines, after 24h incubation. This fact is not surprisingly since we have previously described that INO and adenosine induced C32 melanoma cell proliferation through A_3AR activation, after 48h (Soares et al. 2014a), although INO is

considered only an A_3AR partial agonist (Jin et al. 1997). Nevertheless, activation of A_{2B}AR by adenosine is reported to increase breast tumour cell migration *in vitro* (Stagg et al. 2010). This difference in AR activation could be related, at least in part, to the different cellular models used, reinforcing the fact that AR activation depends on cell type or concentration used (Di Virgilio 2012), even when similar results are observed.

Interestingly, Cl-IB-MECA at our working concentration (10 μM) did not cause any cytotoxic effect on C32 cells, after 24h, while it significantly decreased C32 cell migration elicited by INO or even by vehicle. On the contrary, Cl-IB-MECA alone already induced A375 cytotoxicity at 24h, while it did not cause significant interference in cell migration when compared to vehicle. Specific activation of A_3AR by Cl-IB-MECA was already described to reduce proliferation on A375 cells (Merighi et al. 2002). Moreover, in our data, Cl-IB-MECA blocked the stimulated migration effect elicited by INO. Although we have previously demonstrated that micromolar concentrations of Cl-IB-MECA cause melanoma C32 cell cytotoxicity through AR-independent mechanisms (Soares et al. 2013), herein we may assume that Cl-IB-MECA prevents cellular migration through interaction with A_3AR. In fact, Cl-IB-MECA (at micromolar concentrations) was described as a silent antagonist to A_3AR in the presence of micromolar concentrations of adenosine and INO (Wolber and Fozard 2005). However, it is well established that A_3AR agonists lose their selectivity at high concentrations (Mlejnek et al. 2013), which indicate that Cl-IB-MECA could also mediate its effects by interaction with other AR subtypes, in our model.

Discrepancies between C32 and A375 cells concerning their susceptibility to Cl-IB-MECA were previously described by us (Soares et al. 2014b). This fact may be justified by the different gender cell donator, as C32 were collected from male and A375 from female and different metastatic patterns were already found on female and male melanoma patients (Mervic 2012). Results obtained with PXT also differ between C32 and A375 cells, regarding its anti-migratory effects. Although in both melanoma cell lines, PXT similarly caused cytotoxicity at 24h, this drug only stopped C32 cell migration when compared to vehicle and INO conditions, without significantly affecting A375 cell migration. The classical anti-cancer PXT mechanism is the mitotic spindle stabilization, leading to inhibition of cell proliferation (Ahmed et al. 2011). However, PXT might exert some anti-cancer properties through mechanisms other than its well-known anti-mitotic activity (Tran et al. 2009). In fact, we previously reported that PXT also leads to the generation of reactive oxygen species (ROS) on C32 melanoma cells (Soares et al. 2013). B16F10 mouse melanoma cell migration and growth was described to be controlled by ROS production (Im et al. 2012). Taken together, these overall mechanisms may possible explain the anti-migratory effect of PXT on C32 cells.

When C32 and A375 cells were treated with Cl-IB-MECA+PXT, results demonstrated that this combination caused severe cytotoxicity and blocked INO induced proliferating effects, being these toxic effects more pronounced on A375 cells, after 24h. Moreover, this combination revealed to be more efficient in blocking INO-dependent migration effect on C32 cells, whereas Cl-IB-MECA+PXT elicited similar anti-migration effects on A375 cells to those caused by Cl-IB-MECA alone. Therefore, Cl-IB-MECA+PXT combination is very efficient in preventing A375 cell proliferation, but PXT, alone or in combination, does not contribute for stopping A375 cell migration. This observation is not surprising, since we found that PXT caused ROS generation on A375 cells (Soares et al. 2014b) and ROS production triggered by chemotherapeutic agents may promote cell damage and cell death, but can also lead to oncogenic phenotype of cancer cells (ROS are secondary messengers in intracellular signalling pathways) (Fruehauf and Meyskens 2007).

We found that both melanoma cell lines significantly adhere to ECM and collagen type I, after 1h incubation, which is in agreement with a study where SK-MEL-28 melanoma cells also strongly adhere to ECM and collagen type I and IV (Ohkawa et al. 2010). Although INO is considered an A_3AR partial agonist (Jin et al. 1997), we demonstrated that INO significantly stimulated cell adhesion to collagen type I, through A_3AR-dependent mechanisms. Increased levels of extracellular adenosine were also reported to increase adhesion of several melanoma cell lines (Sadej et al. 2006).

We also showed that Cl-IB-MECA has anti-adhesion properties on C32 and A375 cells, and in both adhesion matrices (ECM and collagen type I). The fact that other AR subtypes than A_3AR might be involved is a possibility, since at micromolar concentrations, agonists lose their selectivity (Mlejnek et al. 2013), and Cl-IB-MECA action as a silent antagonist may justify, again, the prevention INO-stimulatory effect on cell adhesion. On the contrary, PXT did not interfere with melanoma cellular adhesion. Nevertheless, PXT was described to inhibit the adhesion of B16F10 mouse melanoma cells to fibronectin and laminin (Wang et al. 2003), suggesting that human melanoma cells are more resistant to PXT treatments than mouse melanoma cells, concerning cell adhesion. In fact, human melanoma cells have been reported to present high adhesion ability, becoming very resistant to chemotherapy (Locatelli et al. 2009).

The combination Cl-IB-MECA+PXT promoted anti-adhesion effects, similar to those caused by Cl-IB-MECA alone, suggesting that in the combination Cl-IB-MECA+PXT, only Cl-IB-MECA is responsible for preventing cell adhesion.

Melanoma cell invasion was also studied, using human BME (also designated by matrigel), widely used on *in vitro* tumour cell invasion assays (Sallam et al. 2010). We found that INO significantly enhanced the

destruction of the first barrier on the cell invasion process, the basement membrane, being the invasive ability found for A375 cells higher. Moreover, this INO effect was A_3AR-dependent in both melanoma cell lines. Results demonstrated that Cl-IB-MECA prevented the invasion observed with vehicle and INO, without causing cytotoxicity, at 3h incubation. Moreover, PXT did not exhibit any anti-invasion ability on C32 and A375 cells, at 3h, in agreement to the adhesion assay results. However, reduction of cell invasiveness was observed in cell breast cancer cells for PXT concentrations also with no effect on cell viability (Tran et al. 2009). Results also suggested that the anti-invasive ability of the combination Cl-IB-MECA+PXT is only due to Cl-IB-MECA, as similar effects to those caused by Cl-IB-MECA alone were observed. We believe that Cl-IB-MECA blocked the stimulatory effect of INO (Jin et al. 1997), suggesting again the possibility of Cl-IB-MECA behaves as a silent A_3AR antagonist (Wolber and Fozard 2005).

To the best of our knowledge, it is the first time that Cl-IB-MECA is reported to cause anti-migration, anti-adhesion, and anti-invasion effects on human melanoma cells, and this can, at least in part, explain the positive results in clinical assays with hepatocellular carcinoma patients (Stemmer et al. 2013).

Detection of ERK1/2 levels, at the same time incubation of the invasion assay, seems to indicate that the expression of this protein is significantly increased by INO through A_3AR-dependent activation, on both melanoma cell lines. Higher levels of ERK1/2 were found on A375 cells, which is the cell line with higher invasion ability. Adenosine 100 μM was also found to stimulate ERK1/2 activation on A375 cells (Merighi et al. 2002). Cl-IB-MECA blocked the INO effect, and PXT did not cause any effect on ERK1/2 level, on both C32 and A375 cells, in agreement with the invasion assay results. Time-course studies have been published with Cl-IB-MECA and A375: 10 μM of Cl-IB-MECA was shown to had no effect on the expression level of ERK1/2 on A375 cells, at 1h incubation (Merighi et al. 2002), but years later other study stated that Cl-IB-MECA, in the same melanoma model, reduced basal levels of ERK1/2 in a 2h incubation period, by A_3AR activation, which in turn inhibited cell proliferation (Merighi et al. 2005). An adaptation process therefore occurs with Cl-IB-MECA incubation and, overall, we suggest that regulation of ERK1/2, one of the end proteins of the MAPK signalling pathway, is probably involved on adhesion and/or invasion processes induced by INO. Accordingly, adhesion-dependent ERK1/2 cascade activation was also found in human SK-MEL-24 and SK-MEL28 melanoma cells (Conner et al. 2003). Moreover, targeting ERK1/2 was also described as an efficient strategy to reduce B164A5 melanoma cell invasion (Romanchikova et al. 2013), as we observed for Cl-IB-MECA.

The ability to exhibit anchorage-independent cell growth (colony-forming ability) was also evaluated since it has been linked to the tumour's metastatic potential (Mori et al. 2009). We found that C32 cells did not form colonies, while A375 cells exhibited anchorage-independent cell growth. This fact may indicate that the aggressiveness of A375 cells is higher than C32 cells, thus suggesting higher metastatic potential for A375 cells. Moreover, the colony formation of these cells was enhanced by INO through A_3AR activation. The fact that Cl-IB-MECA decreased the size of the colonies, contrary to PXT that decreased the overall colony number, suggests that although both compounds combined are capable of diminishing vehicle and INO-induced colony formation, through different pathways, therefore enhancing the full potential of the combination. Similar approach was reported for the related Cl-IB-MECA compound, IB-MECA, which was reported to improve the chemotherapeutic effect of 5-fluorouracil, inhibiting colony formation of HCT-16 colon carcinoma cells, through downregulation of AKT and NF-kappaB protein expression (Bar-Yehuda et al. 2005). Previously, contrary effects induced by Cl-IB-MECA (10 μM) to those reported by us, described Cl-IB-MECA as to promote cell survival, increasing the number of colonies on A375 cells (Merighi et al. 2002).

Tumour cell survival and growth are dependent of adequate nutrient supply by blood. Thus, when cells are distant from blood vessels, expansion of tumour mass depends on angiogenesis (Sung et al. 2007). Our data indicate that INO significantly enhanced microvessel sprouting through A_3AR-independent mechanisms, and Cl-IB-MECA was able to prevent not only the INO-induced sprouting effect but also the normal vessel sprouting elicited by VEGF. Although Cl-IB-MECA was never reported to cause anti-sprouting effects, thio-Cl-IB-MECA, a related Cl-IB-MECA compound has been recently reported to decrease microvessel sprouting in mouse aortic rings through downregulation of PI3K/AKT/mTOR and ERK signalling of endothelial cells (Kim et al. 2013). In addition, we previously reported that Cl-IB-MECA decreases mTOR levels in melanoma cells (Soares et al. 2014b), suggesting that mTOR could represent a possible pathway by which Cl-IB-MECA mediates this observed anti-angiogenic effect. We demonstrated that although PXT alone did not prevent the development of microvessels promoted by INO, Cl-IB-MECA+PXT was the mostly effective condition in blocking microvessel sprouting.

In summary, we characterized, for the first time, the metastatic potential of two human melanoma cell lines, C32 and A375, and demonstrated that INO functions as an aggressiveness enhancer for both cells. We also provided evidence that, although some effects are prevented by using the selective A_3AR antagonist, MRE3008F20, the combination Cl-IB-MECA+PXT revealed to be almost always more efficient in stopping

metastatic progression. Moreover, the mechanisms not impaired by the clinically used PXT in melanoma are stopped upon Cl-IB-MECA addition. Therefore, we propose this combination as a new therapeutic approach for metastatic melanoma since it not only increases cytotoxicity but also inhibits metastatic progression, by affecting several mechanisms, namely migration, adhesion, invasion and angiogenesis (Fig. 8), overcoming PXT common chemotherapeutic resistance.

Acknowledgments

Work was funded by FEDER through the Program of Operational Competitiveness Factors – COMPETE and National Funds through FCT – Foundation for Science and Technology. ASS and VMC thank FCT for their PhD grant (SFRH/BD/64911/2009) and Post-doc grant (SFRH/BPD/63746/2009), respectively.

Conflict of interest

We declare that we have no conflict of interest in relation to this article.

References

Abdollahi A, Folkman J (2010) Evading tumor evasion: current concepts and perspectives of anti-angiogenic cancer therapy. Drug resistance updates : reviews and commentaries in antimicrobial and anticancer chemotherapy 13 (1-2):16-28

Ahmed AA, Wang X, Lu Z, Goldsmith J, Le XF, Grandjean G, Bartholomeusz G, Broom B, Bast RC, Jr. (2011) Modulating microtubule stability enhances the cytotoxic response of cancer cells to Paclitaxel. Cancer research 71 (17):5806-5817

Attoub S, Arafat K, Gelaude A, Al Sultan MA, Bracke M, Collin P, Takahashi T, Adrian TE, De Wever O (2013) Frondoside a suppressive effects on lung cancer survival, tumor growth, angiogenesis, invasion, and metastasis. PloS one 8 (1):e53087

Baker M, Robinson SD, Lechertier T, Barber PR, Tavora B, D'Amico G, Jones DT, Vojnovic B, Hodivala-Dilke K (2012) Use of the mouse aortic ring assay to study angiogenesis. Nature protocols 7 (1):89-104

Bandarchi B, Ma L, Navab R, Seth A, Rasty G (2010) From melanocyte to metastatic malignant melanoma. Dermatology research and practice 2010

Bar-Yehuda S, Madi L, Silberman D, Gery S, Shkapenuk M, Fishman P (2005) CF101, an agonist to the A3 adenosine receptor, enhances the chemotherapeutic effect of 5-fluorouracil in a colon carcinoma murine model. Neoplasia 7 (1):85-90

Bhatia S, Tykodi SS, Thompson JA (2009) Treatment of metastatic melanoma: an overview. Oncology 23 (6):488-496

Chaturvedi P, Singh AP, Moniaux N, Senapati S, Chakraborty S, Meza JL, Batra SK (2007) MUC4 mucin potentiates pancreatic tumor cell proliferation, survival, and invasive properties and interferes with its interaction to extracellular matrix proteins. Molecular cancer research : MCR 5 (4):309-320

Conner SR, Scott G, Aplin AE (2003) Adhesion-dependent activation of the ERK1/2 cascade is by-passed in melanoma cells. The Journal of biological chemistry 278 (36):34548-34554

Di Virgilio F (2012) Purines, purinergic receptors, and cancer. Cancer research 72 (21):5441-5447

Fruehauf JP, Meyskens FL, Jr. (2007) Reactive oxygen species: a breath of life or death? Clinical cancer research : an official journal of the American Association for Cancer Research 13 (3):789-794

Gessi S, Varani K, Merighi S, Cattabriga E, Avitabile A, Gavioli R, Fortini C, Leung E, Mac Lennan S, Borea PA (2004) Expression of A3 adenosine receptors in human lymphocytes: up-regulation in T cell activation. Molecular pharmacology 65 (3):711-719

Haass NK, Herlyn M (2005) Normal human melanocyte homeostasis as a paradigm for understanding melanoma. The journal of investigative dermatology Symposium proceedings / the Society for Investigative Dermatology, Inc [and] European Society for Dermatological Research 10 (2):153-163

Haass NK, Smalley KS, Li L, Herlyn M (2005) Adhesion, migration and communication in melanocytes and melanoma. Pigment cell research / sponsored by the European Society for Pigment Cell Research and the International Pigment Cell Society 18 (3):150-159

Huang YW, Baluna R, Vitetta ES (1997) Adhesion molecules as targets for cancer therapy. Histology and histopathology 12 (2):467-477

Im YS, Ryu YK, Moon EY (2012) Mouse Melanoma Cell Migration is Dependent on Production of Reactive Oxygen Species under Normoxia Condition. Biomolecules & therapeutics 20 (2):165-170

Jemal A, Siegel R, Xu J, Ward E (2010) Cancer statistics, 2010. CA: a cancer journal for clinicians 60 (5):277-300

Jin X, Shepherd RK, Duling BR, Linden J (1997) Inosine binds to A3 adenosine receptors and stimulates mast cell degranulation. The Journal of clinical investigation 100 (11):2849-2857

Kim GD, Oh J, Jeong LS, Lee SK (2013) Thio-Cl-IB-MECA, a novel A(3) adenosine receptor agonist, suppresses angiogenesis by regulating PI3K/AKT/mTOR and ERK signaling in endothelial cells. Biochemical and biophysical research communications 437 (1):79-86

Liang CC, Park AY, Guan JL (2007) In vitro scratch assay: a convenient and inexpensive method for analysis of cell migration in vitro. Nature protocols 2 (2):329-333

Locatelli C, Leal PC, Yunes RA, Nunes RJ, Creczynski-Pasa TB (2009) Gallic acid ester derivatives induce apoptosis and cell adhesion inhibition in melanoma cells: The relationship between free radical generation, glutathione depletion and cell death. Chemico-biological interactions 181 (2):175-184

Madonna G, Ullman CD, Gentilcore G, Palmieri G, Ascierto PA (2012) NF-kappaB as potential target in the treatment of melanoma. Journal of translational medicine 10:53

Merighi S, Benini A, Mirandola P, Gessi S, Varani K, Leung E, Maclennan S, Borea PA (2005) A3 adenosine receptor activation inhibits cell proliferation via phosphatidylinositol 3-kinase/Akt-dependent inhibition of the extracellular signal-regulated kinase 1/2 phosphorylation in A375 human melanoma cells. The Journal of biological chemistry 280 (20):19516-19526

Merighi S, Mirandola P, Milani D, Varani K, Gessi S, Klotz KN, Leung E, Baraldi PG, Borea PA (2002) Adenosine receptors as mediators of both cell proliferation and cell death of cultured human melanoma cells. The Journal of investigative dermatology 119 (4):923-933

Mervic L (2012) Time course and pattern of metastasis of cutaneous melanoma differ between men and women. PloS one 7 (3):e32955

Mlejnek P, Dolezel P, Frydrych I (2013) Effects of synthetic A3 adenosine receptor agonists on cell proliferation and viability are receptor independent at micromolar concentrations. Journal of physiology and biochemistry 69 (3):405-417

Mori S, Chang JT, Andrechek ER, Matsumura N, Baba T, Yao G, Kim JW, Gatza M, Murphy S, Nevins JR (2009) Anchorage-independent cell growth signature identifies tumors with metastatic potential. Oncogene 28 (31):2796-2805

Mosmann T (1983) Rapid colorimetric assay for cellular growth and survival: application to proliferation and cytotoxicity assays. Journal of immunological methods 65 (1-2):55-63

Ohkawa Y, Miyazaki S, Hamamura K, Kambe M, Miyata M, Tajima O, Ohmi Y, Yamauchi Y, Furukawa K, Furukawa K (2010) Ganglioside GD3 enhances adhesion signals and augments malignant properties of melanoma cells by recruiting integrins to glycolipid-enriched microdomains. The Journal of biological chemistry 285 (35):27213-27223

Romanchikova N, Trapencieris P, Zemitis J, Turks M (2013) A novel matrix metalloproteinase-2 inhibitor triazolylmethyl aziridine reduces melanoma cell invasion, angiogenesis and targets ERK1/2

phosphorylation. Journal of enzyme inhibition and medicinal chemistry. doi:10.3109/14756366.2013.855207

Sadej R, Spychala J, Skladanowski AC (2006) Expression of ecto-5'-nucleotidase (eN, CD73) in cell lines from various stages of human melanoma. Melanoma research 16 (3):213-222

Sallam AA, Ramasahayam S, Meyer SA, El Sayed KA (2010) Design, synthesis, and biological evaluation of dibromotyrosine analogues inspired by marine natural products as inhibitors of human prostate cancer proliferation, invasion, and migration. Bioorganic & medicinal chemistry 18 (21):7446-7457

Soares AS, Costa VM, Diniz C, Fresco P (2013) Potentiation of cytotoxicity of paclitaxel in combination with Cl-IB-MECA in human C32 metastatic melanoma cells: A new possible therapeutic strategy for melanoma. Biomedicine & pharmacotherapy 67 (8):777-789

Soares AS, Costa VM, Diniz C, Fresco P (2014a) Combination of Cl-IB-MECA with paclitaxel is a highly effective cytotoxic therapy causing mTOR-dependent autophagy and mitotic catastrophe on human melanoma cells. Journal of Cancer Research and Clinical Oncology. doi:10.1007/s00432-014-1645-z

Soares AS, Costa VM, Diniz C, Fresco P (2014b) Inosine strongly enhances human C32 melanoma cells proliferation through PLC-PKC-MEK1/2-ERK1/2 and PI3K pathways. Manuscript submitted for publication.

Spychala J (2000) Tumor-promoting functions of adenosine. Pharmacology & therapeutics 87 (2-3):161-173

Stagg J, Divisekera U, Duret H, Sparwasser T, Teng MW, Darcy PK, Smyth MJ (2011) CD73-deficient mice have increased antitumor immunity and are resistant to experimental metastasis. Cancer research 71 (8):2892-2900

Stagg J, Divisekera U, McLaughlin N, Sharkey J, Pommey S, Denoyer D, Dwyer KM, Smyth MJ (2010) Anti-CD73 antibody therapy inhibits breast tumor growth and metastasis. Proceedings of the National Academy of Sciences of the United States of America 107 (4):1547-1552

Stemmer SM, Benjaminov O, Medalia G, Ciuraru NB, Silverman MH, Bar-Yehuda S, Fishman S, Harpaz Z, Farbstein M, Cohen S, Patoka R, Singer B, Kerns WD, Fishman P (2013) CF102 for the treatment of hepatocellular carcinoma: a phase I/II, open-label, dose-escalation study. The oncologist 18 (1):25-26

Sung SY, Hsieh CL, Wu D, Chung LW, Johnstone PA (2007) Tumor microenvironment promotes cancer progression, metastasis, and therapeutic resistance. Current problems in cancer 31 (2):36-100

Taliaferro-Smith L, Nagalingam A, Zhong D, Zhou W, Saxena NK, Sharma D (2009) LKB1 is required for adiponectin-mediated modulation of AMPK-S6K axis and inhibition of migration and invasion of breast cancer cells. Oncogene 28 (29):2621-2633

Tran TA, Gillet L, Roger S, Besson P, White E, Le Guennec JY (2009) Non-anti-mitotic concentrations of taxol reduce breast cancer cell invasiveness. Biochemical and biophysical research communications 379 (2):304-308

Wang F, Cao Y, Liu HY, Xu SF, Han R (2003) Anti-invasion and anti-angiogenesis effect of taxol and camptothecin on melanoma cells. Journal of Asian natural products research 5 (2):121-129

Wolber C, Fozard JR (2005) The receptor mechanism mediating the contractile response to adenosine on lung parenchymal strips from actively sensitised, allergen-challenged Brown Norway rats. Naunyn-Schmiedeberg's archives of pharmacology 371 (2):158-168

Yamazoe Y, Tsubaki M, Matsuoka H, Satou T, Itoh T, Kusunoki T, Kidera Y, Tanimori Y, Shoji K, Nakamura H, Ogaki M, Nishiura S, Nishida S (2009) Dimethylfumarate inhibits tumor cell invasion and metastasis by suppressing the expression and activities of matrix metalloproteinases in melanoma cells. Cell biology international 33 (10):1087-1094

Figure captions

Fig.1 MTT reduction (% from vehicle) assay, after 1h (A, B), 3h (C, D), and 24h (E, F). Human C32 (A, C, and E) and A375 (B, D, and F) melanoma cells treated with INO (50 μM; INO50), MRE3008F20 (10 nM), Cl-IB-MECA (10 μM; Cl10), PXT (10 ng/mL; PXT10), and different combinations (INO50+MRE3008F20, INO50+Cl10, INO50+PXT10, INO50+Cl10+PXT10, and Cl10+PXT10). DMSO (final concentration of 0.1% v/v) in DMEM-HG was used as vehicle. Results are presented as means ± SEM, n=9-12 of 3-4 independent experiments. Significant differences (One-Way ANOVA test, followed by the Student-Newman-Keuls post-hoc test): *p<0.05 vs. vehicle; **p<0.01 vs. vehicle; ***p<0.001 vs. vehicle; $^{\#}$p<0.05 vs. INO50; $^{\#\#\#}$p<0.001 vs. INO50; $^{\$}$p<0.05 vs. corresponding condition without INO50; $^{\$\$\$}$p<0.001 vs. corresponding condition without INO50

Fig.2 Melanoma cell migration elicited by INO50 is A_3AR-mediated and impaired by Cl-IB-MECA in combination with PXT. Human C32 and A375 melanoma cells treated with INO (50 μM; INO50), MRE3008F20 (10 nM), Cl-IB-MECA (10 μM; Cl10), PXT (10 ng/mL; PXT10), and different (INO50+MRE3008F20, INO50+Cl10, INO50+PXT10, INO50+Cl10+PXT10, and Cl10+PXT10). DMSO (final concentration of 0.1% v/v) in DMEM-HG was used as vehicle. Representative photographs of melanoma cell migration of C32 cells (A) and A375 cells (B) of n=8 (4 independent experiments), after 0, 12, and 24h incubation. Black lines and dashed lines indicate the final and the initial scratched edges, respectively. Scale bar, 200 μm

Fig.3 Melanoma cell adhesion on ECM gel and collagen type I. Human C32 and A375 melanoma cells treated with INO (50 μM; INO50), MRE3008F20 (10 nM), Cl-IB-MECA (10 μM; Cl10), PXT (10 ng/mL; PXT10), and different combinations (INO50+MRE3008F20, INO50+Cl10, INO50+PXT10, INO50+Cl10+PXT10, and Cl10+PXT10). DMSO (final concentration of 0.1% v/v) in DMEM-HG was used as vehicle. Results of cell adhesion on ECM gel (% from vehicle) of C32 (A) and A375 (C) cells are presented as means ± SEM, n=9 of 3 independent experiments, after 1h incubation. Significant differences (One-Way ANOVA test, followed by the Student-Newman-Keuls post-hoc test): ***p<0.001 vs. vehicle; $^{\#\#\#}$p<0.001 vs. INO50; $^{\$}$p<0.05 vs. corresponding condition without INO50. Results of cell adhesion on collagen type I (% from vehicle) of C32 (B) and A375 (D) cells are presented as means ± SEM, n=9 of 3 independent experiments, after 1h incubation. Significant differences (One-Way ANOVA test, followed by

the Student-Newman-Keuls post-hoc test): *p<0.05 vs. vehicle; **p<0.01 vs. vehicle; ***p<0.001 vs. vehicle; $^{###}$p<0.001 vs. INO50; $^{\$\$}$p<0.01 vs. corresponding condition without INO50; $^{\$\$\$}$p<0.001 vs. corresponding condition without INO50

Fig.4 Melanoma cell invasion on BME. Human C32 and A375 melanoma cells treated with INO (50 μM; INO50), MRE3008F20 (10 nM), Cl-IB-MECA (10 μM; Cl10), PXT (10 ng/mL; PXT10), and different combinations (INO50+MRE3008F20, INO50+Cl10, INO50+PXT10, INO50+Cl10+PXT10, and Cl10+PXT10). DMSO (final concentration of 0.1% v/v) in DMEM-HG was used as vehicle. Results of cell invasion on BME (% from vehicle) of C32 (A) and A375 (B) cells are presented as means ± SEM, n=9 of 3 independent experiments, after 3h incubation. Significant differences (One-Way ANOVA test, followed by the Student-Newman-Keuls post-hoc test): *p<0.05 vs. vehicle; **p<0.01 vs. vehicle; ***p<0.001 vs. vehicle; $^{\#}$p<0.05 vs. INO50; $^{\#\#}$p<0.01 vs. INO50; $^{\#\#\#}$p<0.001 vs. INO50; $^{\$}$p<0.05 vs. corresponding condition without INO50; $^{\$\$}$p<0.01 vs. corresponding condition without INO50

Fig.5 Levels of ERK1/2 on human C32 (A) and A375 (B) melanoma cells treated with INO (50 μM; INO50), INO50+MRE3008F20, INO50+Cl10, INO50+PXT10, and INO50+Cl10+PXT10, after 3h incubation. DMSO (final concentration of 0.1% v/v) in DMEM-HG was used as vehicle. Results of ERK1/2 levels (OD_{450}/ng protein) are presented as means ± SEM of 3 independent experiments. Significant differences (One-Way ANOVA test, followed by the Student-Newman-Keuls post-hoc test): *p<0.05 vs. vehicle; $^{\#}$p<0.05 vs. INO50; $^{\#\#}$p<0.01 vs. INO50; $^{\#\#\#}$p<0.001 vs. INO50

Fig.6 Colony formation assay of human A375 melanoma cells treated with INO (50 μM; INO50), MRE3008F20 (10 nM), Cl-IB-MECA (10 μM; Cl10), PXT (10 ng/mL; PXT10), and different combinations (INO50+MRE3008F20, INO50+Cl10, INO50+PXT10, INO50+Cl10+PXT10, and Cl10+PXT10), after six days. DMSO (final concentration of 0.1% v/v) in DMEM-HG was used as vehicle. (A) Images from colonies stained with crystal violet were obtained with a digital camera (I) or with a microscope coupled to a digital camera [in this case with magnification of 40x (II)]. Scale bar, 500 μm. (B) Results of the number of colonies *per* well are means ± SEM of n=8, 4 independent experiments. Significant differences (One-Way ANOVA test, followed by the Student-Newman-Keuls post-hoc test): **p<0.01 vs. vehicle; ***p<0.001 vs. vehicle; $^{\#\#}$p<0.01 vs. INO50; $^{\#\#\#}$p<0.001 vs. INO50; $^{\$\$\$}$p<0.001 vs. corresponding condition without INO50. (C)

Results of optical density (540 nm) are means ± SEM of n=8, 4 independent experiments. Significant differences (One-Way ANOVA test, followed by the Student-Newman-Keuls post-hoc test): *p<0.05 vs. vehicle; ***p<0.001 vs. vehicle; $^{\#}$p<0.05 vs. INO50; $^{\#\#\#}$p<0.001 vs. INO50

Fig.7 Mouse aortic rings treated with VEGF (100 ng/mL with 0.1% v/v DMSO) in the absence or in the presence of INO (50 μM; INO50), MRE3008F20 (10 nM), Cl-IB-MECA (10 μM; Cl10), PXT (10 ng/mL; PXT10), and different combinations (INO50+MRE3008F20, INO50+Cl10, INO50+PXT10, INO50+Cl10+PXT10, and Cl10+PXT10), after nine days. (A) Images presented were obtained with a microscope coupled to a digital camera, magnification of 40x (I; scale bar, 500 μm) and 100x (II; scale bar, 200 μm). (B) Results of relative microvessel sprouting areas (% from VEGF) are presented as means ± SEM of n=3-5 independent experiments. Significant differences (One-Way ANOVA test, followed by the Student-Newman-Keuls post-hoc test): ***p<0.001 vs. vehicle; $^{\#\#\#}$p<0.001 vs. INO50; $^{\$\$\$}$p<0.001 vs. corresponding condition without INO50

Fig.8 Illustration representing enhanced proliferation, migration, adhesion, invasion, and increase on ERK1/2 levels stimulated by inosine on human C32 and A375 melanoma cells through A_3AR activation. Inosine also increases the ability of A375 cells to form colonies which is mediated by A_3AR. INO induces microvessel sprouting through A_3AR independent mechanisms. These pathways involved in melanoma progression are drastically decreased by the combination of Cl-IB-MECA with PXT

Table.1 Quantification of scratch closure (% from initial scratched edges) after cell treatment with INO (50 μM; INO50), MRE3008F20 (10 nM), Cl-IB-MECA (10 μM; Cl10), PXT (10 ng/mL; PXT10), and different combinations of these compounds (INO50+MRE3008F20, INO50+Cl10, INO50+PXT10, INO50+Cl10+PXT10, and Cl10+PXT10), at 12 and 24h incubation. DMSO (final concentration of 0.1% v/v) in DMEM-HG was used as vehicle. Results presented are means ± SEM, n=8 of 4 independent experiments. Significant differences (One-Way ANOVA test, followed by the Student-Newman-Keuls post-hoc test): *p<0.05 vs. vehicle; **p<0.01 vs. vehicle; ***p<0.001 vs. vehicle; $^{\#}$p<0.05 vs. INO50; $^{\#\#\#}$p<0.001 vs. INO50; $^{\$}$p<0.05 vs. corresponding condition without INO50; $^{\$\$}$p<0.01 vs. corresponding condition without INO50; $^{\$\$\$}$p<0.001 vs. corresponding condition without INO50

Fig. 1

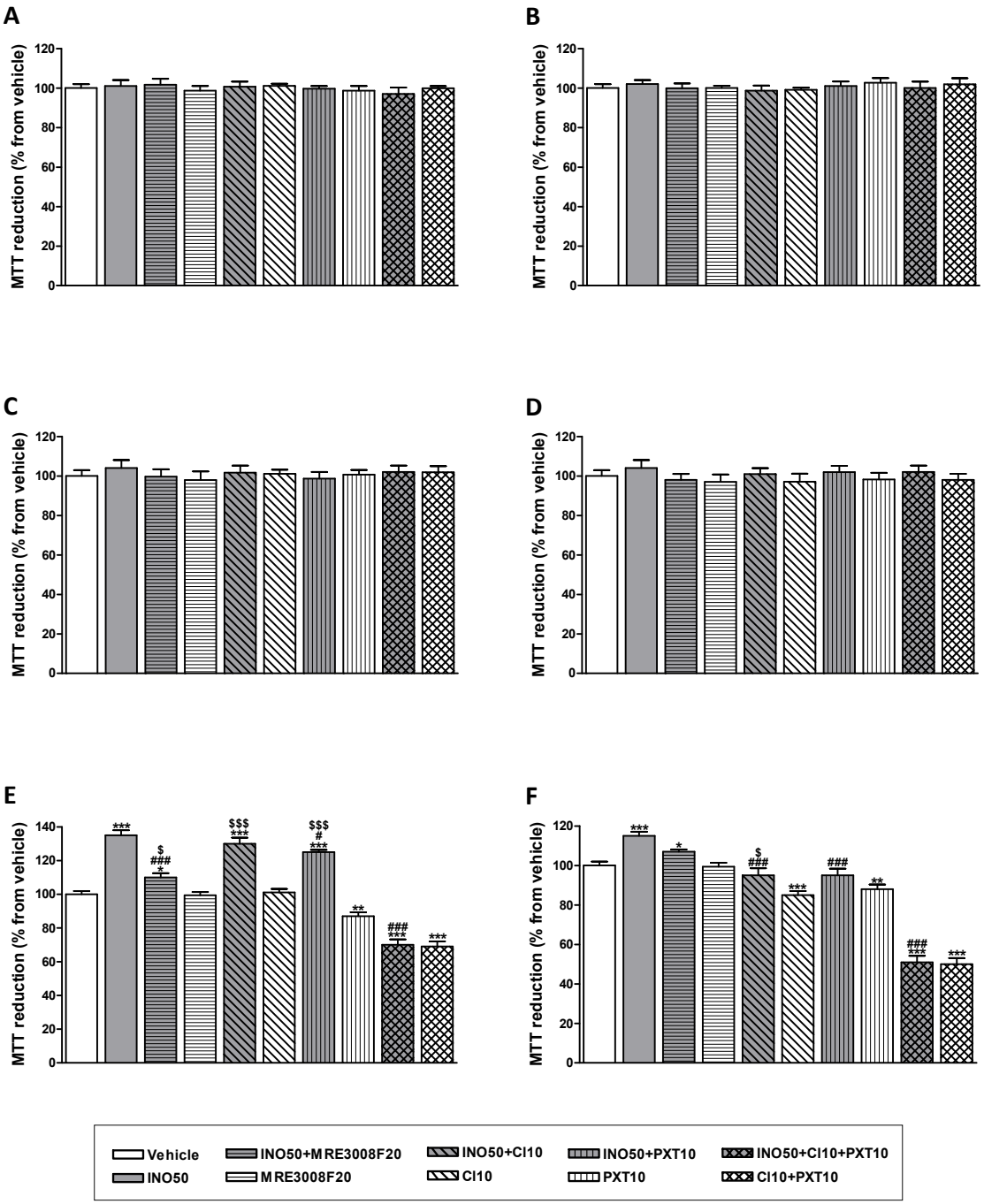
A
B
C
D
E
F
MTT reduction (% from vehicle)
Vehicle
INO50
INO50+MRE3008F20
MRE3008F20
INO50+CI10
CI10
INO50+PXT10
PXT10
INO50+CI10+PXT10
CI10+PXT10

Fig.2

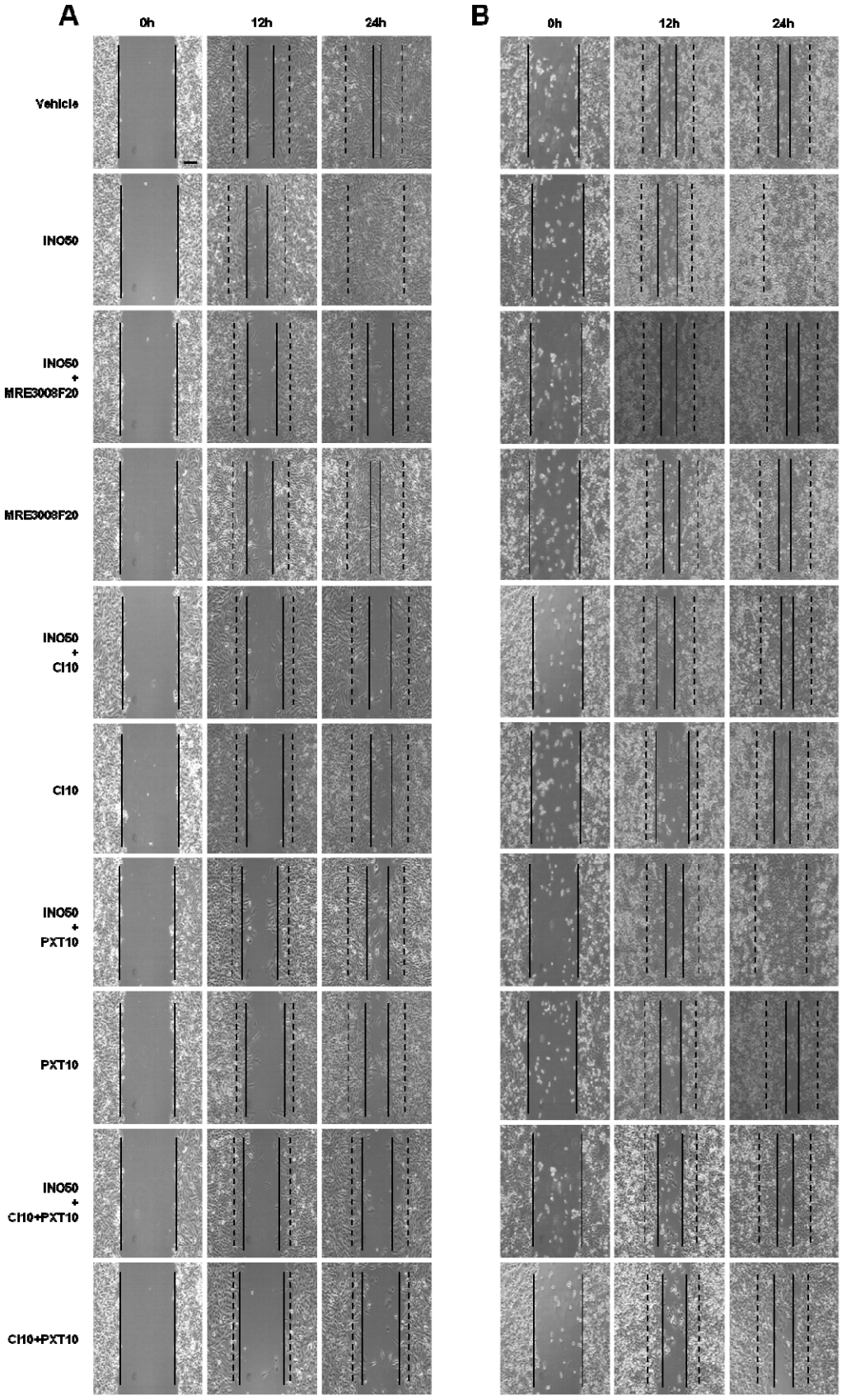
A
0h
12h
24h
Vehicle
INO50
INO50 + MRE3008F20
MRE3008F20
INO50 + CI10
CI10
INO50 + PXT10
PXT10
INO50 + CI10+PXT10
CI10+PXT10
B
0h
12h
24h

Fig.3

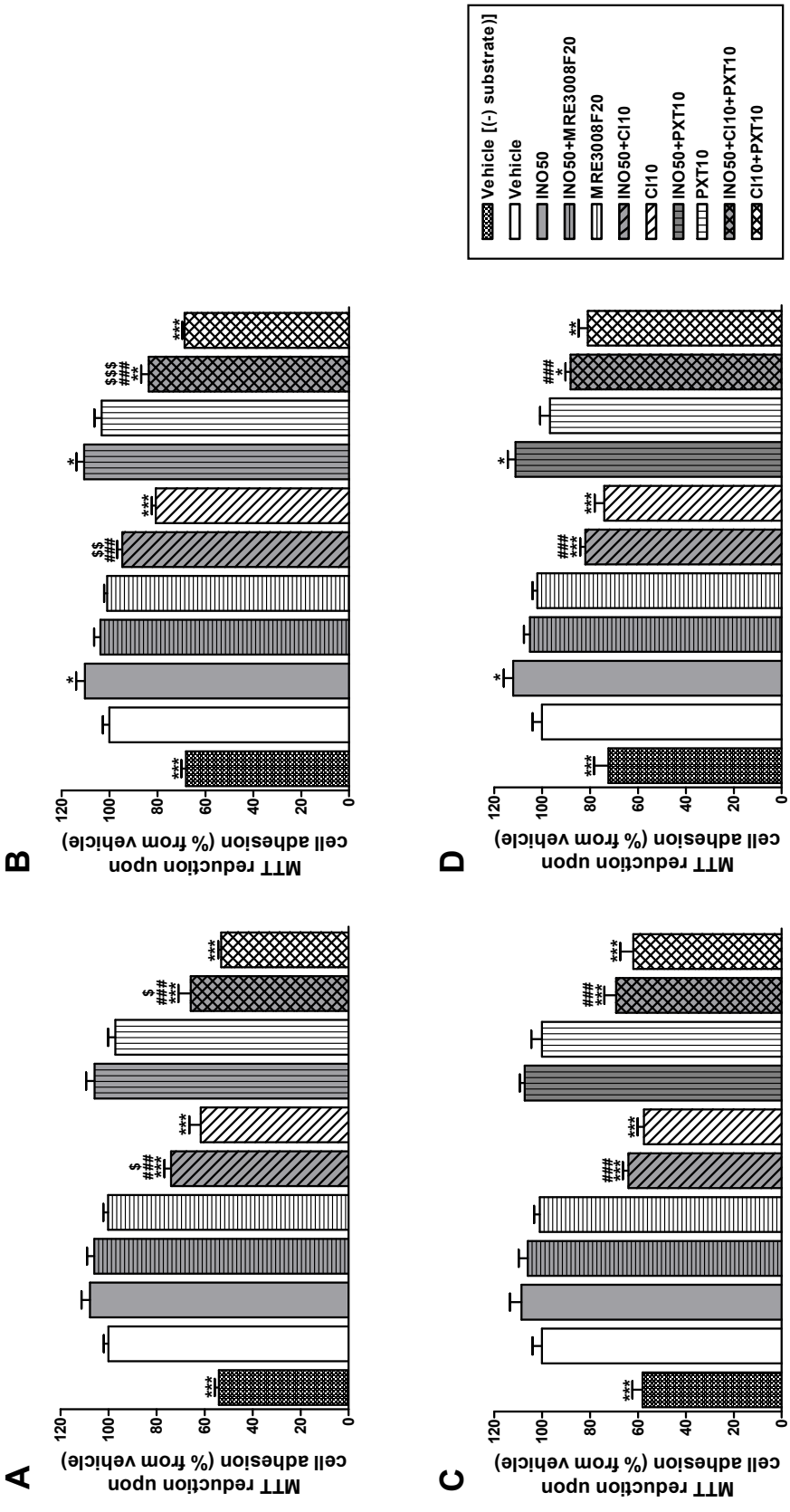
A
B
C
D
MTT reduction upon cell adhesion (% from vehicle)
Vehicle [(-) substrate)]
Vehicle
INO50
INO50+MRE3008F20
MRE3008F20
INO50+CI10
CI10
INO50+PXT10
PXT10
INO50+CI10+PXT10
CI10+PXT10

Fig.4

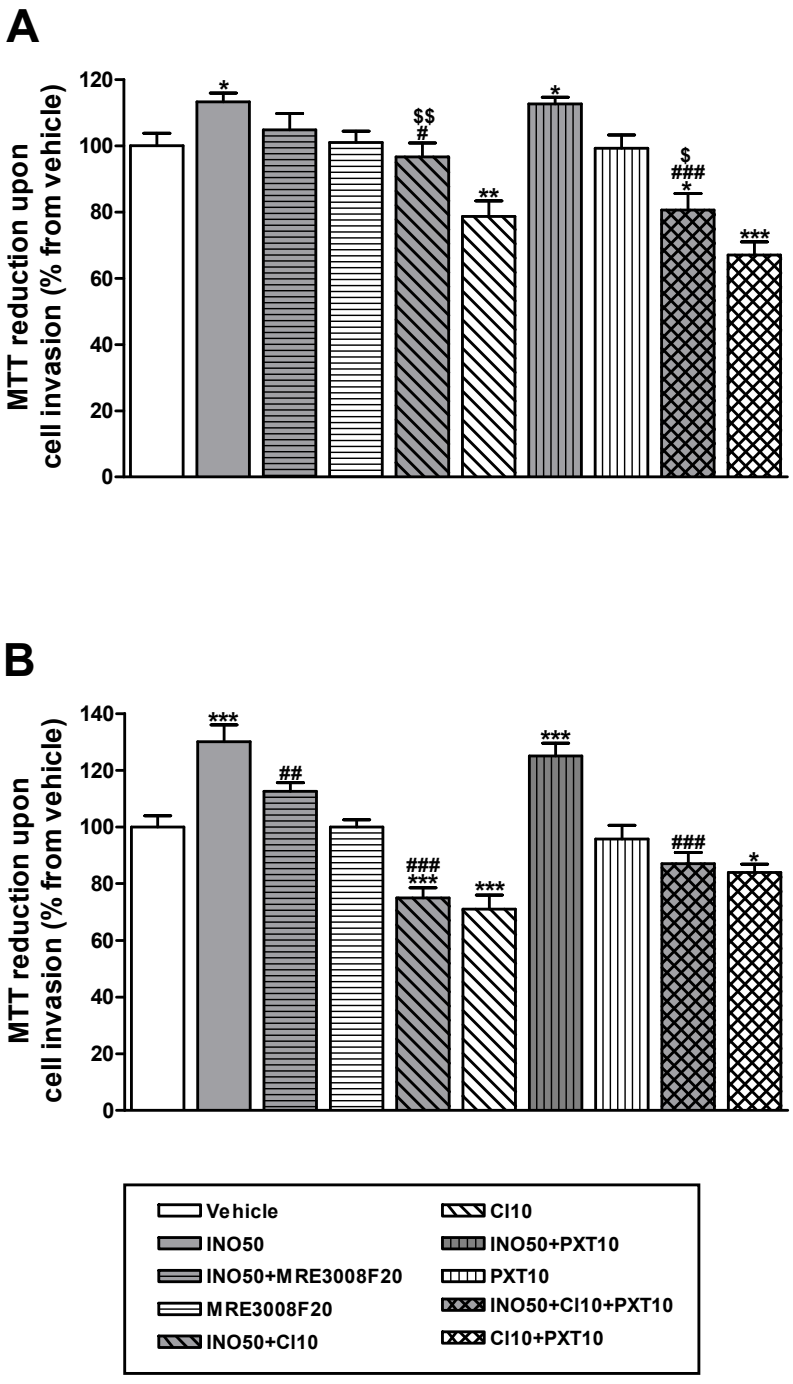
A
MTT reduction upon cell invasion (% from vehicle)
120
100
80
60
40
20
0
*
$$
#
**
*
$
###
*
***
B
MTT reduction upon cell invasion (% from vehicle)
140
120
100
80
60
40
20
0
***
##
###
***
***
***
###
*
Vehicle
INO50
INO50+MRE3008F20
MRE3008F20
INO50+CI10
CI10
INO50+PXT10
PXT10
INO50+CI10+PXT10
CI10+PXT10

Fig.5

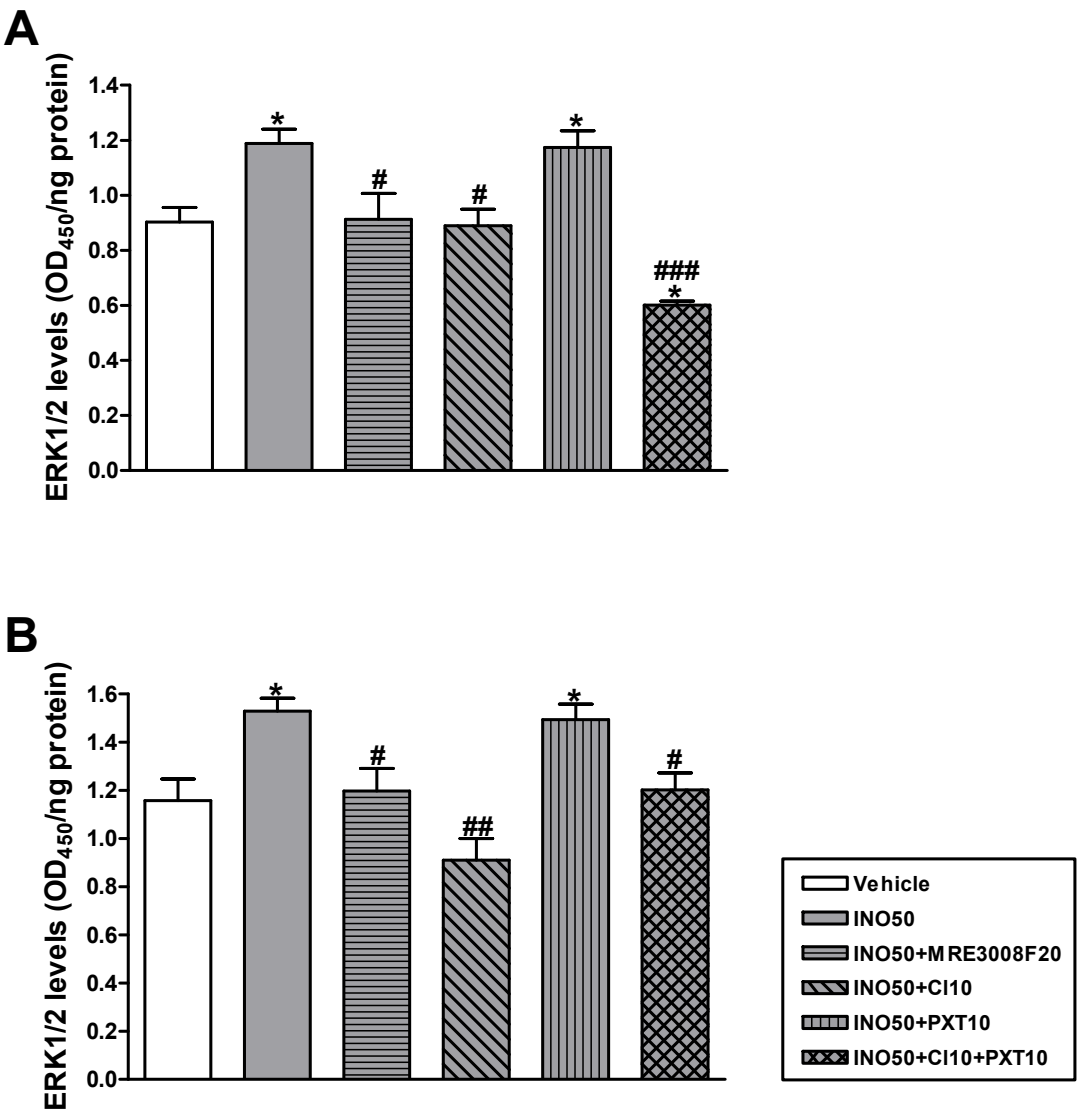
A
ERK1/2 levels (OD450/ng protein)
1.4
1.2
1.0
0.8
0.6
0.4
0.2
0.0
*
#
#
*
###
*
B
ERK1/2 levels (OD450/ng protein)
1.6
1.4
1.2
1.0
0.8
0.6
0.4
0.2
0.0
*
#
##
*
#
Vehicle
INO50
INO50+MRE3008F20
INO50+CI10
INO50+PXT10
INO50+CI10+PXT10

Fig.6

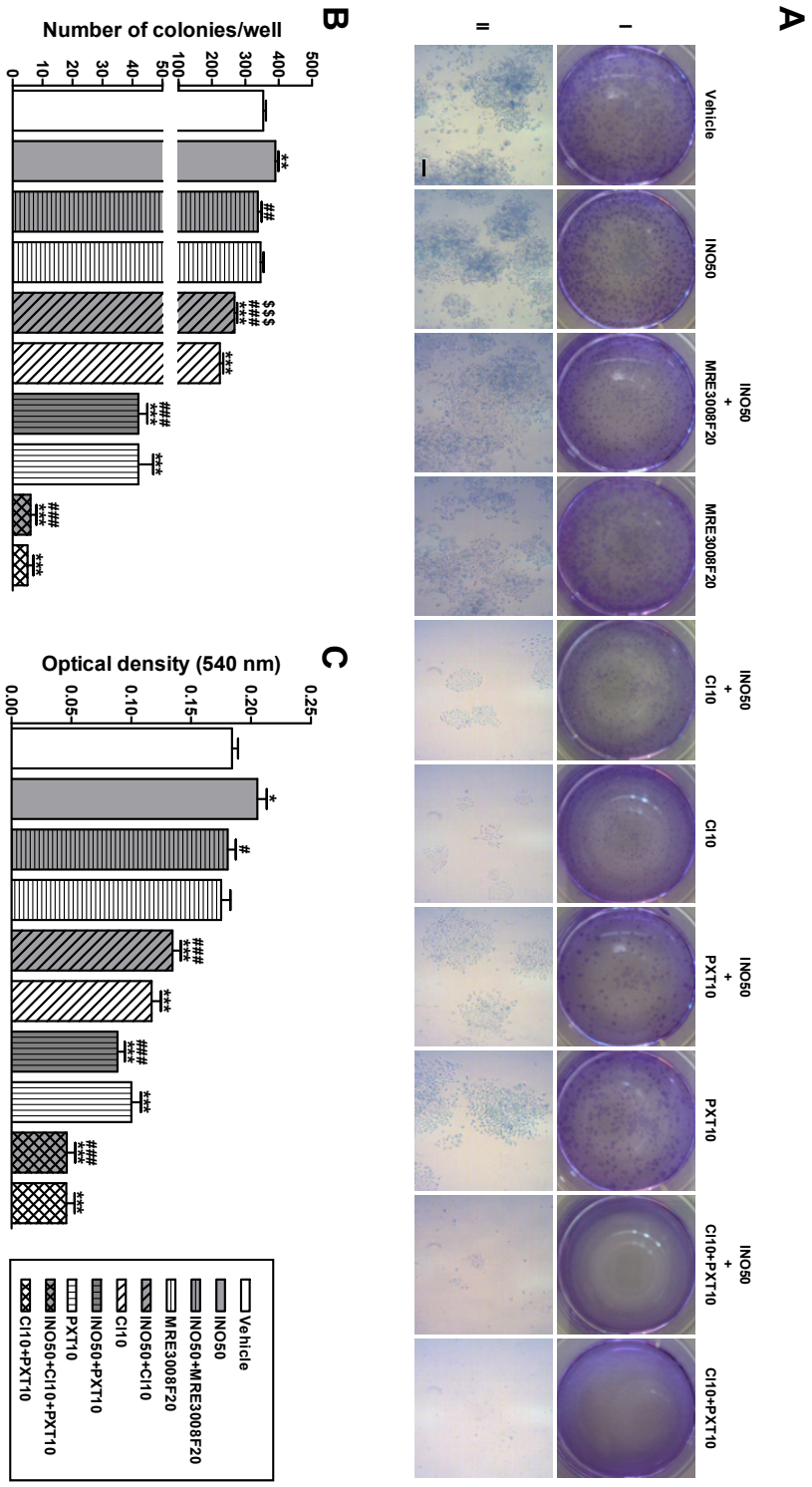
A
Vehicle
INO50
INO50 + MRE3008F20
MRE3008F20
INO50 + CI10
CI10
INO50 + PXT10
PXT10
INO50 + CI10+PXT10
CI10+PXT10
B
Number of colonies/well
C
Optical density (540 nm)
Vehicle
INO50
INO50+MRE3008F20
MRE3008F20
INO50+CI10
CI10
INO50+PXT10
PXT10
INO50+CI10+PXT10
CI10+PXT10

Fig.7

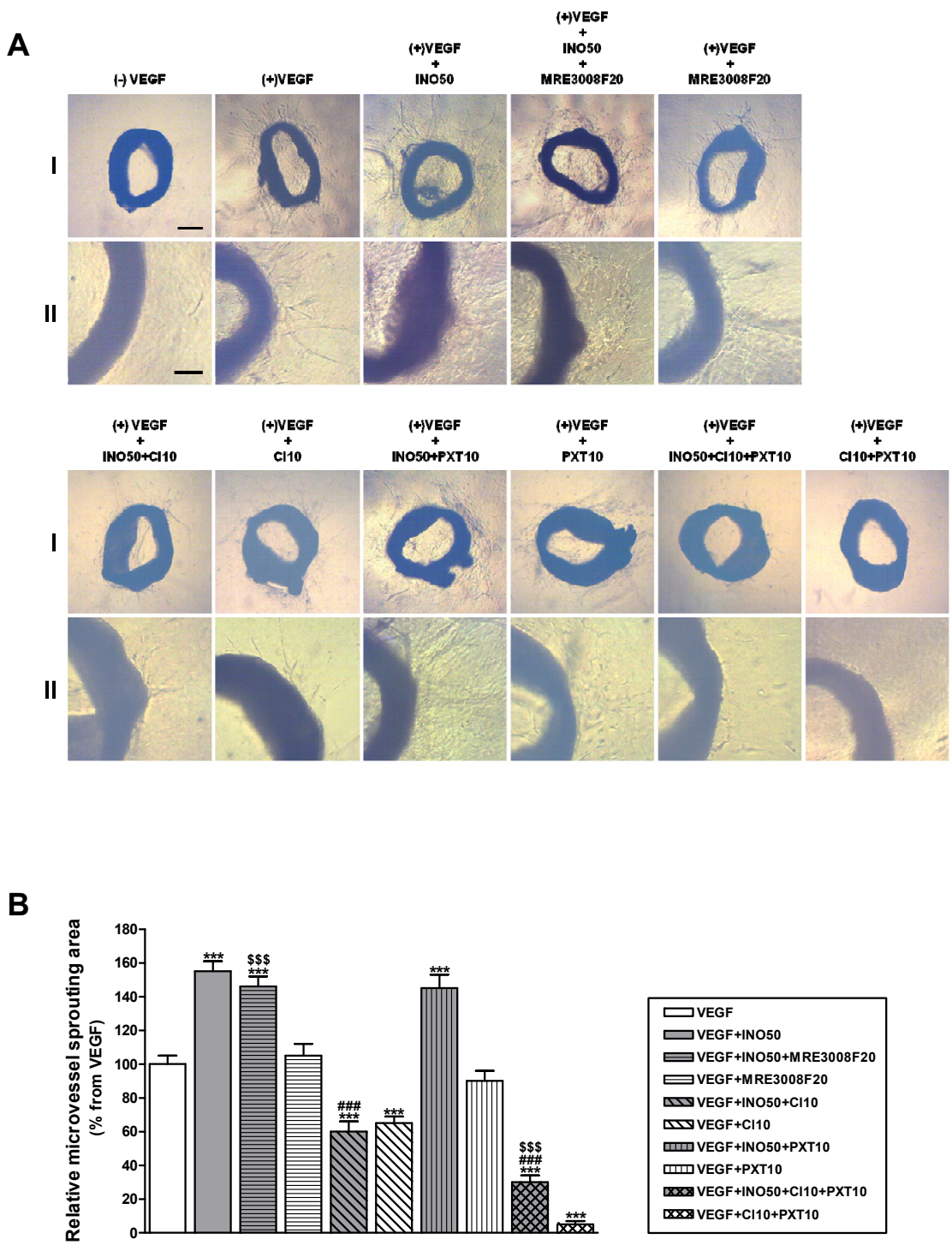
A
(-) VEGF
(+)VEGF
(+)VEGF + INO50
(+)VEGF + INO50 + MRE3008F20
(+)VEGF + MRE3008F20
I
II
(+) VEGF + INO50+CI10
(+)VEGF + CI10
(+)VEGF + INO50+PXT10
(+)VEGF + PXT10
(+)VEGF + INO50+CI10+PXT10
(+)VEGF + CI10+PXT10
B
Relative microvessel sprouting area (% from VEGF)
VEGF
VEGF+INO50
VEGF+INO50+MRE3008F20
VEGF+MRE3008F20
VEGF+INO50+CI10
VEGF+CI10
VEGF+INO50+PXT10
VEGF+PXT10
VEGF+INO50+CI10+PXT10
VEGF+CI10+PXT10

Fig.8

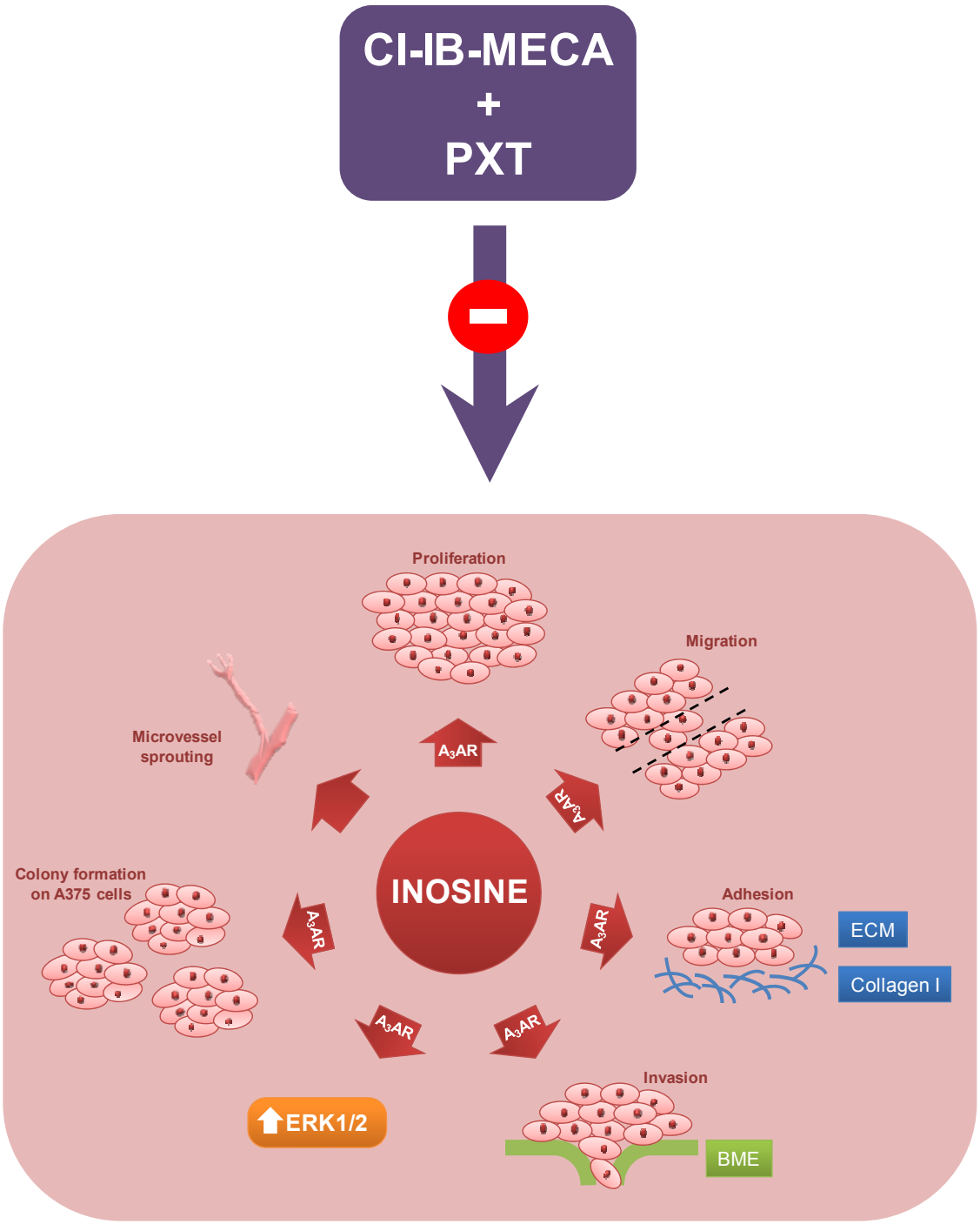
Cl-IB-MECA
+
PXT
Proliferation
Migration
Microvessel sprouting
A3AR
A3AR
INOSINE
Colony formation on A375 cells
A3AR
A3AR
A3AR
Adhesion
ECM
Collagen I
Invasion
BME
ERK1/2

TABLE 1 Quantification of scratch closure (% from initial scratched edges) after cell treatment, at 12 and 24h incubation.

	Scratch closure (% from initial scratched edges) (mean ± SEM)			
	C32 cells		**A375 cells**	
	12h	**24h**	**12h**	**24h**
Vehicle	56±2	89±4	68±3	75±4
INO50	67±1***	99±3*	62±1	99±2*
INO50+MRE3008F20	50±3$^{###}$	54±1***$^{;###;\$\$\$}$	64±2	76±3$^{\#}$
MRE3008F20	55±2	83±2	64±4	74±5
INO50+Cl10	28±1***$^{;###}$	61±4***$^{;###}$	62±1$^{\$\$\$}$	75±2$^{\#}$
Cl10	33±2***	60±4***	31±4***	68±6
INO50+PXT10	32±3***$^{;###}$	62±2***$^{;###}$	62±3	98±8*$^{;\$}$
PXT10	34±1***	56±4***	61±4	75±7
INO+Cl10+PXT10	38±3***$^{;###;\$\$\$}$	44±1***$^{;###;\$\$}$	49±7**$^{;\#}$	76±7$^{\#}$
Cl10+PXT10	22±1***	32±2***	49±8**	61±6

CHAPTER III

Discussion and Conclusions

1. GENERAL DISCUSSION

Data highlight the role of ADO as a crucial regulatory autocrine and paracrine factor that accumulates in the tumour microenvironment [124], favouring the neoplastic process [125]. The concentration of this nucleoside can rapidly increase in response to pathophysiological conditions, making it possible to activate AR, generating various cellular responses [126].

The overall aim of this thesis was to explore the role of the ADO-AR system in the complex interplay of proliferation, death and metastatic progression of melanoma cells and, if possible, find new therapeutic approaches for this deadliest form of skin cancer. To accomplish this goal human C32 [127], A375 [128] and K1735-M2 [129] melanoma cells were selected as these are well-accepted models to evaluate cytotoxic compounds that can be of interest against melanoma. The choice of these amelanotic cells is related to the fact that dedifferentiation is often associated with higher ability for cell proliferation [130].

Results showed, for the first time, the expression of all subtypes of AR (A_1, A_{2A}, A_{2B} and A_3) on human C32 and mouse K1735-M2 melanoma cells, by immunocytochemistry, and confirm their presence on human A375 melanoma cell line [131]. The A_3AR seems to be poorly expressed in all cell lines [131], which is in agreement with previous work showing that A_3 mRNAs are less abundant then A_{2A} and A_{2B} mRNAs in human A375 melanoma cells [109]. Moreover, although melanoma and other tumours express high levels of A_3AR [108], this fact is not true for all types of cancer cells, as human MCF-7 breast cancer cells have undetectable AR expression, whereas human MDA-MB-231 breast cancer cells only express high levels of A_{2B}AR [132].

Pharmacological characterization showed that activation of A_1AR, A_{2A}AR, and A_3AR at 24h did not interfere on cell proliferation of human A375 and mouse K1735-M2 melanoma cells [131]. However, on human C32 melanoma cells, A_3AR activation elicited by micromolar concentrations of ADO or by nanomolar concentrations of the selective A_3AR agonist Cl-IB-MECA induced cell proliferation. These findings suggest that activation of AR subtypes on melanoma cells is dependent on species and gender. In fact, C32 and A375 cells were collected from male and female, respectively, and different melanoma metastatic patterns were found on male and female patients [133]. The aforementioned results highlight the fact that caution should be taken in data extrapolation from mice to humans, and generalization of AR activation in human disease should be avoided. Nevertheless, these findings suggest that high expression of A_3AR is not essential to obtain effects. In fact, it seems that although being poorly expressed, it is the only receptor subtype that mediates ADO effects on human C32 melanoma cells.

On the other hand, Cl-IB-MECA at micromolar concentrations caused severe cytotoxicity on C32 cells, through A_3AR-independent mechanisms [131,134]. This data is in accordance with the fact that Cl-IB-MECA inhibits cell proliferation of human thyroid cancer cells without A_3AR activation [119]. Several possibilities could explain this effect, namely, loss of A_3AR selectivity and/or A_3AR desensitization [135]. Other possibilities include i) high concentrations of Cl-IB-MECA can bind to a yet unidentified membrane receptor and trigger downstream signalling or ii) Cl-IB-MECA can be transported into the cell via a NT, and once inside the cell signal through direct interaction with intracellular targets. However, the cytotoxic effect of Cl-IB-MECA in C32 cells was not prevented by the NT inhibitor NBTI (10 μM) [131,134], discarding the possibility that Cl-IB-MECA enters the cell by a NT-dependent mechanism, in our model. Nevertheless, one cannot discard the last possibility since Cl-IB-MECA can enter the cell through a NT-independent mechanism.

Evidence suggests that an increase in ADA activity can cause a reduction in the extracellular levels of ADO and, therefore, reduce tumour promotion [105]. The hypothesis that degradation of ADO would prevent melanoma cells proliferation was tested, since ADO induced proliferative effects on C32 melanoma cells [131]. The effects of ADO and its degradation (addition of ADA) were further studied, with the associated mechanisms being clarified. One major and surprising finding was that INO caused C32 cell proliferation more pronouncedly than ADO itself, those effects being mediated by A_3AR activation [136]. Moreover, reduction of cell proliferation by AOPCP (a ecto-5'NTase inhibitor, 100 μM) was demonstrated, suggesting that increased levels of AMP, in contrast to ADO, have an inhibitory effect on C32 cell proliferation [136]. Similar results obtained with AOPCP were reported in glioma [137] and breast [138] cancer cells. These findings highlight the complexity of the effects of ADO metabolism, suggesting that ADO degradation, through addition of ADA, is not a successful approach in preventing cell proliferation in this model. Indeed, this strategy may even worsen the clinical condition, since not only ADO, but also INO increases melanoma cell proliferation. Studies reporting increased levels of ADA in serum of patients with bladder [106], breast [139] and lung [140] cancer could be linked to our finding, suggesting a relevant role of the metabolic product of ADO in cancer. Attempts were also made in order to clarify the intracellular mechanisms by which INO mediates cell proliferation. Constitutive activation of PLC-PKC-MEK1/2-ERK1/2 and PI3K pathways was found in C32 melanoma cells and INO showed to increase cell proliferation through further increments of these pathways [136]. Moreover, we provide proof that A_3AR-MEK1/2-ERK1/2 activation is the major pathway responsible for the C32 proliferative effects elicited by INO. This finding is in agreement with the observation that normal melanocytes do not have detectable ERK activity,

requiring growth factors secreted by keratinocytes to survive, whereas melanoma cell lines have enhanced ERK activity due, in part, to autocrine factors stimulation [46]. Taking this into consideration, we propose INO as a stimulation autocrine factor for C32 melanoma cells. Moreover, although the MAPK pathway is primordial for cell proliferation, PI3K pathway is also essential, suggesting that both pathways may be possible targets for future melanoma anticancer therapy. These findings are in agreement with the fact that Ras-Raf-MEK-ERK and PI3K-AKT signalling pathways being constitutively activated in melanoma exerting several key functions in melanoma development and progression [39]. Therefore, these pathways may represent promising therapeutic targets for the effective treatment of metastatic melanoma.

In view of the fact that micromolar concentrations of Cl-IB-MECA caused cytotoxicity in C32 cells [131], the following aim was to understand the intracellular mechanisms elicited by this synthetic nucleoside on melanoma cells. Moreover, attempts were made to explore the potential cytotoxic synergistic effects of the combination of Cl-IB-MECA with a chemotherapeutic agent presently used in therapeutics, PXT. Combinations of cytotoxic agents may yield a slightly higher survival rate than monotherapies already in use for metastatic melanoma (reviewed in [66]). However, these combinations have been associated with higher toxicities [141]. In addition, melanoma usually relapses because most patients develop resistance to chemotherapeutics, namely to PXT [142]. The findings in this thesis demonstrate, for the first time, that the cytotoxicity induced by PXT is potentiated by the simultaneous use of Cl-IB-MECA (10, 20, and 50 μM), at clinically relevant concentrations, in human C32 melanoma cells [143]. PXT concentrations used in this study (10-50 ng/ml) are much lower than those already tested in human bone marrow cells without collateral toxicity [144] and much higher than concentrations found in plasma of PXT-treated cancer patients [145]. A_3AR agonists reveal differential effects on normal and malignant cells, without inhibiting normal cell growth [107] and Cl-IB-MECA is currently being tested in hepatocellular carcinoma patients and considered safe and well-tolerated [122]. Our proposed therapeutic combination seems to act synergistically in causing apoptosis in C32 cells, through enhancement of caspase 9, 8 and 3 activities, although lower concentrations of Cl-IB-MECA (10 and 20 μM) alone did not lead to caspases activation [143]. These findings proved to be very important as even concentrations for which Cl-IB-MECA has no effect, when this compound was combined with the chemotherapeutic agent PXT, the cytotoxic effects were enhanced. However, the cytotoxicity found for the combination of Cl-IB-MECA (10, 20, and 50 μM) and PXT (10 ng/mL) does not involve A_3AR activation. Micromolar concentrations of Cl-IB-MECA (5-80 μM) were also found to inhibit human thyroid carcinoma cell proliferation by a mechanism independent of the classical A_3AR activation [119]. In fact, when the non

selective AR antagonist (CGS 15943, 100 nM) was combined with Cl-IB-MECA and PTX, cytotoxicity was even more pronounced, suggesting that blocking AR probably prevents the binding of endogenous ADO and/or its metabolic product INO, which could be involved in C32 cell survival. The putative protective role of these molecules is in agreement with previous findings that showed the ability of ADO and/or INO to enhance proliferation of human C32 melanoma cells [131,136].

The combination of Cl-IB-MECA and PXT revealed a good therapeutic strategy (cytotoxicity) on metastatic melanoma treatment by induction of caspase-dependent apoptosis on human C32 melanoma cells. However, other mechanisms of cell death are definitively involved since the caspase inhibitor (Ac-DEVD-CHO, 50 μM) only prevented approximately 10% of the cytotoxic effects [143]. It is well accepted that the limited success of most current chemotherapeutic agents used in metastatic melanoma is, at least in part, related to cancer cells ability in escaping apoptosis, acquiring drug resistance [40]. Recently, another type of cell death, autophagy, has become an alternative approach to anticancer therapy, as pro-autophagic drugs seem to overcome drug resistance [146].

Efforts were made in order to elucidate the other mechanisms of cell death elicited by the cytotoxic combination of Cl-IB-MECA and PXT, namely the possible involvement of autophagy. Moreover, to increase knowledge on the potential use of this anticancer therapeutic strategy, this combination was also tested in another melanoma cellular model besides C32 cells. Importantly, Cl-IB-MECA in combination with PXT not only causes apoptosis but also induces autophagy, causing cell death on human C32 and A375 melanoma cells [147]. Activation of both apoptosis and autophagy has also been reported to occur in other human melanoma cells treated with a binuclear palladacycle complex [148]. While autophagy represents the main cell death mechanism of the drug combination for C32 cells, in A375 cells apoptosis and autophagy contribute equally to cell death [147]. This discrepancy between C32 and A375 cells concerning their susceptibility to the drug combination in study could be, in part, justified by the gender of each cell line donor, since different metastatic patterns were found on gender of patients with metastatic melanoma and C32 and A375 were collected from male and female donors, respectively [133]. This fact raises again the importance that generalization on gender human melanoma disease should be avoided as the progression of this disease is different in men and women. Therefore, individualized therapies would represent more efficient strategies for melanoma.

Despite mechanisms of autophagy regulation are not yet completely understood, evidence has shown that mTOR (a member of PI3K family) is involved in cell proliferation and plays a major role in preventing autophagy activation [149]. Results obtained with the combination of Cl-IB-MECA and PXT showed that levels of mTOR were decreased in C32

and A375 cells, as revealed by immunocytochemistry. Thus, it is conceivable that this combination inhibits the PI3K pathway, which was found to be constitutively activated in C32 cells [136]. The downregulation of mTOR and autophagy activation was found to be similar to that elicited by the PI3K inhibitor (LY294002, 50μM) [147]. In fact, autophagy has been reported to be regulated by suppression of mTOR expression [150].

At this point the PXT mechanisms for cell death are poorly understood [151] and apoptosis was found to be more related to PXT whereas Cl-IB-MECA was with autophagy. Strong disruption of microtubule networks and induction of micro- and multinucleation, hallmarks of mitotic catastrophe, were observed to occur for PXT and for the combination of Cl-IB-MECA with PXT [147]. Moreover, induction of mitotic catastrophe was found to be both caspase-dependent and independent. Although caspase-dependent mitotic catastrophe is being suggested as a special case of apoptosis [152], mitotic catastrophe through mechanisms dependent and/or independent of caspase activation has been also reported [153], corroborating our findings [147]. Overall, these findings provide appealing mechanisms concerning melanoma chemotherapy, as induction of autophagy in melanoma cells that are also undergoing apoptosis, drives more cells to die. Therefore, this therapeutic strategy will potentially improve the effectiveness of PXT through activation of other forms of melanoma cell death.

It is well accepted that cellular proliferation is fundamental for melanoma metastasis [154]. The development of metastasis starts with cell migration from the primary tumour, followed by re-adhesion and tissue invasion, with complex interactions between tumour cells and their environment [155]. Based on the variety of cellular mechanisms involved in metastatic progression, attempts were made in order to find new effective drugs that might inhibit tumour cell proliferation, cell migration and/or invasion, and also drugs with anti-angiogenic properties. We had previously demonstrated that INO dramatically increases melanoma cell proliferation [136] and the combination of Cl-IB-MECA with PXT revealed to be very efficient in the induction of melanoma cell death [143,147]. As such, the metastatic potential of human C32 and A375 melanoma cells was characterized. Afterwards, the role of INO on the promotion of the metastatic mechanisms and ability of the combination of Cl-IB-MECA with PXT in counteracting these effects were also investigated [156]. Our findings were the first demonstration that the combination of Cl-IB-MECA with PXT, is very efficient in preventing the metastatic process, stimulated by INO, on human C32 and A375 melanoma cells by (i) inhibiting cell proliferation; (ii) stopping cell migration; (iii) preventing cell adhesion; (iv) blocking cell invasion through the reduction of ERK1/2 levels; (v) diminishing colony formation ability; and (vi) reducing angiogenesis. In fact, although INO is considered a weaker but selective A_3AR agonist [157], it works as an aggressiveness agent for these melanoma cells [156].

Moreover, the effects enhanced by INO are A_3AR-dependent, with the exception of the pro-angiogenic effect which is A_3AR-independent. Nevertheless, the combination of Cl-IB-MECA with PXT was able to abolish all of them, although with dissimilar importance on the two melanoma cell lines. A surprising finding was the fact that Cl-IB-MECA alone is able to block the metastatic processes enhanced by INO. Although micromolar concentrations of Cl-IB-MECA caused melanoma C32 cell cytotoxicity through AR-independent mechanisms [134,143], it is conceivable that Cl-IB-MECA may prevent effects of INO involved in melanoma progression, through interaction with A_3AR. These results are in agreement with works that describe Cl-IB-MECA (at micromolar concentrations) as a silent A_3AR antagonist in the presence of micromolar concentrations of INO [158]. However, it is well established that A_3AR agonists lose their selectivity at high concentrations [159], which suggest that Cl-IB-MECA could also mediate its effects by interaction with other AR subtypes, in these melanoma cellular models. To the best of our knowledge, it is the first time that Cl-IB-MECA is reported to cause anti-migration, anti-adhesion, and anti-invasion effects on human melanoma cells, and this can, at least in part, explain the positive results of this compound in clinical assays [122]. Overall, the combination of Cl-IB-MECA with PXT revealed to be very efficient in stopping metastatic progression, as mechanisms not affected by PXT were impaired upon Cl-IB-MECA addition, thus overcoming the possible PXT chemotherapeutic resistance.

2. FINAL CONCLUSIONS AND FUTURE PERSPECTIVES

The ability of melanoma to metastasize results in early and general spread, causing very high mortality rates [1]. Resistance to chemotherapy and radiotherapy [66] is the main reason for patients with metastatic melanoma to have an overall survival rate of less than two years [1]. Chemotherapeutic drugs including alkylating agents (dacarbazine), platinum analogues (cisplatin, carboplatin) and anti-microbular agents (PXT) have been used, alone or in combination, although without significant survival rate improvement [66]. The lack of effective pharmacological approaches could be, at least in part, due to an incomplete understanding of the pathophysiological mechanisms involved in melanoma cells proliferation and, ultimately, tumour progression.

In this thesis, Cl-IB-MECA with PXT emerges as a promising cytotoxic combination for metastatic melanoma, acting through the induction of multiple mechanisms of cell death and blockade of several pathways involved in the metastatic potential of melanoma. This therapeutic strategy seems to overcome melanoma

multiresistance to chemotherapy and to stop, or delay, its progression, therefore, potentially improving metastatic melanoma treatment (Figure 8).

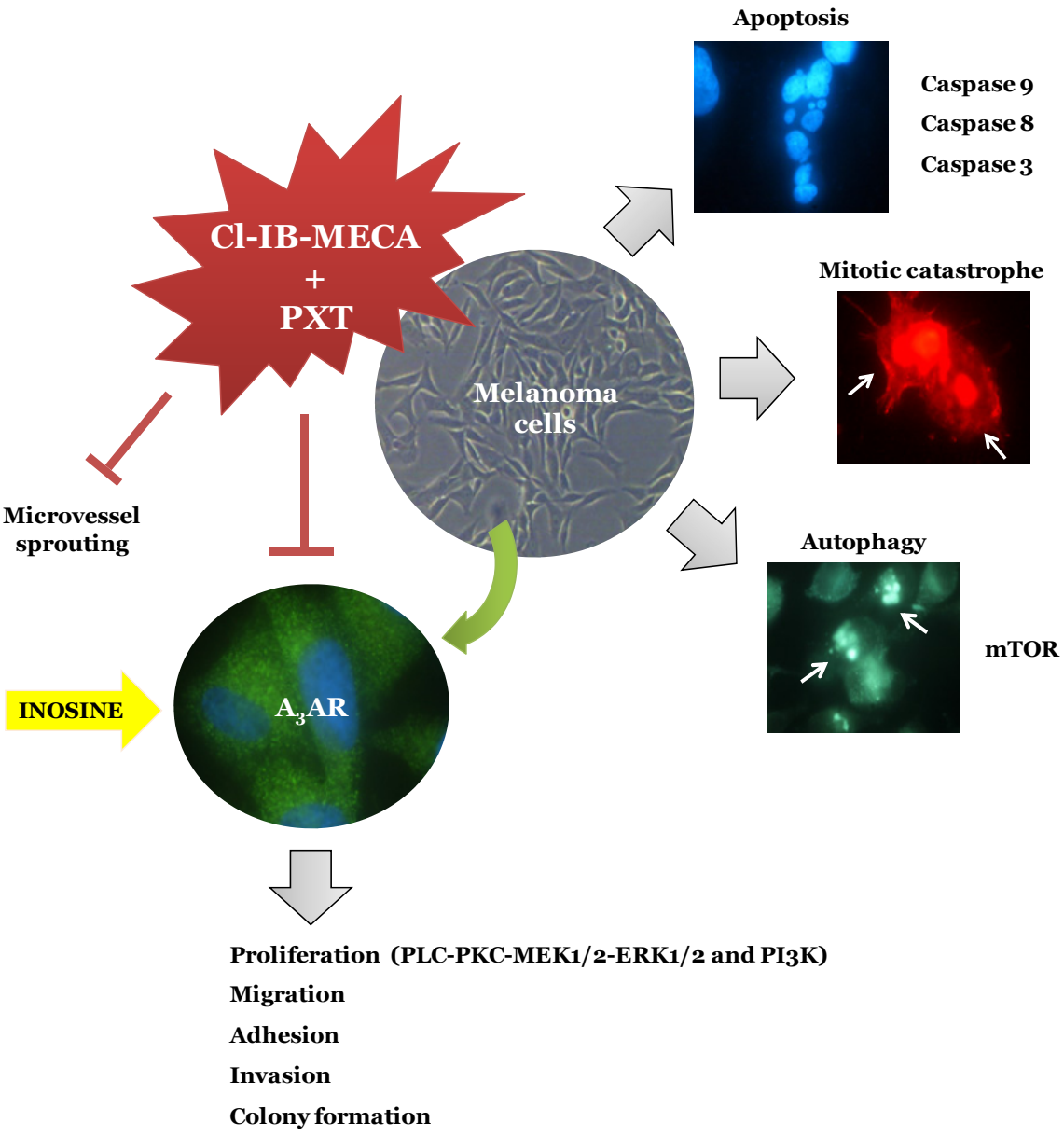

Figure 8. Postulated mechanisms for the cellular signalling pathways altered by the combination of Cl-IB-MECA and PXT. This combination induces multiple mechanisms of cell death (apoptosis with the involvement of mitotic catastrophe, and mTOR-dependent autophagy) and blocks several processes involved in melanoma progression, enhanced by inosine, namely, proliferation, migration, adhesion, invasion, colony formation (A_3AR activation), and microvessel sprouting (independent of A_3AR activation) as an angiogenesis indicator.

Although the strategy of counteracting the *in vitro* growth and progression of melanoma through the combination of Cl-IB-MECA and PXT seems to represent a promising therapeutic approach, the effects of this combination on normal melanocytes and co-cultures of melanoma cells with fibroblasts and/or keratinocytes, would be important to evaluate, as collateral toxicity represents enormous limitations in the development of novel therapies. Moreover, future studies using animal models are also needed to better understand the potential of this combination in anticancer therapy towards melanoma before clinical trials can be performed.

REFERENCES

1. REFERENCES

1 Bandarchi B, Ma L, Navab R, Seth A, Rasty G. From melanocyte to metastatic malignant melanoma. Dermatology research and practice 2010;2010. doi:10.1155/2010/583748.

2 Jemal A, Siegel R, Xu J, Ward E. Cancer statistics, 2010. CA: a cancer journal for clinicians 2010;60:277-300.

3 MacKie RM, Hauschild A, Eggermont AM. Epidemiology of invasive cutaneous melanoma. Annals of oncology : official journal of the European Society for Medical Oncology / ESMO 2009;20 Suppl 6:vi1-7.

4 Eggermont AM, Spatz A, Robert C. Cutaneous melanoma. Lancet 2013

5 Erdei E, Torres SM. A new understanding in the epidemiology of melanoma. Expert review of anticancer therapy 2010;10:1811-1823.

6 Neves AC, Ferreira GM, Teixeira MdC, Monteiro E. Early detection of skin cancer in primary care - an experience. Rev Port Clin Geral 2011;27:381-387.

7 Uong A, Zon LI. Melanocytes in development and cancer. Journal of cellular physiology 2010;222:38-41.

8 Sommer L. Generation of melanocytes from neural crest cells. Pigment cell & melanoma research 2011;24:411-421.

9 Cichorek M, Wachulska M, Stasiewicz A, Tyminska A. Skin melanocytes: Biology and development. Postepy dermatologii i alergologii 2013;30:30-41.

10 Whiteman DC, Pavan WJ, Bastian BC. The melanomas: A synthesis of epidemiological, clinical, histopathological, genetic, and biological aspects, supporting distinct subtypes, causal pathways, and cells of origin. Pigment cell & melanoma research 2011;24:879-897.

11 Nordlund JJ. The melanocyte and the epidermal melanin unit: An expanded concept. Dermatologic clinics 2007;25:271-281, vii.

12 Van Den Bossche K, Naeyaert JM, Lambert J. The quest for the mechanism of melanin transfer. Traffic 2006;7:769-778.

13 Kincannon J, Boutzale C. The physiology of pigmented nevi. Pediatrics 1999;104:1042-1045.

14 Halaban R, Langdon R, Birchall N, Cuono C, Baird A, Scott G, Moellmann G, McGuire J. Paracrine stimulation of melanocytes by keratinocytes through basic fibroblast growth factor. Annals of the New York Academy of Sciences 1988;548:180-190.

15 Curtin JA, Fridlyand J, Kageshita T, Patel HN, Busam KJ, Kutzner H, Cho KH, Aiba S, Brocker EB, LeBoit PE, Pinkel D, Bastian BC. Distinct sets of genetic alterations in melanoma. The New England journal of medicine 2005;353:2135-2147.

16 Bevona C, Goggins W, Quinn T, Fullerton J, Tsao H. Cutaneous melanomas associated with nevi. Archives of dermatology 2003;139:1620-1624.

17 Bandarchi B, Jabbari CA, Vedadi A, Navab R. Molecular biology of normal melanocytes and melanoma cells. Journal of clinical pathology 2013;66:644-648.

18 Pfeifer GP, Besaratinia A. Uv wavelength-dependent DNA damage and human non-melanoma and melanoma skin cancer. Photochemical & photobiological sciences 2012;11:90-97.

19 Wilkerson BL. Malignant melanoma. Plastic surgical nursing : official journal of the American Society of Plastic and Reconstructive Surgical Nurses 2011;31:105-107.

20 Besaratinia A, Pfeifer GP. Sunlight ultraviolet irradiation and braf v600 mutagenesis in human melanoma. Human mutation 2008;29:983-991.

21 Svobodova A, Walterova D, Vostalova J. Ultraviolet light induced alteration to the skin. Biomedical papers of the Medical Faculty of the University Palacky, Olomouc, Czechoslovakia 2006;150:25-38.

22 McMillan TJ, Leatherman E, Ridley A, Shorrocks J, Tobi SE, Whiteside JR. Cellular effects of long wavelength uv light (uva) in mammalian cells. The Journal of pharmacy and pharmacology 2008;60:969-976.

23 Hoerter JD, Bradley P, Casillas A, Chambers D, Weiswasser B, Clements L, Gilbert S, Jiao A. Does melanoma begin in a melanocyte stem cell? Journal of skin cancer 2012;2012:571087.

24 Jhappan C, Noonan FP, Merlino G. Ultraviolet radiation and cutaneous malignant melanoma. Oncogene 2003;22:3099-3112.

25 Mahabeleshwar GH, Byzova TV. Angiogenesis in melanoma. Seminars in oncology 2007;34:555-565.

26 Hsu MY, Meier F, Herlyn M. Melanoma development and progression: A conspiracy between tumor and host. Differentiation; research in biological diversity 2002;70:522-536.

27 Lee JT, Herlyn M. Microenvironmental influences in melanoma progression. Journal of cellular biochemistry 2007;101:862-872.

28 Gaggioli C, Sahai E. Melanoma invasion - current knowledge and future directions. Pigment cell research 2007;20:161-172.

29 Miller AJ, Mihm MC, Jr. Melanoma. The New England journal of medicine 2006;355:51-65.

30 Brozyna AA, Jozwicki W, Carlson JA, Slominski AT. Melanogenesis affects overall and disease-free survival in patients with stage III and IV melanoma. Human pathology 2013;44:2071-2074.

31 Rohren EM, Turkington TG, Coleman RE. Clinical applications of pet in oncology. Radiology 2004;231:305-332.

32 Li G, Satyamoorthy K, Meier F, Berking C, Bogenrieder T, Herlyn M. Function and regulation of melanoma-stromal fibroblast interactions: When seeds meet soil. Oncogene 2003;22:3162-3171.

33 Haass NK, Smalley KS, Li L, Herlyn M. Adhesion, migration and communication in melanocytes and melanoma. Pigment cell research 2005;18:150-159.

34 Mori S, Chang JT, Andrechek ER, Matsumura N, Baba T, Yao G, Kim JW, Gatza M, Murphy S, Nevins JR. Anchorage-independent cell growth signature identifies tumors with metastatic potential. Oncogene 2009;28:2796-2805.

35 Michaylira CZ, Nakagawa H. Hypoxic microenvironment as a cradle for melanoma development and progression. Cancer biology & therapy 2006;5:476-479.

36 Bennett DC. How to make a melanoma: What do we know of the primary clonal events? Pigment cell & melanoma research 2008;21:27-38.

37 Jones V, Katiyar SK. Emerging phytochemicals for prevention of melanoma invasion. Cancer letters 2013;335:251-258.

38 Meier F, Busch S, Lasithiotakis K, Kulms D, Garbe C, Maczey E, Herlyn M, Schittek B. Combined targeting of mapk and akt signalling pathways is a promising strategy for melanoma treatment. The British journal of dermatology 2007;156:1204-1213.

39 Meier F, Schittek B, Busch S, Garbe C, Smalley K, Satyamoorthy K, Li G, Herlyn M. The Ras/Raf/MEK/ERK and PI3K/AKT signaling pathways present molecular targets for the effective treatment of advanced melanoma. Frontiers in bioscience 2005;10:2986-3001.

40 Soengas MS, Lowe SW. Apoptosis and melanoma chemoresistance. Oncogene 2003;22:3138-3151.

41 Hilger RA, Scheulen ME, Strumberg D. The Ras-Raf-MEK-ERK pathway in the treatment of cancer. Onkologie 2002;25:511-518.

42 Rodolfo M, Daniotti M, Vallacchi V. Genetic progression of metastatic melanoma. Cancer letters 2004;214:133-147.

43 Lazar-Molnar E, Hegyesi H, Toth S, Falus A. Autocrine and paracrine regulation by cytokines and growth factors in melanoma. Cytokine 2000;12:547-554.

44 McCubrey JA, Steelman LS, Chappell WH, Abrams SL, Wong EW, Chang F, Lehmann B, Terrian DM, Milella M, Tafuri A, Stivala F, Libra M, Basecke J, Evangelisti C, Martelli AM, Franklin RA. Roles of the Raf/MEK/ERK pathway in cell growth, malignant transformation and drug resistance. Biochimica et biophysica acta 2007;1773:1263-1284.

45 Godeny MD, Sayeski PP. ERK1/2 regulates ANG II-dependent cell proliferation via cytoplasmic activation of rsk2 and nuclear activation of Elk1. American journal of physiology Cell physiology 2006;291:C1308-1317.

46 Smalley KS. A pivotal role for erk in the oncogenic behaviour of malignant melanoma? International journal of cancer 2003;104:527-532.

47 Kortylewski M, Heinrich PC, Kauffmann ME, Bohm M, MacKiewicz A, Behrmann I. Mitogen-activated protein kinases control p27/kip1 expression and growth of human melanoma cells. The Biochemical journal 2001;357:297-303.

48 Vivanco I, Sawyers CL. The Phosphatidylinositol 3-Kinase AKT pathway in human cancer. Nature reviews Cancer 2002;2:489-501.

49 Curtin JA, Stark MS, Pinkel D, Hayward NK, Bastian BC. PI3-Kinase subunits are infrequent somatic targets in melanoma. The Journal of investigative dermatology 2006;126:1660-1663.

50 Singh RS, Diwan AH, Zhang PS, Prieto VG. Phosphoinositide 3-kinase is not overexpressed in melanocytic lesions. Journal of cutaneous pathology 2007;34:220-225.

51 Robertson GP. Functional and therapeutic significance of akt deregulation in malignant melanoma. Cancer metastasis reviews 2005;24:273-285.

52 Dhawan P, Singh AB, Ellis DL, Richmond A. Constitutive activation of AKT/Protein Kinase B in melanoma leads to up-regulation of Nuclear Factor-kappaB and tumor progression. Cancer research 2002;62:7335-7342.

53 Dai DL, Martinka M, Li G. Prognostic significance of activated AKT expression in melanoma: A clinicopathologic study of 292 cases. Journal of clinical oncology 2005;23:1473-1482.

54 Fulda S, Debatin KM. Extrinsic versus intrinsic apoptosis pathways in anticancer chemotherapy. Oncogene 2006;25:4798-4811.

55 Elmore S. Apoptosis: A review of programmed cell death. Toxicologic pathology 2007;35:495-516.

56 Sekulic A, Haluska P, Jr., Miller AJ, Genebriera De Lamo J, Ejadi S, Pulido JS, Salomao DR, Thorland EC, Vile RG, Swanson DL, Pockaj BA, Laman SD, Pittelkow MR, Markovic SN, Melanoma Study Group of Mayo Clinic Cancer C. Malignant melanoma in the 21st century: The emerging molecular landscape. Mayo Clinic proceedings 2008;83:825-846.

57 Green DR, Kroemer G. The pathophysiology of mitochondrial cell death. Science 2004;305:626-629.

58 Saelens X, Festjens N, Vande Walle L, van Gurp M, van Loo G, Vandenabeele P. Toxic proteins released from mitochondria in cell death. Oncogene 2004;23:2861-2874.

59 Nagata S. Apoptotic DNA fragmentation. Experimental cell research 2000;256:12-18.

60 Walczak H, Krammer PH. The CD95 (Apo-1/Fas) and the TRAIL (Apo-2L) apoptosis systems. Experimental cell research 2000;256:58-66.

61 Chen G, Goeddel DV. TNF-r1 signaling: A beautiful pathway. Science 2002;296:1634-1635.

62 Hengartner MO. The biochemistry of apoptosis. Nature 2000;407:770-776.

63 Hartman ML, Czyz M. Anti-apoptotic proteins on guard of melanoma cell survival. Cancer letters 2013;331:24-34.

64 Hussein MR, Haemel AK, Wood GS. Apoptosis and melanoma: Molecular mechanisms. The Journal of pathology 2003;199:275-288.

65 Velho TR. Metastatic melanoma - a review of current and future drugs. Drugs in context 2012;2012:212242.

66 Bhatia S, Tykodi SS, Thompson JA. Treatment of metastatic melanoma: An overview. Oncology 2009;23:488-496.

67 Serrone L, Zeuli M, Sega FM, Cognetti F. Dacarbazine-based chemotherapy for metastatic melanoma: Thirty-year experience overview. Journal of experimental & clinical cancer research 2000;19:21-34.

68 Gasent Blesa JM, Grande Pulido E, Alberola Candel V, Provencio Pulla M. Melanoma: From darkness to promise. American journal of clinical oncology 2011;34:179-187.

69 Chiarion Sileni V, Nortilli R, Aversa SM, Paccagnella A, Medici M, Corti L, Favaretto AG, Cetto GL, Monfardini S. Phase II randomized study of dacarbazine, carmustine, cisplatin and tamoxifen versus dacarbazine alone in advanced melanoma patients. Melanoma research 2001;11:189-196.

70 Wiernik PH, Einzig AI. Taxol in malignant melanoma. Journal of the National Cancer Institute Monographs 1993:185-187.

71 Nathan FE, Berd D, Sato T, Mastrangelo MJ. Paclitaxel and tamoxifen: An active regimen for patients with metastatic melanoma. Cancer 2000;88:79-87.

72 Flaherty KT, Brose M, Schuchter L, Tuveson D, Lee R, Schwartz B, Lathia C, Weber B, P. OD. Phase I/II trial of bay 43-9006, carboplatin (c) and paclitaxel (p) demonstrates preliminary antitumor activity in the expansion cohort of patients with metastatic melanoma. Journal of Clinical Oncology 2004;22:7507.

73 Atkins MB, Lotze MT, Dutcher JP, Fisher RI, Weiss G, Margolin K, Abrams J, Sznol M, Parkinson D, Hawkins M, Paradise C, Kunkel L, Rosenberg SA. High-dose recombinant interleukin 2 therapy for patients with metastatic melanoma: Analysis of 270 patients treated between 1985 and 1993. Journal of clinical oncology 1999;17:2105-2116.

74 Atkins MB, Kunkel L, Sznol M, Rosenberg SA. High-dose recombinant interleukin-2 therapy in patients with metastatic melanoma: Long-term survival update. The cancer journal from Scientific American 2000;6 Suppl 1:S11-14.

75 Hodi FS, O'Day SJ, McDermott DF, Weber RW, Sosman JA, Haanen JB, Gonzalez R, Robert C, Schadendorf D, Hassel JC, Akerley W, van den Eertwegh AJ, Lutzky J, Lorigan P, Vaubel JM, Linette GP, Hogg D, Ottensmeier CH, Lebbe C, Peschel C, Quirt I, Clark JI, Wolchok JD, Weber JS, Tian J, Yellin MJ, Nichol GM, Hoos A, Urba WJ. Improved survival with ipilimumab in patients with metastatic melanoma. The New England journal of medicine 2010;363:711-723.

76 Finn L, Markovic SN, Joseph RW. Therapy for metastatic melanoma: The past, present, and future. BMC medicine 2012;10:23.

77 Eggermont AM, Robert C. New drugs in melanoma: It's a whole new world. European journal of cancer 2011;47:2150-2157.

78 End DW, Smets G, Todd AV, Applegate TL, Fuery CJ, Angibaud P, Venet M, Sanz G, Poignet H, Skrzat S, Devine A, Wouters W, Bowden C. Characterization of the antitumor effects of the selective farnesyl protein transferase inhibitor r115777 in vivo and in vitro. Cancer research 2001;61:131-137.

79 Margolin KA, Moon J, Flaherty LE, Lao CD, Akerley WL, 3rd, Othus M, Sosman JA, Kirkwood JM, Sondak VK. Randomized phase ii trial of sorafenib with temsirolimus or tipifarnib in untreated metastatic melanoma (s0438). Clinical cancer research 2012;18:1129-1137.

80 Chapman PB, Hauschild A, Robert C, Haanen JB, Ascierto P, Larkin J, Dummer R, Garbe C, Testori A, Maio M, Hogg D, Lorigan P, Lebbe C, Jouary T, Schadendorf D, Ribas A, O'Day SJ, Sosman JA, Kirkwood JM, Eggermont AM, Dreno B, Nolop K, Li J, Nelson B, Hou J, Lee RJ, Flaherty KT, McArthur GA, Group B-S. Improved survival with vemurafenib in melanoma with braf v600e mutation. The New England journal of medicine 2011;364:2507-2516.

81 Hauschild A, Grob JJ, Demidov LV, Jouary T, Gutzmer R, Millward M, Rutkowski P, Blank CU, Miller WH, Jr., Kaempgen E, Martin-Algarra S, Karaszewska B, Mauch C, Chiarion-Sileni V, Martin AM, Swann S, Haney P, Mirakhur B, Guckert ME, Goodman V, Chapman PB. Dabrafenib in braf-mutated metastatic melanoma: A multicentre, open-label, phase 3 randomised controlled trial. Lancet 2012;380:358-365.

82 Heidorn SJ, Milagre C, Whittaker S, Nourry A, Niculescu-Duvas I, Dhomen N, Hussain J, Reis-Filho JS, Springer CJ, Pritchard C, Marais R. Kinase-dead braf and oncogenic ras cooperate to drive tumor progression through craf. Cell 2010;140:209-221.

83 Flaherty KT, Infante JR, Daud A, Gonzalez R, Kefford RF, Sosman J, Hamid O, Schuchter L, Cebon J, Ibrahim N, Kudchadkar R, Burris HA, 3rd, Falchook G, Algazi A, Lewis K, Long GV, Puzanov I, Lebowitz P, Singh A, Little S, Sun P, Allred A, Ouellet D, Kim KB, Patel K, Weber J. Combined braf and mek inhibition in melanoma with BRaf v600 mutations. The New England journal of medicine 2012;367:1694-1703.

84 Lopez-Fauqued M, Gil R, Grueso J, Hernandez-Losa J, Pujol A, Moline T, Recio JA. The dual PI3K/mTOR inhibitor PI-103 promotes immunosuppression, in vivo tumor growth and increases survival of sorafenib-treated melanoma cells. International journal of cancer 2010;126:1549-1561.

85 Borowiec A, Lechward K, Tkacz-Stachowska K, Skladanowski AC. Adenosine as a metabolic regulator of tissue function: Production of adenosine by cytoplasmic 5'-nucleotidases. Acta biochimica Polonica 2006;53:269-278.

86 Gessi S, Merighi S, Sacchetto V, Simioni C, Borea PA. Adenosine receptors and cancer. Biochimica et biophysica acta 2011;1808:1400-1412.

87 Zimmermann H, Braun N, Kegel B, Heine P. New insights into molecular structure and function of ectonucleotidases in the nervous system. Neurochemistry international 1998;32:421-425.

88 Deaglio S, Robson SC. Ectonucleotidases as regulators of purinergic signaling in thrombosis, inflammation, and immunity. Advances in pharmacology 2011;61:301-332.

89 Zhang J, Visser F, King KM, Baldwin SA, Young JD, Cass CE. The role of nucleoside transporters in cancer chemotherapy with nucleoside drugs. Cancer metastasis reviews 2007;26:85-110.

90 Hasko G, Cronstein BN. Adenosine: An endogenous regulator of innate immunity. Trends in immunology 2004;25:33-39.

91 Fredholm BB. Adenosine receptors as drug targets. Experimental cell research 2010;316:1284-1288.

92 Ballarin M, Fredholm BB, Ambrosio S, Mahy N. Extracellular levels of adenosine and its metabolites in the striatum of awake rats: Inhibition of uptake and metabolism. Acta physiologica Scandinavica 1991;142:97-103.

93 Hasko G, Sitkovsky MV, Szabo C. Immunomodulatory and neuroprotective effects of inosine. Trends in pharmacological sciences 2004;25:152-157.

94 Fredholm BB, AP IJ, Jacobson KA, Klotz KN, Linden J. International union of pharmacology. Xxv. Nomenclature and classification of adenosine receptors. Pharmacological reviews 2001;53:527-552.

95 Fredholm BB, AP IJ, Jacobson KA, Linden J, Muller CE. International union of basic and clinical pharmacology. Lxxxi. Nomenclature and classification of adenosine receptors--an update. Pharmacological reviews 2011;63:1-34.

96 Schulte G, Fredholm BB. Signalling from adenosine receptors to mitogen-activated protein kinases. Cellular signalling 2003;15:813-827.

97 Gessi S, Merighi S, Varani K, Leung E, Mac Lennan S, Borea PA. The a3 adenosine receptor: An enigmatic player in cell biology. Pharmacology & therapeutics 2008;117:123-140.

98 Zezula J, Freissmuth M. The a(2a)-adenosine receptor: A gpcr with unique features? British journal of pharmacology 2008;153 Suppl 1:S184-190.

99 Sheth S, Brito R, Mukherjea D, Rybak LP, Ramkumar V. Adenosine receptors: Expression, function and regulation. International journal of molecular sciences 2014;15:2024-2052.

100 Antonioli L, Blandizzi C, Pacher P, Hasko G. Immunity, inflammation and cancer: A leading role for adenosine. Nature reviews Cancer 2013;13:842-857.

101 Burnstock G, Di Virgilio F. Purinergic signalling and cancer. Purinergic signalling 2013;9:491-540.

102 Linden J. Adenosine metabolism and cancer. Focus on "adenosine downregulates dppiv on ht-29 colon cancer cells by stimulating protein tyrosine phosphatases and reducing erk1/2 activity via a novel pathway". American journal of physiology Cell physiology 2006;291:C405-406.

103 Spychala J. Tumor-promoting functions of adenosine. Pharmacology & therapeutics 2000;87:161-173.

104 Ceruti S, Abbracchio MP. Adenosine signaling in glioma cells. Advances in experimental medicine and biology 2013;986:13-30.

105 Stagg J, Smyth MJ. Extracellular adenosine triphosphate and adenosine in cancer. Oncogene 2010;29:5346-5358.

106 Pirincci N, Gecit I, Gunes M, Yuksel MB, Kaba M, Tanik S, Demir H, Aslan M. Serum adenosine deaminase, catalase and carbonic anhydrase activities in patients with bladder cancer. Clinics 2012;67:1443-1446.

107 Fishman P, Bar-Yehuda S, Madi L, Cohn I. A3 adenosine receptor as a target for cancer therapy. Anti-cancer drugs 2002;13:437-443.

108 Madi L, Ochaion A, Rath-Wolfson L, Bar-Yehuda S, Erlanger A, Ohana G, Harish A, Merimski O, Barer F, Fishman P. The a3 adenosine receptor is highly expressed in tumor versus normal cells: Potential target for tumor growth inhibition. Clinical cancer research 2004;10:4472-4479.

109 Merighi S, Varani K, Gessi S, Cattabriga E, Iannotta V, Ulouglu C, Leung E, Borea PA. Pharmacological and biochemical characterization of adenosine receptors in the human malignant melanoma a375 cell line. British journal of pharmacology 2001;134:1215-1226.

110 Gessi S, Varani K, Merighi S, Morelli A, Ferrari D, Leung E, Baraldi PG, Spalluto G, Borea PA. Pharmacological and biochemical characterization of a3 adenosine receptors in jurkat t cells. British journal of pharmacology 2001;134:116-126.

111 Suh BC, Kim TD, Lee JU, Seong JK, Kim KT. Pharmacological characterization of adenosine receptors in pgt-beta mouse pineal gland tumour cells. British journal of pharmacology 2001;134:132-142.

112 Fishman P, Madi L, Bar-Yehuda S, Barer F, Del Valle L, Khalili K. Evidence for involvement of Wnt signaling pathway in ib-meca mediated suppression of melanoma cells. Oncogene 2002;21:4060-4064.

113 Madi L, Bar-Yehuda S, Barer F, Ardon E, Ochaion A, Fishman P. A_3 adenosine receptor activation in melanoma cells: Association between receptor fate and tumor growth inhibition. The Journal of biological chemistry 2003;278:42121-42130.

114 Yoshikawa N, Yamada S, Takeuchi C, Kagota S, Shinozuka K, Kunitomo M, Nakamura K. Cordycepin (3'-deoxyadenosine) inhibits the growth of B16-Bl6 mouse melanoma cells through the stimulation of adenosine A_3 receptor followed by glycogen synthase kinase-3beta activation and cyclin d1 suppression. Naunyn-Schmiedeberg's archives of pharmacology 2008;377:591-595.

115 Fishman P, Bar-Yehuda S, Barer F, Madi L, Multani AS, Pathak S. The a3 adenosine receptor as a new target for cancer therapy and chemoprotection. Experimental cell research 2001;269:230-236.

116 Merighi S, Benini A, Mirandola P, Gessi S, Varani K, Leung E, Maclennan S, Borea PA. A3 adenosine receptor activation inhibits cell proliferation via Phosphatidylinositol 3-Kinase/AKT-dependent inhibition of the extracellular signal-regulated kinase 1/2 phosphorylation in A375 human melanoma cells. The Journal of biological chemistry 2005;280:19516-19526.

117 Merighi S, Mirandola P, Milani D, Varani K, Gessi S, Klotz KN, Leung E, Baraldi PG, Borea PA. Adenosine receptors as mediators of both cell proliferation and cell death of cultured human melanoma cells. The Journal of investigative dermatology 2002;119:923-933.

118 Merighi S, Simioni C, Gessi S, Varani K, Mirandola P, Tabrizi MA, Baraldi PG, Borea PA. A(2b) and a(3) adenosine receptors modulate vascular endothelial growth factor and interleukin-8 expression in human melanoma cells treated with etoposide and doxorubicin. Neoplasia 2009;11:1064-1073.

119 Morello S, Petrella A, Festa M, Popolo A, Monaco M, Vuttariello E, Chiappetta G, Parente L, Pinto A. Cl-ib-meca inhibits human thyroid cancer cell proliferation independently of a3 adenosine receptor activation. Cancer biology & therapy 2008;7:278-284.

120 Kim SG, Ravi G, Hoffmann C, Jung YJ, Kim M, Chen A, Jacobson KA. P53-independent induction of fas and apoptosis in leukemic cells by an adenosine derivative, Cl-IB-MECA. Biochemical pharmacology 2002;63:871-880.

121 Morello S, Sorrentino R, Porta A, Forte G, Popolo A, Petrella A, Pinto A. Cl-IB-MECA enhances trail-induced apoptosis via the modulation of NF-kappaB signalling pathway in thyroid cancer cells. Journal of cellular physiology 2009;221:378-386.

122 Stemmer SM, Benjaminov O, Medalia G, Ciuraru NB, Silverman MH, Bar-Yehuda S, Fishman S, Harpaz Z, Farbstein M, Cohen S, Patoka R, Singer B, Kerns WD, Fishman P. Cf102 for the treatment of hepatocellular carcinoma: A phase I/II, open-label, dose-escalation study. The oncologist 2013;18:25-26.

123 de Souza CF, Morais AS, Jasiulionis MG. Biomarkers as key contributors in treating malignant melanoma metastases. Dermatology research and practice 2012;2012:156068.

124 Blay J, White TD, Hoskin DW. The extracellular fluid of solid carcinomas contains immunosuppressive concentrations of adenosine. Cancer research 1997;57:2602-2605.

125 Sitkovsky MV, Kjaergaard J, Lukashev D, Ohta A. Hypoxia-adenosinergic immunosuppression: Tumor protection by t regulatory cells and cancerous tissue hypoxia. Clinical cancer research Research 2008;14:5947-5952.

126 Hasko G, Linden J, Cronstein B, Pacher P. Adenosine receptors: Therapeutic aspects for inflammatory and immune diseases. Nature reviews Drug discovery 2008;7:759-770.

127 Chodurek E, Orchel A, Gruchlik A, Aleksander E, Golabek K, Dzierzewicz Z. Valproic acid enhances cisplatin cytotoxicity in melanoma cells. Acta poloniae pharmaceutica 2012;69:1298-1302.

128 Niles RM, McFarland M, Weimer MB, Redkar A, Fu YM, Meadows GG. Resveratrol is a potent inducer of apoptosis in human melanoma cells. Cancer letters 2003;190:157-163.

129 Serafim TL, Matos JA, Sardao VA, Pereira GC, Branco AF, Pereira SL, Parke D, Perkins EL, Moreno AJ, Holy J, Oliveira PJ. Sanguinarine cytotoxicity on mouse melanoma k1735-m2 cells--nuclear vs. Mitochondrial effects. Biochemical pharmacology 2008;76:1459-1475.

130 Bennett DC. Differentiation in mouse melanoma cells: Initial reversibility and an on-off stochastic model. Cell 1983;34:445-453.

131 Falcato-Soares A, Diniz C, Fresco P. Characterization of adenosine receptors in human and mouse melanoma cells. Medimond International Proceedings: 6th European Congress of Pharmacology, Granada (Spain) 2013:29-34.

132 Panjehpour M, Castro M, Klotz KN. Human breast cancer cell line MDA-MB-231 expresses endogenous A_{2B} adenosine receptors mediating a Ca^{2+} signal. British journal of pharmacology 2005;145:211-218.

133 Mervic L. Time course and pattern of metastasis of cutaneous melanoma differ between men and women. PloS one 2012;7:e32955.

134 Soares AF, Diniz C, Fresco P. A_3 adenosine receptor effects on malignant melanoma cells. FEBS J 2012;279(Suppl. 1):547.

135 Klaasse EC, Ijzerman AP, de Grip WJ, Beukers MW. Internalization and desensitization of adenosine receptors. Purinergic signalling 2008;4:21-37.

136 Soares AS, Costa VM, Diniz C, P F. Inosine strongly enhances human C32 melanoma cells proliferation through PLC-PKC-MEK1/2-ERK1/2 and PI3K pathways. Manuscript submitted for publication.

137 Bavaresco L, Bernardi A, Braganhol E, Cappellari AR, Rockenbach L, Farias PF, Wink MR, Delgado-Canedo A, Battastini AM. The role of ecto-5'-nucleotidase/CD73 in glioma cell line proliferation. Molecular and cellular biochemistry 2008;319:61-68.

138 Mazurek S, Michel A, Eigenbrodt E. Effect of extracellular amp on cell proliferation and metabolism of breast cancer cell lines with high and low glycolytic rates. The Journal of biological chemistry 1997;272:4941-4952.

139 Aghaei M, Karami-Tehrani F, Salami S, Atri M. Adenosine deaminase activity in the serum and malignant tumors of breast cancer: The assessment of isoenzyme ADA1 and ADA2 activities. Clinical biochemistry 2005;38:887-891.

140 Zanini D, Schmatz R, Pelinson LP, Pimentel VC, da Costa P, Cardoso AM, Martins CC, Schetinger CC, Baldissareli J, do Carmo Araujo M, Oliveira L, Chiesa J, Morsch VM, Leal DB,

Schetinger MR. Ectoenzymes and cholinesterase activity and biomarkers of oxidative stress in patients with lung cancer. Molecular and cellular biochemistry 2013;374:137-148.

141 Mouawad R, Sebert M, Michels J, Bloch J, Spano JP, Khayat D. Treatment for metastatic malignant melanoma: Old drugs and new strategies. Critical reviews in oncology/hematology 2010;74:27-39.

142 van Herpen CM, Eskens FA, de Jonge M, Desar I, Hooftman L, Bone EA, Timmer-Bonte JN, Verweij J. A phase ib dose-escalation study to evaluate safety and tolerability of the addition of the aminopeptidase inhibitor tosedostat (chr-2797) to paclitaxel in patients with advanced solid tumours. British journal of cancer 2010;103:1362-1368.

143 Soares AS, Costa VM, Diniz C, Fresco P. Potentiation of cytotoxicity of paclitaxel in combination with cl-ib-meca in human c32 metastatic melanoma cells: A new possible therapeutic strategy for melanoma. Biomedicine & pharmacotherapy 2013;67:777-789.

144 Pessina A, Bonomi A, Cocce V, Invernici G, Navone S, Cavicchini L, Sisto F, Ferrari M, Vigano L, Locatelli A, Ciusani E, Cappelletti G, Cartelli D, Arnaldo C, Parati E, Marfia G, Pallini R, Falchetti ML, Alessandri G. Mesenchymal stromal cells primed with paclitaxel provide a new approach for cancer therapy. PloS one 2011;6:e28321.

145 Bulitta JB, Zhao P, Arnold RD, Kessler DR, Daifuku R, Pratt J, Luciano G, Hanauske AR, Gelderblom H, Awada A, Jusko WJ. Mechanistic population pharmacokinetics of total and unbound paclitaxel for a new nanodroplet formulation versus taxol in cancer patients. Cancer chemotherapy and pharmacology 2009;63:1049-1063.

146 Hanahan D, Weinberg RA. Hallmarks of cancer: The next generation. Cell 2011;144:646-674.

147 Soares AS, Costa VM, Diniz C, Fresco P. Combination of Cl-IB-MECA with paclitaxel is a highly effective cytotoxic therapy causing mTOR-dependent autophagy and mitotic catastrophe on human melanoma cells. Journal of cancer research and clinical oncology 2014. DOI: 10.1007/s00432-014-1645-z.

148 Aliwaini S, Swarts AJ, Blanckenberg A, Mapolie S, Prince S. A novel binuclear palladacycle complex inhibits melanoma growth in vitro and in vivo through apoptosis and autophagy. Biochemical pharmacology 2013;86:1650-1663.

149 Mizushima N. Autophagy: Process and function. Genes & development 2007;21:2861-2873.

150 Quidville V, Alsafadi S, Goubar A, Commo F, Scott V, Pioche-Durieu C, Girault I, Baconnais S, Le Cam E, Lazar V, Delaloge S, Saghatchian M, Pautier P, Morice P, Dessen P, Vagner S, Andre F. Targeting the deregulated spliceosome core machinery in cancer cells triggers mtor blockade and autophagy. Cancer research 2013;73:2247-2258.

151 Bhalla KN. Microtubule-targeted anticancer agents and apoptosis. Oncogene 2003;22:9075-9086.

152 Castedo M, Perfettini JL, Roumier T, Valent A, Raslova H, Yakushijin K, Horne D, Feunteun J, Lenoir G, Medema R, Vainchenker W, Kroemer G. Mitotic catastrophe constitutes a special case of apoptosis whose suppression entails aneuploidy. Oncogene 2004;23:4362-4370.

153 Mansilla S, Priebe W, Portugal J. Mitotic catastrophe results in cell death by caspase-dependent and caspase-independent mechanisms. Cell cycle 2006;5:53-60.

154 Madonna G, Ullman CD, Gentilcore G, Palmieri G, Ascierto PA. Nf-kappab as potential target in the treatment of melanoma. Journal of translational medicine 2012;10:53.

155 Attoub S, Arafat K, Gelaude A, Al Sultan MA, Bracke M, Collin P, Takahashi T, Adrian TE, De Wever O. Frondoside a suppressive effects on lung cancer survival, tumor growth, angiogenesis, invasion, and metastasis. PloS one 2013;8:e53087.

156 Soares AS, Costa VM, Diniz C, Fresco P. The combination of Cl-IB-MECA with paclitaxel: A new anti-metastatic therapeutic strategy for melanoma. Manuscript submitted for publication.

157 Jin X, Shepherd RK, Duling BR, Linden J. Inosine binds to A3 adenosine receptors and stimulates mast cell degranulation. The Journal of clinical investigation 1997;100:2849-2857.

158 Wolber C, Fozard JR. The receptor mechanism mediating the contractile response to adenosine on lung parenchymal strips from actively sensitised, allergen-challenged brown norway rats. Naunyn-Schmiedeberg's archives of pharmacology 2005;371:158-168.

159 Mlejnek P, Dolezel P, Frydrych I. Effects of synthetic a3 adenosine receptor agonists on cell proliferation and viability are receptor independent at micromolar concentrations. Journal of physiology and biochemistry 2013;69:405-417.